

**Optimization Study Of Incineration
In A MSW Incinerator With A
Vertical Radiation Shaft**

A Thesis Submitted by

Vida Nasserzadeh Sharifi, B.Eng.

to

**The University of Sheffield for the
degree of Doctor of Philosophy**

**Department of Mechanical and Process Engineering,
Chemical Engineering and Fuel Technology Group,
The University of Sheffield,**

October 1990

Acknowledgements

The author would like to thank Professor J. Swithenbank for his supervision of this research project, and to acknowledge the financial support of Warren Spring Laboratory (Department of Environment).

In addition the help of the following organisations, laboratories and companies for providing some of the experimental equipment and their technical assistance during the experimental work is, hereby, gratefully acknowledged:

1. Cleansing Services Department, Sheffield City Council,
2. Mr B. Jones, plant manager, Mr G. Sykes maintenance superintendent and the technicians at the Sheffield municipal incinerator plant;
3. Warren Spring Laboratory, Materials Recovery and Pollution Abatement Divisions, Mr D.W. Scott and Mr A.J. Poll;
4. United States Environmental Protection Agency, Hazardous Waste Engineering Research Laboratory, Office of Research and Development, Cincinnati, Ohio, Dr H.M. Freeman;
5. Babcock and Wilcox Power Ltd., London, Mr M. Knowles;
6. Babcock and Wilcox Ltd., Office of Research and Development, Scotland, Dr L. King;
7. Motherwell Bridge Ltd., Dr W. McKingly;
8. Land Combustion Ltd., Dr K. West.

Thanks are also due to Dr A.B. Hedley, Dr P.J. Foster, Dr R.G. Siddall and Dr K. Littlewood for their useful suggestions and discussions concerning various aspects of the work.

The technicians and laboratory staff at the Mechanical and Process Engineering Workshop (University of Sheffield): Mr J.Lane, Mr D.Hancock, Mr J.Simpson, Mr B.Stobbs,

Mr C.Wright, Mr T.Rochford, Mr M.Smith, Mr M.Hudson, Mr B.Milner, Mr A.Sanby, Mr A.Barber and Mr J.Wragg were most helpful in constructing experimental equipment and providing encouragement.

The author also wishes to thank Dr. P.N. Wild from Flow Simulation Ltd. for his help with the mathematical modelling of the flow field inside the furnace using the FLUENT code.

Finally, many thanks to D.Savaz and M.Wild for their help with the computing work and producing the photographs.

Contents

| | | |
|----------|--|-----------|
| 1 | Introduction | 1 |
| 2 | Experimental Programme and Procedure | 7 |
| 2.1 | Introduction | 7 |
| 2.2 | Description of Sheffield municipal incinerator plant | 7 |
| 2.3 | Incinerator Testing Program: | 13 |
| 2.3.1 | Physical and Chemical Analysis of Sheffield Refuse | 13 |
| 2.3.2 | Temperature Measurements | 24 |
| 2.3.3 | Pressure Measurements | 29 |
| 2.3.4 | Gas Sampling Measurements | 34 |
| 2.3.5 | Miscellaneous Measurements | 46 |
| 3 | Calculations | 49 |
| 3.1 | Furnace Calculations; Analysis of Actual Data Obtained From A Series Of Tests At Sheffield Incinerator [42], [43], [44] | 49 |
| 3.2 | Estimation of Average Refuse Residence Time | 61 |
| 3.3 | Calculations: Drying, Pyrolysis, and Char gasification rates on top of each roller inside the incinerator | 62 |
| 3.4 | Overbed Air Regime Calculations | 68 |
| 3.5 | Calculation of Incinerator - Boiler Efficiency (Heat - Balances) | 69 |
| 3.6 | Incinerator Material Balance | 76 |
| 3.7 | Combustion Calculation | 79 |

| | | |
|----------|--|------------|
| 4 | Mathematical Modelling of Combustion Processes | 85 |
| 4.1 | Simplified Combustion Model [59], [60] | 85 |
| 4.2 | Mathematical Model For The Refuse Bed | 87 |
| 4.2.1 | Ignition of Refuse Bed | 88 |
| 4.2.2 | Drying Front | 89 |
| 4.2.3 | Pyrolysis Front | 90 |
| 4.2.4 | Active Burning And Zero Free O ₂ Zones | 92 |
| 4.2.5 | Solid Bed Gasification | 92 |
| 4.3 | Mathematical Model for Over-Bed Region (Gaseous Phase) | 97 |
| 4.3.1 | Primary Air Distributions (Modelling of Riddling Hoppers and Hollow Grate Assemblies) | 98 |
| 4.3.2 | Mathematical Model for Overbed Region; Gaseous Phase | 102 |
| 5 | Discussion | 109 |
| 5.1 | Results for the Sheffield municipal incinerator | 109 |
| 5.1.1 | Isothermal Flow Field Model | 109 |
| 5.1.2 | Reacting Flow Case | 111 |
| 5.2 | Comparison with Experimental Results for the Sheffield Municipal Incin- erator | 115 |
| 6 | Conclusions and Suggestions for Future Work | 117 |
| 6.1 | Conclusions | 117 |
| 6.2 | Suggestions for Future Work | 120 |
| | Bibliography | 122 |
| | Appendices | 129 |
| | Tables | - |
| | Figures | - |

Plates

Nomenclature

| Symbol | Description | Imperial Unit | SI Unit |
|-------------|--|----------------------------------|--------------------------------|
| A | Combustion model constant | - | - |
| a | Stoker efficiency correction factor | - | - |
| A_s | Average pore surface area per unit volume of refuse bed | ft ² /ft ³ | m ² /m ³ |
| \bar{A} | Ash fraction in refuse | lb/lb | kg/kg |
| \bar{C} | Combustible fraction in refuse | lb/lb | kg/kg |
| C_a | Furnace capacity | lb/hr | kg/hr |
| C_p | Specific heat capacity | Btu/lb °F | J/kg °K |
| d | Average refuse particle size | ft | m |
| D | Refuse bed depth | ft | m |
| F_A | Area rate of char gasification | lb/ft ² hr | kg/m ² hr |
| F'_A | Stoker burning rate | lb/ft ² hr | kg/m ² hr |
| f_{rcs} | Relative carbon saturation factor | - | - |
| G_A | Underfire air flow per unit weight of refuse | lb/lb | kg/kg |
| g | Gravitational constant | ft/min ² | m/sec ² |
| \bar{H}_v | Effective latent heat of vaporization | Btu/lb | J/kg |
| h | Enthalpy | Btu/mol | J/mol |
| K_w | Essenhigh waste factor | - | - |
| k, k' | Reaction rate constants | - | - |
| L | Length | ft | m |
| \bar{M} | Free moisture fraction in refuse | lb/lb | kg/kg |

| | | | |
|---------------|--|------------------------|----------------------|
| M_i | Molecular weight of species i | lb/mol | kg/mol |
| m | Index of CO-O ₂ reaction | - | - |
| m_i | Mass of the i-th species | lb | kg |
| \dot{m} | Mass flow rate per unit area | lb/hr ft ² | kg/hr m ² |
| n | $\frac{k}{\epsilon}$ | - | - |
| N_i | Molar concentration of i-th species | moles/min | moles/min |
| P | Pressure | lbf/in ² | Pa |
| P_m | Oxygen mass fraction in air | lb/lb | kg/kg |
| Q_T | Total underfire air flow | ft ³ /min | m ³ /sec |
| \dot{Q}_s | Flame heat release per unit time | Btu/hr | J/hr |
| Q_s | Heat of surface pyrolysis per unit mass per unit area | Btu/lb ft ² | kJ/kg m ² |
| R | Gas constant | Btu/ °F | J/ °K |
| R_{co} | Rate of CO consumption by chemical reaction | mol/sec | mol/sec |
| R_{fu} | Rate of fuel consumption by chemical reaction | mol/sec | mol/sec |
| S_h | Enthalpy source term due to chemical reaction | Btu/mol | j/mol |
| S_s | Species source term due to chemical reaction | lb | kg |
| t | Time | hr | hr |
| T_s | Solid temperature | °F | °C |
| T_o | Ambient temperature | °F | °C |
| T_g | Gas temperature | °F | °C |
| u | Velocity | ft/min | m/min |
| u_i | Time average velocity component | ft/min | m/sec |
| \tilde{u}_i | Instantaneous velocity component | ft/min | m/sec |

| | | | |
|---------------|---|-----------------------------------|----------------------------------|
| u'_i | Fluctuating component of velocity | ft/min | m/sec |
| U | Mass velocity of solid | lb ft/hr | kg m/hr |
| v | Velocity | ft/min | m/min |
| v_p | Velocity in the pores of bed | ft/min | m/min |
| δV_s | Volume element in solid bed | ft ³ | m ³ |
| V | Volatiles fraction of dry combustible | - | - |
| W_a | Stoichiometric air | lb/lb | kg/kg |
| \dot{W} | Mass input rate | lb/hr | kg/hr |
| \dot{W}_p | Mass of pyrolyzable material per unit volume of refuse | lb/ft ³ | kg/m ³ |
| x, y | Horizontal and vertical distances | ft | m |
| X | Molar concentration in pores | mole | mole |
| y^* | Flame height | ft | m |
| Y_i | Mole fraction of i-th species | - | - |
| γ | Refuse bed depth correction factor | - | - |
| μ | Dynamic viscosity | lb/ft sec | kg/m sec |
| ρ_a | Air density | lb/ft ³ | kg/m ³ |
| ρ_g | Gas density | lb/ft ³ | kg/m ³ |
| ρ_s | Solid density | lb/ft ³ | kg/m ³ |
| ϵ | Porosity | - | - |
| ϵ | Dissipation rate of energy | ft ² /min ³ | m ² /sec ³ |
| τ | Turbulence time scale | sec | sec |
| γ_{ij} | Kronecker Delta | - | - |
| δ | Empirical constant | - | - |

Abbreviations:

| | |
|-------------|--|
| <i>CFM</i> | ft ³ /min |
| <i>CV</i> | Calorific value of the refuse |
| <i>F.D.</i> | Forced draught fan |
| <i>FWL</i> | Full water level of the boiler drum |
| <i>HHV</i> | High heat value of refuse |
| <i>I.D.</i> | Induced draught fan |
| <i>LHS</i> | Left hand side |
| <i>MCR</i> | Maximum continuous rating of the incinerator |
| <i>MSW</i> | Municipal solid waste |
| <i>NWL</i> | Normal water level of the boiler drum |
| <i>RHS</i> | Right hand side |
| <i>S.A.</i> | Secondary air fan |
| <i>Wt</i> | Weight |

Summary

An extensive series of experimental tests were carried out at the Sheffield municipal solid waste incinerator plant (30 MW) from September 1988 to July 1989 to investigate the influence of the design and operating parameters on the performance of the incinerator which burns domestic and commercial wastes (500 ton/day).

The following measurements were made around the plant: temperature measurements, pressure measurements, flue gas composition analysis and determination of physical and chemical properties of Sheffield refuse. Several other miscellaneous measurements were also made to monitor the effect of variation of operating parameters on the performance characteristics of the incinerator.

A combustion model of Essenhigh type was then employed to model the combustion processes inside the solid refuse bed on top of the travelling grate. In addition a mathematical model of the finite difference type (FLUENT) was used to predict the three dimensional reacting flows (gaseous phase) within the incinerator geometry. Experimental measurements of gas composition, temperature and exit velocity were compared with model predictions. Modelling results were generally in good agreement with measurements.

As a result of the test data and the mathematical modelling of the whole process, suggestions for design improvements for the Sheffield municipal solid waste incinerator were made which will substantially increase the efficiency, reduce emissions of pollutants and reduce the maintenance costs at the plant. These are: a) replacing the existing secondary air system with secondary air nozzles and the use of more secondary air (up to 20 % of total air) in order to generate turbulence in the high intensity combustion zone where it is most needed and b) introducing a baffle into the main stream inside the radiation shaft in order to lower the gas temperatures entering the precipitator and to remove the existing recirculation zone in the shaft.

Chapter 1

Introduction

Wastes; a survey

Like energy, waste can be changed into different forms but it can never be wholly destroyed. Whether it is burned, buried or recycled, some residue will always remain.

The statistics are staggering, if not well known. Since 1984 the number of landfills for municipal solid waste in the United States has dwindled by 30 percent from 9284 to 6499 [1]. According to the 1973 report of the U.S. Conference of Mayors, over half the cities in the U.S.A will run out of landfill capacity by 1995.

As landfill capacity declines, the rate at which Americans produce waste is increasing rapidly. It is estimated that the solid waste generated in the United States will grow at an average of 1.8 percent per year between 1980 and 2000. While two thirds of this will be due to population growth, a third will come from the increased amount of waste generated per individual. By the beginning of the 21st century, the Americans will produce more than 280 million tons of domestic solid waste every year, or 1.7 kg per day per person.

In the UK alone the total amount of wastes and residues produced annually has been estimated to be 250 million tonnes, of which about 140 million tonnes has no commercial value and is discarded [2]. Table 1.1 shows the various sources and the estimated recoverable and available wastes; some waste materials are already recovered but the

majority are not. To this annual production figure can be added a further 50 million tonnes of colliery spoil, 50 million tonnes of quarrying waste and 12 million tonnes of power station residues. The cost of disposal is enormous; for that portion of the waste handled by Waste Disposal Authorities (WDAs), the net expenditure over the period 1985 to 1986 was £127 million [3]. This however only accounted for the relatively innocuous domestic and commercial wastes. Over a similar period the nine English Water Authorities and the Welsh Authority jointly spend £554 million on sewage treatment and disposal, mainly by land or sea dumping. A Department of the Environment report in 1978 concluded that unless the costs to the community outweigh the benefits then waste should be reclaimed [4] ; most is still tipped and only a fraction of the potential value is realised.

Disposal of Municipal Solid Wastes

The burgeoning problem of the disposal of solid wastes in metropolitan areas has presented many municipalities with a dilemma when choosing suitable disposal methods. The traditional means of disposal have been either open dumping or landfill, but these practices which require large land acreages and in the case of sanitary landfill require costly earth, are becoming less attractive as the areas available for disposal near metropolitan areas rapidly disappear. Incineration will therefore, in all likelihood, play an important role in the future as a practical disposal method in urban areas.

There has been very little fundamental design work on incinerators and designs that have proven "satisfactory" in the field have simply been sized to suit the required loading, often with disregard for basic scaling laws. Consequently, municipal incinerators have been subjected to mounting criticism as to their inefficiency. The processes occurring within a burning refuse bed include drying, pyrolysis, solid and gas phase combustion, convective, conductive and radiative heat transfer, mass transfer and gas flow through randomly packed heterogeneous beds, whose elements differ widely in size, shape and in their physical and chemical structure; moreover, the size, shape, chemical constitution

and orientation of these elements continually change with the course of combustion. There is no more complex unit operation presently in use. Designs have, therefore, evolved as an art rather than as a science.

Typically designs are based on gross overall heat and material balances, on allowable combustion intensities in the overfire volume and on achievable burning rates per unit area of grate surface with different refuse (Table 1.2). Of these three requirements the most difficult to estimate has been the achievable burning rate. The heat and mass balances are straight forward to calculate, particularly as the air requirements for most solid fuels are remarkably uniform when expressed on a basis of energy liberated (Table 1.4). The achievable burning rates per unit of grate are estimated from guidelines such as those provided by Table 1.2 or from the rule of thumb that the heat release rate within the fuel bed should be about 300,000 Btu/hr ft² of grate area. For a typical as-fired heating value for refuse (5,000 Btu/lb), the burning rate for the above criterion would be 60 lb/hr ft² of grate area which agrees with the Incinerator Institute of America's guideline for a class 5 incinerator (see appendix 1) and the values given in Table 1.2.

The maximum allowable heat release rate within a fuel bed is usually determined from consideration of the maximum bed temperature that would prevail and therefore must take heat losses from the bed into account. Temperatures that are too high cause difficulties with clinkering and problems with grates clogged with molten glass and aluminum. There are indications that successful operation has been achieved at heat release rates up to three times the suggested maximum value of 300,000 Btu/hr ft², hinting at the tempting prospect of reduced investment cost per ton of refuse processed.

A similar situation to that encountered when selecting grate sizes is found in the overbed region where few design criteria are available. The only specifications given are for furnace volumes based on guidelines such as those given in Table 1.2, or on the rule of thumb that the volumetric heat release should be around 20,000 Btu/hr ft³, and on allowable gas velocities at different points in the incinerator. The value of the maximum combustion intensity is given without any regard for the amount of combustibles that

have to be burnt in the overbed region. No guidelines are given as to the desirable ratio of primary air introduced through the fuel bed to secondary air injected into the overbed region. There is general agreement in the literature that the secondary air must be supplied with sufficient momentum to provide adequate mixing with combustible gases. There are, however, no reliable methods presently available for determining how this should be accomplished.

The early experimental work by Kreisinger, Ovitz and Augustine [5] and Nicholls [6] provided valuable information on the combustion characteristics of both overfeed and underfeed fuel beds. Although the combustion characteristics of a refuse bed, where the moisture and volatile contents are greater than those for a typical bituminous coal, may not be the same as found in these studies, the work of Kreisinger, Augustine and Harpster [7] with lignite has suggested that the general behaviour may be somewhat similar.

Few laboratory-scale experiments on refuse or simulated refuse combustion have been reported in the literature. The first studies were conducted at the U.S. Bureau of Mines in the late 1960s and since that time their studies have leaned towards the development of a vortex incinerator where the secondary air was injected tangentially above the bed and little or no underfire air was used. The work at the U.S. Bureau of Mines by Weintraub et al [8] provided some information from the measurement of burning rates and bed temperature profiles, on the bed burning characteristics of a simulated refuse (a mixture of paper, cardboard, and leafy vegetable matter). No underfire air was used and in all runs a substantial portion of the secondary air was induced through the bed by natural draft and the vortex flow.

The only other study on fixed-bed incinerators that has been reported was the work of Essenhigh and colleagues at Pennsylvania State University. This work has been summarized in a paper by Essenhigh and Shieh [9]. The Pennsylvania State study was directed towards conditions prevailing in a semicontinuous-feed overfeed bed. The simulated refuse used in these studies was limited to computer cards whose characteristic thickness was

much smaller than that typically encountered in refuse.

There has been little theoretical work reported on models suitable for predicting burning and ignition rates within refuse beds. The literature on coal bed combustion appears to be ill-suited for refuse bed conditions, where the rate of heat transfer into the fuel elements provides a controlling resistance to the combustion processes.

Designs based on these methods may have been satisfactory in the past but with the effects of the new legislation concerning acceptable levels of gaseous and particulate emission as well as ash and residue quality beginning to be felt, increasing numbers of practitioners are becoming interested in developing more fundamental ways of designing their incinerators. For example, Hollender [10] has pointed out the need for indicators for determining the probable burning characteristics of different fuels, and the selection of the size, number and location of secondary jet systems and the ratios of primary and secondary air. In addition the long term trends in refuse quality as predicted by Niessen and Alsobrook [11] and Niessen and Chansky [12] have suggested that the volatile content of refuse which is a measure of the quantity of secondary air that is required to complete the combustion of the volatile products distilling from the fuel bed, will increase over the years (Table 1.3). The projected increase of this component in refuse is also expected to require that more significance be placed on the successful operation of the secondary air jets. This will require a more sophisticated approach to the design of these jets.

The problems of operating an incinerator effectively are enormous when one realizes the tremendous variation in feed material that is handled from day to day. The variation in the feedstock quality of an incinerator is very much greater than that in a pulverized coal fired utility boiler, yet incinerator controls are barely existent compared to the sophisticated controls of modern utility boilers.

It is self-evident that the above design criteria are severely inadequate for present-day purposes and are critically deficient in meeting the challenge of tighter air pollution requirements. The increasing investment costs for suitable incinerators coupled with the challenges posed by more stringent pollution codes, the difficulty of finding skilled

labour, and the financial pressures on municipalities, bring out the basic need to improve the designs and to develop inexpensive and reliable methods of controlling them. These improvements will only be forthcoming as a result of extensive research on a laboratory scale and careful experimentation on full-scale units.

For this reason, work was carried out at the Sheffield MSW incinerator to study the performance of the plant. The main objective of this research project was to specify the incinerator design. The experimental data together with the FLUENT computational code were used to develop a physical and mathematical model of the incinerator. As a result of the test data and the mathematical modelling of the whole process, suggestions for design improvements for the Sheffield MSW incinerator were made which will substantially reduce emissions of pollutants and reduce the maintenance costs at the plant.

The following chapters present and discuss the mathematical model and the results obtained from various experimental measurements made at the Sheffield incinerator plant. Conclusions drawn from the study together with recommendations for future work are finally discussed in chapter 6.

Chapter 2

Experimental Programme and Procedure

2.1 Introduction

This chapter is concerned with the acquisition of the experimental data which was necessary for model input and actual characterisation of the incinerator. Plant performance figures are based upon an assumed ambient temperature in the plant of 15 °C (60 °F). The Incinerator - Boiler unit house ground floor datum 0.00m (0.00"), is located 53.50 m (175') above the Site Ordance Datum level.

Tests were all carried out on Incinerator - Boiler no. 1 (Bernard Rd, Sheffield) from September 1988 to July 1989. The following procedures describe the data collection and the points of collection of the various inputs and outputs around the plant.

2.2 Description of Sheffield municipal incinerator plant

The installation is a continuous refuse disposal plant (30 MW) of direct incineration type consisting of two-stepped-grate roll incinerator grates combined with two natural circulation bi-drum boilers. The primary purpose of the plant is the disposal of refuse collected locally (500 ton/day). The cross sectional view of the plant and the general

section of the process are shown in figures 2.1 and 2.2 respectively. Diagrammatic layout of the Sheffield district heating scheme and damper diagram are also presented in figures 2.3 and 2.4.

Refuse Handling:

Refuse collection vehicles received in the Tipping Area, enter tipping stalls of which six are provided. Each stall having an automatically controlled door to the main refuse bunker. The main fuel for the incinerators is mixed household refuse. There are occasions when collections are made of trade and industrial refuse and of other waste. The former type of refuse can contain unusually large amounts of wet or putrescible matter and the latter type largely paper and cardboard waste. At the head of the two feed conveyors, the refuse is fed to the incinerator feed chutes, a chute being provided for each unit. Each chute is flat-bottomed, the flat bottom forming the ram floor for a hydraulically operated ram charging the incinerator. The level of the ram floor is 8.38 m above the boiler house ground level datum.

The rate of movement of the charging ram feeding the incinerator grate is controlled by the incinerator operator. The section of each refuse chute leading into the furnace is fully water-cooled.

Operating Conditions:

The plant is designed to operate on a basis of continuous incineration of refuse with one incinerator - boiler unit working seven days each week and the other unit working up to five days each week.

Design Data-Boiler:

The Bi-drum waste heat boilers, each with the following characteristics are installed.

| | | |
|--|---|-------------|
| Evaporation at MCR | = | 32300 kg/hr |
| Design Pressure | = | 12.3 bars |
| Feed water temperature | = | 186 °C |
| Water content of boiler and furnace (NWL) | = | 32.58 ton |
| Water content of boiler and furnace (FWL) | = | 35.63 ton |

Heat Source:

Domestic, trade and industrial refuse provides the heat source. A typical analysis of Sheffield refuse is given below, each constituent item being given as a percentage weight of total. The analysis was carried out by Warren Spring Laboratory on 12th of March 1989 (weight sample = 341 kg). The general density of the refuse as collected is taken as 200 kg/m³. There will be variations in density of refuse as grabbed from the refuse pits because of compacting in the pits and inclusion at times of trade and industrial waste and of material collected from offices.

| | |
|--|--------------|
| Fine dust and small cinder (under $\frac{1}{2}$ ") | 11.98% |
| Cinder (12 mm to 45 mm) | - |
| Putrescible matter | 15.20 |
| Paper content | 30.20 |
| Rags content | 4.00 |
| Glass content | 7.80 |
| Tins | 6.45 |
| Plastics | 2.22 |
| Garden refuse | 17.80 |
| Miscellaenous combustible | 2.86 |
| Miscellaneous non-combustible | 1.49 |
| Total | <u>100.0</u> |

The gross calorific value of the crude refuse collected would be 11000 kJ/kg (10428

Btu/lb) although this value could fall to 7000 kJ/kg (6631 Btu/lb).

Bi-drum Boiler:

The bi-drum boiler is a naturally circulated two drum water tube unit. It has a vertically arranged water tube generating bank connecting an upper drum (the steam drum) with a lower drum (the water drum). These drums are positioned transversely with respect to the hot gas flow. The boiler furnace is water-cooled and is designed to absorb radiant heat from the combustion zone. Gases are cooled to a lower temperature before passage over the boiler bank convection surfaces. Steam is generated in the furnace wall tubes and in a major part of the boiler tube bank and flow is up these tubes. Recirculating water descends from the steam drum to the water drum through the final and cooler part of the boiler on the gas outlet side of the boiler.

Furnace:

This is fully water-cooled, of membrane construction comprising 64 mm OD tubes on 76 mm pitch. The side walls of the furnace terminate above grate level and the front wall above the refuse fuel chute. The rear wall of the furnace forms the rear arch and the exit screen which is two rows deep on a 152 mm square pitch. Walls are covered with silica carbide refractory to a height of 5.64 m above the mean stoker level at the centre of the radiation shaft.

The furnace has a width of 3.05 m and a depth of 4.57 m, with a mean height above grate at the centre of the shaft of 11.80 m. It has a heating surface of 172 m² and the volume of the radiation shaft from the nose of the arch is 136 m³. The mean height of the screen is 5.49 m. Furnace tubes are 63 mm O.D to B.S. 3059 Pt. 1.33., Furnace boxes are 244 mm by 16 mm to B.S. 3602 HFS 27.

Boiler bank:

The boiler bank is a single pass bi-drum bank comprising 36+2 elements wide on a pitch of 83 mm across the gas flow. The 1.37 m diameter steam drum and the 1.07 diameter water drum are located 7.62 m away from each other. The total commercial heating surface is 1013 m². Tubes are to BS 3059 Part 1.33, the boiler tubes being 50 mm and supply tubes 100 mm O.D.

The steam drum is of 22 mm thick plate with torospherical ends. There is a 0.40 m x 0.30 m man-hole door at each end. The water drum has a shell of 22 mm thick plate, the ends of the drum are torospherical and are of 19 mm plate. Boiler scantlings generally are to a design pressure of 12.06 bars.

Incinerator:

Two incinerator grate units are installed, one under each boiler. These are used singly or together, according to the amount of refuse available for disposal. The grates used are the "Dusseldorf" continuous incineration rotating roll type (figure 2.5). Each grate is designed to incinerate 10 ton/hr of crude refuse.

Grate roll units:

Six rolls are used to form each complete incinerator grate. The grate is installed at an angle of 30 degrees to the horizontal so that a natural step occurs between each roll. As refuse is carried through the furnace by rotation of the individual grate roll units, it falls from roll to roll down the successive natural steps, being agitated and turned over by the time that the end roll is reached. Each individual grate roll is 2.5 m wide and 2.4 m diameter and the total combustion grate area is 36 m². The grate roll itself consists of a hollow shaft with a basket-type support carrying segmented type grate bars.

Draught system fans:

The induced air fan is a type S.T. BAB 141 fan with a backward aerofoil bladed runner and a duty of 2393 m³/min in conditions of 6.75 mbar and 316 °C. It is driven by a 40.3 KW, 740 RPM motor.

Combustion primary air is admitted to the undergrate areas by six ports, one for each grate roll. Secondary air is taken into the furnace by ports located over the top and the bottom areas of the incinerator grate.

The F.D. fan is a type D122B fan with a backward aerofoil bladed runner and a duty of 1025 m³/min in conditions of 20 mbar and 15 °C, it is driven by a 44 kW, 970 RPM motor.

The secondary air fan is a type SI BCB 42 fan with a backward curved bladed runner and a duty of 281.8 m³/min in conditions of 76.6 mbar and 15 °C, it is driven by a 43.6 kW, 2940 RPM motor.

Steam Utilisation:**a) Heat exchangers:**

One heat exchanger is installed for the provision of hot water to the district heating services. It is a shell and tube exchanger, 0.61 m diameter by 6.40 m long of “U-tube” type. The exchanger has one pass on the shell side with two passes on the tube side. The exchanger is capable of heating 28,150 kg of water from 71 °C to 126 °C using 32500 kg of steam per hour at 8.6-10.4 bar. The heat exchanged is 24,074,100 kJ/hr. The exchanger has design pressures of 12.06 bar on the shell side and 15.86 bar on the tube side, with design temperatures of 192 °C on both shell side and the tube side. Two other heat exchangers are installed for the purpose of providing hot water services for the works, offices and houses in the area. The exchangers are generally similar in construction and in the fittings supplied, to the exchanger used for the district heating scheme.

b) Dump Condensers:

Steam which is in excess of the requirements of the heat exchangers is passed to one or both of two dump condensers. These are type IFPGS air-cooled condensers and are cooled by means of variable pitch eight bladed fans, each condenser being in two units and each unit having its own fan. Salient features of the condensers are: each is 6172 mm long by 4014 mm wide and capable of handling 32,365 kg of steam per hour, condensing it to water under all operating conditions. Tube bundles are of 25 mm O.D. by 13 BWG wall steel tubes with aluminium fins. These tubes are arranged horizontally between fabricated plug type headers.

2.3 Incinerator Testing Program:

2.3.1 Physical and Chemical Analysis of Sheffield Refuse

Characterization of refuse by physical and chemical analysis and by determination of the calorific value is fundamental to the engineering design of the incinerator systems. Chemical analysis and Btu values of refuse and residue supplement furnace calorimetry data in arriving at valid mass and energy balances of incinerator tests. In order to obtain this information, procedures for the sampling and analysis of refuse materials are required. Although there are well established sampling procedures for materials such as mineral ores [13], [14] and [15], the widely differing physical characteristics of the components, the non ideal materials handling properties (non free flowing) and wide ranging particle size distributions of refuse materials make direct use of these techniques inappropriate. Thus for the refuse processing industry, sampling and analytical procedures have been adapted or modified in order to obtain the required information.

Other workers, particularly in Europe, have also been developing refuse sorting processes and have followed similar approaches [16] , [17] to sampling and analysis. Standards have been defined by some countries, for example the American Society for the Testing of Materials (ASTM) in the USA. However the number of possible procedures, particularly

for chemical analysis, can make it difficult to compare the results unless procedures used and the basis on which the results are reported are stated clearly and unambiguously. The purpose of this section is to report on five studies of Sheffield refuse and incinerator residue, all carried out over a period of nine months. The chemical analysis of Sheffield refuse was conducted by the Warren Spring Laboratory. The physical and chemical analysis results obtained, are on an "as received" basis unless otherwise stated. Bulk density is reported in kg/m^3 and moisture content is calculated and reported on a wet weight basis.

Chemical Composition Analysis of Sheffield Refuse

A complete chemical composition analysis of Sheffield waste was carried out by Warren Spring Laboratory. The samples were taken directly from the refuse collection vehicles prior to tipping into the reception bunker. Each time between 13 to 15 separate vehicles were sampled (approximately 30 kg per sample, equivalent to 2 to 3 bins full) to give a feed sample of about 400 kg. Portions of each sample were shovelled into large plastic bags and then sent to Warren Spring Laboratory for analysis.

Tests showed a variation range of refuse analysis and composition. The variation of moisture content of the refuse from 16 to 42 percent was experienced when no rain fell. During a rainy period, the variation in refuse moisture content was in the range between 23 to 60 percent. The variation in refuse noncombustibles and metals was estimated to vary between 18 to 34 percent of total refuse. Paper ranged between 27 to 53 percent of refuse. The garbage (food waste) fraction ranged from 8 to 19 percent, two thirds of which was moisture.

The refuse analysis which probably represents an average, was as follows:

Typical Analysis by Weight and
Volume of a Domestic Refuse
Sample in the City of Sheffield

| | Weight% | Volume% |
|---------------------------|-------------|-------------|
| Screening | 12.31 | 4.30 |
| Vegetable and Putrescible | 35.46 | 25.85 |
| Paper | 31.12 | 38.91 |
| Metals | 5.34 | 8.65 |
| Textiles | 1.70 | 3.41 |
| Glass | 9.31 | 6.44 |
| Plastics | 2.97 | 10.43 |
| Unclassified | 1.79 | 2.01 |
| | <u>100%</u> | <u>100%</u> |

Proximate Analysis (as fired):

| | |
|-----------------|-------|
| Moisture | 36.0% |
| Volatile matter | 32.0% |
| Fixed carbon | 8.2% |
| Ash | 23.8% |

Ultimate Analysis (as fired)

| | |
|----------|-------|
| Moisture | 36.0% |
| Carbon | 20.8% |
| Hydrogen | 2.4% |
| Sulphur | 0.3% |
| Chlorine | 0.2% |
| Nitrogen | 0.4% |
| Oxygen | 17.5% |
| Ash | 23.8% |

Estimated Calorific Value of Domestic
Refuse Sample in the City of Sheffield

| | Vol.% | Btu/lb | kJ/kg |
|---------------------------|-------------|----------------|----------------|
| Screening below 2 cm | 4.30 | 307.78 | 717.13 |
| Vegetable and Putrescible | 25.85 | 871.88 | 2031.48 |
| Paper | 38.91 | 1900.62 | 4428.44 |
| Metal | 8.65 | - | - |
| Textiles | 3.41 | 113.78 | 265.11 |
| Glass | 6.44 | - | - |
| Plastics | 10.43 | 486.49 | 1133.52 |
| Unclassified | 2.01 | 139.93 | 326.04 |
| | <u>100%</u> | | |
| Gross Calorific Value | | <u>3820.48</u> | <u>8901.72</u> |
| Net Calorific Value | | 3285.20 | 7655.72 |

(Base December 1988)

The total yield of domestic waste in the City of Sheffield is in the order of 2500 tonnes/week.

Determination of Calorific Value of Sheffield Refuse

Method of determination: The calorific value of refuse was determined by two methods ; a) by sampling and laboratory analysis and b) by an overall heat balance of the plant.

Method a: Samples of refuse were taken from the pit at approximately 30-minute intervals during the test period. Portions of each sample were shovelled into large plastic bins and retained for ultimate analysis and calorific value determinations. These were carried out by Warren Spring Laboratory. The gross calorific values of the refuse determined by this method were 8769 kJ/kg (17th January 1989) and 6559 kJ/kg (21 February 1989) respectively.

Method b: Measurements made during the incinerator performance tests were used to evaluate an overall heat balance of the plant. The reference temperature selected for the heat balance was taken to be the average ambient temperature measured over the two days of the test (23rd and 24th January 1989) and it was assumed that the refuse in the bunker and the water supply from the main tank were at the same temperature.

It was thus only necessary to consider three sources of heat input to the incinerator, i.e.; the heat from the combustion of refuse, the latent heat of water vapour in the combustion air and the heat input from the forced draught and secondary air fan powers. The heat output of the plant is a summation of the following:

- Heat supplied to boiler feed water
- Sensible heat of dry flue gases
- Latent heat and sensible heat of water vapour in flue gases
- Sensible heat of clinker and dust
- Calorific heat of carbon in clinker and dust (assumed to have a calorific value of 14500 Btu/lb)
- Sensible heat of moisture in clinker and dust
- Radiation and convection losses (assumed to be one percent of the heat output of the plant)

Results of Determination: A summary of the overall heat balance of the plant is given below. The gross calorific value of the refuse determined by heat balance method was 8732 kJ/kg.

Calorific Value of Refuse Determination by Heat Balance:

1) Heat Output:

Heat to boiler feed water = 14347 kJ/sec.

Sensible heat of dry flue gases = 4743 kJ/sec.

Latent heat and sensible heat of water vapour in flue gases = 6641 kJ/sec.

Clinker and dust (excluding moisture):

- sensible heat = 59 kJ/sec.

- calorific heat of carbon = 923 kJ/sec.

Sensible heat of moisture in clinker and dust = 25 kJ/sec.

Radiation and convection losses (assumed 1% of output) = 267 kJ/sec.

Total heat output = 27005 kJ/sec.

2) Heat Input:

Latent heat of water vapour in combustion air = 237 kJ/sec.

Forced draught and secondary air fan power (estimated) = 50 kJ/sec.

Heat from combustion of refuse (by difference) = 26718 kJ/sec.

Total heat input = 27005 kJ/sec.

Incineration rate = 3.45 kJ/sec.

Gross calorific value of refuse = 8732 kJ/kg.

We consider the heat balance method to provide the most accurate determination of the calorific value. The differences between the two values obtained using method (a) and between those values and the heat balance value evidently occur because of the difficulty in obtaining representative samples of the refuse.

Bulk Density Tests

A series of 8 samples runs were performed in order to determine the density of Sheffield refuse. For density measurements the settled volume technique was used as it was considered that this gave more reproducible results, even though the values determined were up to 15% higher than those measured when the contents were not settled [18]. During all tests the refuse was devoid of oversized wastes. Bulk density of refuse was determined by filling a container of known volume (1 m^3) with the fresh refuse. After filling the container, it was dropped 3 times from a height of about 100 mm and then the resulting space was topped up with additional refuse. The weight of refuse was then determined. The samples were taken directly from the collecting vehicles.

The first density test was conducted on Friday, November 18, 1988. There had been no rain or snow during the previous several days. The residential sources were in the heating season which would cause a low moisture content of waste paper. No grass or other yard debris was presented. The next 3 tests were carried out in December 88, January 89 and February 89. The fourth density test was conducted on Monday April 11, 1989 following a humid, cool period during which no rain fell. The refuse was collected from residences the same morning. Grass and leaves from lawn care were present. The refuse was so damp that difficulty was experienced in maintaining the fires on the travelling grate stoker.

During incineration of the November 18 refuse, the moisture content of the flue gas was measured. It indicated a refuse moisture content of 24 per cent. The moisture content of the April 11 refuse was probably close to 47 percent as shown by a test on sampled refuse. Tests were also carried out to determine the bulk density of the residues. The method used was the same as the one described above. The results obtained from these tests are shown below:

Bulk Density Determination

| Date | Refuse Density (kg/m ³) | Residue Density (kg/m ³) |
|-------------|-------------------------------------|--------------------------------------|
| November 88 | 137.0 | 1050.1 |
| December 88 | 176.1 | 998.1 |
| January 89 | 180.2 | 890.5 |
| February 89 | 230.7 | 1140.6 |
| March 89 | 254.6 | 986.8 |
| April 89 | 310.1 | 953.5 |
| May 89 | 246.1 | 896.9 |
| June 89 | 180.6 | 932.3 |

Determination of Moisture Content of Sheffield Refuse

There are several ways in which moisture can influence the combustion intensity in an incinerator. The most obvious is by straight dilution. The reduction in incinerator capacity when burning waste of high moisture is directly due to the reduced reactivity of the reactants (mostly smoke, volatiles and similar gaseous combustibles). The presence of evaporated moisture increases the gas volume so that the concentrations of the fuel (smoke, volatiles and gaseous combustibles) and the oxygen is reduced. At the same time the increased volume of gas decreases the residence time in the combustion chamber so that, either combustion is completed outside the chamber or else the residence time is increased again by reducing the air input which in turn must be balanced by reducing the overall combustion rate. The presence of moisture also provides an extra thermal load so that the flame temperature will drop.

Moisture content of Sheffield refuse was determined by drying samples to constant weight at a temperature of 100 - 105 °C. The following equation was then used to calculate the moisture content percentage, wet weight basis [19]:

$$i.e. \text{ Moisture content \%} = 100 \times \frac{(\text{Wet Wt} - \text{Dry Wt})}{\text{Wet Wt}}$$

Wet samples were investigated on separate days at the plant. Samples were protected from moisture loss and weighed using a platform scale. They were then transferred to the drying oven and were dried to constant weight at about 105 °C. In most of the tests, the constant weight was achieved in 24 hours or less for oven temperatures in the range 100 to 105 °C. This suggests that the time for drying is less dependent on the initial moisture content and more likely to be influenced by surface area, material packing characteristics and the depth of material on the sample tray. It was observed that drying time for large samples was reduced if the sample was spread thinly over 2 or 3 trays rather than being piled up on a single tray. In addition, samples with a higher bulk density, particularly those containing a high proportion of fines, tended to take longer to dry.

The variation of moisture content of Sheffield refuse from 16 to 42 percent was experienced when no rain fell. The refuse moisture during a raining period was observed to increase up to 60 percent.

Clinker and Precipitator Hopper Dust Analysis

In order to fulfil the aim of investigating the combustion efficiency under the various operating conditions, it was necessary to measure the carbon loss from the system. Two sources of loss were considered as carbon monoxide in the flue gases, and as the carbon lost with the carryover and flyash. The gross samples of the burn out clinker were collected during three days of testing. To obtain the samples, the disposal skip was shunted to one side and a skip used solely for the collection of the clinker sample, was placed in position at the conveyor belt discharge. On obtaining the desired amount of sample the disposal skip was shunted back into position. Each sample was picked clean of metals as far as was practicable and the metals set to one side for weighing. On completion of each day of testing the gross samples were crushed. It was then spread and samples taken for analysis. The gross samples of dust from the precipitator hopper discharge were collected during the three days of testing in increments of about 10 kg taken at hourly intervals. The samples were ground down and then analysed for moisture,

carbon, hydrogen and putrescible content determination.

The weighted average carbon content of the clinker and precipitator hopper dust was 3.4 % on a dry and metal free basis (2.9% dry basis). The weighted average putrescible content of the clinker and precipitator hopper dust was 0.095 % on a dry and metal free basis (0.09 % dry basis).

The average value was then taken to be representative of the whole. The method of collection was probably the largest source of error. The error introduced by the sampling and analysis was taken to be small. The results of the second day of the testing program were as follows:

Residue Analysis

| | Average% |
|-------------------------------------|----------|
| Moisture | 14.7% |
| Unburnt carbon (dry and metal free) | 6.6% |
| Putrescible content | 0.099% |

Precipitator Hopper Dust Analysis

| | Average% |
|-------------------------------------|----------|
| Moisture | 16.4% |
| Unburnt carbon (dry and metal free) | 13.9% |
| Putrescible content | 0.247% |

The results obtained for the C/H ratio of the fly ash and the incinerator residues are shown below:

Carbon - Hydrogen Analysis

Fly ash (Dry Basis)

| Run no. | C/H Ratio | Carbon % | Hydrogen % |
|---------|-----------|----------|------------|
| 1 | 28.7 | 4.5 | 0.16 |
| 2 | 46.1 | 5.9 | 0.12 |
| 3 | 40.3 | 5.3 | 0.13 |
| 4 | 37.1 | 5.0 | 0.16 |
| 5 | 24.8 | 5.1 | 0.40 |

Carbon - Hydrogen Analysis

Incinerator Residue (Dry Basis)

| Run no. | C/H Ratio | Carbon % | Hydrogen % |
|---------|-----------|----------|------------|
| 1 | 13.3 | 4.4 | 0.33 |
| 2 | 16.4 | 3.5 | 0.21 |
| 3 | 9.5 | 2.4 | 0.26 |
| 4 | 16.9 | 4.9 | 0.29 |
| 5 | 13.8 | 4.1 | 0.27 |

Grate Siftings Tests

During these tests, the refuse burnt at the plant was primarily from households, with minor commercial source wastes. The refuse appeared to be normal for a rain-free period. The sifting test was conducted at the plant on October 27 and 28, 1988, for nearly 6 hours on both units (Boiler nos. 1 and 2). The clearances around the grate totalled 1.93 percent of the section area. The siftings that passed through the clearances of the grate dropped into the hopper and were emptied. The grate openings (at the surface of rollers) consisted of gaps, $\frac{3}{8}$ inch wide, with a total area of 7% of the sections. The siftings from these sections were also dropped into the hopper and were collected from there. The grate sifting samples were analysed. The combined siftings had a low (4.19 percent) content of combustible matter. At a measured bulk density of 210 kg/m³, the

siftings volume was about 0.10 m³ per refuse ton. Large amount of glass, ceramics and stones were observed in the grate sifting samples. The metal fraction included nails, screws, bottle caps, tin can covers, etc. The density of the siftings was measured and it was about 822 kg/m³. The samples of siftings were all collected when the furnace was shut down. Siftings weight was estimated at 399.5 kg per 3500 tons of raw refuse.

2.3.2 Temperature Measurements

A series of tests was carried out to establish an approximate temperature profile throughout the incinerator. The test temperature logs showed operation with the temperature control set point at 900 °C at the boiler inlet. Simultaneous temperature readings, giving the actual temperature profile of the furnace enclosure, radiation shaft and the refuse bed were obtained. The thermocouple used was of Ni-Cr-Al type covered with stainless steel 310 material. Temperature readings were recorded using the BASIC program (see appendix 6 for printout of the program) run on a CBM computer (plate no. 2). Due to heat transfer considerations the thermocouple bead temperature is not equal to the true gas temperature as discussed in [20] and [21]. A heat balance in fact is necessary to relate the two. Appendix 2 outlines the method [22] by which the flame temperature was derived from thermocouple bead temperature.

Furnace Temperature Measurements:

To record the temperature fluctuations in the hottest zone inside the furnace (position TC10, see fig.2.6), it was decided to use a Ni-Cr-Al thermocouple and try to get the thermocouple as close to the hot zone as possible. This of course meant potential errors due to the effects of radiation but no practical alternative was available. It was decided to use the access port on the back corner approximately 7m away from the hottest zone. Whilst this was thought to be the best choice, it still presented many problems. One of which was that the wall of the radiation shaft sloped at an angle of 60 ° below the access port, thus preventing the simple introduction of a long length of mineral insulated

thermocouple. The only solution seemed to be to use a water cooled probe long enough to project beyond the slope, and thereby enable the thermocouple to hang vertically down into the hot zone from the end of the probe (plate nos. 3 & 4). The access door made of cast iron and lined with refractory material, was removed and brought to the Physics Department workshop. A hole 50 mm diameter at an angle of 45 ° was drilled on it and a 1¼” BSP socket was welded in the hole. This enabled a 20 cm long tube with a bore of 1.03” to be threaded into the socket which provided a guide for the water cooled probe and the addition of grubscrews enabled it to be locked in position (plate no. 5). The design of the water cooled probe was fairly straight forward; it consisted of 3 concentric 316 stainless steel tubes with spirals of copper wire between the tubes to ensure that the water cooled to the end of the probe (figure 2.7). A heat and mass balance calculation was carried out to estimate the amount of water required to cool the probe. Due to restricted space behind the access door, the probe was made 3.5 m long. Insertion and removal was a 4 man operation including the use of a 3 m support to hold the weight of the probe as it emerges. The water supply system for the probe consisted of a Lowerna P.M.70 pump, a tank (1m³) installed with two cold water supplies, one from the mains (45 m below the access port) and one from a header tank on the roof of the plant which was used as a back up (plate no. 6).

Temperatures were recorded in this high temperature zone for each of the operating conditions examined during this study. The maximum temperature recorded was 1293 °C (see figure 2.8). Each time the Ni-Cr-Al thermocouple was quite effective until the flame temperature became too intense, thereby causing the thermocouple to melt. For this reason, we were only able to record the temperatures for about 3 minutes in this region. The above results show that temperatures in this region are well above 1300 °C.

The Ni-Cr-Al thermocouple and the watercooled probe were also used to record the flame temperature fluctuations above the burning refuse inside the furnace. Readings were taken along the bed cross section on top of roller nos 1, 2, 3 and 4 using the top, middle and bottom ports located on the furnace wall (plate nos 7 & 8). Gas temperature

fluctuations were recorded at 6 locations approximately 120 cm above the grate surface. These locations were spaced approximately 50 cm, beginning from a point 25 cm away from the inner surface of the refractory wall (figure 2.6). The maximum temperature recorded was 1174 °C (on top of roller 2). It was not possible to record temperatures above 1174 °C since a Ni-Cr-Al thermocouple was used for measurements. The results showed an increase from the furnace wall to the centre of the chamber and then a decrease. This indicates that most of the refuse is burnt in the middle of the grate mainly on top of rollers 2 and 3. Visual inspection verified this. Typical temperature variation vs time at position 3 for rollers 1, 2 and 3 are presented in figures 2.10, 2.11 and 2.12 respectively. The temperature near to the furnace wall deviated from the centre line temperature by about 35-40%. Temperatures recorded near to the furnace wall ranged from 450 °C up to 600 °C. Temperatures recorded at the centre line were generally above 1300 °C. Temperature variation across the refuse bed on top of rollers 1, 2, 3 and 4 are shown in figures 2.14, 2.15, 2.16 and 2.17 respectively.

Readings taken on top of roller 4 were lower than those recorded for rollers 2 and 3. The highest temperature recorded here was about 980 °C. The temperature at the wall deviated from the centre line temperature by about 25-30% at an axial location 120 cm above the grate surface (figure 2.13).

The fluctuations in temperatures recorded, were in some cases as high as $\pm 30\%$. All fluctuations were averaged for calculation purposes.

Radiation Shaft Temperature Measurements

A water cooled probe fitted with a Ni-Cr-Al thermocouple was used to establish an approximate temperature profile in the shaft. Temperature measurements were taken at 10 locations (positions 1 to 10, figure 2.6) for each of the operating conditions examined during this study. These locations were spaced approximately every 40 cm, beginning from a point approximately 15 cm vertically down from the end of the probe. The thermocouple TC1 was used as the controlling point (900 °C) in our testing program

(figure 2.18). The examination of the temperatures recorded by thermocouples TC2, TC3 and TC4 showed a maximum temperature differential of 200 °C from the temperatures recorded by the controlling thermocouple TC1. Temperatures at these points varied between 650 °C up to 1000 °C (figures 2.19, 2.20 and 2.21). Occasionally sudden drops in temperature were recorded by thermocouples TC5 and TC6. This was possibly due to the passage of unused secondary air in this region or burning of extremely wet refuse (figures 2.22 and 2.23). Temperatures recorded by thermocouples TC7, TC8 and TC9 followed closely the readings taken by thermocouple TC10 with a maximum deviation of approximately 200 °C in a few isolated instances. Temperatures recorded at these points were in the range between 900 °C up to 1300 °C (figures 2.24, 2.25 and 2.26).

Refuse Bed Temperature Measurements:

While instrumentation was available to measure the temperature of the flue gases in the combustion zone, the temperature of the refuse bed was more difficult to determine. The bed temperature was measured at three different locations across the refuse bed on top of roller nos 1, 2 and 3. Measurements were made at roughly one quarter, one half and three quarter of the bed depth inside the bed above the grate (figure 2.9). These measurements were made using a specially constructed probe with Ni-Cr-Al thermocouple. Setting up the requisite procedure for monitoring and collecting all necessary data about the burning refuse bed was a monumental task which unfortunately left some holes in the data. In an attempt to see if, in fact there was a relationship between furnace temperature and the bed temperature, attempts were made to monitor the bed temperature with a specially built probe (figure 2.27). This probe was quite effective until the flame temperature became too intense, thereby causing the probe to melt. Alternatives such as remote transmitters and heat sensitive dyes were investigated. All of these techniques were rejected for numerous reasons of unreliability. An optical pyrometer was used to estimate the surface bed temperature. It was noted that the surface flame temperatures were usually about 300-400 °C greater than the combustion

chamber temperature (In this comparison, furnace temperatures were averaged over the length of the test). It also should be emphasized that these measurements represent a weighted mean of the temperature of the gas flowing over the thermocouple and the temperatures of the surfaces with which the thermocouple is in radiative exchange.

The accuracy of this method is unknown but the results obtained were used for modelling of the refuse bed and estimation of the rate of heat release on top of each roller. Fluctuations in the temperature of bed were as high as $\pm 15\%$. The temperatures recorded were averaged for calculation purposes. It was realised that a more comprehensive study of the bed temperatures was desirable but it was not thought to be practicable. A summary of the results obtained at different points inside the refuse bed is shown below:

Internal Refuse Bed Temperature (°C)

| Roller no. | Bed Depth Point 1 | | | Bed Depth Point 2 | | | Bed Depth Point 3 | | |
|------------|----------------------|---------------|---------------|----------------------|---------------|---------------|----------------------|---------------|---------------|
| | $\frac{1}{4}$ | $\frac{1}{2}$ | $\frac{3}{4}$ | $\frac{1}{4}$ | $\frac{1}{2}$ | $\frac{3}{4}$ | $\frac{1}{4}$ | $\frac{1}{2}$ | $\frac{3}{4}$ |
| 1 | 1010 | 980 | 1043 | 990 | 1013 | 978 | 1254 | 1135 | 810 |
| | 890 | 980 | 1043 | 1005 | 998 | 973 | 973 | 899 | 910 |
| | 965 | 1105 | 995 | 875 | 965 | 989 | 897 | 934 | 1011 |
| 2 | 980 | 898 | 1120 | 1010 | 980 | 990 | 980 | 1230 | 1100 |
| 3 | 780 | 958 | 980 | 810 | 840 | 960 | 927 | 973 | 897 |
| | 870 | 990 | 1120 | 870 | 855 | 1010 | 945 | 1014 | 997 |
| | 993 | 973 | 989 | 830 | 825 | 880 | 915 | 953 | 1011 |

Flue Gas Temperature Measurements:

The flue gas temperature was recorded at eight points in the precipitator inlet duct and precipitator outlet duct using a Ni-Cr-Al thermocouple. Readings were taken at

15-minute intervals of all other test and panel readings. Flue gas temperatures at the precipitator inlet ranged between 287 °C to 330 °C (figure 2.28). The flue gas temperature at the precipitator inlet was at all times during the tests above the specified minimum value of 250 °C. Flue gas temperatures at the precipitator outlet varied between 270 °C to 310 °C which again was quite high compared to the specified minimum value of 210 °C (figure 2.29).

Miscellaneous Temperature Measurements:

In addition to the above temperature measurements, several other temperature measurements were made in order to identify the temperature profile at different locations around the plant. These are:

- 1) Boiler water flow and return temperatures.
- 2) F.D and S.A fan inlet temperatures.
- 3) Ash trough temperature.
- 4) Boiler gas exit temperature.

The wet and dry bulb temperatures in the vicinity of the pits were measured by means of mercury in the glass thermometers at hourly intervals. For all the above measurements a Ni-Cr-Al thermocouple was used. Readings were recorded using a BASIC program run on a CBM computer. The results obtained are as follows:

- Average air temperature at the F.D fan intake ranged between 13 °C to 24 °C.
- Average ash trough temperatures ranged between 69 °C to 87 °C.
- Boiler gas exit temperatures, ranged from 510 °C to 705 °C.
- Boiler water feed temperature, varied between 150 °C to 170 °C (figure 2.30).

2.3.3 Pressure Measurements

The main object of the cold test work (pressure measurements) was to establish the primary and secondary air distribution through the grate and slots on the furnace roof

and hence through the live fire bed. The results of this test work suggested that about 80-90% of the total combustion air entered the furnace through the grate and most of the time no secondary air was used for combustion purposes. From time to time, the secondary air was supplied through a series of slots (4cm width by 10 cm long) located above the top and the bottom areas of the incinerator grate, discharging into the furnace enclosure (figure 2.6). The amount of secondary air used for the cooling purposes varied between 100-125 m³/min (50-60% secondary front and 30-40% secondary rear). In the original design of the plant, it was assumed that the long, luminous flame rising from the refuse bed would mix with the secondary combustion air introduced through the roof arch of the furnace, and that the combustion would be essentially completed in the chamber with only minor parts of the combustion processes continuing in the radiation shaft [23]. In actual operation our tests showed, however, that this condition was seldom reached. When the refuse quality was such that a long, luminous flame could be obtained, the introduction of the secondary air through the roof arch resulted, in some cases, in localized high temperatures, sometimes in excess of 1000 °C. Because the secondary air was distributed in this manner (slots), the turbulence required for complete mixing and good combustion would probably not be achieved due to the absence of high velocity passages or directional baffles. The cooling of the roof arch and the upper portion of the walls by the secondary air, while the lower portions of the walls were exposed to flame temperatures, resulted in high refractory maintenance costs because of partial slagging and thermal gradients (see plate nos. 9 & 10). During the experimental work, boiler no. 1 was shut down twice for refractory maintenance work, once in January 89 and a second time in May 89.

Test work was also carried out to estimate the undergrate air distribution through the grate. The amount of primary air passing through each control damper was estimated using figure 2.32. The results obtained were as follows:

Undergrate Air Distribution

| Roller no. | % air distribution |
|------------|--------------------|
| 1 | 14 - 32 |
| 2 | 28 - 40 |
| 3 | 25 - 35 |
| 4 | 11 - 18 |
| 5 | 4 - 8 |
| 6 | 1 - 3 |

On average, about 75% of the total undergrate air passes through the front half of the grate (roller nos. 1, 2 and 3) and the remainder through the rear of the grate (roller nos. 4, 5 and 6), i.e. through the 2 mm gaps at the roller surface. It was observed that most of the time, these gaps were blocked by dirt and the rollers were not in a good condition which resulted in poor air distribution and low combustion efficiency.

Variation of the amount of air supplied for 18 tests (in order to determine the effect of operating variables such as air on the incinerator performance) could not be achieved as originally planned. There is too much potential for leakage (e.g. through access ports, charging chute and inspection windows) which results in unwanted air being drawn into the furnace. The induced draft fan was the major factor in being able to alter the amount and ratio of the combustion air. Flow irregularities were observed inside the furnace (visual inspection through the access port in the control room) when attempts were made to change the air flow rate and total air applied. The flow patterns which existed when no attempts were made to alter the percentage of air applied were destroyed when the attempts were made. It was noted that air leakage into the furnace occurred continuously. An estimate of the amount was made as the difference between the sum of all forced draught and the induced draught. Estimated performance curves for F.D. and I.D. fans [24] are shown in figures 2.33 and 2.34 respectively. By using these curves, the

amount of the air leakage into the furnace was estimated to be about 3.33 to 5.83 m³/sec. The forced draught fan is rated at 50,000 CFM (23.33 m³/sec), actual measurements were much less than this value and were between 23,000 up to 35,000 CFM (10.73 to 16.33 m³/sec).

The S.A. fan is rated at 9950 CFM (4.64 m³/sec), the actual measurements were again less than this value and were between 3000 to 5500 CFM (1.4 to 2.5 m³/sec), see figure 2.35.

Pressure measurements were carried out at 27 different points around the plant:

a) Measurements were made of ΔP across the control dampers fitted in the side of the hoppers in order to determine the amount of undergrate air passing through the dampers and entering the furnace through each grate roll.

This was done by tapping in (before and after the dampers) and reducing to a 6 mm OD tube which was connected by a flexible tube to a manometer. The results were used to get the flow characteristic curves for each damper (rollers 1 to 6). Pressure traverses were carried out using a pitot - static tube to estimate: 1) the average undergrate air pressures and 2) ΔP across the refuse bed on top of each roller. (At the Sheffield plant, the system is designed on an U/G air pressure of 40 mm WG). The results obtained were as follows:

Average U/G Air Pressures (mmWg)

Roller no. 1, P varied between 18 to 35 mmWg

Roller no. 2, P varied between 25 to 40 mmWg

Roller no. 3, P varied between 14 to 29 mmWg

Roller no. 4, P varied between 8 to 15 mmWg

Roller no. 5, P varied between 4 to 10 mmWg

Roller no. 6, P varied between -4 to 1 mmWg

ΔP across the bed was measured in January 89. The data obtained are as follows:

Roller 1 (From L.H.S to R.H.S) ΔP across the bed varied between 28 mmWG to 44 mmWG.

Roller 2 (From L.H.S to R.H.S) ΔP across the bed varied between 44 mmWG to 37 mmWG.

Roller 3 (From L.H.S to R.H.S) ΔP across the bed varied between 37 mmWG to 20 mmWG.

Roller 4 (From L.H.S to R.H.S) ΔP across the bed varied between 20 mmWG to 10 mmWG.

Roller 5 (From L.H.S to R.H.S) ΔP across the bed varied between 10 mmWG to -1 mmWG.

Roller 6 (From L.H.S to R.H.S) ΔP across the bed varied between 5 mmWG to -10 mmWG.

The same test was done in May 89 with relatively dry refuse and the results obtained are as follows:

Roller no. 1 = 13 to 15 mmWG.

Roller no. 2 = 12 to 17 mmWG.

Roller no. 3 = 10 down to 1 mmWG.

Roller no. 4 = 4 down to 1 mmWG.

Roller no. 5 = 2 down to -1 mmWG.

Roller no. 6 = - .

b) Draft measurements - Total undergrate air pressure, total secondary air pressure, furnace suction, boiler exit suction and the precipitator exit suction were all measured and recorded using the plant instruments, readings being taken at 30 minute intervals.

c) Flue gas velocities and hence the gas flow rates in each duct (at the inlet to and the outlet from the precipitator) were measured by a pitot tube in conjunction with an inclined water manometer. Pitot traverses of the inlet and outlet ducts were carried out

at the commencement and completion of the test period, measurements also being made at each position immediately prior to gas sampling. Velocities measured at the boiler exit varied between 1.8 to 2.7 m/sec.

d) To estimate the F.D fan and S.A. fan output, pressure measurements were made of the inlet to and the outlet from the fans. This was done by tapping in and reducing to a 6 mm OD tube which was connected by flexible tubing to a manometer. Forced air enters a common duct from which two branches evolve. Each branch, in itself, divides into 6 branches. Pitot tubes were used in the ducts at each one of the junction points to measure the amount of air applied. The same tests were repeated with the S.A. fan and an estimation of the amount of secondary air entering the furnace for different operating conditions was obtained.

2.3.4 Gas Sampling Measurements

The emissions from municipal waste incineration processes can be divided into three categories:

- Combustible gases or vapours,
- Particulates consisting of ash plus unburned carbon and metallic fumes or oxides,
- Acid gases.

Emissions of combustible gases and vapours and the carbon content of emitted particulates are functions of the combustion process in the furnace, which is in turn a function of temperature and combustion chamber design. Given a reasonable design and sufficient mixing above the refuse bed, then complete reaction of pyrolysis products should be achieved.

Emissions of particulates are one of the most perceptible forms of pollution and considerable effort is expended in attempting to reduce them. The emission standards for the combustion of municipal refuse is covered by the Report of the Second Working Party on Grit and Dust Emission [25], which recommends 915.6 mg/m³ for an appliance rated less than 0.879 MW and 228.9 mg/m³ for appliances up to 14.7 MW (Table 2.1). There

are several emission control devices currently used on incinerator plants including wet scrubbers and electrostatic precipitators , the latter having guaranteed collection efficiencies of over 95 % [26]. The amount of the particulate emissions is clearly dependent on the ash content of the refuse [27] and with some of the higher ash fuels the particulate loading of the flue gases could cause problems.

Acid gas emissions particularly those of hydrogen chloride could be a further cause for concern, although there is scope for the reduction of emissions. The more familiar problems of the oxides of nitrogen and sulphur also associated with coal combustion, are generally found to be lower for waste combustion than for coal combustion [28]. These lower emission levels are associated with the lower nitrogen and sulphur contents of refuse compared to coal. However, it must be remembered that halving the potential heating value of a fuel (waste c.f. coal) is equivalent to multiplying the inherent nitrogen and sulphur by two for a constant thermal output.

A primary aim of our experimental program at Sheffield municipal waste incinerator was the measurement of the incinerator exit flue gas composition with respect particularly to the pollutants CO, NO and SO₂. The sampling and analysis of the flue gas was required for the following purposes:

- 1 - Checking and controlling the efficiency of combustion.
- 2 - Calculating heat balances.
- 3 - Detecting air or gas in-leakage.
- 4 - Determining compositions and hence calculating volumes of waste gases.
- 5 - Determining the effect of the gas on the other parts of the plant, e.g. corrosion or tube blockage.
- 6 - Determining toxic gases.

This section describes and presents the design, construction and testing of the gas sampling systems together with the analytical results obtained from the tests.

Problems Associated with Gas Sampling

Sampling of incinerator gases requires special consideration of several characteristics unique to this operation: the necessity to obtain the representative sampling of relatively large gas flows in a large duct cross-section, the presence of large low density particulates entrained in the gas stream and the necessity to sample gases at temperatures in the range of 500 °C to 700 °C. An analysis of the experience of a number of organizations active in sampling incinerator gases and a summary of the recommendations on the proper approach to the design of sampling equipment for incinerator gases, is contained in a series of papers; [29], [30] and [31]. These recommendations are as follows:

- The minimum size of sampling nozzles should be 3/4 in. (18 mm).
- Sampling nozzles in high temperature gases (i.e. above approximately 500 °C) should be of stainless steel.
- Sampling probes in high temperature conditions (i.e. above approximately 500 °C) should be water cooled to prevent combustion of entrained particulates after entry into the sampling nozzle.
- Sampling equipment should be designed to assure isokinetic conditions on an instantaneous basis, i.e. null type sampling.

Usually a number of problems are raised when a gas sampling probe is introduced into a two phase flow. Apart from the obvious fouling by droplet or particulate trajectories, the probe distorts the gaseous streamlines at the point in the flow where it is located. This distortion of the stream lines causes a perturbation of the concentration gradients of all species in the flow.

For a large scale system, i.e. an incinerator, a large water cooled sampling probe is normally used, the internal diameter is of the order of 1 mm and the external diameter of the order of say 6 mm. Adiabatic expansion is not usually employed and heat conduction is used to cool the sampled gases. The probe is usually cooled with water although heated water under pressure or steam are sometimes used in an endeavour to prevent the condensation of water vapour present in the sample when wet analyses are needed.

The thermal stresses which a metallic sampling probe experiences when immersed in a turbulent high temperature flow field are considerable, this constitutes an additional complexity which has to be taken into account when designing a water cooled probe. Although sufficient sample mass flow can be extracted, the water cooled probe has a considerable draw-back in that transition metals which are normally employed for probe construction, can provide ideal environments for surface chemical reactions. All chemical reactions within the probe being extremely undesirable. This surface reaction problem is most acute when sampling for NO_x species since it is known [32], [33] that under reducing environment conditions the chemical reduction of nitrogen oxides by carbon monoxide, hydrogen and other reducing agents occurs in the presence of a metallic surface. The result is that NO_x concentrations lower than the true values are measured by the analyser. In an effort to overcome this problem many investigators [32], [34] have constructed their probes from stainless steel since this material does not display as high a tendency as pure transition metals (e.g. Cu, Ni and Fe) to promote surface reactions. Stainless steel also possesses good mechanical strength and oxidizes only very slowly.

Another problem encountered when sampling probes are used concerns the rate at which the sample is withdrawn from the probe. As mentioned above a distortion of the streamlines upstream of the probe occurs and it is obvious that this distortion is a function of sampling rate. To minimize unwanted distortion, the mean velocity of the gases at the probe entrance must be equal to the mean velocity of the gases in this vicinity which would exist in the absence of the probe. The effect of sampling velocity upon measured gas composition has been examined by Lengelle and Verdier [35] who found a significant dependence.

Measurement of CO, CO₂ and O₂ concentrations in the stack gas

A water cooled stainless steel probe was designed and constructed for the purpose of measuring CO, CO₂ and O₂ concentrations in the stack gas. The overall length of the probe was 4 m. Measurements were made at the inlet to and the outlet from the

precipitator. Sampling was carried out for 10 minutes at each of 12 positions at both the inlet and the outlet (see figure 2.36), giving a nominal sampling time of 2 hours at both positions (tests were carried out each day over a period of 6 weeks). The probe consisted of three concentric stainless steel tubes which were attached to a stainless steel tip by means of silver soldering. The probe overall OD was 40 mm and the inner capillary through which the sample flowed, was 2 mm ID (figure 2.7). It was vital that the 3 tubes remained concentric so that the cooling water could flow easily along the narrow probe annuli. In order to ensure that the tip which experiences considerable thermal and mechanical stress, was adequately cooled and the sample efficiently quenched, the cooling water flowed through the inner most channel first before reaching the tip. No difficulty with any excessive sample condensation in the probe were encountered. A water tank (1m^3) connected to a small Stuart Turner pump was used as the water supply for this probe. Cooling water was supplied from the header tank on the plant roof. A detailed heat transfer analysis of the probe was not attempted as a design aid since such an analysis would be very complex mathematically due to the large range of temperatures and hence the thermal properties which are encountered throughout the probe. Instead an approximate heat transfer evaluation was made to estimate the necessary cooling water mass flow rate, and then relatively detailed calculations were performed to assess the efficiency of the resultant probe design in quenching chemical reactions occurring in the sample flow through the probe. A computer program nearly similar to the one presented in [22] was used for this purpose. Flexible polythene tubing was used to transfer cooling water to and from the probe and brazing was used in the cooling water manifold construction. The probe inner sample capillary was expanded to $\frac{3}{8}$ " OD stainless steel tubing in this manifold and connected to the $\frac{3}{8}$ " OD Teflon sample line by means of a swagelock $\frac{3}{8}$ " stainless steel fitting. Figure 2.37 illustrates the gas sampling line. As it shows, the system was operated in either of two modes; 1) normal sampling and 2) purging of the probe with air. The second mode of operation was selected at all times during which actual withdrawal of samples from the stack was not required. Two Grubb

Parsons SB2 infra red gas analysers (IRGA) were used for the purpose of continuously measuring CO and CO₂ concentrations in the sampled gases. As plate no. 6 shows, they were connected in series. This posed no real disadvantage from a response time point of view since steady state readings only were required. An O₂ paramagnetic analyser was used for oxygen measurements. A water manometer was connected to them so that sufficient flow to the analysers was assured if a pressure drop across them of 5 in.W.G., i.e. approximately 0.5 lit/min was registered. Both IRGA's and the O₂ paramagnetic analyser were connected to the channels of the Chessell miniature chart recorder after the output potentiometers on each analyser were first substituted with a lower range type which enabled sensitive adjustment of the output signal in the range 0 - 10 mV (see plate nos. 11, 12 and 13).

Nitrogen was employed as zero gas and a standard gas containing 10% CO₂, 10% CO and zero O₂ was used for the calibration purposes. Both IRGA's and the O₂ analyser were serviced before use and were left permanently switched on to assure steady state operation. Each time the zero/calibration of each instrument was checked before making any actual measurements. Provision was also made in the sampling line for the connection of another analyser, however, this take-off point was normally used whenever batch samples were required to be accumulated in the sample bottles for analysis by the gas chromatograph. This method of analysis was used for checking IRGA operation and for the estimation of H₂, CH₄ and N₂ levels.

Pitot-static pressure and flue gas temperature measurements were made at regular intervals across each duct (inlet to the precipitator and at the outlet from the precipitator) to enable the accurate determination of the mean flue gas temperatures and flowrates. These measurements were made using a pitot tube and inclined manometer, whilst the temperature measurements were made using a Ni-Cr-Al thermocouple.

The percent excess air was calculated using the stack gas analysis. These tests on the Sheffield incinerator showed an average excess air of 210 percent and a range from 70 to 380 percent. The excess air percentage was calculated from the stack gas analysis using

the following equation [36] :

$$\% \text{ Excess air} = \left(\frac{O_2 - CO/2}{0.264N_2 - (O_2 - CO/2)} \right) \times 100$$

where N_2 , O_2 and CO are volumetric percentages of the components in the stack flue gas determined by experiments (dry basis).

The CO_2 concentration ranged from 3.6 to 16.2 percent with an average of 6.1. Carbon monoxide content varied between 76 ppm up to 430 ppm with an average of 185 ppm. Figures 2.38 to 2.42 show the CO_2 , CO and O_2 concentration variation as a function of time at the precipitator inlet and outlet. It should be noted that all the gas sampling data was obtained under isokinetic sampling conditions and is expressed on a dry basis. The mean combustion efficiency of the incinerator plant was calculated using the following equation [37]:

$$\text{combustion efficiency} = ((CO_2 - CO)/CO_2) \times 100$$

From the stack gas analysis results, the C/H ratio of refuse burned at the time of gas sampling was also determined. The flue gas analyses for fuels containing carbon and net hydrogen are affected by the C/H ratio in accordance with the following equation [38] :

$$\frac{C}{H} = \frac{CO_2}{8.80 - 0.421(CO_2 + O_2)}$$

The above equation is derived from the molal relations and the oxygen content of air (20.9%). Sulphur and nitrogen in refuse cause only slight error in the use of the equation. Since the volume of SO_2 will be less than 0.1 percent that of CO_2 and the refuse nitrogen will be about 0.1 percent of the nitrogen in the stoichiometric air, nitrogen and sulphur in refuse may be neglected in considering the gas analysis. The CO_2 content of air (0.03 percent) is also usually neglected except in precision work.

From above, the C/H ratio calculated for the Sheffield incinerator ranged from 4.15 to 32.6, with an average of 11.8 based on the average gas analysis obtained at the plant. The reason for a low C/H ratio observed in some runs is not apparent.

The moisture content of the stack gases was determined by the condensate method. A weighted condensation trap followed by a magnesium perchlorate trap were used for

moisture determination. The change in weight of the condensation trap and the perchlorate absorbent together with the gas volume gave the flue gas moisture concentration (appendix 3). The moisture content of the stack gas varied between 5.7 to 17.8 % with an average of 13.5%.

Burning Rate Determination

The actual burning rate was calculated using the gas analysis and air mass flow rate (see appendix 4 for the method used for burning rate calculation). It represented only that part of the charge (refuse) which was burned to carbon dioxide and water. The theoretical burning rate was calculated using Essenhigh's model [39], [40]. The instantaneous values of the actual burning rate calculated from gas samples taken at regular intervals were compared with the theoretical values. The maximum burning rate was approximately 64 percent of the theoretical value. The average burning rate was 57 percent of the theoretical rate. These relations differed somewhat for various test conditions.

Burning rates calculated from gas analysis ranged between 26.1 to 46.9 kg/hr (128.5 to 230.9 kg/m² hr).

Measurement of NO - SO₂ concentrations in the stack gas

For the measurement of the NO and SO₂ concentrations in the stack gas (precipitator inlet) two specially made probes were used to take samples. The NO probe and SO₂ probe were set adjacent to each other and were passed through a blading plate into the duct and were traversed across the width of the duct (1m) by means of a lathe bed supporting both probes and also supporting a board on which the condenser and the glass vessels for taking SO₂ samples were mounted (see plate nos. 14 and 15). The NO probe was 1.7 m long and was a conventional water cooled probe similar to the CO/CO₂ probe as described before. In order to eliminate the possibility of NO_x surface cooled sample interactions, the actual line was constructed completely of $\frac{1}{8}$ in. OD Teflon tubing and Swagelok $\frac{1}{8}$ stainless steel fittings were used throughout to connect the various

components in the line. As shown in figure 2.37, the system was operated in either of two modes; a) Normal sampling, and b) Purging of the probe with air. The second mode of operation was selected at all times during which actual withdrawal of samples from the stack was not required and served two important purposes. Firstly it enabled the sampling line and the probe to be maintained free of any solid/liquid deposits, and secondly it was used to directly check for any probe - NO_x interference reactions. In the second mode of operation the water trap, filter and sample flow rotameter were bypassed and filtered air was pumped back through the probe.

During the sampling mode the sample was passed through a water trap in order to condense out any water vapour present in the sample. The sample then flowed through a filter to remove any small particles, before reaching a Gasmeter (0.1 - 2 lit/min) rotameter which had an integral regulator that was used to meter the sample flow. The pump used to transport the sample was of the reciprocating diaphragm type (Charles Austen M391) and was driven by 3 phase power. The upstream side of the pump was under vacuum and hence a pressure gauge, 0 - 760 mmHg Bourdon type, was used to monitor this pressure.

Three glass 3-way taps were also employed in the system to enable either of the two operating modes to be set. The lengths of all interconnecting Teflon tubing were minimised so that the overall residence time of the sample in the system was correspondingly minimised. Due to:

- low sample line residence times.
- inert materials used to construct the actual line.
- relatively low NO_2 concentrations anticipated in the sample.

the gaseous oxidation of NO to NO_2 in the sample line was assumed negligible. This check was later confirmed experimentally. Leakages into the sample line were found to be negligible. This was performed by passing a standard NO containing gas through the probe and determining the composition of the resulting gas which reached the NO_x analyser.

The analyser selected for NO measurement was of the continuous type and was the Thermo Electron model 10A modular type (see plate no. 16). It utilises the chemiluminescent chemical reaction between NO and O₃:



$$(\lambda \cong 0.6 - 3\mu)$$

Light emission occurs when electronically excited NO₂ molecules revert to their ground state. Instrument output is linear so that, in all cases, calibration is performed using a single standard gas (500 ppm). The range over which the analyser was used was zero up to 1000 ppm.

Sample gas was withdrawn continually through the analyser by means of a bypass pump. A rotameter in the analyser indicated the bypass flowrate and a set of capillaries plus two pressure regulators maintained the correct flowrates of O₃ and the sample to the reaction chamber, which was evacuated by a Welch 1399 vacuum pump. The zero reference gas used was air.

The instrument output response was monitored by means of a Chessel 301 miniature chart recorder. The operating conditions under which the NO_x analyser was run were:

- 1) O₂ pressure; 2 psi.
- 2) Reaction chamber vacuum; 8-12 mmHg.
- 3) Sample vacuum; 5 in.Hg.
- 4) Sample flow; 0.23 - 0.93 lit/min, of which 5% reached the reaction chamber, the remainder being bypassed.

Whenever the instrument was required for actual data acquisition, it was turned on at least 24 hours beforehand to ensure that it had completely warmed up.

A heated silica sampling probe was used for taking SO₂ samples from the stack. The probe consisted of a stainless steel tube (1.7 m long), inside which was a silica tube (13 mm OD and 2 m long). This was wound with kanthal wire and insulated with refractory cement (figure 2.27). A current was passed through the kanthal wire in order that the

temperature of the flue gas remained above 260 °C [30]. Heating tape was wrapped around the glassware (connected to the probe) to keep the temperature above 260 °C. The concentration of SO₂ was measured by passing the gas samples through solutions of 0.5 Molar Sodium Hydroxide, contained in two sintered drechsel bottles in series. Flow rates were limited to about 0.8 l/min of dry flue gas (figure 2.44). The solutions were retained for sulphate analysis at the department laboratory. The NO concentration at the precipitator inlet was in the range between 125 ppm up to 380 ppm with an average of 250 ppm (figure 2.43). The SO₂ concentrations varied between 98 ppm up to 168 ppm with an average of 135 ppm.

A Land SO₂/NO_x electrochemical probe/analyser was used at the base of the chimney to take readings for NO and SO₂ concentrations in the flue gases (see plate nos. 17 and 18 and refer to the manufacturer handbook for a more detailed description of the probe). The NO concentrations at the precipitator outlet were in the range between 98 ppm up to 257 ppm with an average of 145 ppm. The SO₂ concentrations were in the range between 35 ppm to 67 ppm with an average of 57 ppm (figure 2.45). A summary of the gas analysis results at the precipitator inlet is shown in the following table;

| Stack Gas Emissions | | | | | | |
|---------------------|-----|-----------------|----------------|-----|-----------------|------------------|
| Precipitator Inlet | | | | | | |
| Run no. | CO | CO ₂ | O ₂ | NO | SO ₂ | H ₂ O |
| | ppm | % | % | ppm | ppm | % |
| 1 | 83 | 5.6 | 16.0 | 125 | 54 | 11.8 |
| 2 | 151 | 4.1 | 15.8 | 128 | 48 | 16.3 |
| 3 | 101 | 4.8 | 17.1 | 124 | 51 | 14.3 |
| 4 | 172 | 4.3 | 15.6 | 131 | 53 | 12.8 |
| 5 | 62 | 5.8 | 16.1 | 121 | 49 | 11.9 |
| 6 | 143 | 5.8 | 14.8 | 118 | 51 | 14.3 |
| 7 | 184 | 3.8 | 16.5 | 124 | 58 | 13.8 |

Flue Gas Analysis Above The Refuse Bed

A series of tests were made above the refuse bed approximately 120 cm above the grate surface in order to determine the effect of varying secondary and primary air rates on the oxygen distribution and burning conditions in the combustion chamber. These tests showed that excess air was present from the wall to the centre and along the grate from the first roller to the roller no.6. These results were used for combustion calculations as described in chapter 3.

Gas Analysis inside the Refuse Bed

Representative samples of the gases were withdrawn from the fire bed approximately 10 in. below the initial height of the refuse bed (Roller nos. 2 and 3). The carbon content of the gases at the sample point were compared with that in the stack. The value at the centre of the bed was approximately 25 percent higher than that in the stack sample, suggesting that air flows preferentially near the furnace wall. Maximum CO₂ contents of about 15% to 18% were recorded at the sampling points. The oxygen concentration fell to near 2.1. Methane concentrations of up to 2.5 percent, dry basis were also measured. CO concentrations were in the range between 3% up to 11%. Hydrogen concentrations varied between 2.5 to 5.0 percent during the active burning period. In some runs significant concentrations of O₂ were found within the bed at times at which the CO concentration was also high, no doubt due to channeling of the underfire air through the bed. The results obtained were not consistent and therefore only general conclusions could be drawn. A more detailed study of gases within the refuse bed would have been of interest but would have required the design and construction of specialized equipment. This was not carried out because the project time scale did not allow for this.

Overbed Air Requirements - From the gas analysis above the refuse bed, it is apparent that the oxygen required to complete the combustion of the gases leaving the refuse bed will vary with operating conditions and with position along the grate. The stoichiometric

air requirement for a pound of moisture-free, ash free refuse is approximately five pounds [41]. The amount of air required in the overbed section can therefore be readily deduced from the difference between the stoichiometric requirement per unit area of grate calculated from burning rates and the underfire air supply rate. During the periods of most active burning as much as 60 percent of the air needs to be supplied above the grate while in some runs where significant channeling occurred the overbed air requirements were small.

2.3.5 Miscellaneous Measurements

The feeder ram speed and the roller speed were recorded in order that the refuse feed rate can be estimated since their speed limits the rate at which refuse can be charged to the furnace.

Meteorological conditions at the time of the test were monitored and recorded. These measurements include barometric pressure and ambient temperature.

General Effects of Operational Conditions

It should be noted that there is some 1 to 1.5 hours lag time between the refuse loading onto the feed conveyor and the bottom ash discharge (30 - 40 minutes on the conveyor, 30 - 40 minutes on the grate) and therefore determining the effect of changes in operating conditions is a slow process. Hence only a limited range of variables was looked at before selecting the steady test conditions needed for the sampling period.

The primary and secondary air rates were varied in a series of 18 tests in order to study their effects on the overall incinerator performance. There were cases when CO concentration fell down to about 58 ppm or high temperatures were recorded inside the furnace. Of the 18 conditions investigated, the air distribution using 59% primary, 26% secondary front and 15% secondary rear gave the best combustion conditions. The mean carbon monoxide concentration was then only 58 ppm and showed few excursions.

General observation made throughout the experimental program

Visual inspection of the rollers, secondary air slots and refractories inside the furnace were made during the plant shut down periods. It was noted that the rollers were broken at some places and not in good condition. The 2 mm gaps at the roller surface and the secondary air slots were mostly blocked by dirt.

On occasions, when a large surge of waste entered the chamber, the roller grates had difficulty loosening up and spreading the waste and the surge tended to travel down the grate as a coherent lump. This led to short periods of poor ash burnout and although the operators tried to reduce the effect of such surges by reversing rollers and adjusting combustion air settings, this only led to a marginal improvement as such action tended to be taken only when the surge was well down the grate.

Conclusions:

This experimental program was devised to get as closely as possible the overall performance characteristics of the Sheffield incinerator plant. The conclusions of this study are summarized below.

The testwork data showed that at the time of testing, the time averaged combustion efficiency was relatively low. The carbon in the ash was relatively high and the carbon dioxide concentration in the flue gases was, sometimes, outside the range expected for an incinerator with heat recovery. The total supply of the combustion air and its distribution throughout the system was inadequate. At times, large volumes of excess air was used for the burnout of the refuse. This led to relatively poor gas phase combustion, overloading of the electrostatic precipitator and higher pollutant emissions. The boiler performance at such high excess air rates was relatively poor and the ratio of steam produced per kg of the refuse was small.

The flue gases were discharged to the EP at a high temperature ($\approx 300^\circ\text{C}$), consequently the volume of the flue gases tended to be greater than anticipated and the particulate abatement plant was often overloaded. Furnace temperature distribution was found to

be nonuniform which affected the incinerator performance and resulted in high refractory maintenance costs because of partial slagging and thermal gradients (in the side areas directly above the grate). It was suspected that the roof secondary air openings (slots), arranged in rows perpendicular to the center line of the furnace were the major cause of localized high temperatures inside the furnace.

Chapter 3

Calculations

Combustion and heat calculations are invaluable in designing the incinerator and in evaluating its performance. They establish a) the quantities of the constituents involved in the chemistry of combustion, b) the quantity of heat released and c) the efficiency of the combustion process under both ideal and actual conditions. This chapter presents details of the calculations that were made using experimental data to determine the performance characteristics of the incinerator. Some of the results were used for mathematical modelling of the refuse bed and overbed region.

3.1 Furnace Calculations; Analysis of Actual Data Obtained From A Series Of Tests At Sheffield Incinerator [42], [43], [44]

Dates of experiments: 18th, 19th and 20th May 1989

Waste type: 70% domestic waste & 30% wastes from market (mainly dry)

Refuse feed rate: 6.4 ton/hr (6400 kg/hr or 14,128 lb/hr)

Total combustion air flow: 210 percent excess air

Underfeed air flow: 80 - 90% of total combustion air flow

Heat losses: Siftings: 3% of total feed (3 - 4% combustibles)

Fly ash: 2% of total feed (6.6% carbon)

Residue: 29.5% of total feed (4.1% combustibles)

Figure 3.1 shows a schematic elevation and plan view of the Sheffield incinerator furnace with the individual stoker air zones (rollers) and furnace pressures and approximate positions of the gas sampling points. Although it would have been desirable to sample all points in this test program simultaneously to remove possibility of conditions changing greatly at any one point during the test, the manpower and the equipment requirements made this impractical. Attempts were made to operate the incinerator as uniformly as possible throughout the test period. Thus the test results are thought to be, in general, indicative of combustion conditions in the incinerator.

Also for the purpose of simplification, it was assumed that the refuse bed depth followed a triangular shape with the depth equal to zero at the discharge end of the stoker and with the maximum depth at the throat of the charging chute. Between two points along the stoker length the refuse bed depth would follow a trapezoidal configuration.

A summary of the mean composition of the gas samples taken at the indicated points above the refuse bed and inside the bed (figure 3.1) are given in the following tables:

Summary of Gas Sampling Data

(10 cm above the bed)

| Location | % By Volume | | | | | |
|--------------------------------|-----------------|----------------|------|----------------|-----------------|----------------|
| | CO ₂ | O ₂ | CO | H ₂ | CH ₄ | N ₂ |
| <i>A</i> ₁ | 4.00 | 14.67 | 1.35 | 1.10 | 0.29 | 75.1 |
| Roller 1 <i>B</i> ₁ | 3.08 | 15.18 | 1.96 | 1.43 | 1.14 | 71.8 |
| <i>C</i> ₁ | 8.83 | 6.72 | 6.58 | 10.99 | 2.81 | 61.2 |
| <i>D</i> ₁ | 10.65 | 7.06 | 1.84 | 0.98 | 0.32 | 75.4 |

| Location | % By Volume | | | | | | |
|----------|-----------------|----------------|-------|----------------|-----------------|----------------|-------|
| | CO ₂ | O ₂ | CO | H ₂ | CH ₄ | N ₂ | |
| Roller 2 | A ₂ | 5.07 | 14.53 | 0.001 | 0.01 | 0.01 | 80.2 |
| | B ₂ | 17.55 | 5.22 | 1.97 | 1.28 | 0.33 | 78.1 |
| | C ₂ | 13.08 | 2.95 | 7.12 | 4.27 | 2.35 | 68.5 |
| | D ₂ | 6.47 | 12.7 | 3.18 | 1.97 | 0.69 | 72.34 |
| Roller 3 | A ₃ | 6.81 | 16.44 | 2.08 | 0.98 | 0.81 | 79.8 |
| | B ₃ | 13.34 | 7.51 | 4.09 | 1.12 | 0.04 | 80.9 |
| | C ₃ | 9.71 | 9.83 | 3.89 | 1.74 | 0.47 | 78.5 |
| | D ₃ | 5.94 | 15.71 | 1.87 | 1.32 | 0.28 | 77.8 |
| Roller 4 | A ₄ | 2.90 | 10.4 | 1.73 | 1.36 | 0.30 | 83.3 |
| | B ₃ | 3.10 | 11.6 | 3.1 | 2.21 | 0.63 | 79.3 |
| | C ₄ | 8.40 | 10.4 | 1.73 | 1.36 | 0.31 | 77.8 |
| | D ₄ | 3.45 | 10.9 | 1.97 | 0.92 | 0.43 | 82.3 |
| Roller 5 | A ₅ | 0.25 | 6.98 | - | - | 0.20 | 81.2 |
| | B ₄ | 0.42 | 6.76 | - | - | 0.32 | 80.3 |
| | C ₅ | 0.18 | 6.54 | - | - | 0.17 | 79.4 |
| | D ₅ | 0.09 | 7.14 | - | - | 0.11 | 82.1 |
| Roller 6 | - | - | - | - | - | - | |

Summary of Gas Sampling Data

(inside the bed, \simeq 50 cm above the grate surface)

| | Location | % By volume | | |
|----------|----------|-----------------|------|----------------|
| | | CO ₂ | CO | O ₂ |
| Roller 1 | A | 6.1 | 12.4 | 10.6 |
| | B | 13.8 | 11.2 | 4.2 |
| | C | 11.9 | 14.9 | 5.1 |
| | D | 11.2 | 10.6 | 6.9 |
| Roller 2 | A' | 7.1 | 10.2 | 4.6 |
| | B' | 13.7 | 11.3 | 4.3 |
| | C' | 13.6 | 10.8 | 6.8 |
| | D' | 12.3 | 14.2 | 7.5 |
| Roller 3 | A'' | 8.7 | 7.3 | 6.8 |
| | B'' | 10.4 | 4.7 | 7.5 |
| | C'' | 13.2 | 8.9 | 7.8 |
| | D'' | 9.3 | 6.7 | 6.9 |
| Roller 4 | A''' | 4.1 | 1.7 | 6.2 |
| | B''' | 6.8 | 2.1 | 8.7 |
| | C''' | 8.3 | 2.8 | 7.3 |
| | D''' | 7.4 | 3.1 | 7.8 |
| Roller 5 | - | - | - | - |
| Roller 6 | - | - | - | - |

Based on the above data, the energy release inside and above the refuse bed were calculated and the results obtained are shown in figure 3.2. Now, integrating the areas under

the curve for the total heat release (in bed and above the bed) in figure 3.2, we can estimate the heat release for each of the stoker zones.

The heat release rate inside the refuse bed on top of rollers 1 to 6 were estimated [45] as follows;

$$\text{Roller 1} = 6.31 \times 10^3 \text{ MJ/hr}$$

$$\text{Roller 2} = 8.97 \times 10^3 \text{ MJ/hr}$$

$$\text{Roller 3} = 5.98 \times 10^3 \text{ MJ/hr}$$

$$\text{Roller 4} = 4.41 \times 10^3 \text{ MJ/hr}$$

$$\text{Roller 5} = 0.11 \times 10^3 \text{ MJ/hr}$$

$$\text{Roller 6} = -$$

Stoker Heat Release Rate

| Roller no. | Btu/hr $\times 10^6$ | MJ/hr $\times 10^3$ | % |
|--------------|----------------------|---------------------|---------------|
| Roller no. 1 | 14.26 | 15.05 | 23.9 |
| Roller no. 2 | 19.39 | 20.46 | 32.4 |
| Roller no. 3 | 16.59 | 17.51 | 27.4 |
| Roller no. 4 | 9.21 | 9.72 | 16.2 |
| Roller no. 5 | 0.23 | 0.24 | 0.10 |
| Roller no. 6 | - | - | - |
| <i>Total</i> | <u>62.22</u> | <u>65.65</u> | <u>100.00</u> |

Converting the gas compositions above the refuse bed to a % by weight basis and combining the readings at locations A₁B₁C₁D₁, A₂B₂C₂D₂, A₃B₃C₃D₃ and A₄B₄C₄D₄, the values for the stoker burning rates including the gasification phase were calculated.

Neglecting the Nitrogen content in refuse, the percentages of the combined and bypassing oxygen were calculated (“Bypassing air” is the air which remains after the combustion of CO, H₂ and CH₄ above the refuse bed is completed).

| Location | Average % By Weight | | | | | |
|-------------------------------|---------------------|------|-------|--------|--------|-------|
| | O_2 | CO | H_2 | CH_4 | CO_2 | N_2 |
| $A_1B_1C_1D_1$ | 12.7 | 3.0 | 0.26 | 0.66 | 10.6 | 72.6 |
| O_2 for complete combustion | - | 1.71 | 2.08 | 2.64 | - | - |
| Excess O_2 | 6.27 | - | - | - | - | - |
| $A_2B_2C_2D_2$ | 9.6 | 2.9 | 0.12 | 0.45 | 15.7 | 71.1 |
| O_2 for complete combustion | - | 1.65 | 0.96 | 1.8 | - | - |
| Excess O_2 | 5.19 | - | - | - | - | - |
| $A_3B_3C_3D_3$ | 12.0 | 2.0 | 0.1 | 0.23 | 6.0 | 78.6 |
| O_2 for complete combustion | - | 1.18 | 0.80 | 0.92 | - | - |
| Excess O_2 | 9.1 | - | - | - | - | - |
| $A_4B_4C_4D_4$ | 7.8 | - | - | 0.121 | 0.37 | 91.6 |
| O_2 for complete combustion | - | - | - | 0.44 | - | - |
| Excess O_2 | 7.36 | | | | | |
| $A_5B_5C_5D_5$ | - | - | - | - | - | |
| $A_6B_6C_6D_6$ | - | - | - | - | - | |

Based on the above data, the percentages of the combined and by passing oxygen were estimated as shown below:

Location % of combined and by passing O_2

Roller no.

| | combined O_2 | Uncombined O_2 |
|---|----------------|------------------|
| 1 | 69% | 31% |
| 2 | 77% | 23% |
| 3 | 68% | 32% |
| 4 | 49% | 51% |
| 5 | 7% | 93% |
| 6 | - | - |

The burning rate of each of the stoker sections can now be determined as can be the actual burning rates based on the heat release rate percentages [39].

Burning Rates

| Roller no. | lb/hr | kg/hr |
|------------|--------|--------|
| 1 | 1854.3 | 839.9 |
| 2 | 3028.7 | 1372.0 |
| 3 | 2472.4 | 1119.9 |
| 4 | 1236.2 | 559.9 |
| 5 | 100.6 | 45.5 |
| 6 | - | - |

Total grate area = $36 \text{ m}^2 = 387 \text{ ft}^2$

Each roller area = $6 \text{ m}^2 = 64.5 \text{ ft}^2$

Now using the above data, the actual burning rates per unit area of each roller were estimated. The results obtained are shown below:

Actual Burning Rates Per Unit Area Of Roller

| | lb/ft ² hr | kg/m ² hr |
|----------|-----------------------|----------------------|
| Roller 1 | 28.74 | 139.9 |
| Roller 2 | 46.95 | 228.6 |
| Roller 3 | 38.33 | 186.6 |
| Roller 4 | 19.16 | 93.3 |
| Roller 5 | 1.55 | 7.58 |
| Roller 6 | - | - |

To obtain a reasonable calorific value of the refuse, we can sum up the heat release in and above the refuse bed and the heat losses, by assuming a high heat value of the combustible fraction of refuse at approximately 9000 Btu/lb (20.934 MJ/kg), see ref.[46]:

Heat release in and above the refuse bed = 62.22×10^6 Btu/hr (65.65×10^3 MJ/hr)

Siftings = $14128 \times 0.03 \times 0.035 \times 9000 = 133509.6$ Btu/hr (140.86 MJ/hr)

Residue = $14128 \times 0.29 \times 0.04 \times 9000 = 1474963.2$ Btu/hr (1556.23 MJ/hr)

Fly ash (Carbon) = $14128 \times 0.02 \times 0.06 \times 14544 = 246573.1$ Btu/hr (260.15 MJ/hr)

Total = 64.08×10^6 Btu/hr (66.89×10^3 MJ/hr)

From above the high heat value of the refuse is calculated approximately as:

$$HHV = \frac{64,084,608}{14,128} = 4536 \text{ Btu/lb (10.55 MJ/kg)}$$

and the combustible fraction,

$$\bar{C} = \frac{4536}{9000} = 0.504 \text{ lb/lb of refuse (kg/kg of refuse)}$$

Based on the Sheffield refuse composition determined at the time of experiments (19th January 1989), the stoichiometric air requirement can be calculated as follows:

Refuse composition (Ultimate Analysis)

| | |
|--------|-------|
| C | 22.3% |
| H_2 | 2.52% |
| N_2 | 0.71% |
| O_2 | 12.4% |
| S | 0.2% |
| H_2O | 31.4% |
| Ash | 30.5% |

Stoichiometric air required is 2.847 kg air/kg refuse or the stoichiometric air required is 5.648 kg air/kg combustible fraction \bar{C} .

Optimum stoker burning rate (lb/ft² hr) [39] can be calculated using the following equation:

$$F_A = K_w C_a^{1/3}$$

where F_A = optimum stoker burning rate (lb/ft² hr), K_w = Essenhigh waste factor (dimensionless factor expressed as a function of combustion intensity, high heat value of the refuse and furnace configuration factor) and C_a = furnace capacity. Now, from figure 3.3, $K_w = 3.39$ for refuse with HHV = 4536 Btu/lb ; So,

$$F_A = (14128)^{1/3} \times 3.39 = 81.95 \text{ lb/ft}^2\text{hr} \text{ (403.5 kg/m}^2\text{hr)}$$

If all the oxygen supplied with the underfire air would react with the combustible fraction of the refuse, the ratio of the [44];

$$\frac{G_A}{W_a} = \frac{\text{Under fire air flow (lb/lb of refuse)}}{\text{Stoichiometric air (lb/lb of refuse)}}$$

would be equal to the ratio of [44];

$$\frac{\text{Optimum stoker burning rate}}{\text{Optimum stoker burning rate corrected for underfire air flow and stoker efficiency}}$$

Therefore we can proceed to use the percentage of combined O₂ to determine $\frac{G_A}{W_a}$ ratios of each of the stoker zones:

$$\text{Zone 1} = \frac{G_A}{W_a} = \frac{28.74}{81.95 \times 0.69} = 0.508$$

$$\text{Zone 2} = \frac{G_A}{W_a} = \frac{46.95}{81.95 \times 0.77} = 0.744$$

$$\text{Zone 3} = \frac{G_A}{W_a} = \frac{38.33}{81.95 \times 0.68} = 0.687$$

$$\text{Zone 4} = \frac{G_A}{W_a} = \frac{19.16}{81.95 \times 0.49} = 0.477$$

$$\text{Zone 5} = \frac{G_A}{W_a} = \frac{1.55}{81.95 \times 0.07} = 0.270$$

$$\text{Zone 6} = -$$

and therefore the optimum stoker burning rate corrected for underfire air flow and stoker efficiency on top of each roller (F'_A) is [44]:

$$\text{Roller1 } F'_A = 81.95 \times 0.508 = 41.63 \text{ lb/ft}^2.\text{hr} \text{ (204.9 kg/m}^2\text{hr)}$$

$$\text{Roller2 } F'_A = 81.95 \times 0.744 = 60.97 \text{ lb/ft}^2.\text{hr} \text{ (300.2 kg/m}^2\text{hr)}$$

$$\text{Roller3 } F'_A = 81.95 \times 0.687 = 56.29 \text{ lb/ft}^2.\text{hr} \text{ (277.1 kg/m}^2\text{hr)}$$

$$\text{Roller4 } F'_A = 81.95 \times 0.477 = 39.09 \text{ lb/ft}^2.\text{hr} \text{ (192.4 kg/m}^2\text{hr)}$$

$$\text{Roller5 } F'_A = 81.95 \times 0.270 = 22.12 \text{ lb/ft}^2.\text{hr} \text{ (108.9 kg/m}^2\text{hr)}$$

$$\text{Roller6 } - \quad - \quad - \quad - \quad - \quad -$$

The fact that there is uncombined oxygen bypassing the refuse bed and the combustion zone above the refuse bed, can only be attributed to stoker efficiency (inefficiency) and the influence of the refuse bed depth. Using the following equation [44], the stoker efficiency factor for each roller was estimated as follows ($\frac{\gamma}{a}$ = efficiency factor);

$$F_A = F'_A \times \frac{\gamma}{a}$$

where γ = refuse bed correction factor, a = stoker efficiency correction factor and $\frac{\gamma}{a}$ = Optimum efficiency factor.

| | | | | | |
|----------------|-------|---|-------|---|------------------------|
| <i>Roller1</i> | 28.74 | = | 41.63 | × | $(\frac{\gamma}{a})_1$ |
| <i>Roller2</i> | 46.95 | = | 60.97 | × | $(\frac{\gamma}{a})_2$ |
| <i>Roller3</i> | 38.33 | = | 56.29 | × | $(\frac{\gamma}{a})_3$ |
| <i>Roller4</i> | 19.16 | = | 39.09 | × | $(\frac{\gamma}{a})_4$ |
| <i>Roller5</i> | 1.55 | = | 22.12 | × | $(\frac{\gamma}{a})_5$ |
| <i>Roller6</i> | - | - | - | - | - |

$$\begin{aligned} \text{so } (\frac{\gamma}{a})_1 &= 0.69 \\ (\frac{\gamma}{a})_2 &= 0.77 \\ (\frac{\gamma}{a})_3 &= 0.68 \\ (\frac{\gamma}{a})_4 &= 0.49 \\ (\frac{\gamma}{a})_5 &= 0.07 \\ (\frac{\gamma}{a})_6 &= - \end{aligned}$$

Now, the stoichiometric air requirements of 2.847 kg/kg of refuse will yield a total underfire air flow at 21 °C [47] of;

$$Q_T = 2.847 \times \frac{14128}{60} \times (13.34) \times 3.082 = 27561.6 \text{ CFM } (12.81 \text{ m}^3/\text{sec})$$

Therefore,

$$\begin{aligned} Q_1 &= 6004.7 \text{ CFM } (8.83 \text{ m}^3/\text{sec}) \\ Q_2 &= 8777.5 \text{ CFM } (10.86 \text{ m}^3/\text{sec}) \\ Q_3 &= 7158.8 \text{ CFM } (9.01 \text{ m}^3/\text{sec}) \\ Q_4 &= 4987.5 \text{ CFM } (6.86 \text{ m}^3/\text{sec}) \\ Q_5 &= 2645.6 \text{ CFM } (3.98 \text{ m}^3/\text{sec}) \\ Q_6 &= - \end{aligned}$$

According to the manufacturer's data, the free open area of the stoker is \simeq 7% of the stoker surface, hence the air velocities through the surfaces of the stoker sections can be

estimated as follows [48]:

$$\begin{aligned}
 Vel.1 &= 830.8 \text{ ft/min} = 252.5 \text{ m/min} \quad (4.20 \text{ m/sec}) \\
 Vel.2 &= 1215.3 \text{ ft/min} = 369.4 \text{ m/min} \quad (6.15 \text{ m/sec}) \\
 Vel.3 &= 992.1 \text{ ft/min} = 301.5 \text{ m/min} \quad (5.02 \text{ m/sec}) \\
 Vel.4 &= 781.2 \text{ ft/min} = 237.4 \text{ m/min} \quad (3.95 \text{ m/sec}) \\
 Vel.5 &= 2.47 \text{ ft/min} = 0.750 \text{ m/min} \quad (0.01 \text{ m/sec}) \\
 Vel.6 &= - \quad - \quad = \quad - \quad - \quad -
 \end{aligned}$$

The above zone air velocities will yield the following dynamic pressures:

$$\begin{aligned}
 VP_1 &= 10.58 \quad P_a = 1.079 \quad mmWG \\
 VP_2 &= 22.69 \quad " = 2.31 \quad " \\
 VP_3 &= 15.12 \quad " = 1.54 \quad " \\
 VP_4 &= 9.36 \quad " = 0.955 \quad " \\
 VP_5 &= 6 \times 10^{-5} \quad " = 6.12 \times 10^{-6} \quad " \\
 VP_6 &= - \quad - = - \quad -
 \end{aligned}$$

The total pressure differentials across the stoker and the refuse bed are:

$$\begin{aligned}
 TP_1 &= 40.64 \text{ mmWG} \\
 TP_2 &= 41.50 \quad " \\
 TP_3 &= 30.18 \quad " \\
 TP_4 &= 17.08 \quad " \\
 TP_5 &= 5.7 \quad " \\
 TP_6 &= -
 \end{aligned}$$

Therefore the friction losses through the refuse bed are:

$$\begin{aligned}
 FP_1 &= 39.57 \text{ mmWG} \\
 FP_2 &= 39.19 \quad " \\
 FP_3 &= 28.64 \quad " \\
 FP_4 &= 16.12 \quad " \\
 FP_5 &= 5.7 \quad " \\
 FP_6 &= -
 \end{aligned}$$

Since the friction losses are directly proportional to the refuse bed depth, then; D=
 Refuse bed depth can be estimated as follows:

$$D_1 = 0.75 \text{ m}$$

$$D_2 = 0.74 \text{ m}$$

$$D_3 = 0.54 \text{ m}$$

$$D_4 = 0.30 \text{ m}$$

$$D_5 = 0.10 \text{ m}$$

$$D_6 = - -$$

3.2 Estimation of Average Refuse Residence Time

An analysis was made of the estimated time of refuse residence time on the grate inside the furnace from the feed ram to the ash chute. Figure 3.4 shows the so-called “Duesseldorf” system of incineration at the Sheffield incinerator plant. It consists of an inclined row of rotating grate cylinders. The rotating cylinder action transports the refuse from roller to the roller in a gentle agitation for thorough combustion. Each roller has its own variable speed drive to suit the refuse feed and combustion rate. The speed can be varied from 1 to 10 revolutions per hour.

The average rollers’ speed measured at the time of our experiments are given below;

| Roller no. | Measured Roller Speed (rev/hr) |
|------------|--------------------------------|
| 1 | 2.5 |
| 2 | 2 |
| 3 | 1.5 |
| 4 | 0.9 |
| 5 | 0.9 |
| 6 | 0.9 |

Using these values and assuming that α (approx.) = $120^\circ = \frac{2\pi}{3}$ (each roller rotates at 120° before the refuse on top of it transfers to the next roller), we have;

For roller 1, average speed of roller = 2.5 rev/hr, so $t_1 = \frac{2\pi/3}{2.5 \times 2\pi} = 0.13 \text{ hr} = 8 \text{ min}$

For roller 2, average speed of roller = 2 rev/hr, so $t_2 = \frac{2\pi/3}{2 \times 2\pi} = 0.16 \text{ hr} = 10 \text{ min}$

For roller 3, average speed of roller = 1.5 rev/hr, so $t_3 = \frac{2\pi/3}{1.5 \times 2\pi} = 0.22 \text{ hr} = 13.3 \text{ min}$

For roller 4, average speed of roller = 0.9 rev/hr, so $t_4 = \frac{2\pi/3}{0.9 \times 2\pi} = 0.37 \text{ hr} = 22.3 \text{ min}$

For roller 5, average speed of roller = 0.9 rev/hr, so $t_5 = \frac{2\pi/3}{0.9 \times 2\pi} = 0.37 \text{ hr} = 22.3 \text{ min}$

For roller 6, average speed of roller = 0.9 rev/hr, so $t_6 = \frac{2\pi/3}{0.9 \times 2\pi} = 0.37 \text{ hr} = 22.3 \text{ min}$

Therefore, estimated total refuse residence time inside the furnace from the feed ram to the ash chute is:

$$8 + 10 + 13.3 + (22.3 \times 3) = 98.2 \text{ min} = 1.63 \text{ hr}$$

3.3 Calculations: Drying, Pyrolysis, and Char gasification rates on top of each roller inside the incinerator

The following calculations were carried out to allow quantitative estimation of the generation rate of combustibles along the refuse bed, thus specifying the secondary air requirement and distribution. The results obtained were used as preliminary input data for the development of the mathematical model of the Sheffield incinerator (FLUENT modelling).

Drying Rate:

The propagation rate of drying is determined by the rate at which energy is transferred ahead of the propagating front; a function of undergrate air supply, particle size, air preheat, moisture content and fuel type. For refuse, the rate estimated by Essenhigh et al [49] vary from 0.09 m/min for wet refuse to 0.15 m/min for average refuse. The U.S.B.M. tests [8] indicate that the distance of separation of the ignition and drying wave is of the order of 0.15 m, but their ignition rates measured with little underfire air were lower than those observed by Essenhigh et al.

Now, using the following equation [43];

$$\frac{dx}{dt} = \sqrt{\frac{k_s^d(T_s^o - T_s^v)}{2\Delta\bar{H}_v\rho_s^d t}}$$

where k_s^d = thermal conductivity of the dry solid bed, T_s^v = temperature of the drying front, ρ_s^d = dry density of solid, t = time, T_s^o = fixed surface temperature and H_v = latent heat of vapourization, the drying rate can be estimated.

Putting the typical values for Sheffield refuse; $k_s^d = 0.2$ Btu/hr ft °F, $\rho_s^d = 50$ lb/ft³, $T_s^o = 1800$ °F, $T_s^v = 212$ °F, $\Delta\bar{H}_v = 600$ Btu/lb (for refuse with approximately 35% moisture content), the rate of propagation of the vaporization plane (drying rate) can be obtained as follows [43];

$$\frac{dx}{dt} = \sqrt{\frac{317.6}{60000t}} = 0.072\sqrt{\frac{1}{t}} = 0.072t^{-0.5}$$

where $\frac{dx}{dt}$ = rate of propagation of vaporization plane;

$$\begin{aligned} t &= 1 \text{ min} , \quad \frac{dx}{dt} = 0.557 \text{ ft/min} \quad (0.16\text{m/min}) \\ t &= 2 \text{ min} , \quad \frac{dx}{dt} = 0.394 \text{ ft/min} \quad (0.11\text{m/min}) \\ t &= 3 \text{ min} , \quad \frac{dx}{dt} = 0.321 \text{ ft/min} \quad (0.09\text{m/min}) \\ t &= 10 \text{ min} , \quad \frac{dx}{dt} = 0.176 \text{ ft/min} \quad (0.05\text{m/min}) \\ t &= 15 \text{ min} , \quad \frac{dx}{dt} = 0.144 \text{ ft/min} \quad (0.04\text{m/min}) \\ t &= 20 \text{ min} , \quad \frac{dx}{dt} = 0.124 \text{ ft/min} \quad (0.03\text{m/min}) \end{aligned}$$

The above calculations show that the rate of propagation of the vaporization plane decreases at $t^{-0.5}$, since the potential for heat transfer $\frac{dT}{dx}$ decreases as $t^{-0.5}$.

Pyrolysis Rate:

Combustible pollutants appear to be generated along the full length of the incinerator grate, although their discharge rate into the overbed volume is relatively low in the drying and ignition zones prior to the introduction of the underfire air. From the standpoint of the total kg per hour per square meter release rate, the pyrolysis zone probably qualifies as the single most important source of carbon monoxide, soot and hydrocarbon.

In order to estimate the rate of generation of the pyrolysis products at the Sheffield incinerator model, the following equation [50] was used, assuming that the pyrolysis reactions occur instantaneously above a critical temperature T_s^c (260 °C), the rate of generation of pyrolysis products is then:

$$\dot{R}_\rho = \frac{W_\rho(T_s^o - T_s^c)}{2(T_s^o - T_s^v)} \sqrt{\frac{k_s^d(T_s^o - T_s^v)}{2\Delta\bar{H}_v\rho_s^d t}}$$

where \dot{R}_ρ = rate of generation of pyrolysis products,

W_ρ = mass of pyrolysis products per unit volume of refuse,

H_v = latent heat of vapourization,

ρ_s^d = dry density of solid,

T_s^o = fixed surface temperature,

T_s^v = temperature of drying front,

T_s^c = critical temperature (260 °C),

and t = time.

Usually a pyrolysis product generation rate greater than 1.84 lb/hr ft² (8.96 kg/hr m²) is necessary for spontaneous combustion to occur [50].

Now, putting the typical values for Sheffield refuse into the above equation, we get;

$\rho_s^d = 50 \text{ lb/ft}^3$, $k_s^d = 0.2 \text{ Btu/hr ft } ^\circ\text{F}$, $T_s^o = 1800 \text{ } ^\circ\text{F}$, $T_s^v = 212 \text{ } ^\circ\text{F}$, $T_s^c = 600 \text{ } ^\circ\text{F}$, $W_\rho = 30 \text{ lb/ft}^3$, $\Delta\bar{H}_v = 600 \text{ Btu/lb}$ (for approximately 35% moisture content)

$$\dot{R}_\rho = \frac{0.85}{\sqrt{t}}$$

Using this equation, the rate of pyrolysis product generation would fall below the threshold level only after a period of 0.2 hr (12 mins).

The results obtained are shown below;

| | | | | |
|-----------|----------------------------|-------------------------------|----------|--------------|
| $t = 1$ | $\min \dot{R}_\rho = 6.58$ | $lb/hr ft^2$ | $(32.39$ | $kg/hr m^2)$ |
| $t = 2$ | $\min \dot{R}_\rho = 4.65$ | $lb/hr ft^2$ | $(22.89$ | $kg/hr m^2)$ |
| $t = 3$ | $\min \dot{R}_\rho = 3.80$ | $lb/hr ft^2$ | $(18.71$ | $kg/hr m^2)$ |
| $t = 4$ | $\min \dot{R}_\rho = 3.29$ | $lb/hr ft^2$ | $(16.19$ | $kg/hr m^2)$ |
| $t = 5$ | $\min \dot{R}_\rho = 2.94$ | $lb/hr ft^2$ | $(14.47$ | $kg/hr m^2)$ |
| $t = 6$ | $\min \dot{R}_\rho = 2.68$ | $lb/hr ft^2$ | $(13.19$ | $kg/hr m^2)$ |
| $t = 7$ | $\min \dot{R}_\rho = 2.48$ | $lb/hr ft^2$ | $(12.21$ | $kg/hr m^2)$ |
| $t = 8$ | $\min \dot{R}_\rho = 2.32$ | $lb/hr ft^2$ | $(11.42$ | $kg/hr m^2)$ |
| $t = 9$ | $\min \dot{R}_\rho = 2.19$ | $lb/hr ft^2$ | $(10.78$ | $kg/hr m^2)$ |
| $t = 10$ | $\min \dot{R}_\rho = 2.08$ | $lb/hr ft^2$ | $(10.24$ | $kg/hr m^2)$ |
| $t = 11$ | $\min \dot{R}_\rho = 1.98$ | $lb/hr ft^2$ | $(9.15$ | $kg/hr m^2)$ |
| $t = 12$ | $\min \dot{R}_\rho = 1.90$ | $lb/hr ft^2$ | $(9.05$ | $kg/hr m^2)$ |
| $(t = 13$ | $\min \dot{R}_\rho = 1.82$ | <i>below threshold level)</i> | | |

The above calculations show that in the Sheffield incinerator, pyrolysis reactions take place on top of roller 1 and half way through on top of roller 2 until all the volatile materials in the refuse are given off ($\simeq 12$ minutes).

Char gasification rate (as a function of primary air supply rate):

Once the refuse has been completely devolatilized, the rate of burnout of the char will be determined by the rate of oxygen supply with the combustion first yielding CO_2 , which then reacts with more carbon to yield CO . The amount of char provided is expected to be in the range 0.10 to 0.20 kg per kg of the refuse [51]. The oxygen requirement for the 0.80 to 0.90 kg of refuse gasified will be determined by the water gas shift reaction and enthalpy requirements.

Char gasification rate (as a function of primary air supply rate) on top of each roller was estimated for the Sheffield incinerator using the following equation [51];

$$F_A = \frac{0.75 f_{rcs} P_m \dot{G}_A}{(1 - \bar{A} - \bar{M})(1 - \bar{V})}$$

where P_m is the oxygen mass fraction in the air. \dot{G}_A is the air supply rate, V is the volatile matter fraction of the dry, inert-free refuse, and A and M are the inert and moisture fractions respectively. f_{rcs} is a factor defined by Thring [52] known as the relative carbon saturation (RCS) factor. It represents the degree of potential saturation of oxygen by carbon with a value of zero for pure air and a value of unity at the maximum saturation which is carbon monoxide. In our model the RCS factor was calculated from the O_2 and CO_2 in the gas analysis at the top of the refuse bed using the following equation [52];

$$f_{rcs} = \frac{1 - 0.019(CO_2\%) - 0.048(O_2\%)}{1 + 0.010(CO_2\% + O_2\%)}$$

where $CO_2\%$ and $O_2\%$ are the volumetric or molar percentages of these two gases in the gasification products.

To calculate the total refuse gasification rate from this carbon burning rate, the volatile, moisture and ash content of the refuse must be considered. If the volatile fraction of the refuse on a dry ash-free basis is \bar{V} , each kg of carbon is produced from $\frac{1}{1-\bar{V}}$ kg of dry, inert-free refuse and one kg of char is produced from $\frac{1}{(1-\bar{V})(1-\bar{A}-\bar{M})}$ kg of as-fired refuse if A and M are the ash and moisture content of as-fired refuse.

Following the above discussion, the char gasification rate was calculated on top of each roller as shown below;

$$\text{Total feed rate} = 6400 \text{ kg/hr}$$

$$\text{Total primary air rate} = 11.8 \text{ m}^3/\text{sec}$$

| Roller | % Air flow rate | Vol. flow (m ³ /sec) | kg/m ² .hr |
|--------|-----------------|---------------------------------|-----------------------|
| 1 | 20% | 2.36 | 0.79 |
| 2 | 26% | 3.06 | 1.03 |
| 3 | 26% | 2.83 | 0.95 |
| 4 | 16% | 1.88 | 0.63 |
| 5 | 12% | 1.41 | 0.47 |
| 6 | 2% | 0.23 | 0.07 |

Using the following equation,

$$F_A = \frac{0.75 \cdot f_{res} \cdot P_m \cdot \dot{G}_A}{(1 - \bar{A} - \bar{M})(1 - \bar{V})}$$

The char gasification rate on top of each roller can now be estimated as follows:

| Roller no. | Char gasification rate kg/hr m ² |
|------------|--|
| 1 | 126.6 |
| 2 | 230.7 |
| 3 | 210.3 |
| 4 | 140.8 |
| 5 | 50.7 |
| 6 | - |

The following table summarizes in Metric units the average conditions in the six zones of the grate (top of rollers 1 to 6) roughly equivalent to the underfire air zones available. This data was utilized as the preliminary input data in the mathematical modelling work.

| Roller no. | 1 | 2 | 3 | 4 | 5 | 6 |
|---|-------|-------|-------|-------|-------|------|
| Grate length (m) | 2.04 | 2.04 | 2.04 | 2.04 | 2.04 | 2.04 |
| Grate area (m ²) | 6.19 | 6.19 | 6.19 | 6.19 | 6.19 | 6.19 |
| Percentage of charge burnt | 21.6% | 30.9% | 26.5% | 15.2% | 5.8% | - |
| kg air/kg refuse burned | 5.25 | 8.75 | 10.5 | 24.1 | 38.7 | - |
| Excess air percentage | 50% | 150% | 200% | 590% | 680% | - |
| Air flow (m ³ /m ²) | 30.22 | 51.60 | 31.07 | 53.31 | 44.12 | - |
| Burning rate (kg/m ² hr) | 209.8 | 300.2 | 257.4 | 147.6 | 56.3 | - |
| Char gasification rate (kg/m ² hr) | 126 | 230 | 210 | 140 | 50.7 | - |

3.4 Overbed Air Regime Calculations

From the refuse bed concentrations obtained experimentally, it is apparent that the oxygen required to complete the combustion of gases leaving the refuse bed varies with the operating conditions and with the time. For a travelling grate incinerator, this means that the secondary air requirements will vary with position along the grate as well as with operating conditions. Oxygen can be supplied to the bed both in the underfire air and in any secondary air induced through the bed by temperature gradients. For the latter case, the overbed air (which has a lower mass fraction of oxygen than the underfire air) will tend to sink down at the “cold ” walls of the furnace and to rise up through the “hot” core of the bed. The oxygen in this air would be expected to be rapidly consumed near the edges of the bed. The estimation of the quantity of air being induced into the bed in this manner is difficult but a rough estimate of the expected magnitude of this effect can be found for the Sheffield incinerator as follows:

If the only significant forces are those of momentum ($U^2 \rho L^3$) and buoyancy ($L^3 \Delta \rho g$), the entrainment velocity U is found to be [53];

$$U = \sqrt{\frac{L\Delta\rho g}{\rho_c}}$$

where, L = characteristic length given by distance from the top of the bed to the roof of the incinerator,

$\Delta\rho$ = the density difference of the gas at the hot and cold temperatures,

ρ_c = the density of cold gas,

g = gravitational constant.

The mass flux of oxygen through a unit area of the bed by the natural draught (\dot{G}_{ND}) will be [53];

$$\dot{G}_{ND} = U\rho_c(M_{O_2})_c\sqrt{\frac{L\Delta\rho g}{\rho_c}}$$

where $(M_{O_2})_c$ = mass fraction of oxygen in the overbed air.

The mass flux of oxygen through a unit of bed in the underfire air (\dot{G}_{FD}) is given by

[53];

$$\dot{G}_{FD} = V \rho_a (M_{O_2})_a$$

where V = superficial velocity of the underfire air,

ρ_a = density of air,

and $(M_{O_2})_a$ = mass fraction of oxygen in the underfire air.

If the effect of the natural draught is to be negligible, then,

$$V \rho_a (M_{O_2})_a \gg \rho_c (M_{O_2})_c \sqrt{\frac{L \Delta \rho g}{\rho_c}}$$

and using $\rho_c = \frac{\rho_a T_a}{T_c}$ and $\rho_H = \frac{\rho_a T_a}{T_H}$, where T_a , T_c and T_H are the ambient cold and hot air and gas temperatures, gives;

$$V (M_{O_2})_a \gg \frac{T_a (M_{O_2})_c}{T_c} \sqrt{L \left[1 - \frac{T_c}{T_H} \right] g}$$

Putting typical values for the Sheffield incinerator plant into the above equation, we get:

$V = 2.5$ ft/sec, $(M_{O_2})_a = 0.23$, $(M_{O_2})_c = 0.08$, $T_a = 15$ °R (27 °C), $T_c = 555$ °R (999 °C),
 $T_H = 840$ °R (1512 °C) gives;

$$0.575 \gg 0.006 \sqrt{L}$$

For many furnaces, L , one of the driving forces for the buoyancy term is of the order of 10 - 20 ft. For the Sheffield incinerator plant, L is about 3 m (10 ft).

An estimation of the quantity of air being induced into the bed was made by substituting this value for L in the above equation. The results indicate that the oxygen mass flux induced by natural draught may well be greater than that supplied in the underfire air.

3.5 Calculation of Incinerator - Boiler Efficiency (Heat - Balances)

Unfortunately there is no method of continuously monitoring the feed rate at the Sheffield incinerator (e.g. a belt weigher or crane grab weigher) and hence the feed rate had to be calculated on the basis of the overall run time and the total number of 'grabs' taken

to empty the known weight of raw refuse deposited in the pit. This provides an average weight of refuse per grab load and by recording the number of grabs per hour an estimate of hourly feed rate was made. There are inevitably errors involved in this procedure, the bulk density of the waste in the pit varies, different crane operators use different procedures to fill the grab and full grab loads become more difficult to obtain when the pit is nearly empty. Figure 3.5 shows the hourly feed rate and it can be noted that the average feed rate was 6.8 ton/hr with a standard deviation of 1.3 ton/hr (or $\pm 12\%$).

The following gives the detailed calculations and the principal values used for calculating the mass and energy balances for the Sheffield refuse incineration [54], [55], [56] and [57]:

CALCULATIONS:

Note: For convenience (e.g. use of UK Callender steam tables, etc) the calculations were carried out to give heat as British thermal units (Btu). Values in MJ are also provided on the basis that 1 Btu = 1054.5 Joules.

Basis: One hour.

INPUT:

1 - Heat in refuse:

CV of refuse = 5295 Btu/lb , Feed rate = 14991 lb (6400 kg)

$5295 \text{ Btu/lb} \times 14991 \text{ lb} = 79.38 \times 10^6 \text{ Btu} (83755 \text{ MJ})$

2 - Heat in boiler feed water:

Wt of water \times temperature above 60 °F and specific heat

$41534 \text{ lb of steam} \times (296 - 60) \times 1 = 9.80 \times 10^6 \text{ Btu} (10341 \text{ MJ})$

OUTPUT:

3 - Heat in steam:

Btu per lb from steam tables for saturated steam at 151 psi (10.26 bar),

Heat in steam = 1197 Btu/lb;

correcting for difference in datum line chosen and datum line in steam table;

$1197 - 28.1 = 1168.9 \text{ Btu/lb}$

Multiply Btu/lb by pounds of steam;

$$1169 \times 41534 = 48.55 \times 10^6 \text{ Btu (51,223 MJ)}$$

$$\text{Heat in steam - heat in feed water} = (48.55 - 9.80) \times 10^6 = 38.75 \times 10^6 \text{ (40,881 MJ)}$$

4 - Loss due to unburnt fuel in ash:

$$\text{Measured \% carbon in bottom ash} = 5.8 \% \text{ (dry basis)}$$

$$\text{Dry basis flowrate of ash} = 2.42 \text{ te/hr}$$

$$\text{Wt of carbon in bottom ash} = 309.43 \text{ lbs (140.36 kg)}$$

$$\begin{aligned} \text{Heat in bottom ash} &= 309.43 \times 14544 \text{ (combustion heat)} \\ &= 4.50 \times 10^6 \text{ Btu (4747 MJ)} \end{aligned}$$

$$\text{Measured \% carbon in EP ash} = 6.8 \% \text{ (dry basis)}$$

$$\text{Dry basis flowrate of EP ash} = 967 \text{ lb/hr (438.05 kg/hr)}$$

$$\text{Wt of carbon in EP ash} = 65.75 \text{ lbs (29.78 kg)}$$

$$\text{Heat in EP ash} = 65.75 \times 14544 = 0.95 \times 10^6 \text{ Btu (1008 MJ)}$$

Total heat in bottom

$$\text{ash and EP ash} = 5.45 \times 10^6 \text{ Btu (5749 MJ)}$$

5 - Heat Loss in Stack Gases:

5a) Sensible heat loss in dry stack gas;

Calculate moles of carbon in stack gas,

$$\text{carbon in refuse} = 14991 \times 22.3/100$$

$$= 3342.99 \text{ lb}$$

$$\text{carbon in ash} = 375.18 \text{ lbs}$$

$$\text{carbon in stack gas} = 2967.81 \text{ lbs}$$

$$\text{moles of carbon in gas} = 2967.81 \div 12 = 247 \text{ moles}$$

Calculate moles of dry stack gas from dry vol/vol composition,

$$\frac{247 \times 100}{5.8} = 4259 \text{ moles}$$

Calculate moles of each gas,

$$CO_2 = \frac{4259 \times 5.8}{100} = 247 \text{ moles}$$

$$O_2, N_2, CO = 4259 - 247 = 4012 \text{ moles}$$

From sensible heat chart, read heat in gas at 509 °F (298 °C),

| | Btu/moles |
|--------------------------------------|-----------|
| CO ₂ | = 4300 |
| O ₂ , N ₂ , CO | = 3150 |
| H ₂ O | = 3700 |

Multiply moles by Btu per mole,

$$CO_2 : 247 \times 4300 = 1,062,100 \text{ Btu}$$

$$O_2, N_2, CO : 4012 \times 3150 = 12,637,800 \text{ Btu}$$

Total heat in dry stack gas = 13.69×10^6 Btu (14,453 MJ).

5b - Heat loss in water vapour from moisture and from hydrogen in refuse:

$$H_2O \text{ from moisture in refuse} = 14991 \times \frac{28}{100}$$

$$= 4197.48 \text{ lbs}$$

$$\text{Wt. of hydrogen in refuse} = 14991 \times \frac{3.55}{100}$$

$$= 532.18 \text{ lbs}$$

$$\text{Wt of } H_2O \text{ from refuse} = \frac{532.18 \times 18}{2}$$

$$= 4789.62 \text{ lbs}$$

$$\text{Total wt of } H_2O \text{ from refuse combustion} = 8987.10 \text{ lbs}$$

$$\text{Total moles of } H_2O = \frac{8987.10}{18} = 499 \text{ moles}$$

$$\text{Calculate sensible heat content} = 499 \times 3700$$

$$\text{of water vapour} = 1.84 \times 10^6 \text{ Btu (1947 MJ)}$$

$$\text{Calculate latent heat of vapourisation} = 8987.10 \times 1057 = 9.49 \times 10^6 \text{ (10,021 MJ)}$$

$$\text{Total heat loss in water vapour} = 11.33 \times 10^6 \text{ Btu (11,968 MJ)}$$

5c - Undeveloped heat:

Total moles of dry gas = 4259 moles

Concentration of CO = 183 ppm (dry)

Moles of CO = $\frac{0.018 \times 4259}{100} = 0.766$ moles

Heat loss as CO = $0.766 \times 122,400 = 0.09 \times 10^6$ Btu (98.99 MJ)

5d - Radiation and unaccounted for losses:

Determined by difference,

| | Btu $\times 10^6$ | MJ $\times 10^3$ |
|--------------------------------------|-------------------|------------------|
| Total heat input | = 75.25 | 79.38 |
| Accounted for output | = 69.31 | 73.12 |
| Radiation and unaccounted for losses | = 5.94 | 6.26 |

COMPLETE HEAT BALANCE, BASIS 1 HOUR, DATUM LINE 60 °F

| Input: | Btu $\times 10^6$ | MJ $\times 10^3$ | % |
|--------------------------------------|-------------------|------------------|-------|
| 1 Heat in raw refuse | 75.25 | 79.38 | 100.0 |
| Output: | | | |
| 3 Heat in steam -heat in boiler feed | 38.75 | 40.88 | 51.48 |
| 4 Heat loss in ash (unburnt) | 5.45 | 5.74 | 7.24 |
| 5 Heat loss in stack gases | | | |
| a) sensible heat (dry gas) | 13.69 | 14.45 | 18.19 |
| b) heat in water vapour | 11.33 | 11.95 | 15.05 |
| c) undeveloped heat | 0.09 | 0.09 | 0.15 |

6 Radiation and unaccounted for losses 5.94 6.26 7.89

\overline{T}_{total} 75.25 79.38 100.00

STACK GAS VOLUME CHECK

Pitot measurement = 16.93 m³/sec STP, wet.

Moisture content = 14.94 %

Therefore, dry volume 14.4 m³/sec (508 ft³/sec)

Dry gas composition CO₂ = 5.8% : CO₂ density = 0.1237 lb/ft³

O₂ = 15.1% : O₂ density = 0.0892 lb/ft³

N₂ = 80.4% : N₂ density = 0.0782 lb/ft³

Wt of CO₂ = 508 × 3600 × 0.058 × 0.1237 = 13120.90 lbs

Moles of CO₂ = $\frac{13120.90}{44}$ = 298 moles

Wt of O₂ = 508 × 3600 × 0.15 × 0.0892 = 24469.34 lbs

Moles of O₂ = $\frac{24469.34}{32}$ = 764 moles

Wt of N₂ = 508 × 3600 × 0.80 × 0.0782 = 114409.73 lbs

Moles of N₂ = $\frac{114409.73}{28}$ = 4086 moles

Therefore;

Total dry gas moles based on the

measured stack volume = 5148 moles

Total wet gas moles based on the

measured volume = 5367 moles

Total wet gas moles based on the

calculated mass balance of C and H₂O = 4758 moles

% increase in measured gas volume = $\frac{609 \times 100}{4758}$

= 12.79%

Boiler Efficiency Calculation

The efficiency of the boiler was calculated, using the following equation [57];

$$E = \frac{\text{Total heat per kg of steam} \times \text{Weight of steam}}{\text{Calorific value of fuel} \times \text{Weight of refuse}} \times 100$$
$$E = \frac{(2719.01 \text{ kJ/kg}) \times (18814.9 \text{ kg/hr})}{(12316.1 \text{ kJ/kg}) \times (6400 \text{ kg/hr})}$$

Therefore, Efficiency of boiler = 64.9%

The overall efficiency based on the net calorific value of the refuse was estimated as follows [57] ;

$$\text{Efficiency} = \frac{\text{Heat in steam} - \text{Heat in boiler water}}{\text{Heat in refuse} - \text{sensible heat in stack gases}}$$
$$\text{Efficiency} = \frac{38.75 \times 10^6}{61.56 \times 10^6} = 62.9\%$$

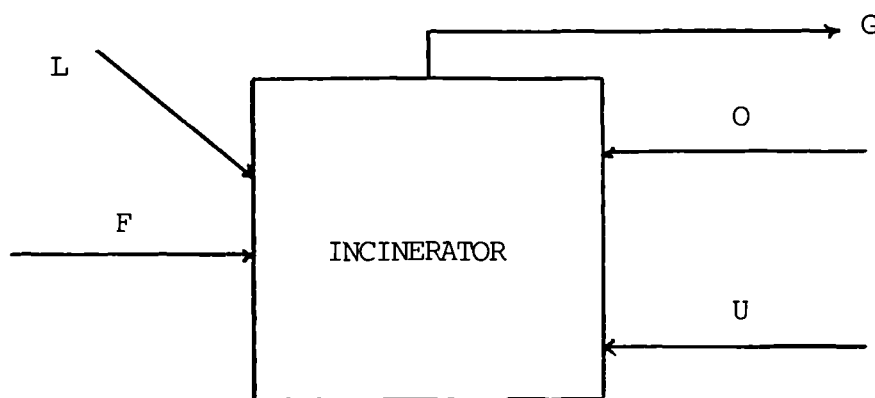
From the above calculations, it can be noted that 51.48% of the gross heating value in the waste was converted to steam with the major losses associated with the stack gas, in particular the water vapour losses which include the latent heat as well as sensible heat losses. 7.89% of the heat input was unaccounted for directly and represents radiation losses, heat loss in solid discharge and any sampling/measurement errors. Considering the direct combustion efficiency losses, 7.24% of heat content of raw refuse was lost due to inefficient combustion. In terms of net calorific value input, i.e. accounting for the moisture, hydrogen and ash content of refuse which inevitably lead to efficiency losses in a combustion system, the overall efficiency was 62.9% and as noted, the efficiency loss is almost entirely associated with the boiler section of the incinerator.

Considering the potential errors involved in calculating the heat balance, it can be noted that the gas flow was calculated assuming the carbon balance was correct. As a measured stack volume was also available, this was compared and there was a difference of 12.79% between the two values (the measured value being higher). This is within the errors expected for such an experimental work, given the problems associated with sampling refuse materials and measurement of air flows. If the measured volumes had been used in the heat balance, this would have reduced unaccounted losses to less than 1% of the total,

a value considered to be unrealistically low. The schematic mass and energy balance for raw waste incineration at the Sheffield incinerator is shown in figure 3.6. The typical steam production rate is presented in figure 3.7.

3.6 Incinerator Material Balance

A material balance was carried out in order to estimate the hourly rate of consumption of the carbon, hydrogen and oxygen content of the refuse inside the incinerator [58].



F = Refuse consumed (kg/hr),

G = Stack gas flow rate (kg mol/hr)

L = Air leakage flow rate (kg/hr)

O = Secondary air flowrate (kg/hr)

U = Underfire air flow rate (kg/hr)

The above diagram shows the material inputs to and outputs from the incinerator. The material balance took the amount of air leakage into the overbed region into account.

Now, at any particular instant during the experimental run four material balances for carbon, hydrogen, oxygen and nitrogen could be written as follows (In these equations the refuse was assumed to contain only carbon, hydrogen and oxygen which was a valid assumption for the raw refuse used in this study).

Carbon balance;

$$\frac{F \cdot F_C}{12} = G (Y_{CO_2}^G + Y_{CO}^G)$$

Oxygen balance;

$$\frac{F \cdot F_O}{32} = G (Y_{CO_2}^G + Y_{O_2}^G + Y_{CO}^G + \frac{1}{2} Y_{H_2O}^G) - (U + O + L)(Y_{O_2}^A + \frac{1}{2} Y_{H_2O}^A)$$

Hydrogen balance;

$$\frac{F \cdot F_H}{2} = G Y_{H_2O}^G - (U + O + L) Y_{H_2O}^A$$

Nitrogen balance;

$$G Y_{N_2}^G = (U + O + L) Y_{N_2}^A$$

In the above equations F_C , F_H and F_O are respectively the weight fraction of carbon, hydrogen and oxygen in the refuse; Y_i^G is the mole fraction of the component "i" in the stack gases and Y_i^A is the mole fraction of the component "i" in the ambient air.

The above equations together with the testwork data obtained on 23rd of November 1988 were used to solve for the rate of consumption of oxygen, carbon and hydrogen content of the refuse, i.e. $F \cdot F_O$, $F \cdot F_C$ and $F \cdot F_H$. The results obtained are as follows;

Calculation

Basis = 1 hour

| | m ³ /sec | kg/hr | moles/hr |
|--------------------------|---------------------|-------|----------|
| Total undergrate air (U) | 11.8 | 78120 | 2697 |
| Total secondary air (O) | 1.3 | 10697 | 369 |
| Air leakage volume (L) | 0.7 | 7907 | 273 |

Stack gases;

Pitot measurement = 18.32 m³/sec at STP, wet

Moisture content = 13.9 %

Therefore, dry volume = 15.7 m³/sec

Dry gas composition obtained from gas analysis;

| component | % by volume | density (kg/m ³) |
|-----------------|-------------|------------------------------|
| CO ₂ | 6.1 | 1.980 |
| CO | 0.009 | 1.549 |
| O ₂ | 14.7 | 1.428 |
| N ₂ | 80.4 | 1.251 |

Then, we have;

$$\text{Wt of CO}_2 = 15.7 \times 3600 \times 0.061 \times 1.980 = 6826 \text{ kg/hr}$$

$$\text{Moles of CO}_2 = \frac{6826}{44} = 155 \text{ moles/hr}$$

$$\text{Wt of CO} = 15.7 \times 3600 \times 0.00009 \times 1.549 = 7.87 \text{ kg/hr}$$

$$\text{Moles of CO} = \frac{7.87}{28} = 0.281 \text{ moles/hr}$$

$$\text{Wt of O}_2 = 15.7 \times 3600 \times 0.147 \times 1.428 = 11864 \text{ kg/hr}$$

$$\text{Moles of O}_2 = \frac{11864}{32} = 371 \text{ moles/hr}$$

$$\text{Wt of N}_2 = 15.7 \times 3600 \times 0.804 \times 1.251 = 56848 \text{ kg/hr}$$

$$\text{Moles of N}_2 = \frac{56848}{28} = 2030 \text{ moles/hr}$$

Therefore, the total dry gas moles based on measured volume = 2556 moles/hr and the total wet gas moles based on measured volume = 3354 moles/hr.

Using the above values, the rate of consumption of the oxygen, carbon and hydrogen content of the refuse can be calculated as follows:

$$\frac{F \cdot F_C}{12} = 3354 (6.1\% + 0.009\%) = 204.89 \text{ moles/hr (2458.6 kg/hr)}$$

$$\begin{aligned} \frac{F \cdot F_O}{32} &= 3354 (6.1\% + 0.009\% + 14.7\% + \frac{1}{2}(13.9)) - (2697 + 369 + 273)(21\% + \frac{1}{2}(0.013)) \\ &= 208 \text{ moles/hr (6656 kg/hr)} \end{aligned}$$

$$G Y_{N_2}^G = (2697 + 369 + 273)(79\%) = 2637 \text{ moles/hr (73836 kg/hr)}$$

Thus the total burning rate in one hour is approximately :

$$2458.6 + 6656 + 846 = 9960.6 \text{ kg/hr}$$

3.7 Combustion Calculation

The quantities and the products of combustion air involved per kg of refuse were determined as follows [57]. In the following calculations, the amount of moisture in the combustion air is taken as 0.013 lb/lb of dry air, corresponding to conditions of 80 ° F dry bulk temperature and 60% relative humidity.

CALCULATION OF THEORETICAL AIR NEEDED FOR COMBUSTION;

WEIGHT METHOD :

Assume : complete combustion (100% total air, no excess air).

| ULTIMATE ANALYSIS | | MULTIPLIER | REQUIRED FOR COMBUSTION | |
|-----------------------------|-------|-------------|-------------------------|---------|
| kg/kg of refuse as fired | | | O ₂ | DRY AIR |
| C | 0.223 | 2.66, 11.53 | 0.593 | 2.571 |
| H ₂ | 0.025 | 7.94, 34.34 | 0.198 | 0.858 |
| O ₂ | 0.124 | | - | - |
| N ₂ | 0.007 | | - | - |
| S | 0.002 | 1.0, 4.29 | 0.002 | 0.0085 |
| H ₂ O | 0.314 | | - | - |
| ASH | 0.305 | | - | - |
| SUM | 1.000 | | 0.793 | 3.437 |
| Less O ₂ in fuel | | -0.124 | -0.590 | |
| Required at 100% total air | | | 0.669 | 2.847 |

Now, the theoretical air required for combustion using 210% excess air can be calculated as follows;

| | O ₂ | Dry Air |
|---|----------------|---------|
| O ₂ and air × 210/100, total | 1.404 | 5.978 |
| Excess air = 5.978 - 2.847 | - | 3.131 |
| Excess O ₂ = 1.404 - 0.669 | 0.735 | - |

CALCULATION OF THEORETICAL AIR NEEDED FOR COMBUSTION;

MOLE METHOD:

Assume complete combustion (100% total air - no excess air).

| Ultimate Analysis kg/100 kg refuse as fired | Moles per 100 kg refuse | Multiplier | Required combustion moles/100 kg refuse | |
|---|----------------------------|------------|---|---------|
| | | | O ₂ | dry air |
| C 22.3/12 | 1.85 | 1,4.76 | 1.85 | 8.80 |
| H ₂ 2.52/2 | 1.26 | 0.5,2.38 | 0.63 | 2.99 |
| O ₂ 12.4/32 | 0.38 | - | - | - |
| N ₂ 0.71/28 | 0.025 | - | - | - |
| S 0.28/32 | 0.008 | 1,4.76 | 0.008 | 0.038 |
| H ₂ O 31.4/18 | 1.74 | - | - | - |
| Ash 30.5 | - | - | - | - |
| Sum 100.00 | | | 2.48 | 11.82 |
| Less O ₂ in refuse | | | -0.38 | -1.809 |
| Required at 100% total air(stoichiometric) | | | 2.1 | 10.01 |

CALCULATION OF THE PRODUCTS OF COMBUSTION USING

THEORETICAL AIR:

The following table shows the amounts of oxygen and air required for the combustion of 1 kg of each combustible element of refuse and the products of the combustion obtained.

| Combustible Element | kg air components, or products of combustion | | | | | | |
|---------------------------|--|-------|-------|--------|------|--------|--------|
| | per kg of element | | | | | | |
| | O_2 | N_2 | Air | CO_2 | CO | H_2O | SO_2 |
| C(when burned to CO_2) | 2.66 | 8.82 | 11.48 | 3.66 | - | - | - |
| C(when burned to CO) | 1.33 | 4.41 | 5.74 | - | 2.33 | - | - |
| Hydrogen | 8 | 26.4 | 34.4 | - | - | 9 | - |
| Sulphur | 1 | 3.3 | 4.3 | - | - | - | 2 |

The volume of the products of combustion in m^3 at STP are as follows:

| | CO_2 | CO | N_2 | H_2O | SO_2 |
|---------------------------------|--------|------|-------|--------|--------|
| From 1kg C to CO_2 | 1.86 | - | 6.53 | - | - |
| From 1 kg C to CO | - | 1.87 | 3.51 | - | - |
| From 1 kg H_2 to water vapour | - | - | 20.99 | 11.16 | - |
| From 1 kg sulphur to SO_2 | - | - | 2.62 | - | 0.686 |

From the above data the weight and volume of the air required and the weights and volumes of products of combustion using theoretical air can be calculated as follows:

| Refuse | Analysis | kg constituent/kg fuel |
|--------|----------|------------------------|
| C | 22.3% | 0.22 |
| H_2 | 2.52% | 0.02 |
| O_2 | 12.4% | 0.12 |
| S | 0.28% | 0.0028 |
| N_2 | 0.71% | 0.007 |
| H_2O | 31.4% | 0.31 |
| Ash | 30.5% | 0.30 |

Using theoretical air:

0.22 kg C requires 0.22×2.66 kg $O_2 = 0.585$ kg O_2 /kg C

0.22 kg H₂ requires $0.02 \times 8 \text{ kg O}_2 = 0.16 \text{ kg O}_2/\text{kg H}_2$

0.0028 kg S requires $0.0028 \times 1 \text{ kg O}_2 = 0.0028 \text{ kg O}_2/\text{kg S}$

Total Wt. O₂ required = 0.747 kg

Wt. O₂ present in refuse = -0.124

O₂ to be supplied from air = 0.623 kg

Wt. of air required = $0.623 \times \frac{100}{23.2} = 2.685 \text{ kg} = 2.23 \text{ m}^3$ at STP air

Wt. of Nitrogen in refuse = 0.007 kg/kg refuse

Wt. of Nitrogen in air = $2.68 - 0.623 = 2.057 \text{ kg}$

Wt. of Nitrogen in flue gases = 2.05 kg

Wt. of CO₂ produced = $0.22 \times 3.66 = 0.805 \text{ kg/kg refuse}$

Wt. of H₂O produced = $0.02 \times 9 = 0.18 \text{ kg/kg refuse}$

Wt. of H₂O in refuse = 0.31 kg/kg refuse

Therefore we have,

Total water vapour in flue gases = 0.49 kg

Wt. of SO₂ produced = $0.0028 \times 2 = 5.6 \times 10^{-3} \text{ kg}$

Total products of combustion, wet = 1.48 kg

Total products of combustion, dry = 0.990 kg

From above, the volumes of the combustion products can be estimated as shown below;

| Flue gas constituent | Vol. at STP, dry (m ³) |
|----------------------|---------------------------------------|
| N ₂ | 1.62 |
| CO ₂ | 1.73 |
| H ₂ O | 0.60 |
| SO ₂ | 0.002 |
| Total flue gas, wet | 1.08 |
| Total flue gas, dry | 0.71 |

CALCULATION OF EXCESS AIR AND DRY FLUE GASES USING

EXCESS AIR :

Actual flue gas analysis (by volume , dry basis) :

$$\text{CO}_2 = 5.8\%$$

$$\text{CO} = 0.03\%$$

$$\text{O}_2 = 13.9\%$$

$$\text{N}_2 = 79.0\%$$

Actual volume of dry flue gases can be calculated using the following equation [57];

$$\frac{\text{Theory CO}_2}{\text{Actual (CO}_2 + \text{CO)}} \times \text{Theoretical Vol. of dry flue gases}$$

Now, from above;

$$\frac{25.6}{6+3} \times 1.561 = 4.440 \text{ m}^3$$

$$\text{Volume of theoretical dry flue gases} = 1.561 \text{ m}^3$$

But, the difference between these 2 volumes is the volume of the excess air. Therefore;

$$\text{Volume of excess air} = 2.879 \text{ m}^3$$

$$\text{Volume of theoretical air} = 2.23 \text{ m}^3$$

$$\text{and, Excess air \%} = \frac{2.879}{2.23} \times 100 = 129.1\%$$

$$\text{Wt. of dry flue gases} = \text{theoretical Wt} + \text{Wt. excess air} = 1.561 + 3.144 = 5.005 \text{ kg}$$

$$\text{Wt. of wet flue gases} = 2.161 + 2.87 = 5.031 \text{ kg}$$

Conclusions:

On the basis of the above calculations, the following main conclusions can be drawn.

The overall steam raising efficiency of the incinerator was relatively low. It was estimated that 51.48% of the gross heating value in the waste was converted to steam with the major losses associated with the stack gas (33.39%), in particular the water vapour losses which include the latent heat as well as sensible heat losses. Considering the direct combustion efficiency losses, 7.24% of the heat content of the refuse was lost due to inefficient combustion. This shows that significant modifications in design and

operational parameters are required to uprate the boiler section in order to ensure that the heat is effectively converted to steam and also to improve the combustion efficiency of the incinerator.

The computed air flows and burning rates in the furnace revealed an ineffective utilization of the combustion system. The calculated burning rates supported by the heat release rates, showed that the stoker zones 2 and 3 alone yielded an hourly capacity of 4325 kg/hr, or approximately 60 % of the rated furnace capacity. This indicated an ineffective use of the last two stoker sections and excessive burning rates on the second and third stoker sections. The consequence of this type of the operation (exposing the stoker surface to excessive temperatures) was the rapid deterioration of the stoker surface at approximately the midpoint of the second roller from the feed chute.

By computing the required air flow on the basis of the rated burning rate and applying the appropriate stoker efficiency factor, the $\frac{\text{under fire air}}{\text{stoichiometric air}}$ ratio for all the 6 rollers was estimated which showed an inadequate distribution of the underfire air flow throughout the system.

The values obtained for drying, pyrolysis and gasification rates and the air flows were used as the preliminary input data for the development of the mathematical model of the Sheffield incinerator plant (FLUENT modelling).

Chapter 4

Mathematical Modelling of Combustion Processes

Virtually all the new research and development techniques in combustion technology involve the application of computational fluid dynamics to combustor design. This seems to be the best approach to solving design problems. Mathematical modelling thus is seen as an inherent part of practically all combustion research programmes.

This chapter describes modelling of the Sheffield municipal incinerator. A combustion model of the Essenhigh type was employed to model the solid refuse bed on top of the travelling grate. In addition a computational package (FLUENT) was used to model the three dimensional reacting flows within the incinerator geometry. Firstly the solid bed model will be described. Gaseous phase modelling and its application to the Sheffield incinerator plant is then discussed.

4.1 Simplified Combustion Model [59], [60]

The overall solid waste combustion process for a travelling grate-type incinerator can be separated into two distinct regions (figure 4.1):

- Region 1 - The porous solid waste,
- Region 2 - The flame zone adjacent to the regressing surface.

Under the assumption of constant thermal properties in each region, no heat loss to the walls, and a uniform speed of grate travel, the following equations apply:

Region 1:

$$U_{gr}\rho_w C_w \frac{\partial T_1}{\partial x} + U_a \rho_a C_a \frac{\partial T_1}{\partial y} = k_w \frac{\partial^2 T_1}{\partial y^2} \quad (4.1)$$

Region 2:

$$\left(\rho_a U_a - \rho_g U_{gr} \frac{\partial y_s}{\partial x} \right) C_g \frac{\partial T_2}{\partial y} = k_g \frac{\partial^2 T_2}{\partial y^2} + \dot{Q} \quad (4.2)$$

An exact analytical solution of these energy equations seems unlikely. Thus several simplifying assumptions were made to yield a tractable model.

The horizontal temperature gradients were considered to be small compared to vertical gradients. The heat generation term in the combustion zone \dot{Q} was assumed to occur at a boundary only. This is an approximation that is often used in the analysis of combustion for solid rocket propellant.

The regression rate derivative ($\partial y_s / \partial x$) was neglected in eq. 4.2 to obtain a quasi-steady approximation. The surface position can then be obtained by numerical integration in the x-direction. With these simplifications, the energy equation in the waste becomes:

$$\dot{m}_a C_a \frac{\partial T_1}{\partial y} = \bar{k}_w \frac{\partial^2 T_1}{\partial y^2} \quad (4.3)$$

corresponding boundary conditions are:

$$T_1 = T_0 \quad \text{at} \quad y = 0$$

$$T_1 = T_s \quad \text{at} \quad y = y_s$$

Similarly, the simplified energy equation for the combustion region and the corresponding boundary conditions are:

$$\dot{m}_a C_g \frac{\partial T_2}{\partial y} = \bar{k}_g \frac{\partial^2 T_2}{\partial y^2} \quad (4.4)$$

$$T_2 = T_s \quad \text{at} \quad y = y_s$$

$$T_2 = T_f \quad \text{at} \quad y = y_f$$

The two regions (solutions) are coupled at the surface by the heat flux expression,

$$-\bar{k}_g \frac{\partial T_2}{\partial y} = -\bar{k}_w \frac{\partial T_1}{\partial y} + \dot{m}_s Q_s \quad (4.5)$$

The above equations can be solved in a straight-forward manner to yield an expression that relates the surface regression rate to other system parameters,

$$\frac{\dot{m}_a C_a (T_s - T_o)}{1 - \exp(-\dot{m}_a C_a y_s / \bar{k}_w)} - \frac{\dot{m}_g C_g (T_f - T_s) \exp(-\dot{m}_g C_g y^* / \bar{k}_g)}{1 - \exp(-\dot{m}_g C_g y^* / \bar{k}_g)} = \dot{m}_s \dot{Q}_s$$

The mass regression rate of the solid waste surface can be expressed in terms of an Arrhenius expression;

$$\dot{m}_s = A_s \exp(-E_s / RT_s)$$

This results in an implicit expression for the surface temperature T_s and the actual oxidizer to fuel mass ratio.

Finally, the thickness of the flame zone y^* can be approximated;

$$y^* = \frac{\bar{k}_g}{C_g \dot{m}_s}$$

4.2 Mathematical Model For The Refuse Bed

Let us first consider the history of a combustible element in the refuse bed. Typically such an element is heated primarily by radiation from the overfire region and from the burning refuse bed. As its temperature increases it will lose its free moisture at 212 °F (100 °C), pyrolyze at 500 °F (260 °C), ignite at 600 °F (316 °C) and then burn vigorously until either the oxygen surrounding the element is depleted or all the element is devolatilized leaving a carbonaceous char. The residual charred or partially charred element may undergo further pyrolysis, be gasified by CO₂ or H₂O to yield CO or CO and H₂, or be oxidized by free oxygen directly to CO₂ [61].

In the heterogeneous bed all the above processes may be occurring simultaneously within a section of the bed since neighbouring fuel elements vary widely in size and composition. Despite these complications and the additional complexity introduced by the substantial temperature and concentration gradients that may be present in the larger fuel elements, it is convenient for purposes of modelling to subdivide the burning refuse bed into well defined zones as shown in fig. 4.2.

As can be seen from the simplified qualitative model of the refuse bed [43], shown in figure 4.2, drying and ignition waves propagate through the refuse followed by a devolatilization zone. The gases from the pyrolysis section pass through the char bed from the top of which a mixture of mainly low-molecular weight gases emerge with small amounts of soot and tars. The char that is formed follows an overfeed burning mechanism.

4.2.1 Ignition of Refuse Bed

A combustible element in a fuel bed may receive the thermal energy required for drying, pyrolysis and ignition via a number of different mechanisms. In the overfeed bed the thermal energy is supplied by radiation from the overbed region (from both the hot combustion gases and the refractory walls) by convective heating of the combustion gases flowing up through the fuel bed and by radiative heating from the combustion zone of the fuel bed. In the underfeed bed the major portion of the thermal energy is supplied via radiation from the combustion zone directly behind the ignition front, while the remainder is supplied by conduction through the fuel [62]. In case of the travelling grate stoker the fuel at the top of the bed near the feed end of the grate is heated solely by radiation from the overbed region. Once the ignition plane progresses down into the fuel bed, as shown in figure 4.2, the thermal energy required is transferred to the fuel in a manner analogous to the underfeed case. It is important to keep the underfire air rate low at the entrance to the travelling grate stoker in order to insure that ignition is achieved for the larger particles and for those with high moisture contents. Subsequently, as the ignition plane propagates through the bed, it is again necessary to supply the right amount of air through the grate so as not to hinder the progress of the ignition wave. Ideally the underfire air should be set at the value that gives the maximum possible ignition rate. Practically this is impossible, because not enough is known about the processes of ignition propagation for this value to be determined on an appropriate basis. Qualitatively it can be expected that the ignition rate will be a function of underfire air preheat and supply rate [63], particle size [64], refuse type and moisture content [65].

For refuse, Kaiser's tests on the Oceanside Incinerator [46] indicated that the ignition rate varied from 0.3 ft/min for wet refuse to 0.5 ft/min for average refuse. The ignition rate would be expected to decrease as the moisture content of the refuse increased since there will be a decrease in the total heat liberated within the bed that is available for heating up fresh refuse. Present theories do not give an indication of how the underfire air rate should be varied to take into account the different refuse moisture contents.

4.2.2 Drying Front

The heat effects associated with drying are greater than those associated with pyrolysis and therefore for a high moisture content fuel such as refuse, the drying heat load will be the only one of importance. The moisture content of a fuel particle can obviously affect the time required for the particle to ignite and the drying of the particle may provide the limiting step in the overall combustion process. The drying behaviour of a particular particle will depend on many factors; amount of moisture(both free and bound), micro and macroscopic structure of the particle, its diathermicity and the heating rate itself. None of these factors has been studied in enough detail to permit anything but a crude picture to be established for a 'typical' refuse particle.

There will, naturally, be a wide range of behaviour in the drying characteristics of refuse components. Only the two extremes of this range will be discussed here. These limits correspond to the cases where 1) the rate of heat transfer to the particle is much higher than the rate of internal diffusion of water and 2) the rate of internal diffusion of water is high enough for the surface temperature to remain in the vicinity of the vapourization temperature of water [66].

For the first case it is assumed that at the high heating rates associated with a fuel bed, the solid exhibits drying characteristics that resemble the "falling rate period" in drying operations, and that a vapourization plane will retreat into the material as it is heated. This model, at least for wet wood irradiated with intensities from 2.7 to 4.2×10^4 Btu/hr ft², has been observed to fit experimental results reasonably well [66]. For the second

extreme of behaviour, it is assumed that the internal diffusion of water is very rapid. In this case, the drying time can be calculated from the amount of heat that must be transferred to the particle to supply all the heat for drying under the assumption that the surface remains at 212 °F (100 °C).

The next consideration is how the moisture content of fuel (refuse) hinders the combustion rate. This may be estimated as follows. Assuming a fixed surface temperature T_s^o and a linear temperature distribution in the particle (which will be valid for high moisture contents), the progress of the drying front can be readily shown to be given by [43];

$$\frac{dx}{dt} = \sqrt{\frac{k_s^d(T_s^o - T_s^v)}{2\Delta H_v \cdot \rho_s^d \cdot t}}$$

where k_s^d = thermal conductivity of the dry solid bed, T_s^v = temperature at the drying front, ρ_s^d = dry density of the solid, t = time and H_v = latent heat of vapourization of water.

4.2.3 Pyrolysis Front

When the internal rate of diffusion of moisture is low, the surface temperature of the fuel particles will increase slowly until ignition is achieved. Depending on the particle's size and moisture content, this may take place over a period of a few minutes after the main ignition front has passed by. After the surface reaches an ignition temperature, the particle will continue to pyrolyze and burn until either all the oxygen surrounding the element is consumed or the rate of generation of pyrolysis products falls below the level required to sustain ignition. The latter condition would be achieved if the heat supplied to the fuel element was not great enough to drive the vapourization plane at a rate sufficient to supply the required amount of dry pyroizable material. The surface of a fuel element, shortly after the ignition plane has passed it, will begin to char. It will then be oxidized by any available O_2 or will react with CO_2 and H_2O according to the reactions $C + CO_2 = 2 CO$ and $C + H_2O = H_2 + CO$. Only the very small particles will burn out completely at this stage, and the larger ones will still be drying and pyrolyzing

until all the oxygen in the underfire air is consumed [67].

For a fuel element in which the rate of diffusion of moisture is rapid, the heat sink will cause local quenching of ignition and combustion. These particles and those surrounding them will then remain in this quenched state until all the moisture from the fuel element has been removed and there is enough oxygen and heat supplied to the element for it to ignite and burn. If the residence time in the furnace is not long enough, these elements will be discharged incompletely combusted and may cause some of the surrounding particles to be discharged in a similar state.

Bamford, Crank and Malan [68] indicated that a pyrolysis product generation rate greater than 1.84 lb/hr ft² (8.96 kg/hr m²) is necessary for spontaneous combustion to occur. For the conditions in a refuse bed, where some flame is present, this pyrolysis product generation rate should provide an upper bound for the rate required to sustain combustion. Assuming that the pyrolysis reactions occur instantaneously above a critical temperature T_s^c , the rate of generation of pyrolysis products is then:

$$\dot{R}_p = \frac{W_p(T_s^o - T_s^c)}{2(T_s^o - T_s^v)} \sqrt{\frac{k_s^d(T_s^o - T_s^v)}{2\Delta\bar{H}_v \cdot \rho_s^d \cdot t}}$$

Where W_p is the mass of pyrolysis products per unit volume of refuse fuel. Inserting typical values for the Sheffield refuse into the above equation: $\rho_s^d = 50$ lb/ft³, $k_s^d = 0.2$ Btu/hr.ft °F, $T_s^o = 1800$ °F, $T_s^v = 212$ °F, $W_p = 30$ lb/ft³, $\Delta\bar{H}_v = 600$ Btu/lb (for 35% moisture content) gives:

$$\dot{R}_p \simeq \frac{0.85}{\sqrt{t}}$$

Using the Bamford, Crank and Malan criteria for sustaining combustion, the rate of pyrolysis product generation would fall below the threshold level only after a period of 0.2 hr. It can be hypothesized, therefore, that drying may limit the pyrolysis rate to the extent that it will hinder active flaming. Some further elementary calculations show that the heat load associated with the movement of the drying wave will not act as a severe local heat sink, as the enthalpy required can be readily supplied by convective transfer from the combustion gas and radiative heat transfer from surrounding elements.

4.2.4 Active Burning And Zero Free O₂ Zones

The only exothermic reactions taking place within the bed will consist of the reaction of oxygen with char and pyrolysis products. The very high rate of reaction of oxygen with both char and pyrolysis products suggests that all the oxygen in the underfire air will be quickly consumed within a small zone just behind the ignition front; this behaviour was observed in the coal bed studies of Kreisinger et al [7]. The heat released within this zone provides the only source of energy within the fuel bed to dry and pyrolyze the fuel and to sustain ignition.

Active burning will take place in a zone whose depth is determined by the rate of consumption of underfire oxygen in both volatile and char combustion. Burning rates in coal beds were found by Kreisinger et al [7] to be approximately proportional to underfire air supply rate unless the burning rate was restricted by the ignition rate. Roughly the same behaviour can be expected in a refuse bed. Beyond the point of oxygen depletion, additional release of volatiles will occur from the larger particles and the char will be gasified by the CO₂ and H₂O rising from the burning zone. Up to the point where the ignition wave reaches the grate, the burning action will be of the unrestricted underfeed type. After the ignition plane has reached the grate, combustion of the residual char will be limited by the supply of oxygen. The CO₂ released on combustion in this region will partially react with the remaining char to yield CO.

4.2.5 Solid Bed Gasification

The following gasification model of the bed burning process [40] was used to determine the char gasification rate inside the refuse bed. Assumptions made were:

- 1 - The refuse bed is presumed to consist of solid particles that are mainly carbon and inerts, packed randomly on top of the grate, with air supplied from below and fresh fuel from above;
- 2 - A uniform porosity through the bed is assumed;
- 3 - Temperature through the bed is uniform;

4 - The velocity of flow through the pores of the bed is sufficiently slow for the heterogeneous reaction to be dominated by diffusion.

Reactions in the spaces between the particles are then, according to the "Three Zone Theory [69]:

1 - Oxygen reacting heterogeneously with carbon to produce some CO₂ but mainly CO,

2 - CO₂ reacting heterogeneously with carbon being reduced to CO,

3 - CO and oxygen reacting homogeneously in the gas phase to oxidize back to CO₂.

Consider the elemental volume of the bed regarded simply as a porous solid of porosity ϵ . The kinetic equations can now be written for the three reactions listed above. For the two heterogeneous reactions (O₂ and CO₂ with solid carbon), the velocity constant k determines the rate of reaction per unit of the pore surface. Knowing that reaction is diffusion dominated, the reactant-gas concentration (O₂ and CO₂) at the solid surface can be assumed to be nearly zero. Therefore the specific rate of reaction will be proportional to the main stream or average concentration across a pore. If this concentration written as moles per unit volume is X , then assuming A is the average pore surface area of the bed (and will be a function of porosity and particle size, etc.), the molar rates of the carbon removal (dm/dt) by the two reactions in a volume element V are given by:

1 - For C reacting with O₂ to give CO (mainly) by the reaction;



$$(dm_1/dt) = 2(k'_1.A_s).X_1.\partial V_s = 2.K_1.X_1.\partial V_s \quad (4.7)$$

2 - For C reacting with CO₂ to give CO by the reaction;



$$(dm_2/dt) = (k'_2.A_s).X_2.\partial V_s = K_2.X_2.\partial V_s \quad (4.9)$$

where by this formulation the subscripts 1 and 2 refer to the C/O and the C/CO₂ reactions respectively. k' denoting reaction with respect to unit surface area, becomes K by multiplication with A_s which in turn denotes the reaction with respect to unit volume of bed.

For the overall gas phase reaction given by;



the details of the kinetic scheme are involved, requiring reaction with OH as a key intermediate step. Fortunately there is evidence that the rate of CO₂ formation can be represented in the phenomenological kinetics by the following equation [69]:

$$dY_2'/dt = k_3.Y_3.Y_1^m \quad (4.11)$$

where Y_2' indicates the mole fraction of CO₂ formed by this reaction alone and m is an index apparently lying between 0 and 1.0 [69]. As a result of reaction, as a volume element of gas moves up through the bed, the gas concentrations change and the gas volume increases (at constant temperature and pressure) due to CO formation. Suppose at some point in the bed we have a volume element of bed V_s containing a volume V of gas. This gas volume is assumed to remain in this position for a small period of time ∂t during which reaction takes place and at the end of which the gas volume moves on into the next adjacent volume element of bed. Suppose the total number of moles in the gas volume ∂V_g is M_o at the start of reaction. Then,

$$M = N + N_1 + N_2 + N_3 \quad (4.12)$$

where N is the number of inert moles (nitrogen, etc.) and the subscripts 1, 2 and 3 refer to O₂, CO₂ and CO. If δm_1 moles of carbon form CO by reaction with oxygen and δm_2 by reaction with CO₂, the increase in CO from these two reactions is $(\delta m_1 + 2\delta m_2)$ and the increases in N_1 and N_2 are $(-\delta m_1/2)$ and (δm_2) respectively. There is also an increase in CO₂ to the extent (δN_2) moles due to the gas-phase reaction and corresponding increases to O₂ and CO to the extent $(-\delta N_2'/2)$ and $(-\delta N_2')$ respectively. The net molar increases of the three gases are therefore:

$$\delta N_1 = (-\delta m_1/2) - (\delta N_2'/2) \quad (4.13)$$

$$\delta N_2 = (-\delta m_2) + (\delta N_2') \quad (4.14)$$

$$\delta N_3 = (\delta m_1 + 2\delta m_2) - (\delta N_2') \quad (4.15)$$

The total molar increases δM is the sum of the $\delta N_s'$, i.e.;

$$\delta M = \delta N_1 + \delta N_2 + \delta N_3 = \frac{\delta m_1}{2} + \delta m_2 - \delta N_2' = \frac{\delta N_3}{2} \quad (4.16)$$

or,

$$M - M_o = N_3/2 \quad (4.17)$$

If $N_3 = 0$ when the air enters the bed (at time $t = 0$), then $M = M_o$. If Y is the mole fraction of inerts in the gas volume in the bed, then, since N remains unchanged, $N = Y_o \times M_o = Y M$; therefore,

$$Y = Y_o.(M_o/M) \quad (4.18)$$

Similarly defining $Y_3 = N_3/M$, then substituting for N_3 by equation 4.17 and for M by equation 4.18, we obtain

$$Y = Y_o.(1 - Y_3/2) \quad (4.19)$$

Since the total of all mole fractions must be unity, we have for the input condition respectively:

$$Y_1 + Y_2 + Y_3 = 1 - Y \quad (4.20)$$

$$Y_1^o = (1 - Y_o) \quad (4.21)$$

Eliminating Y and Y_o between these last three equations yields:

$$Y_1 + Y_2 + (Y_3/2).(1 + Y_1^o) = Y_1^o \quad (4.22)$$

which is the general molar balance required. It enables calculation of any one of the three gases if either of the other two are measured. Now, the rate of reaction for any one of the above reactions can be found as follows:

Consider a horizontal thin element of the refuse bed of unit horizontal area and thickness Δx . Its volume (δV_s) is therefore Δx and the void volume (δV_g) containing the gas is $\epsilon \Delta x$. If reaction proceeds for a time δt , the mass of carbon removed in that time by the

two heterogeneous reactions (δm) is given by multiplying the rate equations 4.10 and 4.12 by δt ;

$$2\delta N_1 + \delta N_2 = -\delta m_1 - \delta_2 = -2.k_1.X_1\delta V_s.\delta t - k_2X_2\delta V_s\delta t \quad (4.23)$$

Dividing by $\delta V_s = \delta V_g / \epsilon$ converts δN into a change in number of moles per unit volume δX . Dividing again on both sides by the number of moles per unit volume (which is a constant at constant temperature and pressure) yields Y (the mole fraction) in place of X . Dividing by δt and taking limits gives after rearranging,

$$[2\epsilon (dY_1/dt) + 2.k_1Y_1] + [\epsilon (dY_2/dt) + k_2.Y_2] = 0 \quad (4.24)$$

Dividing through by ϵ and writing $(k/\epsilon) = n$, the equation becomes:

$$[2(dY_1/dt) + 2n_1.Y_1] + [(dY_2/dt) + n_2Y_2] = 0 \quad (4.25)$$

Each of the two expressions in the brackets are individually simple standard forms, and each is equal to some function $f(t)$ which is determined by the gas phase reaction. Since conversion of N to Y by the divisions described above converts N'_2 to Y'_2 in equation 4.13, then combining equation 4.13 with 4.11 yields:

$$f(t) = n_3.Y_3.Y_1^m \quad (4.26)$$

Simultaneous solution of this with equation 4.25 will generate the equations required for the calculation of char gasification rate. Now, if we assume that in the above equations k_1 and k_2 depend primarily on diffusion, then they should differ only by the difference between the diffusion coefficients for oxygen diffusing through nitrogen (and neglecting any Stefan flow effects which is valid at the high dilution levels encountered in air). To a first approximation or better, these diffusion coefficients are the same ($0.18 \text{ cm}^2/\text{sec}$ for oxygen, compared with 0.14 for CO_2) and the temperature coefficients are also about the same. Therefore we may write;

$$n_1 \simeq n_2 \simeq n_3 \quad (4.27)$$

Equation 4.25 now integrates directly, giving;

$$Y_1 + (Y_2/2) = Y_1^o.exp(-nt) \quad (4.28)$$

and $Y_2 = 0$ at $t = 0$

Based on the above analysis, the char gasification rate of the refuse bed as a function of the area air supply rate, \dot{G}_A , and the relative carbon saturation factor, f_{rcs} (as proposed by Essenhigh et al [61]) can be written as:

$$F_A = \frac{(3/4) \cdot p_m \cdot \dot{G}_A \cdot f_{rcs}}{(1 - A - M)(1 - V)} \quad (4.29)$$

where V , A and M are the volatile fraction, ash, and moisture of the refuse and p_m is the mass fraction of oxygen in air. (For more detailed analysis of the gasification model and derivation of equation 4.29, refer to references [59] and [61]).

In the equation 4.30, the rate of supply of oxygen to the combustion zone by the undergrate air is $p_m \dot{G}_A$ (lb/ft² hr). Assuming all the carbon dioxide formed in the combustion zone is reduced to carbon monoxide by the time the gases reach the top of the gasification zone, the carbon burning rate will be $\frac{(2M_C)p_m \dot{G}_A}{M_{O_2}}$, where M_C and M_{O_2} are the molecular weights of C and O₂. If the refuse bed is not deep enough to permit complete reduction of CO₂ to CO, the carbon burning rate becomes $0.75 p_m \dot{G}_A f_{rcs}$ (lb/ft² hr).

The limits for f_{rcs} is 1 for complete conversion of char to CO and 0.5 for complete conversion of char to CO₂. Usually for refuse f_{rcs} is about 0.6 to 0.7 (for a bed depth of 0.5 m to 1 m). To calculate the total refuse burning rate from this carbon burning rate, the volatile, moisture and ash content of the refuse must be considered. If the volatile fraction of the refuse on a dry ash-free basis is \bar{V} , each pound of carbon is produced from $\frac{1}{1-\bar{V}}$ pounds of dry inert-free refuse and one pound of char is produced from $\frac{1}{(1-\bar{V})(1-\bar{A}-\bar{M})}$ pounds of as-fired refuse if A and M are the ash and moisture content of as-fired refuse.

4.3 Mathematical Model for Over-Bed Region (Gaseous Phase)

The FLUENT computer code together with experimental data were used to model the over-bed region inside the incinerator.

4.3.1 Primary Air Distributions (Modelling of Riddling Hoppers and Hollow Grate Assemblies)

In the Sheffield incinerator a large proportion of the combustion air (primary air 80-90% of total air) enters the furnace through the 2 mm gaps at the surface of the rollers and the refuse bed on top of the rollers. This flow may be expected to play a major role in the flame stabilisation and complete burning of the refuse inside the incinerator. It was therefore important to ensure that this feature could be simulated correctly before proceeding with full incinerator modelling.

The loss of head by air flow through the roller gaps and the refuse bed on top of each roller was investigated using the FLUENT code. The results obtained from this modelling (velocity profiles and pressure drops across the refuse bed and the rollers) were used as the inlet boundary conditions for modelling of the over-bed region

Description of the individual stoker air zones :

Combustion primary air is admitted to the undergrate areas by six ports, one for each grate roll. Under each grate roll unit, there is a riddlings hopper to receive the particles of grit passing through the grate and products from the hoppers discharge continuously to the disposal system below. The hoppers are fitted along both sides with air plenum chambers and undergrate combustion air is passed to each grate roll through control dampers fitted in the side of the hoppers.

Modelling and Calculation Conditions:

Cartesian coordinates were employed to model the hoppers, 6 rollers and the refuse bed on top of the rollers. Figures 4.3 and 4.4 show the finite difference grid used for the solution as well as the outline of the riddling hopper and the roller. The dense solid lines in this figure indicate grid lines and wall boundaries. Breaks in this boundary indicate inlet and exit zones. 30×38×7 grid nodes were employed in the x, y and z directions respectively. Cartesian coordinates necessiated the use of a stepped wall to

represent the hoppers' side walls. Half the main body of each of the rollers and hoppers in the z direction was modelled by using the symmetry cells. The precise meaning of the symmetry cell is best explained by defining it as a 'wall without shear' or 'slip wall'. This means that fluid can not flow through it but it does not otherwise affect the flow. Using these cells can save a great deal of computation wherever symmetry conditions are known to exist.

Fluent's porous media model was used to model the solid refuse bed on top of each roller inside the incinerator. The model was used to simulate the air flow through the solid bed and to determine the flow resistance of the refuse bed present in the air flow path on top of each roller. This model consists of a modified Birkman's equation (which is an extension of Darcy's law) with a second order inertial correction [70];

$$\nabla P = \frac{\mu}{k} \cdot v + \mu \cdot D^2 \cdot v + C_2 \cdot \frac{1}{2} \cdot \rho \cdot |v| \cdot v$$

The above equation relates the pressure gradient in the porous cell to the flow velocity in the porous cell. Two constants are required as inputs;

k = permeability specified in each component direction,

and C_2 = internal resistance factor (m^{-1})

Permeability has units m^2 in SI units and Darcys in British units (Note that 1 Darcy = $9.87 \times 10^{-13} m^2$)

In our modelling work, first the depth of solid bed on top of each roller was estimated (as shown in chapter 3). The loss coefficient based upon the refuse bed velocity was then converted to the loss coefficient based upon the velocity at 100 % open area [71]. Finally the resultant loss coefficient value was adjusted for the thickness of the refuse bed on top of each roller. These data were supplied to the FLUENT code using the 'physical constant' option.

Porous zone properties (solid bed on top of each roller) were set as follows;

| Roller no. | Zone | Kx m ² | Ky m ² | Kz m ² | C2 m ⁻¹ |
|------------|------|----------------------|----------------------|----------------------|-----------------------|
| 1 | ★1 | 10 ¹¹ | 10 ¹¹ | 10 ¹¹ | 872 |
| 2 | ★1 | 10 ¹¹ | 10 ¹¹ | 10 ¹¹ | 1023 |
| 3 | ★1 | 10 ¹¹ | 10 ¹¹ | 10 ¹¹ | 952 |
| 4 | ★1 | 10 ¹¹ | 10 ¹¹ | 10 ¹¹ | 865 |
| 5 | ★1 | 10 ¹¹ | 10 ¹¹ | 10 ¹¹ | 743 |
| 6 | ★1 | 10 ¹¹ | 10 ¹¹ | 10 ¹¹ | 684 |

where Kx = permeability in x direction, Ky = permeability in y direction, Kz = permeability in z direction and C2 = inertial resistance factor.

Isothermal modelling was carried out separately for each of the riddling hoppers and hollow grate assemblies at a temperature of 300 K and a pressure of 730 mmHg. The inlet boundary conditions (air flows) for each of the rollers are summarized below;

Effective area of 6 rollers (3m wide grate) = 36 m²

Free area through grate = 7%

Free air surface = 36 × 0.07 = 2.52 m²

Free air surface/Roller = $\frac{2.52}{6} = 0.420$ m²

Primary (F.D.) air flow = 80% air required for combustion

Therefore: Vol. primary (F.D) air = 6400 kg/hr × 8 m³/kg refuse × 0.8 = 40960 m³/hr

Total primary air = 11.37 m³/sec

Now, using the experimental data (as shown in chapter 2), we can calculate the area and the amount of undergrate air for each of the primary air inlet cell in our model [72].

Air Flow Distribution for Each Roller

| Inlet | No. of Inlets | Inlet Area (m ²) | %Total Air |
|----------|---------------|------------------------------|------------|
| Roller 1 | 1 | 0.20 | 20 |
| Roller 2 | 1 | 0.20 | 26 |
| Roller 3 | 1 | 0.20 | 26 |
| Roller 4 | 1 | 0.20 | 16 |
| Roller 5 | 1 | 0.20 | 12 |
| Roller 6 | 1 | 0.20 | 2 |

An inlet turbulence intensity of 10% was assumed. Turbulence intensity for this study has been defined as [70];

$$Intensity = \left[\sqrt{\frac{\overline{u'^2}}{\overline{u}}} \right] \times 100\% = \left[\frac{\sqrt{2k/3}}{\overline{u}} \right] \times 100\%$$

The dissipation rate boundary conditions were obtained from the following relationship [70];

$$\epsilon = \frac{(C_\mu)^{0.75} \cdot k^{1.5}}{0.07 \cdot \left[\frac{A}{\pi}\right]^{0.5}}$$

where A is the inlet opening area.

For the isothermal calculation, the u, v, and w momentum equations were solved in cartesian coordinates and the k- ϵ turbulence model was employed. Using the k- ϵ model requires the solution of the conservation of mass and momentum in their time averaged form together with the solution of transport equations for kinetic energy of turbulence (k) and its dissipation rate (ϵ). The set of governing equations for the flow field is given in appendix 5 (equations A1 to A6). For compactness cartesian tensor notation has been employed to present the formulation.

Calculations were performed using an IBM compatible computer where the problem required a memory size of 5 megabytes. With this, iterations were performed until the

sum of normalized residuals fell to a value of 1×10^{-4} . Approximately 3 hours of cpu time were required for the rollers' cold flow modelling calculations. The velocity vector plot in two and three dimensional view (plane 4) and the geometrical outline are shown in figures 4.5, 4.6 and 4.7 respectively.

Under Relaxation Factors For Cold Model

| Variable | Factors (cold flow) |
|-------------|---------------------|
| u | 0.5 |
| v | 0.5 |
| w | 0.5 |
| k | 0.4 |
| ϵ | 0.4 |
| Species | - |
| Enthalpy | - |
| Temperature | - |
| μ | 0.2 |

The printout of the FLUENT case file used for the modelling of the rollers (i.e. roller no. 2) is given in appendix 6.

4.3.2 Mathematical Model for Overbed Region; Gaseous Phase

Fluent code (version 2.95) was used for modelling of the incinerator. For this problem the rollers and the furnace roof were modelled by the use of a stepped wall approximation. Half the main body of the furnace, shaft and the boiler in the z direction was modelled by using the symmetry cells. Cartesian coordinates with $30 \times 38 \times 9$ grid nodes were used in the x, y and z directions respectively. Some *simplifications* to the modelled geometry were made since the incinerator shape was so complicated. This will always be necessary

when cylindrical or cartesian coordinates are employed. At the same time attempts were made to ensure a sufficiently fine grid spacing in regions where steep gradients of the dependent variables were expected. Inevitably in fitting a difficult geometry, some grid nodes were effectively wasted. Efforts were made to minimize this. The entering primary and secondary air were modelled as discrete inlets and porous cells were used to model the boiler tubes.

Often in engineering situations devices are encountered through which the pressure drop is proportional to the velocity head of the fluid. Tube banks are such devices. When they are part of a much larger flow system (as it is in our modelling work), it is often impractical to model them in sufficient detail to predict the losses through them. For this reason, it was convenient to model the tube banks inside the incinerator as a porous region of flow field, defining a known flow resistance using the inertial resistance factor C2.

The porous zone properties (boiler tubes) were set as follows;

Zone = *1,

Kx = Permeability in x direction = 10^{11} m^2 ,

Ky = Permeability in y direction = 10^{11} m^2 ,

Kz = Permeability in z direction = 10^{11} m^2 ,

C2 = Inertial resistance factor = $1.121 \times 10^3 \text{ m}^{-1}$.

The effective grate area within the furnace burning area was established at 37.9 m^2 , this was equivalent to a grate loading of $293 \text{ kg/m}^2 \text{ hr}$, at a 272 metric ton per day loading. Based on a grate 3 m in width by 15.54 m long in the active burning zones, the primary air velocities at the surface of the solid refuse bed were determined for each stoker air zone prior to hot flow modelling. The following table summarizes the combustion air flow distribution for the reacting flow model;

Air Flow Distribution

| Inlet | No. of Inlets | Inlet Area | %Total Air |
|-----------------------|---------------|------------|------------|
| Primary air: | | | |
| Roller 1 | 28 | 0.06 | 14 |
| Roller 2 | 28 | 0.06 | 23 |
| Roller 3 | 28 | 0.06 | 21 |
| Roller 4 | 28 | 0.06 | 12 |
| Roller 5 | 28 | 0.06 | 8 |
| Roller 6 | 28 | 0.06 | 2 |
| Secondary air: | | | |
| Front secondary | 5 | 0.06 | 6 |
| Rear secondary | 5 | 0.06 | 14 |
| <i>Total</i> | - | - | <u>100</u> |

The entering air possessed vertical velocity components but no transverse components. The turbulence intensity for primary air inlets and the dissipation rate boundary condition were calculated and used as input data in the model. These are as follows;

| Roller no. | Inlet Turbulence m^2/s^2 | Dissipation rate m^2/s^3 |
|------------|-------------------------------|-------------------------------|
| I1 | 6.6×10^{-4} | 2.7×10^{-3} |
| I2 | 3.1×10^{-3} | 2.5×10^{-2} |
| I3 | 3.1×10^{-3} | 2.5×10^{-2} |
| I4 | 6.6×10^{-4} | 2.7×10^{-3} |

$$I5 \quad 9.6 \times 10^{-5} \quad 1.5 \times 10^{-4}$$

$$I6 \quad 2.9 \times 10^{-6} \quad 8.2 \times 10^{-7}$$

Isothermal modelling was carried out for a total combustion air flow rate of 11.3 m³/sec at a temperature of 300 K and a pressure of 730 mmHg. The results of this calculation were then employed as a 'first guess' flow field for further trials. For the isothermal calculation, the u, v, and w momentum equations were solved together with the k and ϵ transport equations.

The two step chemical reaction mechanism (equations B4 to B8 , see appendix 5) was used for hot flow modelling.

The parameters employed in the numerical solution procedures are summarized below. The available computer time has not made it practical to fully optimise all of these parameters. Past experience with similar problems is the only guide to parameter selection. In the case of under relaxation factors, the choice was a trade off between stability and speed of convergence.

The under relaxation factors used for the hot flow model are given below;

Under Relaxation Factors for Hot Flow Model

| Variable | Factors (cold flow) | Factors (hot flow) |
|-------------|---------------------|--------------------|
| u | 0.6 | 0.6 |
| v | 0.6 | 0.6 |
| w | 0.6 | 0.6 |
| k | 0.5 | 0.5 |
| ϵ | 0.5 | 0.5 |
| Species | - | 0.9 |
| Enthalpy | - | 0.6 |
| Temperature | - | 0.8 |
| μ | 0.4 | 0.4 |

The refuse model boundary conditions and the physical properties for the Sheffield incinerator model were set as follows;

Refuse density = 200 kg/m^3

Molecular weight = 162

Approximate chemical formula = $C_6 H_{10} O_5$

Heat of combustion = 10^7 J/kg

Stoichiometric ratio = 0.6

Turbulence controlled reaction factors ; A = 4.0 and B = 0.5

Viscosity (gas) = $1.72 \times 10^{-5} \text{ kg/m.sec}$

Thermal conductivity (gas) = $2.4 \times 10^{-4} \text{ kJ/m.sec.K}$

Heat capacity (gas) = 1004 J/kg.K

The amount of raw refuse and the amount gasified on top of each roller was set in the calculation domain by using the patch option. These values were estimated from the experimental work at the plant (as shown in chapter 2). The air entering the incinerator had the same temperature and mass flow rate as did the isothermal case.

Calculations were performed using Walters 386 computer where the problem required a RAM memory size of 5 megabytes. With this, as with the isothermal case, iterations were performed until the sum of normalised residuals fell to a value of 1×10^{-4} . Approximately 5 hours of cpu time were required for the Sheffield incinerator hot flow calculation.

After the gas phase solution was obtained, the secondary phase (particulate) phase was defined using the S2 (set up phase 2) option of the 'Main' menu. Setting up the second phase was considerably more straight forward than the equivalent option for the gas phase since only the initial conditions for the particle phase was required along with some physical data. These were as follows;

A group of 10 inert particles were injected into the furnace. The particles were injected

the Magnussen type was employed with chemistry simplified to a two step process. For solution of the gas phase equations a finite difference technique was employed, using the SIMPLE algorithm and hybrid differencing. An additional Lagrangian model was employed for the prediction of the particle trajectories in the incinerator. The results obtained from mathematical modelling work will be discussed in the following chapter.

the Magnussen type was employed with chemistry simplified to a two step process. For solution of the gas phase equations a finite difference technique was employed, using the SIMPLE algorithm and hybrid differencing. An additional Lagrangian model was employed for the prediction of the particle trajectories in the incinerator. The results obtained from mathematical modelling work will be discussed in the following chapter.

Chapter 5

Discussion

Chapter 5 presents the mathematical modelling results for the overbed region (gaseous phase) and makes comparison with the experimental data. Firstly the overall performance of the model is assessed in terms of its ability to predict the isothermal and reacting flow fields within the incinerator. The model behaviour is then compared with the experimental results obtained at the Sheffield incinerator together with a more detailed discussion of the individual features.

Since the results of the computer modelling are held in storage arrays of very large size and represent complicated three dimensional distributions, presentation of the data in an intelligible form represents almost as much effort as the computations themselves. Vector plots, isometric projections, contour lines and profile graphs have been employed to interpret the results.

5.1 Results for the Sheffield municipal incinerator

5.1.1 Isothermal Flow Field Model

Cartesian coordinates with $30 \times 38 \times 9$ grid nodes were used in the x, y and z directions to model the incinerator. Some simplifications to the modelled geometry were made since the incinerator shape was so complicated. At the same time attempts were made to ensure a sufficiently fine grid spacing in regions where steep gradients of the dependent

variables were expected. Inevitably in fitting a difficult geometry, some grid nodes were effectively wasted. Efforts were made to minimize this. The grid constructed for the incinerator and the modelled incinerator in outline are shown in figures 5.1 and 5.2 respectively. The three dimensional view of the incinerator is given in figure 5.3.

The isothermal flow field prediction for the Sheffield incinerator is shown by the velocity vector plot in figures 5.4. Vectors show both magnitude and direction of the predicted velocities in each grid cell. The length of the arrow and size of the arrow head indicate the magnitude of velocity. Figure 5.4 shows the general flow pattern in a slice through the incinerator in the plane of the secondary air injection inlets for the isothermal case. The velocity vector plots clearly show that a large recirculation zone has formed inside the radiation shaft. Recirculation zones are usually formed in flows when the effect of an adverse axial pressure gradient exceeds the kinetic energy of the fluid particles and a stagnation point is produced. The impingement of undergrate air from the top of rollers 5 and 6 and the rear secondary air appears to be responsible for the small recirculation zone at the discharge end of the incinerator. Velocities at the discharge end are relatively low, i.e. 0.06 m/sec.

The vertical flow patterns at the refuse bed surface (on top of the rollers 2, 3 and 4) continue in a vertical direction entering the shaft with an average velocity of 1 m/sec. However high pressure losses appear at the nose of the rear arch and exit screen (boiler screen) accompanied by high exit velocities of up to 1.3 m/sec. Figures 5.5 and 5.6 present predicted turbulence properties for the isothermal case. As expected the level of turbulence is low inside the furnace. These regions of poor mixing might be expected to result in high localized temperatures near to the walls inside the furnace.

High levels of turbulence and dissipation rate are apparent in the shaft and near to the boiler screen where the tube bank impose a considerably high flow resistance in the gas flow path. Clearly turbulence is causing some mixing to occur in this area in the direction of the mean flow.

5.1.2 Reacting Flow Case

Figure 5.7 shows the velocity vector plot in the plane of secondary air injection slots (plane 4) for the reacting flow case. Contours of u , v and w velocities for this case are shown in figures 5.8, 5.9 and 5.10. Here the fuel is municipal waste. For the purposes of computation ease, the composition of the inert-free content of moist refuse can be simulated by $C(H_2O)_n$ with 'n' having a value of 5/6 for a dry cellulose, 1.55 for a refuse with 23% inerts and 25% moisture and 2.0 for a refuse with 23% inerts and 34% moisture [51]. The amount of the refuse and the amount gasified on top of each roller was set in the calculation domain by using the patch option. These values were obtained from the experimental work (as shown in chapter 2). The air entering the incinerator has the same temperature and mass flow rate as did the isothermal case. The results were obtained using the eddy dissipation type, two step chemistry model (FLUENT, version 2.95).

As would be expected, heat release is seen to have raised the gas flow velocities. Recirculation in the shaft is now considerably reinforced. High velocities created by the limited furnace discharge throat are aggravated by the stack effect of the rise in the shaft roof. Despite the effects outlined above, the basic flow patterns (cf. to isothermal flow field model) remain unaltered by the combustion process. This indicates the usefulness of isothermal flow visualisation methods and the isothermal flow modelling as a combustor design tool.

In the Sheffield municipal incinerator the radiation shaft is located directly over the area of active burning in the furnace (rollers 2 and 3). From figure 5.7 it can be seen that the vertical flame patterns at the refuse bed surface continue in a vertical direction entering the shaft with an average velocity of 5 m/sec. Maximum velocities along the roof arch of the furnace are seen to be as high as 7 m/sec with 1.5 m/sec velocities extending back to drying zone (top of roller 1).

The flow field inside the incinerator appears to be nearly two dimensional. This can be seen by comparing the flow patterns in different planes. The relative uniformity of

the refuse and the air distribution across the grate and the fact that the width of the furnace is relatively small compared to the vertical and horizontal dimension appears to be responsible for this phenomenon.

The predicted temperatures inside the incinerator are shown in figure 5.12 (plane 2, near to the furnace side wall) and figure 5.13 (plane 4, near to the center of furnace) . A long flame rising from the refuse bed on top of rollers 2, 3 and 4 can be seen in figure 5.14. Temperatures in excess of 2000 K are present in this area. The introduction of the secondary air through the roof arch has resulted in localized high temperatures and in stratification of the flue gas stream. This cooling of the roof arch and of the upper portion of the walls by the secondary air, while the lower portions of the walls are exposed to high flame temperatures, is apparent in figure 5.16. This results in partial slagging and general deterioration of the side walls directly above the grate surface. High refractory maintenance costs has been a major problem at the Sheffield incinerator plant in recent years. The predicted temperature at the ash discharge end is higher than expected. Discrepancies at this area may be attributed to the stepped wall approximation for the inner liner surface of the furnace in the model which causes the stagnation of gases in this area.

The predicted temperature contours confirm the presence of much cooler, air rich gases in the recirculation zone inside the radiation shaft with a local temperature of about 800 K. The drop in temperature in this area can have a significant effect on the composition of the combustion products leaving the incinerator. Predicted temperatures at the refuse feed chute end and top of the roller no. 1 (drying zone) are around 1000 K . As is shown in figure 5.13 the temperatures gradually drop as the gas flow passes through the boiler tubes and approaches the exit. Here the predicted temperatures are around 800-900 K. Figure 5.15 shows the colour raster plot of density (kg/m^3) of flue gases at plane 4. A continuous feed incinerator furnace usually produces the hottest gases near the input end of the burning grate while the gases at the discharge end are cooler because of the higher percent excess air. As can be seen from this figure , the flow from the top 'of rollers 2

and 3 is essentially vertical with warm, low density gases tending to remain at the top and to flow with higher velocity as a result of acceleration in the vertical flow from the refuse bed. The hot gases will be accelerated as they flow upwards in the pressure field produced by the denser cool gases.

Contour plots of the predicted kinetic energy of turbulence and its dissipation rate are shown in figures 5.17 and 5.18 (plane 4). These figures present predicted turbulence levels and dissipation rates inside the radiation shaft for the reacting flow case. As expected, the level of turbulence is high in the recirculation zone. It is apparent that the region of maximum mixing is at the entrance to the boiler bank where the main gas flow impinges on the surface of the first row of the tubes (spaced 2.5 inches apart from each other). Although this is clearly a very well stirred region, most of the mixing power is expended mixing air rich gases with air rich gases and is of no benefit to the combustion. Regions of poor mixing are apparent inside the furnace. Very little secondary air is used for the incineration of the municipal waste and the turbulence required for complete secondary combustion is not achieved due to the absence of high velocity secondary jets. The secondary air vertical velocity components seem to decay rapidly once they enter the furnace and there is no indication of efficient mixing of these jets with the main body of the flow.

The characteristics of the combustion process in the Sheffield municipal incinerator can be qualitatively and quantitatively determined by examining the product species concentration distributions within the incinerator enclosure.

A two step kinetic scheme together with a Magnussen type model for determining reaction rate has been able to give some indication of pollutant formation inside the incinerator. Predicted species mass fractions, i.e. F (fuel), B (carbon monoxide), C (carbon dioxide) and O (oxygen) are shown in figures 5.19, 5.20, 5.21 and 5.22 respectively.

The distribution of concentration of unburnt fuel (species F) is shown in figure 5.19 and shows, as expected, that the majority is to be found in the most active burning zone located on top of rollers 2, 3 and 4, giving rise to a fuel rich region near to the nose

of the arch roof of the furnace. Very low concentration of species F (0.02%) exits at the ash discharge end of the furnace where no combustion takes place. The relatively non-uniform distribution of species F inside the furnace enclosure in figure 5.19 indicates that this furnace configuration does not utilize the lower volume of the furnace over the grate discharge. The concentration of unburnt fuel decreases as the flue gases enter the shaft and approach the boiler exit. The concentration at the boiler exit is about 0.03%. Figure 5.20 shows the colour raster plot of species B (CO). The high concentration of CO on top of rollers 2, 3 and 4 indicates that nearly all of the refuse is pyrolyzed and gasified in this region. As can be seen from this figure, these rich CO-containing gases rising from the gasification and char burn out zones (rollers 2, 3, and 4) are accelerated as they flow into the shaft. Very little CO appears to be evolved in the discharge grate section (0.01%). CO discharge rate into the overbed volume is also relatively low in the drying and ignition zones on top of roller 1 (less than 0.005%). Predicted CO concentrations at the boiler exit are about 0.03%.

Figure 5.21 shows the concentration of CO₂ throughout the system. A relatively large percentage of CO₂ concentration is present at the grate discharge end. The slow increase in the CO₂ concentration as the main flow enters the shaft and passes through the boiler tubes can be attributed to the relatively slow oxidation of CO to CO₂. High CO₂ regions are also apparent in the shaft and the boiler section of the incinerator plant. The CO₂ concentration at the boiler exit is about 4%.

A colour raster plot of oxygen concentration (figure 5.22) shows a maxima near to the undergrate and secondary air inlets. Air-rich portions of the flow are seen near to the feed chute end of the furnace (drying zone, roller 1) and near to the ash discharge end (rollers 5 and 6). This probably improves drying and ignition with wet refuse. The low oxygen concentrations directly above the refuse bed (rollers 2, 3 and 4) indicate that fairly good combustion does occur within the bed in this region. The O₂ concentrations in the shaft and boiler tube bank are relatively low.

Detailed information on particle trajectories provides a supplement to the overall un-

derstanding of the flow field structure of the combustion chamber. Figures 5.23 to 5.28 show particle trajectories for different particle injection locations (top of rollers 1 to 6) in the plane of secondary air openings for the Sheffield incinerator plant. As can be expected from the structure of the flow field discussed earlier, particles injected from the top of rollers 2 and 3 followed the gas flow of relatively high velocity and escaped from the shaft without entering the recirculation zone (8 to 11 seconds). However, particles injected from the top of roller 1 were captured by the corner part of the recirculation zone and therefore had a significantly longer residence time (17 to 21 seconds). The particles injected from the top of rollers 4, 5 and 6 collided with the furnace wall and were captured by the small recirculation zone at the discharge end of the travelling grate incinerator.

5.2 Comparison with Experimental Results for the Sheffield Municipal Incinerator

The measurement of temperatures at the furnace exit, boiler exit, radiation shaft and inside the furnace were presented in chapter 2. Temperature measurements were made using a thermocouple and the quoted results were corrected for radiation errors. Over most of the incinerator plant, the model predicts the correct magnitude of temperature and its change with position. In the most active burning zone (top of rollers 2 and 3) the asymmetric character is apparent in both measured and calculated temperature profiles. This can be seen by comparing the temperature colour raster plots in planes 2 and 4 (figures 5.12 and 5.13). The data clearly shows the cool core in the shaft due to the major recirculation eddy and high temperature region on top of rollers 2, 3 and 4, as predicted by the model.

The low temperature secondary air entering the furnace can be seen to be giving rise to corresponding low temperatures. Figures 2.18 and 2.28 (chapter 2) show the available temperature data at furnace exit and boiler exit. Temperatures were again measured

by thermocouple. Comparison with modelling results show the temperatures to be well predicted. There is, however, some over prediction of temperature by the model at the ash discharge end of the furnace. This is too large to be explained by the approximate nature of the radiation correction made in the experimental study, but there may be a probe interference effect when measuring the temperatures in this region or more likely due to the value of the product specific heat capacity used for the modelling.

Comparisons of predicted and measured gas composition were made. Agreement between experiment and predicted carbon monoxide, carbon dioxide and oxygen concentrations are generally good. The two step kinetic model for prediction of carbon monoxide formation has performed well. Of particular note are the large peaks in CO concentrations measured on top of rollers 2 and 3. These are reliably reproduced by the model. It can be seen that close agreement is also achieved at the boiler exit between the computed and measured values. The computed CO₂ and O₂ profiles in the shaft and within the furnace enclosure also show the correct trend, although there are some over predictions. The measurements of combustor exit velocity are presented in chapter 2 and the predicted velocity profiles are shown in figure 5.7. Measurements and prediction are in reasonable agreement.

Chapter 6

Conclusions and Suggestions for Future Work

6.1 Conclusions

An extensive experimental programme was carried out at the Sheffield municipal incinerator in conjunction with the modelling study. Measurements of velocity, gas composition and temperature were made. The modelling results were generally in good agreement with the experimental work.

The principal conclusions are summarized below:

- An evaluation of the data revealed that during the tests, the unit (incinerator - boiler no. 1) operated at 51.5 percent of capacity which was lower than expected. The overall steam raising efficiency of the incinerator plant was relatively low. It was estimated that 51.48% of the gross heating value in the waste was converted to steam with the major losses associated with the stack gas, in particular the water vapour losses which include the latent heat as well as sensible heat losses. Considering the direct combustion efficiency losses, 7.24% of heat content of the waste was lost due to inefficient combustion.
- The calculated burning rates, supported by the heat release rates (estimated from the refuse bed gas analysis), showed that the stoker zones 2 and 3 alone yielded an hourly

capacity of 4325 kg/hr or nearly 60 percent of the rated furnace capacity. This indicates an ineffective use of the last two stoker sections and excessive burning rates on the second and third stoker sections.

- The total supply of the combustion air and its distribution throughout the system was inadequate. Variation of the amount of air supplied for most of the tests could not be achieved as originally planned. There was too much potential for leakage which resulted in unwanted convection air being drawn into the furnace.
- Performance tests showed that the secondary air was used only for cooling purposes and no use was made of these air jets to generate turbulence in the high intensity combustion zone where it was most needed.
- Changes to operational strategies (such as optimizing primary and secondary air distribution) greatly improved the temperature profiles and combustion efficiency. The air distribution using 59% primary, 26% secondary front and 15% secondary rear gave the best combustion conditions. The time average combustion efficiency was 99.989 % and the mean carbon monoxide (CO) concentration was only 58 ppm. The mean temperature at the combustor exit was 945 °C. In view of the importance of maintaining high combustion efficiency both to optimise steam production and minimise emissions of unburnt carbonaceous material, it is recommended that CO₂ and CO monitoring instrumentation is fitted at the plant to measure combustion efficiency on a continuous basis.
- Refuse of high moisture content burned in the incinerator with greater excess of air than drier refuse. However the data were not sufficient to decide whether this difference was due entirely to the refuse or to the other variables.
- Dry refuse yielded more CO in the pyrolysis region (top of rollers 1 and 2) than the wet refuse.
- More CO was released in the char burning zone (rollers 3 and 4) than elsewhere in the furnace and would present a large secondary air demand in this area.
- The furnace temperature distribution was found to be non-uniform which affected the incinerator performance and resulted in high refractory maintenance costs because of

partial slagging and thermal gradients (in the side areas directly above the grate). The roof secondary air openings, arranged in rows perpendicular to the center line of the furnace, were the major cause of localized high temperatures inside the furnace.

- Maximum temperatures usually occurred near the center of the combustion chamber. There were a few cases when the L.H.S. of the furnace was generally hotter than the R.H.S.

- The flue gases were discharged to the electrostatic precipitator at high temperature (approximately 300 °C), consequently the volume of the flue gases tended to be greater than anticipated and the particulate abatement plant was often overloaded.

- The emission performance tests on the Sheffield incinerator showed that the emission levels of pollutants (CO, NO and SO₂) were relatively high possibly as a result of poor mixing inside the furnace.

- Combustible pollutants appeared to be generated along the full length of the incinerator grate mainly on top of rollers 2, 3 and 4 although their discharge rate into the overbed volume was relatively low in the drying and ignition zones (top of roller 1).

- A mathematical model of the finite difference type was employed to predict the three dimensional reacting flows within the incinerator. This model formulation has proved capable of predicting all the major features in the Sheffield incinerator flow field.

- As a result of the test data and modelling of the whole process, suggestions for design improvements for the Sheffield incinerator were made which should substantially reduce emissions of pollutants and reduce the maintenance costs at the plant [73] , [74]. These are : a) replacing the existing secondary air system with secondary air nozzles and the use of more secondary air (up to 20% of total air) in order to generate turbulence in the high intensity combustion zone (top of rollers nos 2 and 3) where it is most needed and b) introducing a baffle into the main stream inside the radiation shaft in order to lower the gas temperatures and to remove the existing recirculation zone in the shaft.

6.2 Suggestions for Future Work

Much work is required in model development, application and experimental testing before the full potential of our three dimensional modelling technique can be realised.

Employing cartesian coordinates to model the complicated incinerator geometry has presented some difficulties. The use of three dimensional body fitted coordinates should take a high priority in any further studies.

Some improvements to the chemical reaction model are required for a more detailed analysis of the gaseous phase above the refuse bed. Models for the prediction of soot, oxides of nitrogen and chlorinated compounds are also required, however these are best incorporated in a post processor for the FLUENT output.

As noted in chapter 4, further work on the refuse solid bed model in a travelling grate incinerator is also an important area for research. Experimental studies will be particularly important here. Knowledge of drying, ignition, pyrolysis and actual burning rates in the incinerator primary zone will be valuable for model testing. However these are likely to be difficult to make in practice and will require extensive research work on a laboratory scale and careful experimentation on full scale units.

The further extension of the proposed model to include the effect of moisture content of the refuse in determining the overall performance of the incinerator is also required.

The mathematical model based on existing refuse burning models gave realistic results when compared to the experimental data of this programme. Data from further experimental programmes utilizing a wider range of combustion conditions could also be used to determine the flexibility of the model.

The only gaseous emissions measured during the present experiments were the combustion gases CO, NO and CO₂. Other toxic gases could be released, e.g. Dioxins during the combustion of municipal waste due to the plastic content and this area too requires investigation.

The need to monitor the composition and temperature of the flue gases leaving the combustion chamber and prior to the abatement equipment has been illustrated from the

present experimental work. Carbon dioxide and/or oxygen measurements are required to modulate the total amount of combustion air fed to the system to suit the refuse feed and composition. Carbon monoxide measurement is required to adjust the distribution of the air to optimise combustion. In addition comprehensive temperature measurements are needed to check that the required temperature at the combustor exit is being maintained. While this instrumentation is commercially available, its use on the incinerators particularly in the U.K. is minimal and considerable work is required to identify suitable equipment and monitoring technologies.

As the temperature and the gas residence time are to be set as key control parameters in the incineration of wastes, their measurements is becoming increasingly important and requires research into more accurate representative methods than those currently available.

Bibliography

- [1] 'Background Report 1: Description Of Incineration Technology', Environmental Protection Agency, Office Of Policy And Planning, Washington, U.S.A, March 1985
- [2] 'The Potential For Waste Burning', A.J. Smith and H. King, Energy From Waste Burning Symposium, Institute Of Energy, Portsmouth, 1979
- [3] 'The Hazardous Waste Inspectorate Second Report', Department Of Environment, U.K., July 1986
- [4] 'Report Of The Working Party On Refuse Disposal', Department Of Environment, HMSO, London, 1978
- [5] 'Combustion In The Fuel Bed Of Hand-Fired Furnaces', H. Kreisinger, F.K. Ovitz and C.E. Augustine, U.S. Bureau Of Mines, Technical Paper No. 137, 1946
- [6] 'Underfeed Combustion; Effect Of Preheat And Distribution Of Ash In Fuel Beds', P. Nicholls, U.S. Bureau Of Mines, Bulletin No. 387, 1954
- [7] 'Combustion Experiments With North Dakota Lignite', H. Kreisinger, C.E. Augustine and W.C. Harpster, U.S. Bureau Of Mines, Technical Paper 207, 1959
- [8] 'Experimental Studies Of Incineration In A Cylindrical Combustion Chamber', M. Weintraub, A.A. Orruing and C.H. Schwartz, U.S. Bureau Of Mines, Technical Paper No. 467, 1967

- [9] 'Combustion Of Computer Cards In A Continuous Test Incinerator; A Comparison Of Theory And Experiment', W.S. Shieh and R.H. Essenhigh, Proceedings Of National Incinerator Conference, A.S.M.E., N.Y., 1972
- [10] 'Developing Thermal Energy Release Intensity Parameter For Solid Waste', H.I. Hollander, Proceedings Of National Industrial Solid Waste Management Conference, Houston, Texas, March 1970
- [11] 'Municipal And Industrial Refuse; Composition And Rates', W.R. Niessen and A.F. Alsobrook, Proceedings Of National Incinerator Conference, A.S.M.E., N.Y., 1972
- [12] 'The Nature Of Municipal Solid Waste', W.R. Niessen and S.H. Chansky, Ibid, 1968
- [13] 'Mineral Processing', E.J. Pryor, 2nd Edition, Elsevier Publishing, 1965
- [14] 'Hand Book Of Mineral Dressing', A.F. Taggart, Elsevier Publishing, 1944
- [15] 'Sampling And Sampling Problems Relating To Minerals', D.N. Collins, Analytical Proceedings, Vol. 23, October 1986
- [16] 'Analysis Of Household Waste And Measurement Of Thermal Emissions, Resources And Conservation', K.E. Lorber, Vol. 14, 1987, pp. 205 - 223
- [17] 'Methods For Sampling And Analysis Of Waste', Paper Presented By Gendan Ltd. (Copenhagen, Denmark), For The Commission Of The European Communities, 1982
- [18] 'Private Communications', D.W. Scott and A.J. Poll, Warren Spring Laboratory, 1988
- [19] 'Sampling And Analysis Of Domestic Refuse; A Review Of Procedures At Warren Spring Laboratory', A.J. Poll, Report No. LR45S, 1987
- [20] 'Evaluation Of Furnace Temperature, Gas Residence Times And Operational Factors Affecting Refuse Incinerators', A. Loader, Report No. LDFT34, Warren Spring Laboratory, 1988

- [21] 'Incinerator Temperature Measurements: How, What And Where', J.L. Laver, Proceedings Of National Incinerator Conference, A.S.M.E., N.Y., 1964
- [22] 'Pollutant Minimisation By Blue Flame Staged Combustion', D.S. Prior, PhD Thesis, Chemical Engineering Department, Sheffield University, 1976
- [23] 'Private Communications', Dr. W.McKingly, Motherwell Bridge Ltd., January 1989
- [24] 'Private Communications', Dr. L. King, Babcock and Wilcox Ltd., Scotland, January 1989
- [25] 'The Environmental Impact Of Refuse Incineration In The U.K.', M. Woodfield, Warren Spring Laboratory, September 1987
- [26] 'Techniques For Air Pollution Control In Municipal Incineration', J.A. Fife, AIChE, Symp. Ser. No. 137, Vol. 70, 1974, pp 405 - 473
- [27] 'An Approach To Incinerator Combustible Pollutant Control', W.R. Nissen and A.F. Sarofim, Proceedings Of National Incinerator Conference, A.S.M.E., N.Y., 1970
- [28] 'Energy World', May 1984, p.5
- [29] 'The Measurement Of Suspended Particle, Heavy Metal And Selected Organic Emissions At Sheffield MSW Incinerator', P. Clayton and D.W. Scott, Report No. LR570 (PA), Warren Spring Laboratory, 1988
- [30] 'Methods For The Sampling And Analysis Of Flue Gases; Part 1 And 2, BS 1756', 1971
- [31] 'Refuse Combustion And Flue Gas Analysis From Municipal Incinerator', E.R. Kaiser, Proceedings Of National Incinerator Conference', A.S.M.E., N.Y., 1964
- [32] 'The Sampling, Analysis And Study Of The Nitrogen Oxides Formed In Natural Gas/Air Flames', C.J. Halstead and A.J.E. Munro, I.G.T./A.G.A. Conference, Chicago, USA, 1971

- [33] 'Hydrogen Interference In Chemiluminescent NO_x Analysers', R.M. Sievert, *Combustion And Flame*, Vol. 25, 1975, p. 273
- [34] 'Private Communications', Dr. K. West, LAND Combustion Ltd., December 1988
- [35] 'Gas Sampling And Analysis In Combustion Phenomena', R. Lengelle and F. Verdier, AGARD Report No. 168, 1973
- [36] 'Steam/Its Generation And Use', 39th Edition, Babcock and Wilcox, 1978
- [37] 'Preliminary Report On Sheffield Incinerator', D.W. Scott, Warren Spring Laboratory, Report No. LHK45, 1988
- [38] 'Sampling And Analysis Of Solid Incinerator Refuse And Residue', E.R. Kaiser, *Proceedings Of National Incinerator Conference*, A.S.M.E., N.Y., 1970
- [39] 'Burning Rates In Incinerators', R.H. Essenhigh, *Ibid*, 1970
- [40] 'Burning Rates And Operational Limits In A Solid Fuel Bed', M. Kuwata, T.J. Kuo and R.H. Essenhigh, *Ibid*, 1970
- [41] 'An Investigation Of Combustion Air For Refuse Burning', L.J. Cohan and R.C. Sherril, *Ibid*, 1964
- [42] 'The Effect Of Furnace Design And Operation On Air Pollution From Incinerators', H.G. Meissner, *Ibid*, 1964
- [43] 'Solid Fuel Combustion And Its Application To The Incineration Of Solid Refuse', J.E.L. Rogers, PhD Thesis, Chemical Engineering Department, Massachusetts Institute Of Technology, 1973, Microfiche
- [44] 'Practical Application Of Incinerator Burning Rate Equations', M. Dvirka, *Proceedings Of National Waste Processing Conference*, A.S.M.E., N.Y., 1976
- [45] 'Industrial Furnaces', L. Trinks, Vol. 1, 2nd Edition, Interscience Publisher, 1944

- [46] 'Refuse Composition And Flue Gas Analysis From Municipal Incinerators', E.R. Kaiser, Proceedings Of National Waste Processing Conference, A.S.M.E., N.Y., 1964
- [47] 'Internal Flow Systems', D.S. Miller, BHRA, 1972
- [48] 'ASHRAE Handbook And Product Directory: Fundamentals', 1977
- [49] 'Combustion And Emission Phenomena In Incinerators; Studies On Combustion Behaviour And Extinction Limits Of Smoke Flames', B.K. Kiswas, T.J. Kuo and R.H. Essenhigh, Proceedings Of National Incinerator Conference, A.S.M.E., N.Y., 1970
- [50] 'The Pyrolysis Of Refuse Components', R.G. Rogers, AIChE 60th Annual Meeting, Reprint 370, N.Y., 1967
- [51] 'Combustion And Emission Phenomena In Incinerators; Physical And Mathematical Model Of A Simple Incinerator', T.J. Kuo, M. Kuwata, W.S. Shieh and R.H. Essenhigh, Proceedings Of National Incinerator Conference, A.S.M.E., N.Y., 1970
- [52] 'The Science Of Flames And Furnaces', M.W. Thring, 2nd Edition, Chapman & Hall, 1962
- [53] 'Mathematical Analysis Of Gas Flow Patterns In Municipal Incinerator Furnace Configuration', W.T. Clarke, Proceedings Of National Incinerator Conference, A.S.M.E., N.Y., 1972
- [54] 'Preparation And Incineration Of Screened Refuse', J. Barton and A.J. Poll, Warren Spring Laboratory, Report No. LR 592 (MR), November 1986
- [55] 'The Efficient Use Of Fuel', H.M. Stationary Office, London, 1958
- [56] 'Steam Plant Calculations Manual', V. Ganapathy, Marcel Dekker Inc., 1976
- [57] 'Fuels And Fuel Technology', W. Francis and M.C. Peters, Second Edition, Pergamon Press, 1975

- [58] 'Combustion Calculations; Theory, Worked Examples And Problems', E.M. Goodger, 1st edition, The MacMillan Press Ltd., 1977
- [59] 'Development Of Physical And Mathematical Models Of Incinerators; Part 1, Statement Of The Problems', R.H. Essenhigh and T.J. Kuo, Proceedings Of National Incinerator Conference, A.S.M.E., N.Y., 1970
- [60] 'Theoretical Model Of Solid Waste Combustion Processes', J.E. Flanagan and G.A. Hosack, Ibid, 1970
- [61] 'Development Of Fundamental Basis For Incinerator Design Equations And Specifications', R.H. Essenhigh and T.J. Kuo, Proceedings Of 3rd Mid-Atlantic Industrial Waste Conference, University Of Maryland, November 1969
- [62] 'Effect Of Underfire Air Rate On A Burning Simulated Refuse Bed', J.E.L. Rogers, A.F. Sarofim and J.B. Howard, Proceedings Of National Incinerator Conference, A.S.M.E., N.Y., 1972
- [63] 'Contribution To The Study Of The Ignition Of Fuel Beds', A.C. Dunningham and E.S. Grammell, Institute Of Fuel Journal, Vol. 11, 1947, pp 117-122
- [64] 'Studies On Combustion Of Carbon Particles In Flames And Fluidized Beds', S. Yagi and D. Kunii, 5th Symposium (International) On Combustion, Reinhold, N.Y., 1955
- [65] 'The Ignition Of Wet And Dry Wood Ignited By Radiation', D.L. Simms and M. Law, Institute Of Fuel Journal, Vol. 11, 1967, pp 377-388
- [66] 'Experimental Study Of Incineration', A.A. Orruing, W.C. Harold and J.F. Schwultz, Proceedings Of National Incinerator Conference, A.S.M.E., N.Y., 1970
- [67] 'The Heat Balance Integral And Its Application To Problems Involving A Change Of Phase', T.R. Goodman, Trans. A.S.M.E., Vol. 8, No. 2, 1958, pp 335-342

- [68] 'The Combustion Of Wood, Part 1', C.H. Bamford, J. Crank and D.H. Malan, Proc. Camb. Phil. Soc., Vol. 42, 1946, pp 146-181
- [69] 'The Degree Of Interaction Between Air And Solid Refuse: The Effect Of Fuel Size', M.W. Thring, Coal Research, BCURA Leatherhead, September 1944, p 70
- [70] 'FLUENT Manual', Flow Simulation Ltd., 1988
- [71] 'Gas Turbine Combustor Modelling And Validation', P.N. Wild, PhD Thesis, Chemical Engineering Department, Sheffield University, 1987
- [72] 'Chemical Engineering Handbook', R.H. Perry and C.H. Chilton, 5th Edition, International Student Edition, 1972
- [73] 'Three Dimensional Modelling Of The Sheffield MSW Incinerator', V. Nasserzadeh, J. Swithenbank, D.W. Scott and B. Jones, To be published in the Journal Of Institute Of Energy, 1990
- [74] 'Design Optimization Of A Large Municipal Incinerator With A Vertical Radiation Shaft', V. Nasserzadeh, J. Swithenbank, D.W. Scott and B. Jones, To be published in the Journal Of Institute Of Energy, 1990
- [75] 'Heat Transmission', W.H. McAdams, 2nd Edition, McGraw Hill, 1967
- [76] '3 Dimensional Gas Turbine Combustor Modelling', P.N. Wild, F. Boysan and J. Swithenbank, Conference Proceedings No. 422, Combustion And Fuels In Gas Turbine Engines, AGARD, France, 1987
- [77] 'Advance Of Research Of Coal Combustion System Modelling', J.Swithenbank, E.S.Garbett, F.Boysan and W.H.Ayers, Proceedings Of The International Symposium On Coal Combustion, Beijing, China, September 1987

Appendix 1

Types Of Refuse And The Classes Of Incinerators

The Incinerator Institute of America (IIA) has categorized the types of refuse and the classes of incinerators as part of a systematic approach to incinerator application and engineering [1]. They are as follows:

Types of Refuse :

Type 1: A mostly dry, primarily rubbish, containing up to 25 % moisture and up to 10 % incombustible solids with a heating value of 8000 kJ/kg as fired.

Type 2: An evenly mixed refuse of rubbish and garbage, containing up to 50 % moisture and up to 7 % incombustible solids with a heating value of 5500 kJ/kg as fired.

Type 3: A mostly wet refuse, generally garbage, consisting of up to 70 % moisture and up to 5 % incombustible solids with a heating value of 2500 kJ/kg as fired.

Type 4: By-product waste, gaseous, liquid or semi-liquid from industrial operations having variable content and Btu values.

Type 5: Solid by-product waste from industrial operations, otherwise unclassified and having little or no moisture with variable content and Btu values.

To consume divergent types of refuse, a wide range of incinerator designs and capacities have developed together with different methods of charging classified by the IIA as follows:

Classes of Incinerators:

Class 1: Portable, packaged, direct fed incinerators with a capacity of up to 50 kg per hour of type 1 or type 2 refuse.

Class 1A: Portable, packaged or site assembled, direct fed incinerators with a capacity of from 50 to 200 kgs per hour of type 1 or type 2 refuse.

Class 2: Chute-fed apartment house incinerators where the refuse chute also acts as the flue for the products of combustion.

Class 2A: Chute-fed apartment house incinerators having a separate refuse chute and a separate flue for the products of combustion.

Class 3: Direct-fed incinerators with a burning rate of 200 kg per hour or more, suitable for type 1 or type 2 refuse.

Class 4: Direct-fed incinerators with a burning rate of 150 kg per hour or more, suitable for type 3 refuse.

Class 5: Municipal incinerators with a burning rate of 1 ton per hour or more.

Class 6: Crematory and pathological incinerators suitable for only type 4 refuse.

Class 7: Incinerators designed for specific type 5 by-product waste.

Appendix 2

Calculation of Ambient Flame Gas Temperature from Thermocouple Bead Temperature

A Ni-Cr-Al Thermocouple was used for the purpose of estimating mean values of flame temperature T_f (°C). Due to heat transfer consideration the thermocouple bead temperature T_b does not equal this value, a heat balance in fact is necessary to relate the two. This appendix outlines the method by which T_f was calculated from T_b [22].

Assume thermocouple bead is spherical and of 1 mm diameter.

Thermocouple bead steady state heat balance [33]:

Rate of heat transferred to bead by convection from gases = Rate of heat transferred from bead by radiation to the combustor walls + Rate of heat transferred from bead by conduction along the leads

$$\dot{q}_1 = \dot{q}_2 + \dot{q}_3$$

Therefore,

$$hA_b(T_f - T_b) = \delta A_b(\epsilon T_b^4 - \alpha T_w^4) + \dot{q}_3$$

where T_w = mean combustor wall temperature, °K

h = heat transfer coefficient $\left(\frac{W}{m^2K}\right)$

ϵ = bead emissivity

δ = Stefan Boltzmann constant, $5.67 \times 10^{-8} \left(\frac{W}{m^2K^4}\right)$

α = absorptivity of walls

D_b = bead diameter, m

Forced convection and turbulence effects constitute additional complexities but were neglected since first order approximations only are required. It is further assumed:

- $\dot{q}_2 \gg \dot{q}_3$, in practice \dot{q}_3 can be minimised by the use of small diameter leads,

• $T_b^4 \gg T_w^4$, T_w is difficult to measure without resorting to the implantation of further thermocouples.

For heat transfer to a cylindrical object;

$$N_u = \frac{hD_b}{\lambda} = 2.0$$

Now λ and ϵ are not constants but functions of temperature. In the interests of mathematical simplicity both these thermal properties were expressed as linear relations:

$$\lambda \propto \lambda_{air} = 6.13 \times 10^{-5} T_f + 3.01 \times 10^{-2} \left(\frac{W}{mK} \right)$$

For $500 \leq T_f \leq 1800^\circ C$, using data available from [74]:

$$\epsilon \propto \epsilon_{Ni-Cr-Al \text{ wire}} = 8.63 \times 10^{-5} T_b + 0.05$$

A FORTRAN program was written to calculate T_f in addition to evaluating T_f for any given T_b the program estimates the density of flue gas at that point.

The program listing used for T_f and flue gas density calculations is given in appendix 6.

Appendix 3

Calculation of % Moisture Content of Flue Gases

The following sample formulae was used in each test case for computing the percentage of moisture by volume that was experimentally determined during each test [31].

Formula 1 yields the volume of sampled flue gas at standard temperature and pressure;

$$V_{std} = \frac{V_m P_m T_{std}}{T_m P_{std}} \quad (1)$$

Formula 2 yields the volume of sampled flue gas at duct temperature and pressure;

$$V_{duct} = \frac{V_{std} P_{std} T_{duct}}{T_{std} P_{duct}} \quad (2)$$

Formula 3 yields the volume of water vapour at duct temperature and pressure based on the amount of water collected by the desiccant;

$$V_{wv} = \left(\frac{w}{P_{duct} 18.00} \right) \times (82.057) \cdot T_{duct} \quad (3)$$

where w = amount of water collected.

Formula 4 yields the volume percentage of water vapour as determined by the desiccant weight change method;

$$\text{Vol. \% water vapour} = \left[\frac{V_{wv}}{V_{duct} + V_{wv}} \right] \times 100 \quad (4)$$

where V_{wv} = volume of water vapour.

The following sample calculations use data gathered on the 16th of November, 1988 at the Sheffield municipal incinerator;

$$V_{std} = \frac{(163.4 \text{ lit})(659 \text{ mm})(330 \text{ K})}{(760 \text{ mm})(332 \text{ K})} = 140.2 \text{ lit}$$

$$V_{duct} = \frac{(140.2 \text{ lit})(760 \text{ mm})(433 \text{ K})}{(761 \text{ mm})(330 \text{ K})} = 188.8 \text{ lit}$$

$$V_{wv} = \frac{(762 \text{ mm})(15.24 \text{ g})(82.05 \text{ cc/g moleK})(433 \text{ K})}{(761 \text{ mm})(18.00 \text{ g/g mole})} = 27700 \text{ cc (27.7 lit)}$$

Therefore;

$$\% \text{ Moisture content of flue gases} = \frac{27.7 \text{ lit}}{188.8 \text{ lit} + 27.7 \text{ lit}} \times 100 = 12.8\%$$

Appendix 4

Burning Rate Determination [40]

Assumption: There are negligible amounts of Nitrogen, Sulphur and other inorganic combustibles in the waste.

The specific gravity of the flue (stack) gas referred to air can be determined by the following equation;

$$Sp.Gr. = \frac{M_{CO_2} + M_{CO} + M_{O_2} + M_{N_2} + M_{H_2O}}{29.0}$$

where;

$$M_{CO_2} = \left(\frac{\%CO_2}{100} \right) \times 44.01$$

$$M_{CO} = \left(\frac{\%CO}{100} \right) \times 28.01$$

$$M_{O_2} = \left(\frac{\%O_2}{100} \right) \times 32.00$$

$$M_{H_2O} = \left(\frac{\%H_2O}{100} \right) \times 18.01$$

$$M_{N_2} = \left(\frac{\%N_2}{100} \right) \times 28.20$$

N.B. Molecular weight of dry air = 29.00.

The density of the flue gas at standard conditions is then;

$$\rho_{fg} = Sp.Gr. \times \rho_{air}$$

where; ρ_{air} = density of dry air at standard conditions = 0.075 lb/ft³

The total mass of the flue gas leaving the system is;

$$M_t = \rho_{fg} Q_s \quad (lb/hr)$$

where ρ_{fg} = density of flue gas (lb/ft³) and Q_s = volumetric flow rate (ft³/hr).

The nitrogen in the flue gas can be used as a tie element to determine the quantity of dry combustion air introduced to the incinerator.

$$M_{air} = Q_s \left(\frac{\%N_2}{100} \right) \left(\frac{\rho_{N_2}}{f_{N_2}} \right) \text{ (lb/hr)}$$

where ρ_{N_2} = density of nitrogen in lb/ft³ at standard conditions.

and f_{N_2} = weight fraction of nitrogen in air = 0.768

By determining the absolute humidity (H_a) of the combustion air at the time of the test, the water contained in the combustion air can be accounted for.

$$M_{ca} = [1 + H_a] \cdot \left[Q_s \left(\frac{\%N_2}{100} \right) \rho_{N_2} \right] \div f_{N_2}$$

where H_a = absolute humidity (lb water/lb dry air).

The burning rate for an incinerator can now be determined on an ash free basis;

$$RAF = M_t - M_{ca} \text{ (lb/hr)}$$

where RAF = Burning rate ash free basis (lb/hr)

Or it can be expressed as;

$$RAF = Q_s [\rho_{fg} - (1 + H_a)(\%N_2/100)(\rho_{N_2}/f_{N_2})]$$

in lb/hr of ash free waste burned.

If the ash content of the waste is known or can be determined, the charging rate can be expressed as;

$$RT = RAF \left[\frac{1}{1 - \left(\frac{\%Ash}{100} \right)} \right]$$

where %Ash = weight percentage of incombustibles in the waste.

Appendix 5

FLUENT Computational Package; An Overview [70]

In this study a computer code, FLUENT, was used to perform the calculations. This computer programme can fulfil a wide range of requirements. Examples of the application of FLUENT presented in references [76] and [77] illustrate the level of versatility and validity of this particular computer code.

Equations of the gas phase model; The equations required for the description of the flow field in the combustion chamber which express the time averaged fluid flow balance of mass and momentum are given below in cartesian tensor notation for compactness.

Conservation of mass

$$\frac{\partial}{\partial x_i}(\rho u_i) = 0 \quad (A1)$$

Conservation of momentum

$$\frac{\partial}{\partial x_i}(\rho u_i u_j) + (\rho u'_i u'_j) = -\frac{\partial \delta_{ij}}{\partial x_i} \quad (A2)$$

$$\delta_{ij} = p\gamma_{ij} - \mu \left[\frac{\partial u_i}{\partial x_j} + \frac{\partial u_j}{\partial x_i} \right] + \frac{2}{3}\mu \left(\frac{\partial u_i}{\partial x_j} \right) \gamma_{ij} \quad (A3)$$

k- ϵ Turbulence model

$$\frac{\partial}{\partial x_i}(\rho u_i k) = \frac{\partial}{\partial x_i} \left[\left(\frac{\mu + \mu_t}{\delta_k} \right) \left(\frac{\partial k}{\partial x_i} \right) \right] + P - \rho \epsilon \quad (A4)$$

$$\frac{\partial}{\partial x_i}(\rho u_i \epsilon) = \frac{\partial}{\partial x_i} \left[\left(\frac{\mu + \mu_t}{\delta_\epsilon} \right) \left(\frac{\partial \epsilon}{\partial x_i} \right) \right] + C_1 \frac{\epsilon}{k} P - C_2 \rho \frac{\epsilon^2}{k} \quad (A5)$$

$$\mu_t = 0.09 \times \frac{\rho k^2}{\epsilon} \quad (A6)$$

Modelling coefficients take the values; $C_1 = 1.44$, $C_2 = 1.92$, $\delta_k = 1.0$ and $\delta_\epsilon = 1.3$.

Equations for gas phase reacting flow

Equation for the conservation of enthalpy;

$$\frac{\partial}{\partial x_i}(\rho u_i h) = \frac{\partial}{\partial x_i} \left[\left(\frac{\mu + \mu_t}{\delta_h} \right) \left(\frac{\partial h}{\partial x_i} \right) \right] + S_h \quad (B1)$$

Equation for conservation of chemical species;

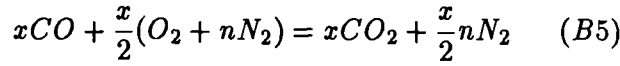
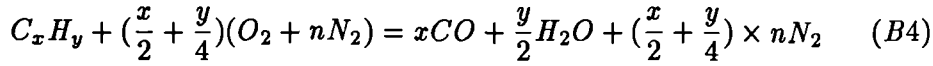
$$\frac{\partial}{\partial x_i}(\rho u_i m_s) = \frac{\partial}{\partial x_i} \left[\left(\frac{\mu + \mu_t}{\delta_s} \right) \left(\frac{\partial m_s}{\partial x_i} \right) \right] + S_s \quad (B2)$$

The equation of state;

$$\rho = \frac{p}{RT \sum m_j / M_j} \quad (B3)$$

Equations for two step chemical reaction model

The two step reaction mechanism is modelled as follows;



Reaction rates for the two steps are determined by;

$$R_{fu} = \left[A_1 \rho m_{fu} \frac{\epsilon}{k}, A_1 \frac{\rho \epsilon}{S_{fu} k} \frac{S_{fu} m_{fu}}{S_{fu} m_{fu} + S_{co} m_{co}}, R_{fu} \text{ kinetic} \right] \quad (B6)$$

$$R_{co} = \left[A_2 \rho m_{co} \frac{\epsilon}{k}, A_2 \frac{\rho m_o \epsilon}{S_{co} k} \frac{S_{co} m_{co}}{S_{fu} m_{fu} + S_{co} m_{co}}, R_{co} \text{ kinetic} \right] \quad (B7)$$

where A is a model constant and the subscript 'kinetic' denotes the rates determined by the Arrhenius equations. S_{fu} and S_{co} are the stoichiometric oxidant/fuel mass ratio for the combustion reactions. These have been included in order to account for the fact that the two reactions are simultaneously competing for available oxygen. The operator [] takes the smaller of the terms within and allows combustion to be controlled by the Arrhenius formula, the dissipation of oxygen containing eddies or the dissipation of fuel eddies. Once the rates R_{fu} and R_{co} are known, the required source terms are determined from knowledge of stoichiometry and the heat of combustion.

Appendix 6

List of Computer Programs Used For The Experimental And Modelling Work

- 1 - BASIC program used for recording the furnace temperature.
- 2 - Flame gas temperature estimation program (in FORTRAN).
- 3 - Mean gas temperature estimation program (in FORTRAN).
- 4 - Standard deviation calculation program (in FORTRAN).
- 5 - FLUENT case file used for modelling of the rollers.
- 6 - FLUENT case file used for modelling of the Sheffield incinerator plant.

READY.

```
1 DIMOP(16)
100 REM***PCI1002ADC**
110 REM
120 REM*****
130 REM*BERNARD RD INCINERATOR *
140 REM*TEMP. MEASUREMENT EXPT.*
150 REM*PCI1002ADC PROGRAM *
160 REM*VIDA NASSERZADEH *
170 REM*UNIVERSITY OF SHEFFIELD*
180 REM* *
190 REM*****
200 REM
205 REM***SELECT T/C RANGE***
206 REM
210 PRINT"PCI 1002 THERMOCOUPLE CONVERTER"
220 PRINT"NTHERMOCOUPLE TYPES AVAILABLE"
230 PRINT"QA, B"
235 PRINT"QA IS FOR K TYPE 0- 400 DEG C ;RANGE IS 30MV"
236 PRINT"QB IS FOR K TYPE 400-1370 DEG C ;RANGE IS 30MV"
237 REM
240 PRINT"ENTER TYPE"CHR$(3);
250 GETT$
252 REM
254 REM***SELECT LINEARISING COFFS***
256 REM
260 IFT$="A"THEN A(0)=0:A(1)=2.4383248E-2:A(2)=9.7830251E-9:CK=40.30
290 IFT$="A"THEN A(3)=3.6276965E-12:A(4)=-2.5756438E-16:GOTO396
300 IFT$="B"THEN A(0)=6.2300671:A(1)=2.4955374E-2:A(2)=-7.8788333E-8:CK=40.30
310 IFT$="B"THEN A(3)=1.3269743E-12:A(4)=1.5580541E-18:GOTO396
340 IFT$="R"THEN A(0)=0:A(1)=1.5239494E-1:A(2)=-1.3755675E-5
350 IFT$="R"THEN A(3)=1.2610922E-9:A(4)=-4.4281251E-14:CK=5.85:GOTO396
395 GOTO250
396 PRINTT$
400 REM
410 REM***ENTER DEVICE NO***
420 REM***DEVICE NO IS 6 IN THIS CASE***
430 UN=6
440 REM
450 REM***CHECK PCI1002 RANGE***
460 REM
470 CH=0:GOSUB 10000
480 IFOP(0)<800THENR=100
490 IFOP(0)>=800ANDOP(0)<2000THENR=30
500 IFOP(0)>=2000THENR=10
510 REM
520 REM***SCAN CH1 TO 15***
530 REM
535 PRINT"Q"
536 PRINT"RANGE"R"MV ; THERMOCOUPLE TYPE "T$
537 FOR#2,"SEQ FILE".D0,W
538 FOR L=1 TO 2
540 FORCH=1TO15:GOSUB10000:NEXTCH
550 REM
620 CH=4
630 GOSUB11000
640 PRINT"TEMP. OF CHANNEL"CH"= "OP(CH)"DEG C"
641 X$="TEMP.RECORD"+STR$(OP(CH))
642 PRINT#2,X$
```

```

643 REM
644 REM
645 REM
646 REM
699 REM
741 OPEN 4,4
742 CMD4
743 PRINT#4,;"TEMPERATURE OF CHANNEL NO"CH"=           "OP(CH)"DEG C"
744 PRINT#4,;
745 CLOSE4
746 FOR Z=1TO15000:NEXTZ
799 NEXT L
800 NEXT
810 END
982 /40
10000 REM
10010 REM*** OPERATING SUBROUTINE***
10020 REM
10030 OPEN1,IN,CH
10040 GET#1,J#,K#
10050 K=ASC(K#)-224
10060 IFK<0THEND=(K+32)*-1
10070 IFK>=0THEND=K
10080 D=D*256
10090 IFJ#=""THENJ=0:GOTO10110
10100 J=ASC(J#)
10110 IFK<0THENJ=J*-1
10120 OP(CH)=J+D
10130 CLOSE1
10140 RETURN
11000 REM
11010 REM***BITS TO DEGC SUBROUTINE***
11020 REM
11030 CJ=CK*(OP(3)*R/400):REM GIVES CJC IN MICROVOLTS
11040 V=OP(CH)*R/4:REM GIVES O/P IN MICROVOLTS
11050 V=V+CJ:REM ADD CJC VOLTAGE
11060 T=A(4)
11070 FORI=3TO8STEP-1
11080 T=T*V+A(I)
11090 NEXTI
11100 OP(CH)=INT(10*(T)+0.5)/10
11110 RETURN
READY.

```

!File <UBRA17>FC2VNS>FLAMD.F77 last modified Friday 11 Aug 89 10:22:44

```
REAL DATA(12,29),TB(29),TF(29),RDHT(29),ESH(29),DEN(29)
INTEGER NOP,NOC,CN
CHARACTER*20 FNAME
WRITE(1,*)'INPUT DATA FILENAME'
READ(1,'(A17)')FNAME
OPEN(UNIT=5,FILE=FNAME)
READ(5,*)NOP,NOC
DO 100 I=1,NOP
READ(5,*)(DATA(J,I),J=1,NOC)
100 CONTINUE
CLOSE(UNIT=5)
WRITE(1,*)'WHICH COLUMN TO USE'
READ(1,*)CN
CN=CN+1
DO 200 I=1,NOP
TB(I)=DATA(CN,I)
DSH=1.75E-03
SBC=5.67E-08
ESH(I)=(0.109*TB(I)/1132.22)+0.05
RDHT(I)=((TB(I)+273)**4)*SBC*ESH(I)
A=12.26E-05
D=0.72E-04
B=D-(A*TB(I))
C=(D*TB(I))+(DSH*RDHT(I)/837.4)
TF(I)=((-B)+SQRT((B**2)+(4*A*C)))/(2*A)
DEN(I)=(28.0/22.4)*(73.0/76.0)*(273/(273+TF(I)))
WRITE(1,3)TF(I),DEN(I)
200 CONTINUE
3  FORMAT(F8.3,5X,F8.3)
STOP
END
```

!File <USRA17>FC2VNS>MEAN.F77 last modified Friday 11 Aug 89 14:46:24

```
REAL DATA(11,52),TB(52),SUM
INTEGER NOP,NOC,CN
CHARACTER*20 FNAME
WRITE(1,*)'INPUT DATA FILENAME'
READ(1,'(A17)')FNAME
OPEN(UNIT=5,FILE=FNAME)
READ(5,*)NOP,NOC
DO 100 I=1,NOP
  READ(5,*)(DATA(J,I),J=1,NOC)
100 CONTINUE
  WRITE(1,*)'WHICH COLUMN TO USE'
  READ(1,*)CN
  CN=CN+1
  SUM=0.0
  DO 200 I=1,NOP
    TB(I)=DATA(CN,I)
    SUM=SUM+TB(I)
200 CONTINUE
  XMEAN=SUM/NOP
  WRITE(1,201)XMEAN
  CLOSE(UNIT=5)
  STOP
201 FORMAT(F8.3)
  END
```

!File <USRA17>FC2VNS>STDEV.F77 last modified Friday 11 Aug 89 14:47:00

```
REAL DATA(11,52),TF(52),B(52)
INTEGER NOP,NOC,CN
CHARACTER*20 FNAME
WRITE(1,*)'INPUT DATA FILENAME'
READ(1,'(A17)')FNAME
OPEN(UNIT=5,FILE=FNAME)
READ(5,*)NOP,NOC
DO 100 I=1,NOP
READ(5,*)(DATA(J,I),J=1,NOC)
100 CONTINUE
WRITE(1,*)'WHICH COLUMN TO USE'
READ(1,*)CN
CN=CN+1
SUM1=0.0
SUM2=0.0
DO 200 I=1,NOP
TF(I)=DATA(CN,I)
C WRITE(1,*) TF(I)
SUM1=SUM1+TF(I)
200 CONTINUE
TFAV=SUM1/NOP
C WRITE(1,*) TFAV
DO 300 I=1,NOP
B(I)=(TF(I)-TFAV)**2
C WRITE(1,*) B(I)
SUM2=SUM2+B(I)
300 CONTINUE
STDEV=SQRT(SUM2/NOP)
WRITE(1.3)STDEV
3 FORMAT(F8.3)
STOP
END
```

 : LICENSED BY AND THE PROPERTY OF CREARE INC. P.O. BOX 71, HANOVER, NEW HAMPSHIRE 03755. (603) 643-3800 I
 I-----

I
 I FFFFF L U U EEEEE N N TTTT
 I F L U U E NN N T
 I FFFF L U U EEEE N N N T
 I F L U U E N NN T
 I F LLLLL UUU EEEEE N N T FLUID FLOW
 O D E L L I N G
 I
 I
 I-----

I
 I OUTPUT PRODUCED BY RELEASE 2.99 ROLLER MODELLING
 I
 I-----

- UNITS SYSTEM -

| INDEX | PROPERTY | UNITS | S.I. CONVERSION FACTOR |
|-------|------------------|------------------|------------------------|
| 1 | | DIMENSIONLESS | 1.000E+00 |
| 2 | MASS | KILOGRAMS | 1.000E+00 |
| 3 | LENGTH | METRES | 1.000E+00 |
| 4 | TIME | SECONDS | 1.000E+00 |
| 5 | VELOCITY | METRES/SEC | 1.000E+00 |
| 6 | FORCE | NEWTONS | 1.000E+00 |
| 7 | ACCELERATION | METRES/SEC/SEC | 1.000E+00 |
| 8 | ENERGY | JOULES | 1.000E+00 |
| 9 | POWER | WATTS | 1.000E+00 |
| 10 | MASSFLOWRATE | KILOGRAMS/SEC | 1.000E+00 |
| 11 | TEMPERATURE | KELVIN | 1.000E+00 |
| 12 | ENTHALPY | JOULES/KILOGRAM | 1.000E+00 |
| 13 | PRESSURE | PASCALS | 1.000E+00 |
| 14 | DENSITY | KILOGRAMS/CU.M | 1.000E+00 |
| 15 | VISCOSITY | KG/M-SEC. | 1.000E+00 |
| 16 | K.E. OF TURBLNCE | M.SQ/SEC/SEC | 1.000E+00 |
| 17 | K.E. DISS. RATE | M.SQ/SEC/SEC/SEC | 1.000E+00 |
| 18 | SPEC. HT. CAP. | JOULES/KG-K | 1.000E+00 |
| 19 | THERMAL COND. | WATTS/M-K | 1.000E+00 |
| 20 | DIFFUSIVITY | M.SQ/SEC. | 1.000E+00 |
| 21 | ACTIVATION ENRGY | JOULES/KGMOL | 1.000E+00 |
| 22 | ANGLE | RADIANS | 1.000E+00 |
| 23 | HEAT FLUX | WATTS/M.SQ. | 1.000E+00 |
| 24 | PARTICLE DIAM. | METRES | 1.000E+00 |
| 25 | MOMENTUM TR RATE | KG M/SEC/SEC | 1.000E+00 |

| | | | |
|----|-----------------------|------------------|-----------|
| 25 | MOMENTUM TRANSF. COEF | KG./M. SEC./SEC. | 1.000E+00 |
| 26 | HEAT TRANSF. COEF | WATTS/M. SQ.-K. | 1.000E+00 |
| 27 | PERMEABILITY | M. SQ. | 1.000E+00 |
| 28 | (INTERNAL MISC.) | UNDEFINED | 1.000E+00 |
| 29 | VOL. FLOWRATE | CU. M./SEC. | 1.000E+00 |
| 30 | AREA | M. SQ. | 1.000E+00 |
| 31 | ARRHENIUS FACTOR | CU. M./KG. -SEC. | 1.000E+00 |
| 32 | INERTIAL FACTOR | PER METRE | 1.000E+00 |
| 33 | VOL. HEAT RATE | WATTS/CU. M. | 1.000E+00 |
| 34 | ABSORB./SCATTER. | PER METER | 1.000E+00 |
| 35 | ANGULAR VELOCITY | PER SECOND | 1.000E+00 |
| 36 | SF ARE | UNDEFINED | 1.000E+00 |

- GEOMETR. -

RECTANGULAR CARTESIAN COORDINATES

NI = 3. NJ = 15 NK = 7

|NODE CENTRES..... | | | |POSITIVE FACES..... | | |
|---------------------------|-------------|-------------|-------------|--------------------------|-----------|-----------|
|CELL DIMENSIONS..... | | | | X-GRID | Y-GRID | Z-GRID |
| NO. | X-GRID | Y-GRID | Z-GRID | X-GRID | Y-GRID | Z-GRID |
| X-GRID | Y-GRID | Z-GRID | NO. | | | |
| 1 | -1.0736E-02 | -1.1111E-01 | -2.0000E-01 | 0.000E+00 | 0.000E+00 | 0.000E+00 |
| 5.357E-02 | 2.222E-01 | 4.000E-01 | 1 | | | |
| 2 | 1.0736E-02 | 1.1111E-01 | 2.0000E-01 | 5.357E-02 | 2.222E-01 | 4.000E-01 |
| 5.357E-02 | 2.222E-01 | 4.000E-01 | 2 | | | |
| 3 | 8.0357E-02 | 3.3333E-01 | 6.0000E-01 | 1.071E-01 | 4.444E-01 | 8.000E-01 |
| 5.357E-02 | 2.222E-01 | 4.000E-01 | 3 | | | |
| 4 | 1.3397E-01 | 5.5556E-01 | 1.0000E+00 | 1.607E-01 | 6.667E-01 | 1.200E+00 |
| 5.357E-02 | 2.222E-01 | 4.000E-01 | 4 | | | |
| 5 | 1.3750E-01 | 7.7778E-01 | 1.4000E+00 | 2.143E-01 | 8.889E-01 | 1.600E+00 |
| 5.357E-02 | 2.222E-01 | 4.000E-01 | 5 | | | |
| 6 | 2.4107E-01 | 1.0000E+00 | 1.8000E+00 | 2.679E-01 | 1.111E+00 | 2.000E+00 |
| 5.357E-02 | 2.222E-01 | 4.000E-01 | 6 | | | |
| 7 | 2.7464E-01 | 1.2222E+00 | 2.2000E+00 | 3.214E-01 | 1.333E+00 | 0.000E+00 |
| 5.357E-02 | 2.222E-01 | 4.000E-01 | 7 | | | |
| 8 | 3.4821E-01 | 1.4444E+00 | 0.0000E+00 | 3.750E-01 | 1.556E+00 | 0.000E+00 |
| 5.357E-02 | 2.222E-01 | 0.000E+00 | 8 | | | |
| 9 | 4.0179E-01 | 1.6667E+00 | 0.0000E+00 | 4.286E-01 | 1.778E+00 | 0.000E+00 |
| 5.357E-02 | 2.222E-01 | 0.000E+00 | 9 | | | |
| 10 | 4.5536E-01 | 1.8889E+00 | 0.0000E+00 | 4.821E-01 | 2.000E+00 | 0.000E+00 |
| 5.357E-02 | 2.222E-01 | 0.000E+00 | 10 | | | |
| 11 | 5.0893E-01 | 2.1111E+00 | 0.0000E+00 | 5.357E-01 | 2.222E+00 | 0.000E+00 |
| 5.357E-02 | 2.222E-01 | 0.000E+00 | 11 | | | |
| 12 | 5.6250E-01 | 2.3333E+00 | 0.0000E+00 | 5.893E-01 | 2.444E+00 | 0.000E+00 |
| 5.357E-02 | 2.222E-01 | 0.000E+00 | 12 | | | |
| 13 | 6.1607E-01 | 2.5556E+00 | 0.0000E+00 | 6.429E-01 | 2.667E+00 | 0.000E+00 |
| 5.357E-02 | 2.222E-01 | 0.000E+00 | 13 | | | |
| 14 | 6.6964E-01 | 2.7778E+00 | 0.0000E+00 | 6.964E-01 | 2.889E+00 | 0.000E+00 |
| 5.357E-02 | 2.222E-01 | 0.000E+00 | 14 | | | |
| 15 | 7.2321E-01 | 3.0000E+00 | 0.0000E+00 | 7.500E-01 | 3.111E+00 | 0.000E+00 |
| 5.357E-02 | 2.222E-01 | 0.000E+00 | 15 | | | |
| 16 | 7.7679E-01 | 3.2222E+00 | 0.0000E+00 | 8.036E-01 | 3.333E+00 | 0.000E+00 |
| 5.357E-02 | 2.222E-01 | 0.000E+00 | 16 | | | |
| 17 | 8.3036E-01 | 3.4444E+00 | 0.0000E+00 | 8.571E-01 | 3.556E+00 | 0.000E+00 |
| 5.357E-02 | 2.222E-01 | 0.000E+00 | 17 | | | |
| 18 | 8.8393E-01 | 3.6667E+00 | 0.0000E+00 | 9.107E-01 | 3.778E+00 | 0.000E+00 |
| 5.357E-02 | 2.222E-01 | 0.000E+00 | 18 | | | |
| 19 | 9.3750E-01 | 3.8889E+00 | 0.0000E+00 | 9.643E-01 | 4.000E+00 | 0.000E+00 |
| 5.357E-02 | 2.222E-01 | 0.000E+00 | 19 | | | |
| 20 | 9.9107E-01 | 4.1111E+00 | 0.0000E+00 | 1.018E+00 | 4.222E+00 | 0.000E+00 |
| 5.357E-02 | 2.222E-01 | 0.000E+00 | 20 | | | |
| 21 | 1.0446E+00 | 4.3333E+00 | 0.0000E+00 | 1.071E+00 | 4.444E+00 | 0.000E+00 |

- BOUNDARIES -

BNDRYBOUNDARY CONDITIONS.....

 ZONE (U) (V) (W) (E) (D) (T)
 (F) (D) (C) (2)
 W0 0.0000E+00W 0.0000E+00W 0.0000E+00W 0.0000E+00S 0.0000E+00S 2.7300E+02W 0.
 000E+00C 0.0000E+00C 0.0000E+00C R
 0 0.0000E+00L 0.0000E+00L 0.0000E+00L 0.0000E+00L 0.0000E+00L 2.7300E+02L 0.
 000E+00L 0.0000E+00L 0.0000E+00L E
 I1 0.0000E+00L 0.0000E+00L 4.0000E+01L 2.4000E+01L 2.2417E+03L 2.7300E+02L 0.
 000E+00L 0.0000E+00L 0.0000E+00L E

- CONSTANTS -

CYCLIC CELLS PRESCRIBED PRESSURE DROP = 0.000E+00
 DIFFERENCING SCHEME - POWER LAW
 REFERENCE PRESSURE AT I= 2 J= 3 K= 2 (ACTUAL PRESSURE = 1.013E+05)
 GAS DENSITY AT STP = 1.293E+00 USE GAS LAW - Y PRESSURE CORRECTED
 - N
 SECOND RELAXATION FACTORS ON AFTER 32000 ITERATIONS.
 PATCH OPTION -N
 CONVERG/DIVERG CHK -Y
 NORMALIZE RESIDS. -Y
 CONTINUITY CHECK -Y
 RESET OPTION -Y
 SWEEP DIRECTION -1
 REYNOLDS STRESS MODEL-N
 NON-NEWTONIAN FLOW -N
 POROSITY MODEL -Y
 ALLOW LINK SETTING -N
 SET INLET TURBULENCE -N
 MONITOR OPTION -N
 LINK OPTION -N
 PARTICLE TRACKING 0 TRACKS EVERY 0 ITNS.

POROUS ZONE PROPERTIES :

| ZONE | KX | KY | KZ | C2 |
|------|------------|------------|------------|------------|
| * | 1.0000E+11 | 1.0000E+11 | 1.0000E+11 | 1.2931E+03 |
| *1 | 1.0000E+11 | 1.0000E+11 | 1.0000E+11 | 7.7110E+02 |

GRAVITATIONAL ACCELERATIONS- X = 0.000E+00 Y = 0.000E+00 Z = 0.000E+
 10
 APARAM = 1.000E+01
 CONRES = 1.000E+03
 CONCHN = 1.000E+03
 ITMAX = 9

TURBULENCE MODEL - CD C1 C2 CMU RSMCD
 5.5E-01 1.4E+00 1.9E+00 9.0E-02 1.0E+00

WALL TURBULENCE MODEL. WALL_ZONE CAPPA ELOG
 W0 4.187E-01 9.793E+00

NON-NEWTONIAN FLOW - N K
 1.0E+00 1.0E+00

|NODE CENTRES..... | | | |POSITIVE FACES..... | | |
|---------------------------|-------------|-------------|-------------|--------------------------|-----------|-----------|
|CELL DIMENSIONS..... | | | | | | |
| NO. | X-GRID | Y-GRID | Z-GRID | X-GRID | Y-GRID | Z-GRID |
| X-GRID | Y-GRID | Z-GRID | NO. | | | |
| 1 | -2.2357E-01 | -2.9514E-01 | -1.0714E-01 | 0.000E+00 | 0.000E+00 | 0.000E+00 |
| 4.471E-01 | 5.903E-01 | 2.143E-01 | 1 | | | |
| 2 | 2.2357E-01 | 2.9514E-01 | 1.0714E-01 | 4.471E-01 | 5.903E-01 | 2.143E-01 |
| 4.471E-01 | 5.903E-01 | 2.143E-01 | 2 | | | |
| 3 | 6.7071E-01 | 8.8542E-01 | 3.2143E-01 | 8.943E-01 | 1.181E+00 | 4.286E-01 |
| 4.471E-01 | 5.903E-01 | 2.143E-01 | 3 | | | |
| 4 | 1.1179E+00 | 1.4757E+00 | 5.3571E-01 | 1.341E+00 | 1.771E+00 | 6.429E-01 |
| 4.471E-01 | 5.903E-01 | 2.143E-01 | 4 | | | |
| 5 | 1.5650E+00 | 2.0660E+00 | 7.5000E-01 | 1.789E+00 | 2.361E+00 | 8.571E-01 |
| 4.471E-01 | 5.903E-01 | 2.143E-01 | 5 | | | |
| 6 | 2.0121E+00 | 2.6563E+00 | 9.6429E-01 | 2.236E+00 | 2.951E+00 | 1.071E+00 |
| 4.471E-01 | 5.903E-01 | 2.143E-01 | 6 | | | |
| 7 | 2.4593E+00 | 3.2465E+00 | 1.1786E+00 | 2.683E+00 | 3.542E+00 | 1.286E+00 |
| 4.471E-01 | 5.903E-01 | 2.143E-01 | 7 | | | |
| 8 | 2.9064E+00 | 3.8368E+00 | 1.3929E+00 | 3.130E+00 | 4.132E+00 | 1.500E+00 |
| 4.471E-01 | 5.903E-01 | 2.143E-01 | 8 | | | |
| 9 | 3.3536E+00 | 4.4271E+00 | 1.6071E+00 | 3.577E+00 | 4.722E+00 | 0.000E+00 |
| 4.471E-01 | 5.903E-01 | 2.143E-01 | 9 | | | |
| 10 | 3.8007E+00 | 5.0174E+00 | 0.0000E+00 | 4.024E+00 | 5.312E+00 | 0.000E+00 |
| 4.471E-01 | 5.903E-01 | 0.000E+00 | 10 | | | |
| 11 | 4.2479E+00 | 5.6076E+00 | 0.0000E+00 | 4.471E+00 | 5.903E+00 | 0.000E+00 |
| 4.471E-01 | 5.903E-01 | 0.000E+00 | 11 | | | |
| 12 | 4.6950E+00 | 6.1979E+00 | 0.0000E+00 | 4.919E+00 | 6.493E+00 | 0.000E+00 |
| 4.471E-01 | 5.903E-01 | 0.000E+00 | 12 | | | |
| 13 | 5.1421E+00 | 6.7882E+00 | 0.0000E+00 | 5.366E+00 | 7.083E+00 | 0.000E+00 |
| 4.471E-01 | 5.903E-01 | 0.000E+00 | 13 | | | |
| 14 | 5.5893E+00 | 7.3785E+00 | 0.0000E+00 | 5.813E+00 | 7.674E+00 | 0.000E+00 |
| 4.471E-01 | 5.903E-01 | 0.000E+00 | 14 | | | |
| 15 | 6.0364E+00 | 7.9687E+00 | 0.0000E+00 | 6.260E+00 | 8.264E+00 | 0.000E+00 |
| 4.471E-01 | 5.903E-01 | 0.000E+00 | 15 | | | |
| 16 | 6.4836E+00 | 8.5590E+00 | 0.0000E+00 | 6.707E+00 | 8.854E+00 | 0.000E+00 |
| 4.471E-01 | 5.903E-01 | 0.000E+00 | 16 | | | |
| 17 | 6.9307E+00 | 9.1493E+00 | 0.0000E+00 | 7.154E+00 | 9.444E+00 | 0.000E+00 |
| 4.471E-01 | 5.903E-01 | 0.000E+00 | 17 | | | |
| 18 | 7.3779E+00 | 9.7396E+00 | 0.0000E+00 | 7.601E+00 | 1.003E+01 | 0.000E+00 |
| 4.471E-01 | 5.903E-01 | 0.000E+00 | 18 | | | |
| 19 | 7.8250E+00 | 1.0330E+01 | 0.0000E+00 | 8.049E+00 | 1.062E+01 | 0.000E+00 |
| 4.471E-01 | 5.903E-01 | 0.000E+00 | 19 | | | |
| 20 | 8.2721E+00 | 1.0920E+01 | 0.0000E+00 | 8.496E+00 | 1.122E+01 | 0.000E+00 |
| 4.471E-01 | 5.903E-01 | 0.000E+00 | 20 | | | |
| 21 | 8.7193E+00 | 1.1510E+01 | 0.0000E+00 | 8.943E+00 | 1.181E+01 | 0.000E+00 |
| 4.471E-01 | 5.903E-01 | 0.000E+00 | 21 | | | |
| 22 | 9.1664E+00 | 1.2101E+01 | 0.0000E+00 | 9.390E+00 | 1.240E+01 | 0.000E+00 |
| 4.471E-01 | 5.903E-01 | 0.000E+00 | 22 | | | |
| 23 | 9.6136E+00 | 1.2691E+01 | 0.0000E+00 | 9.837E+00 | 1.299E+01 | 0.000E+00 |
| 4.471E-01 | 5.903E-01 | 0.000E+00 | 23 | | | |
| 24 | 1.0061E+01 | 1.3281E+01 | 0.0000E+00 | 1.028E+01 | 1.358E+01 | 0.000E+00 |
| 4.471E-01 | 5.903E-01 | 0.000E+00 | 24 | | | |
| 25 | 1.0508E+01 | 1.3872E+01 | 0.0000E+00 | 1.073E+01 | 1.417E+01 | 0.000E+00 |
| 4.471E-01 | 5.903E-01 | 0.000E+00 | 25 | | | |
| 26 | 1.0955E+01 | 1.4462E+01 | 0.0000E+00 | 1.118E+01 | 1.476E+01 | 0.000E+00 |
| 4.471E-01 | 5.903E-01 | 0.000E+00 | 26 | | | |
| 27 | 1.1402E+01 | 1.5052E+01 | 0.0000E+00 | 1.163E+01 | 1.535E+01 | 0.000E+00 |
| 4.471E-01 | 5.903E-01 | 0.000E+00 | 27 | | | |
| 28 | 1.1849E+01 | 1.5642E+01 | 0.0000E+00 | 1.207E+01 | 1.594E+01 | 0.000E+00 |
| 4.471E-01 | 5.903E-01 | 0.000E+00 | 28 | | | |
| 29 | 1.2296E+01 | 1.6233E+01 | 0.0000E+00 | 1.252E+01 | 1.653E+01 | 0.000E+00 |
| 4.471E-01 | 5.903E-01 | 0.000E+00 | 29 | | | |
| 30 | 1.2744E+01 | 1.6823E+01 | 0.0000E+00 | 0.000E+00 | 1.712E+01 | 0.000E+00 |
| 4.471E-01 | 5.903E-01 | 0.000E+00 | 30 | | | |
| 31 | 0.0000E+00 | 1.7413E+01 | 0.0000E+00 | 0.000E+00 | 1.771E+01 | 0.000E+00 |


```

33 WO . . . . . *1*1*1*1*1*1*1*1 . . . 0
32 WO . . . . . *1*1*1*1*1*1*1*1 . . . 0
31 WO . . . . . *1*1*1*1*1*1*1*1 . . . 0
30 WO . . . . . WOWO . *1*1*1*1*1*1*1*1 . . . WO
29 WO . . . . . WOWO . *1*1*1*1*1*1*1*1 . . . WO
28 WO . . . . . WO . *1*1*1*1*1*1*1*1 . . . WO
27 WO . . . . . WO . *1*1*1*1*1*1*1*1 . . . WO
26 WOWO . . . . . WO . *1*1*1*1*1*1*1*1 . . . WO
25 WOWOWO . . . . . WO . *1*1*1*1*1*1*1*1 . . . WO
24 WOWOWOWO . . . . . WO . *1*1*1*1*1*1*1*1 . . . WO
23 WOWOWOWOWO . . . . . WO . *1*1*1*1*1*1*1*1 . . . WO
22 WO . . . . . WO . . . . . WOWO . . . . . WO
21 WO . . . . . WOWOWO . . . . . WOWO . . . . . WOWO
20 WO . . . . . WOWOWOWO . . . . . WOWO . . . . . WOWOWO
19 WO . . . . . WOWOWOWOWO . . . . . WOWO . . . . . WOWOWOWO
18 WO . . . . . WOWOWOWOWOWO . . . . . WOWO . . . . . WOWOWOWOWO
17 WOWO . . . . . I9WO I9WOWOWOWOWOWOWOWOWOWOWOWO
16 WOWOIIIIII . . . . . WOWOWOWOWOWOWOWOWOWOWOWO
15 WOWOWOWO . . . . . WOWOWOWOWOWOWOWOWOWOWOWO
14 WOWOWOWOWOI2I2I2I2 . . . . . WOWOWOWOWOWOWO
13 WOWOWOWOWOWOWO . . . . . WOWOWOWOWOWOWO
12 WOWOWOWOWOWOWOWOWOI3I3I3I3 . . . . . WO
11 WOWOWOWOWOWOWOWOWOWO . . . . . WO
10 WOWOWOWOWOWOWOWOWOWOWOWOWOWOI4I4I4I4 . . . . . WO
9 WOWOWOWOWOWOWOWOWOWOWOWOWOWOWOWO . . . . . WO
8 WOWOWOWOWOWOWOWOWOWOWOWOWOWOWOWOWOWOWOWOWOWOWOI5I5I5I5 . . . . . WO
7 WOWOWOWOWOWOWOWOWOWOWOWOWOWOWOWOWOWOWOWOWOWO . . . . . WO
6 WOWOWOWOWOWOWOWOWOWOWOWOWOWOWOWOWOWOWOWOWOWOWOWOI6I6I6I6 . . . . . WO
5 WOWOWOWOWOWOWOWOWOWOWOWOWOWOWOWOWOWOWOWOWOWOWO . . . . . WO
4 WOWOWOWOWOWOWOWOWOWOWOWOWOWOWOWOWOWOWOWOWOWOWO . . . . . WO
3 WOWOWOWOWOWOWOWOWOWOWOWOWOWOWOWOWOWOWOWOWOWOWO . . . . . WO
2 WOWOWOWOWOWOWOWOWOWOWOWOWOWOWOWOWOWOWOWOWOWOWO . . . . . WO
1 WOWOWOWOWOWOWOWOWOWOWOWOWOWOWOWOWOWOWOWOWOWOWO
J I= 2 4 6 8 10 12 14 16 18 20 22 24 26 28 30

```

K = 7

```

J I= 2 4 6 8 10 12 14 16 18 20 22 24 26 28 30
38 WOWOWOWOWOWOWOWOWOWOWOWOWOWOWOWOWOWOWOWOWOWOWO
37 WO . . . . . *1*1*1*1*1*1*1*1 . . . 0
36 WO . . . . . *1*1*1*1*1*1*1*1 . . . 0
35 WO . . . . . *1*1*1*1*1*1*1*1 . . . 0
34 WO . . . . . *1*1*1*1*1*1*1*1 . . . 0
33 WO . . . . . *1*1*1*1*1*1*1*1 . . . 0
32 WO . . . . . *1*1*1*1*1*1*1*1 . . . 0
31 WO . . . . . *1*1*1*1*1*1*1*1 . . . 0
30 WO . . . . . WOWO . *1*1*1*1*1*1*1*1 . . . WO
29 WO . . . . . WOWO . *1*1*1*1*1*1*1*1 . . . WO
28 WO . . . . . WO . *1*1*1*1*1*1*1*1 . . . WO
27 WO . . . . . WO . *1*1*1*1*1*1*1*1 . . . WO
26 WOWO . . . . . WO . *1*1*1*1*1*1*1*1 . . . WO
25 WOWOWO . . . . . WO . *1*1*1*1*1*1*1*1 . . . WO
24 WOWOWOWO . . . . . WO . *1*1*1*1*1*1*1*1 . . . WO
23 WOWOWOWOWO . . . . . WO . *1*1*1*1*1*1*1*1 . . . WO
22 WO . . . . . WO . . . . . WOWO . . . . . WO
21 WO . . . . . WOWOWO . . . . . WOWO . . . . . WOWO
20 WO . . . . . WOWOWOWO . . . . . WOWO . . . . . WOWOWO
19 WO . . . . . WOWOWOWOWO . . . . . WOWO . . . . . WOWOWOWO
18 WO . . . . . WOWOWOWOWOWO . . . . . WOWO . . . . . WOWOWOWOWO
17 WOWO . . . . . WOWOWOWOWOWOWO . . . . . WOWO . . . . . WOWOWOWO
16 WOWOIIIIII . . . . . WOWOWOWOWOWOWOWOWOWOWOWO
15 WOWOWOWO . . . . . WOWOWOWOWOWOWOWOWOWOWOWO

```


E-01 7.0E-01 7.0E-01
 RESIDUALS 2.3E+00 3.7E-02 4.6E-02 1.8E+00 3.1E-02 3.2E-02 1.0E-02 4.1
 E-02 2.2E-02 4.9E-03

BOUNDARIES -

.....BOUNDARY CONDITIONS.....

| ZONE | (U) | (V) | (W) | (E) | (D) | (T) |
|------|-------------|--------------|-------------|-------------|-------------|-------------------------|
| (1) | (2) | (3) | (4) | (5) | (6) | (7) |
| 00 | 0.0000E+00W | 0.0000E+00W | 0.0000E+00W | 0.0000E+00S | 0.0000E+00S | 6.0000E+02W 0.0000E+00C |
| 01 | 0.0000E+00L | 0.0000E+00L | 0.0000E+00L | 0.0000E+00L | 0.0000E+00L | 2.7300E+02L 0.0000E+00L |
| 11 | 0.0000E+00L | 2.1000E-01L | 0.0000E+00L | 6.6000E-04L | 2.7000E-03L | 3.0000E+02L 0.0000E+00L |
| 12 | 0.0000E+00L | 4.6000E-01L | 0.0000E+00L | 3.1000E-03L | 2.9000E-02L | 3.0000E+02L 0.0000E+00L |
| 13 | 0.0000E+00L | 4.6000E-01L | 0.0000E+00L | 3.1000E-03L | 2.9000E-02L | 3.0000E+02L 0.0000E+00L |
| 14 | 0.0000E+00L | 2.9200E-01L | 0.0000E+00L | 6.6000E-04L | 2.7000E-03L | 3.0000E+02L 0.0000E+00L |
| 15 | 0.0000E+00L | 3.0000E-02L | 0.0000E+00L | 9.6000E-05L | 1.5000E-04L | 3.0000E+02L 0.0000E+00L |
| 16 | 0.0000E+00L | 1.4000E-02L | 0.0000E+00L | 2.9000E-06L | 8.2000E-07L | 3.0000E+02L 0.0000E+00L |
| 18 | 0.0000E+00L | -3.7600E-01L | 0.0000E+00L | 1.6000E-03L | 1.1400E-02L | 2.7300E+02L 0.0000E+00L |
| 19 | 0.0000E+00L | 5.0400E-01L | 0.0000E+00L | 3.8000E-03L | 3.8700E-03L | 2.7300E+02L 0.0000E+00L |

CONSTANTS

CYCLIC CELLS PRESCRIBED PRESSURE DROP = 0.000E+00
 DIFFERENCING SCHEME POWER LAW
 REFERENCE PRESSURE AT I= 27 J= 2 K= 2 (ACTUAL PRESSURE = 1.000E+05)
 GAS DENSITY AT STP = 1.293E+00 USE GAS LAW - Y PRESSURE CORRECTED

N
 SECOND RELAXATION FACTORS ON AFTER 32000 ITERATIONS.

- PATCH OPTION -N
- CONVERG/DIVERG CHP. Y
- NORMALIZE RESIDS. -Y
- CONTINUITY CHECK -Y
- RESET OPTION -Y
- SWEEP DIRECTION 1
- REYNOLDS STRESS MODEL -N
- NON NEWTONIAN FLOW -N
- POROSITY MODEL -Y
- ALLOW LINK SETTING -N
- SET INLET TURBULENCE -Y
- MONITOR OPTION -N
- LINK OPTION -N
- PARTICLE TRACKING 0 TRACKS EVERY 0 ITNS.

POROUS ZONE PROPERTIES :

| ZONE | KX | KY | KZ | C2 |
|-------|-------|-------|-------|-------|
| ----- | ----- | ----- | ----- | ----- |

- TEMPERATURE DEPENDENT PROPERTIES

| PROPERTY | COEFFS | 0 | 1 | 2 | 3 |
|-----------------------|--------|------------|---|---|---|
| ----- | | | | | |
| DYNAMIC VISCOSITY | 1 | 1.7200E-05 | | | |
| LIQ.DENSITY INERTS | 1 | 1.2930E+00 | | | |
| LIQ.DENSITY SPECIES F | 1 | 1.2930E+00 | | | |
| LIQ.DENSITY SPECIES O | 1 | 1.2930E+00 | | | |
| LIQ.DENSITY SPECIES C | 1 | 1.2930E+00 | | | |
| SPECIFIC HEAT (GAS) | 1 | 1.0040E+03 | | | |
| THERMAL COND. (GAS) | 1 | 2.4100E-02 | | | |
| SPECIFIC HEAT (PART.) | 1 | 1.0000E+03 | | | |
| THERMAL COND. (PART.) | 1 | 7.8000E-02 | | | |
| BINARY DIFFUSIVITY | 1 | 3.0000E-05 | | | |
| VAP. PRESS. (PHASE 2) | 1 | 2.5331E+03 | | | |

- SECOND PHASE PARTICLE/DROPLET TRACKING -

MAX. NO. OF STEPS = 5000
 STEP LENGTH FACT. = 2.000E+01
 PARTICLE DENSITY = 1.000E+03
 BOILING POINT = 3.730E+02
 LATENT HEAT OF VAPORIZATION = 1.000E+03
 COEFFICIENT OF RESTITUTION = 1.000E+00
 VAPORIZATION TEMPERATURE = 3.730E+02
 SWELLING COEFFICIENT = 2.000E+00
 FRACTION VOLATILE COMPONENT = 1.000E+00
 FRACTION NON-VOLATILE COMPONENT = 0.000E+00
 STOICHIOMETRIC RATIO FOR SURFACE REACTION = 1.333E+00
 HEAT OF REACTION FOR SURFACE REACTION = 2.000E+07

PARTICLE LAWS ACTIVATED FOR USER-DEFINED HISTORY -

| INERT | VAPORIZE | BOILING | DEVOLAT | BURNOUT | INERT |
|-------|----------|---------|---------|---------|-------|
| Y | N | N | N | N | Y |

INJECT INITIAL VALUES.....
 NO TYP (X) (Y) (Z) (U) (V) (W) (T) (DIAM) (MFLOW)

FLOW FIELD AFTER 0 ITERATIONS--

| | TOTAL | RECOVERABLE | AVAILABLE |
|---------------------------|---------------------------|-------------|-----------|
| | UNITS MILLION (te / year) | | |
| REFUSE : | | | |
| DOMESTIC AND TRADE | 18 - 20 | 18 - 20 | 18 - 20 |
| INDUSTRIAL AND COMMERCIAL | 25 - 35 | 25 - 35 | 25 - 35 |
| SCRAP TYRES AND SPENT OIL | 1.0 - 1.5 | 0.5 - 0.8 | 0.5 - 0.7 |
| SEWAGE SLUDGE : | 30 - 40 | 25 - 35 | 25 - 35 |
| ANIMAL WASTES : | | | |
| CATTLE | 115 - 145 | 40 - 45 | 40 - 45 |
| POULTRY | 3.5 - 4.5 | 3.5 - 4.0 | 3.5 - 4.0 |
| PIGS | 8 - 11 | 8 - 11 | 8 - 11 |
| CROP RESIDUES : | | | |
| STRAW | 10 - 14 | 9 - 13 | 4 - 5 |
| SUGAR BEET | 6 - 8 | 4 - 4.5 | 3 - 3.5 |
| VEGETABLES | 1.8 - 2.3 | 1.8 - 2.3 | 1.6 - 2.0 |
| WOOD RESIDUES : | | | |
| FORESTRY | 2.8 - 3.2 | 0.5 - 1.0 | 0.5 - 1.0 |
| WOOD PROCESSING | 1.7 - 2.0 | 1.7 - 2.0 | 0.7 - 1.0 |
| PROCESS WASTES : | | | |
| FOOD AND DRINKS | 10 - 11 | 10 - 11 | 0.1 - 0.2 |
| OTHER INDUSTRIES | 0.5 - 1.0 | 0.5 - 1.0 | 0.4 - 0.7 |
| TOTALS | 223 - 298 | 147 - 186 | 129 - 163 |

TABLE 1.1 - SOURCES OF WASTES AND RESIDUES IN THE U.K. (REF. 3)

| | Type of refuse * | Grate loadings in lbs of refuse per hour of operation per ft of grate area | Volume in ft per ton of refuse per 24 hours | |
|-----------------|------------------|--|---|---------------------------|
| | | | Furnace primary chamber | Furnace secondary chamber |
| Range of values | M | 58 to 109 | 8.5 - 25 | 12.1 - 28.0 |
| | R | 50 to 72 | 13 - 14.5 | 26.6 - 31.8 |
| | C | 54 to 98 | 9.9- 13.8 | 17.2 - 28.3 |
| Average values | M | 77 | 12.7 | 18.5 |
| | R | 58 | 13.6 | 29.9 |
| | C | 77 | 11.5 | 21.3 |

* M - Mixed refuse made up of garbage, rubbish and non-comustibles.

R - Refuse comprised of burning rubbish only.

C - Refuse containing comustibles only; such as garbage and burnable rubbish.

TABLE 1.2 - PARAMETERS OF DESIGN FOR REFUSE INCINERATORS (REF.1)

| COMPOSITION | 1970 | 1980 | 1990 | 2000 |
|-------------------------------|------|------|------|------|
| WEIGHT % AS DISCARDED : | | | | |
| Paper | 37.4 | 40.1 | 43.4 | 48.0 |
| Yard wastes | 13.9 | 12.9 | 12.3 | 11.9 |
| Food wastes | 20.0 | 16.1 | 14.0 | 12.1 |
| Glass | 9.0 | 10.2 | 9.5 | 8.1 |
| Metal | 8.4 | 8.9 | 8.6 | 7.1 |
| Wood | 3.1 | 2.4 | 2.0 | 1.6 |
| Textiles | 2.2 | 2.3 | 2.7 | 3.1 |
| Leather and rubber | 1.2 | 1.2 | 1.2 | 1.3 |
| Plastic | 1.4 | 3.0 | 3.9 | 4.7 |
| Miscellaneous | 3.4 | 2.7 | 2.4 | 2.1 |
| WEIGHT % AS DISCARDED : | | | | |
| Moisture | 25.1 | 22.0 | 20.5 | 19.9 |
| Volatile carbon | 19.6 | 20.6 | 21.8 | 23.4 |
| Total ash | 22.7 | 23.9 | 22.8 | 20.1 |
| Ash (excluding glass & metal) | 6.4 | 6.1 | 6.0 | 6.0 |

TABLE 1.3 - PROJECTED AVERAGE GENERATED REFUSE COMPOSITION AND QUANTITY, BETWEEN 1970 TO 2000 (REF. 11)

ATMOSPHERIC AIR REQUIRED (lb/10000 Btu)

| FUEL | RANGE | AVERAGE |
|----------------------|-----------|---------|
| Anthracite : | | |
| New Mexico | - | 7.83 |
| Colorado | - | 7.85 |
| Pennsylvania | 7.81-7.93 | 7.88 |
| Semi-Anthracite | 7.68-7.82 | 7.74 |
| Bituminous coal : | | |
| Low volatile | 7.62-7.76 | 7.69 |
| High volatile A | 7.51-7.73 | 7.63 |
| High volatile B | 7.56-7.73 | 7.66 |
| High volatile C | 7.54-7.67 | 7.50 |
| Sub-bituminous coal | 7.56-7.57 | 7.56 |
| Lignite : | | |
| North Dakota | - | 7.47 |
| Texas | - | 7.52 |
| Coke : | | |
| High-temperature | - | 7.96 |
| Low-temperature | - | 7.63 |
| Beenive | - | 8.05 |
| By-product | - | 8.01 |
| Gas works coke | 8.02-8.10 | 8.06 |
| Petroleum coke | - | 7.73 |
| Pitch coke | - | 8.13 |
| Wood: | | |
| Soft wood | 7.02-7.22 | 7.11 |
| Hard wood | 7.09-7.28 | 7.15 |
| Bagasse | 6.25-6.99 | 6.59 |
| Petroleum oils : | | |
| Gasoline | - | 7.46 |
| Kerosine | - | 7.42 |
| Gas oil | - | 7.45 |
| Fuel oil | - | 7.58 |
| Gaseous fuels : | | |
| Natural gas | 7.32-7.41 | 7.37 |
| Refinery and oil gas | 6.52-7.38 | 7.44 |
| Blast furnace gas | 5.73-6.27 | 5.82 |
| Coke oven gas | 6.66-7.02 | 6.80 |
| Miscellaneous : | | |
| Cellulose | - | 6.80 |
| Glucose | - | 6.90 |
| Glycol dipalmitate | - | 7.40 |
| Methyle alcohol | - | 6.70 |

TABLE 1.4 - AIR REQUIREMENT OF COMPLETE COMBUSTION FOR DIFFERENT FUELS ON A DRY BASIS (REF. 7)

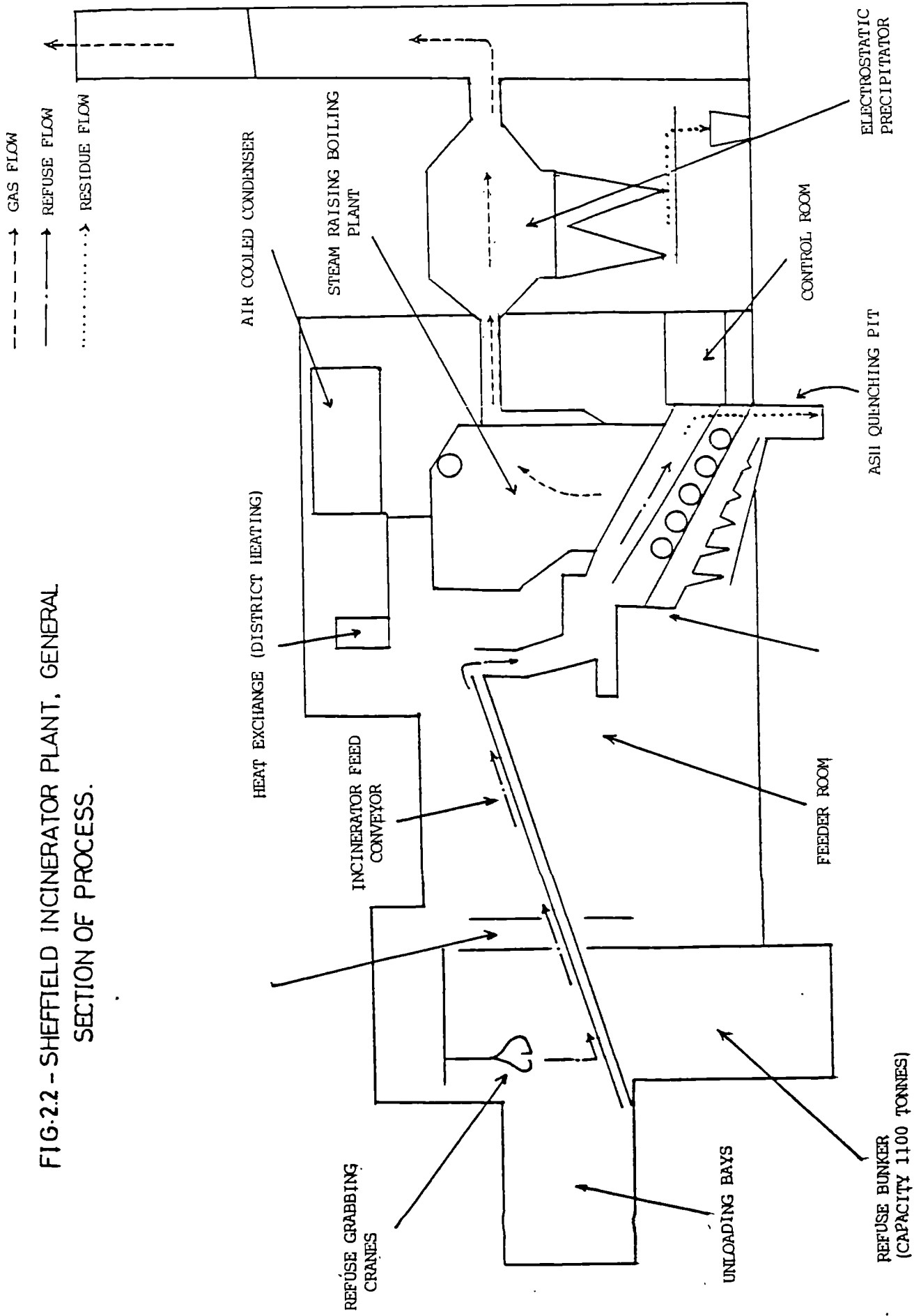
| Heat Release | | Tonnes/h* | Maximum Allowable Emission of Grit and Dust | |
|--------------|---------|-----------|--|-------|
| (MBtu/h) | MJ/h | | (lb/h) | g/s |
| 1.0 | 1055 | 0.091 | 1.0 | 0.126 |
| 2.0 | 2110 | 0.181 | 2.0 | 0.25 |
| 3.0 | 3164 | 0.272 | 3.0 | 0.378 |
| 4.0 | 4219 | 0.363 | 3.5 | 0.441 |
| 5.0 | 5274 | 0.453 | 4.0 | 0.504 |
| 10.0 | 10548 | 0.907 | 6.5 | 0.819 |
| 15.0 | 15822 | 1.36 | 9.0 | 1.134 |
| 20.0 | 21096 | 1.81 | 9.6 | 1.210 |
| 30.0 | 31640 | 2.721 | 10.6 | 1.335 |
| 40.0 | 42190 | 3.63 | 11.7 | 1.474 |
| 50.0 | 52740 | 4.53 | 12.8 | 1.61 |
| 75.0 | 79110 | 6.80 | 19.2 | 2.42 |
| 100.0 | 105500 | 9.07 | 25.6 | 3.226 |
| 200.0 | 210960 | 18.14 | 51.1 | 6.438 |
| 300.0 | 316400 | 27.21 | 76.7 | 9.664 |
| 400.0 | 421900 | 36.28 | 102 | 12.85 |
| 500.0 | 527400 | 45.35 | 128 | 16.13 |
| Above 500.0 | <527400 | | Add 26 lb/h per 100 MBtu/h. 3.276 g/s per 105500 MJ/h | |

Intermediate values in the above table should be found by interpolation.

* Based on an assumed 5000 Btu/lb

TABLE 2.1 - THE RECOMMENDATIONS OF THE SECOND WORKING PARTY ON GRIT AND DUST EMISSIONS (REF.25)

FIG.2.2 - SHEFFIELD INCINERATOR PLANT, GENERAL SECTION OF PROCESS.



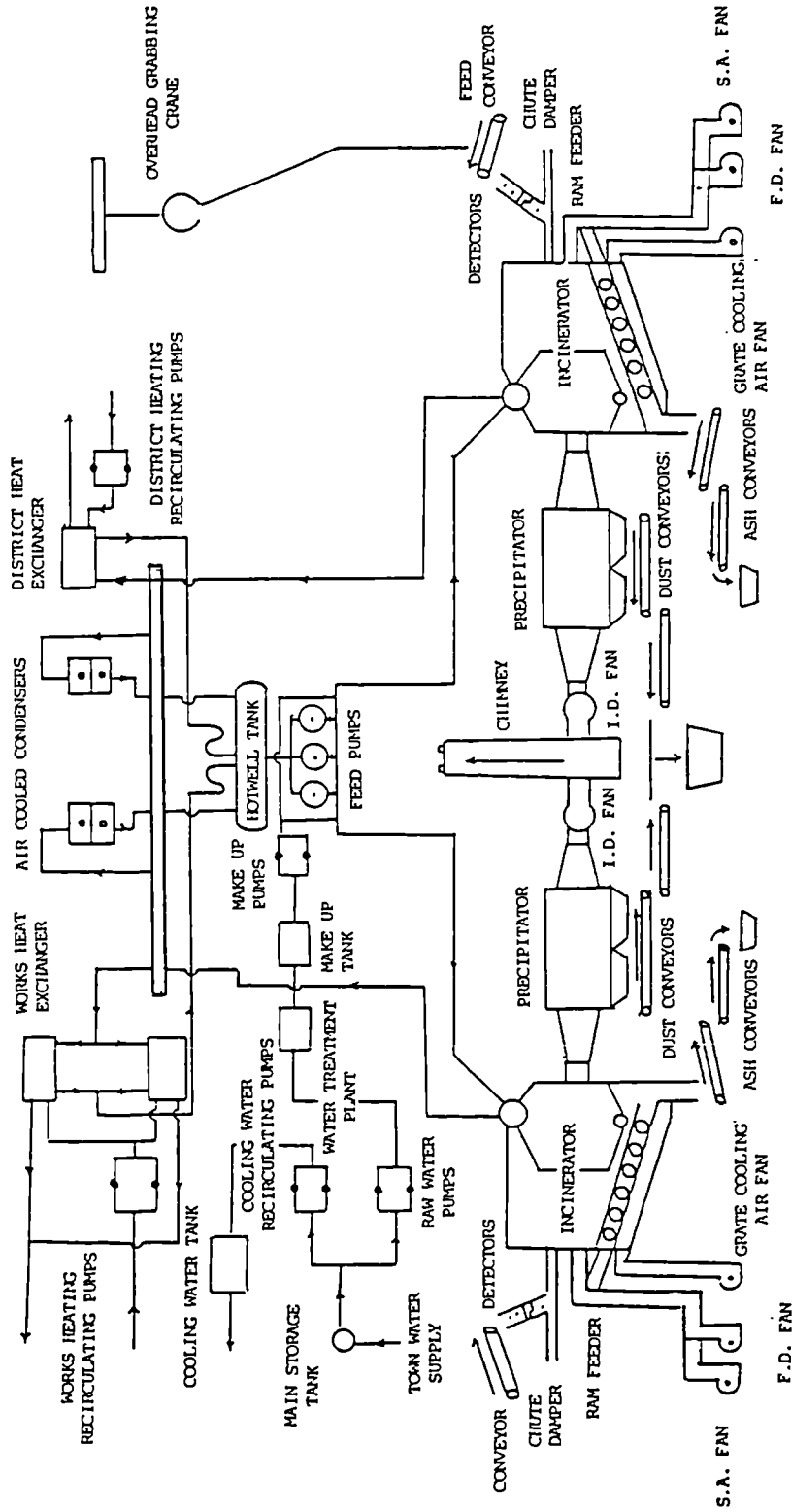


FIGURE 2.3-DIGRAMATIC LAYOUT OF SHEFFIELD DISTRICT HEATING SCHEME.

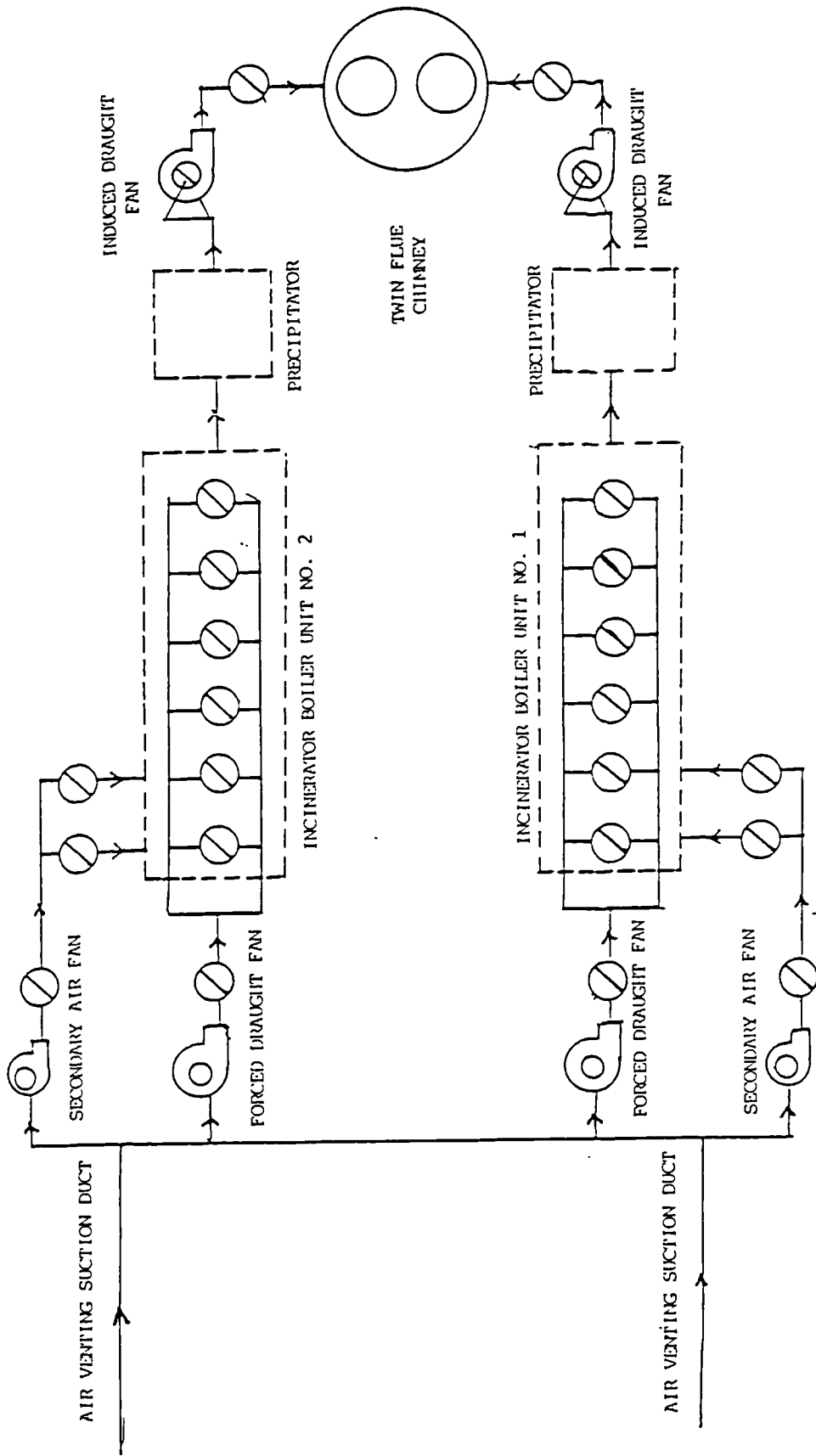
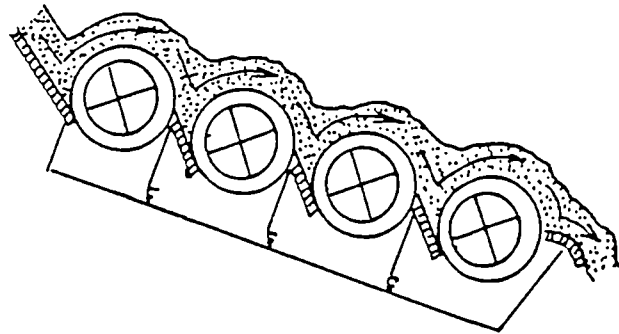
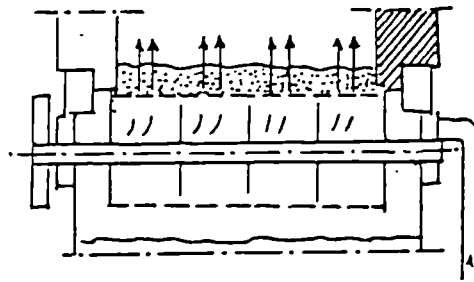


FIGURE 2.4 - DAMPER DIAGRAM (SHEFFIELD INCINERATOR)



SIDE VIEW



CROSS SECTION

FIGURE 2.5 'DUSSELDORF' ROTATING ROLL
GRATE TYPE.

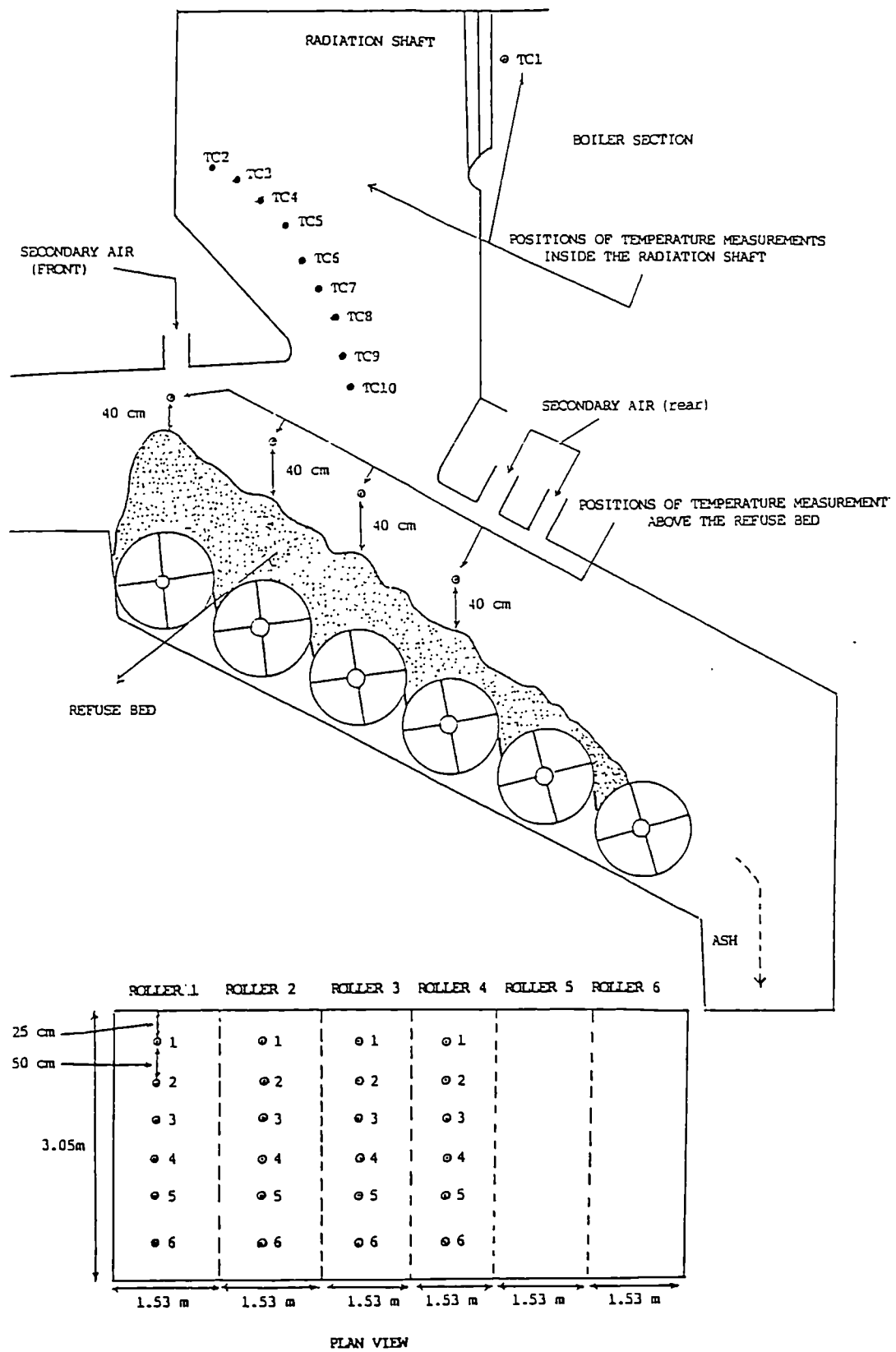
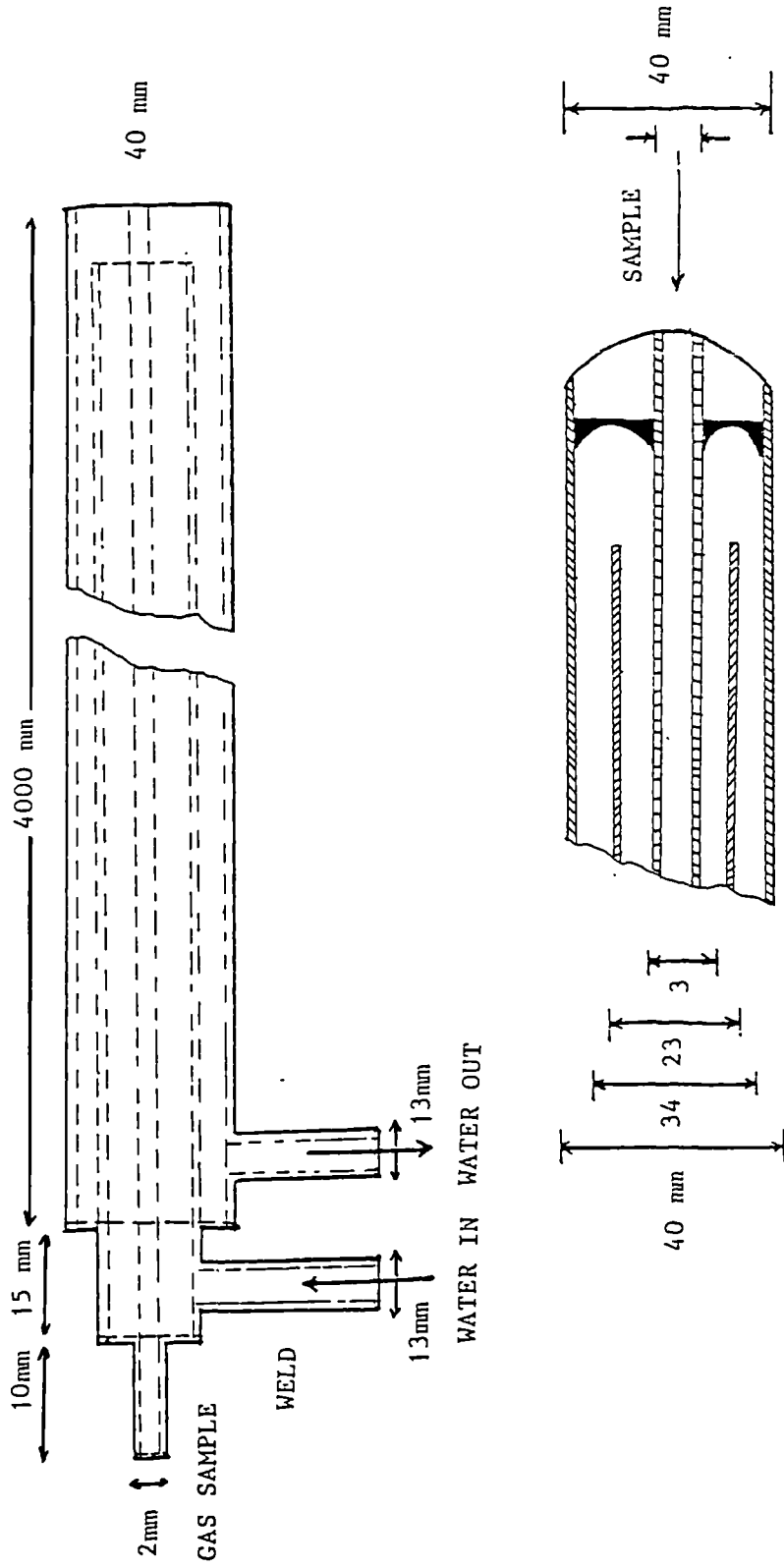


FIGURE 2-6 - SCHEMATIC OF SHEFFIELD MUNICIPAL INCINERATOR SHOWING LOCATION OF TEMPERATURE MEASUREMENTS INSIDE THE FURNACE AND SHAFT.



SAMPLING PROBE : TIP CONSTRUCTION

FIGURE 2.7-WATER COOLED PROBE USED FOR TEMPERATURE MEASUREMENT.

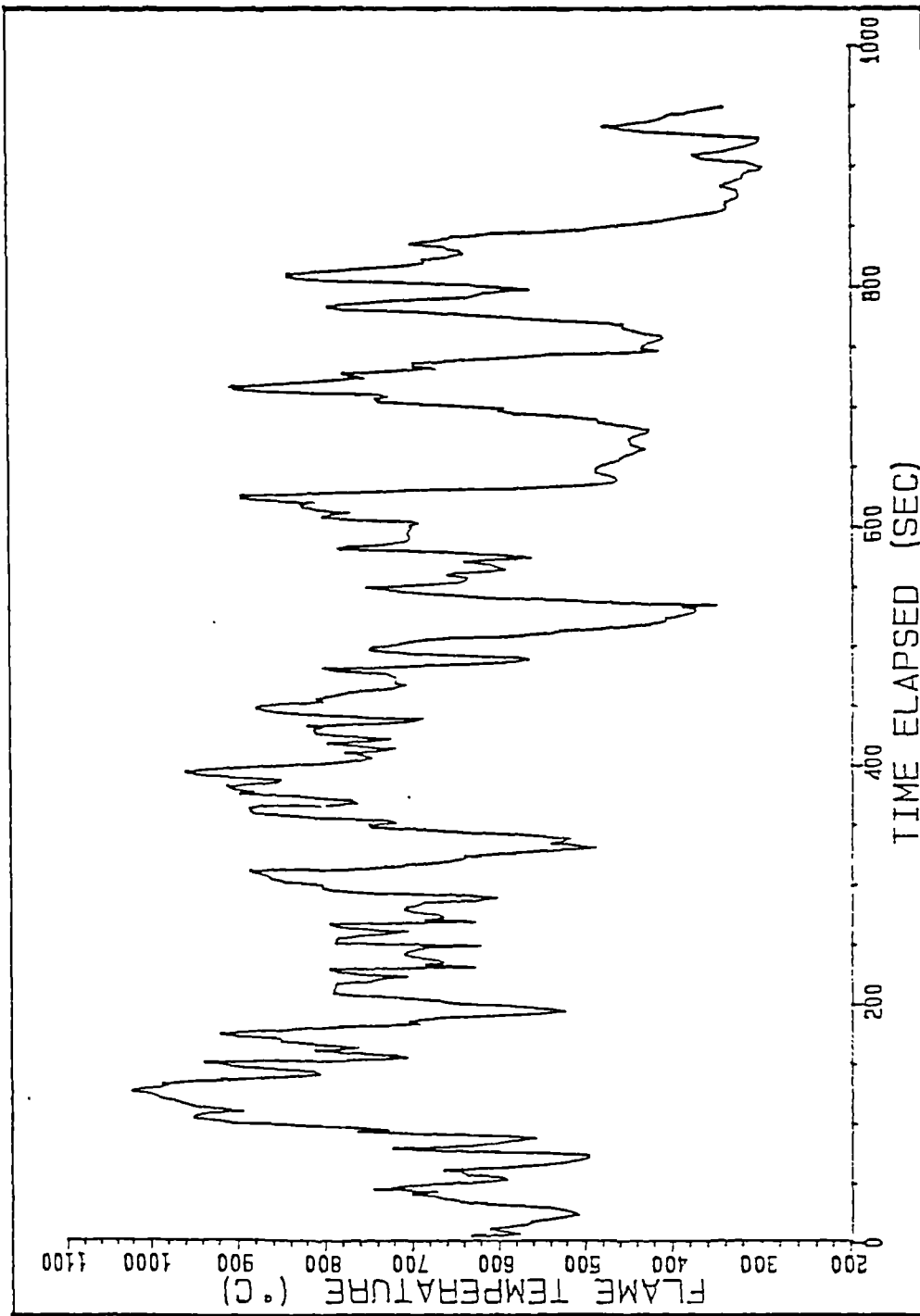


FIGURE 2.8 - TYPICAL TEMPERATURE VARIATION VS TIME AT POSITION TC10 INSIDE THE RADIATION SHAFT.

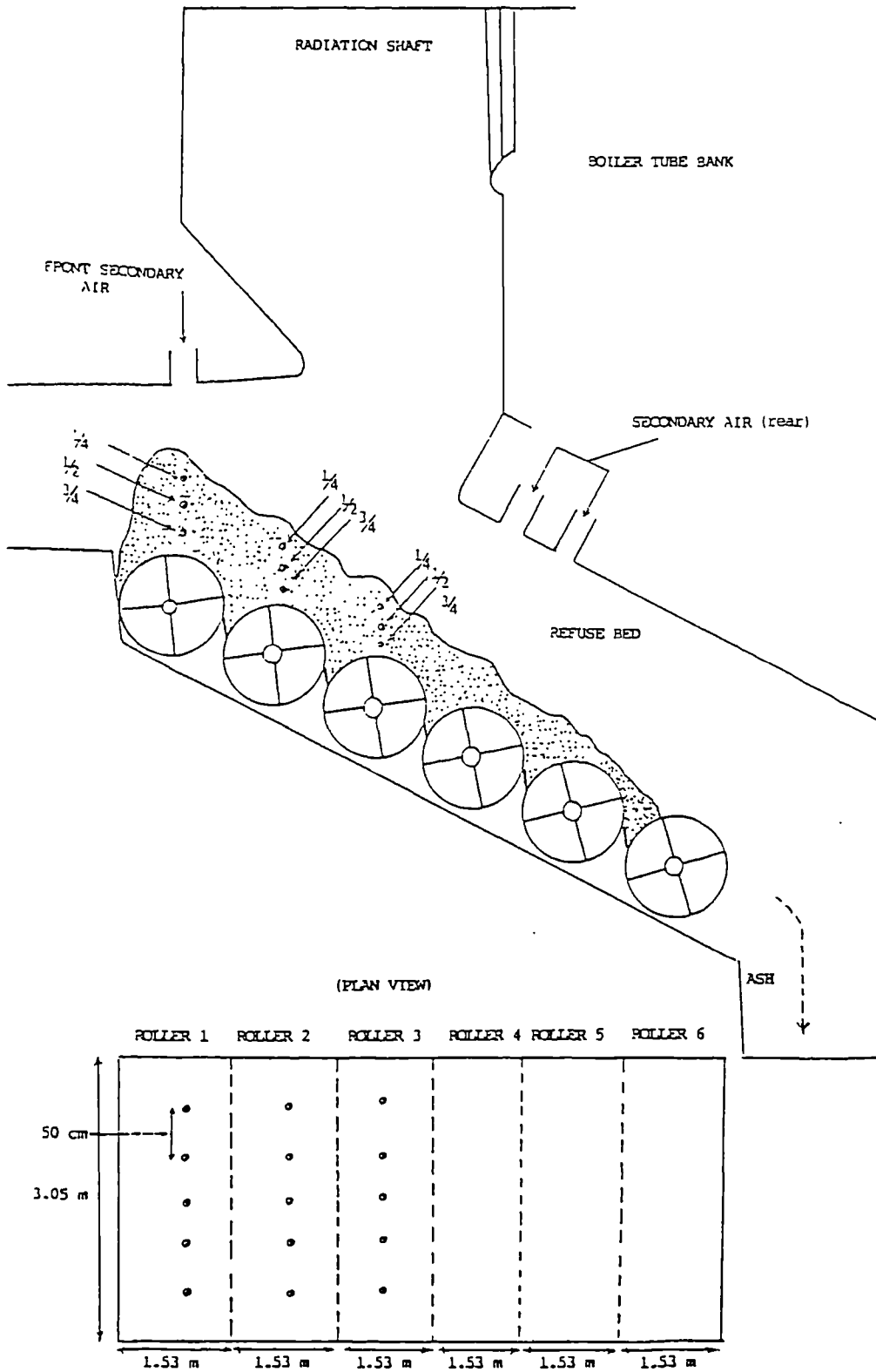


FIGURE 2.9 - SCHEMATIC OF SHEFFIELD MUNICIPAL INCINERATOR SHOWING LOCATION OF TEMPERATURE MEASUREMENTS INSIDE THE REFUSE BED.

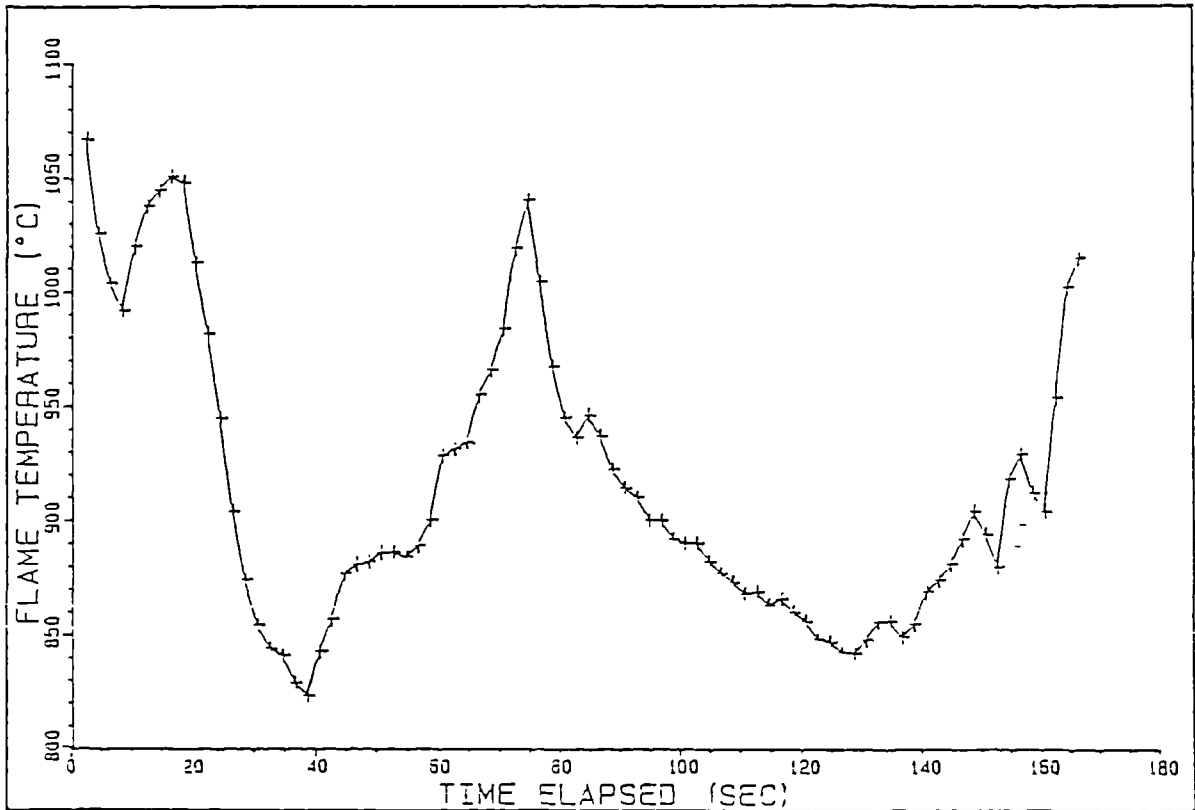


FIGURE 2.10 - TYPICAL TEMPERATURE VARIATION VS TIME AT POSITION 3 ABOVE ROLLER No. 1 , (SEE FIG. 2.6)

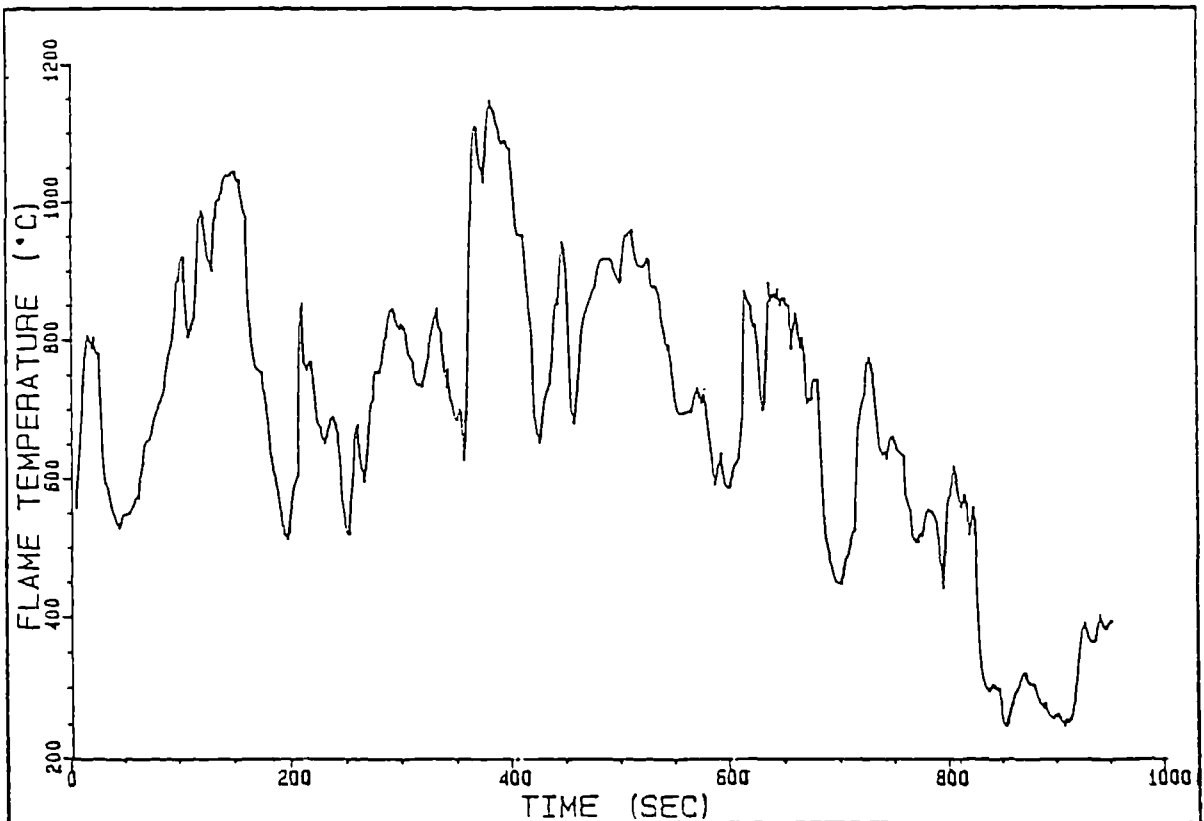


FIGURE 2.11 - TYPICAL TEMPERATURE VARIATION VS TIME AT POSITION 3 ABOVE ROLLER No. 2 , (SEE FIG. 2.6)

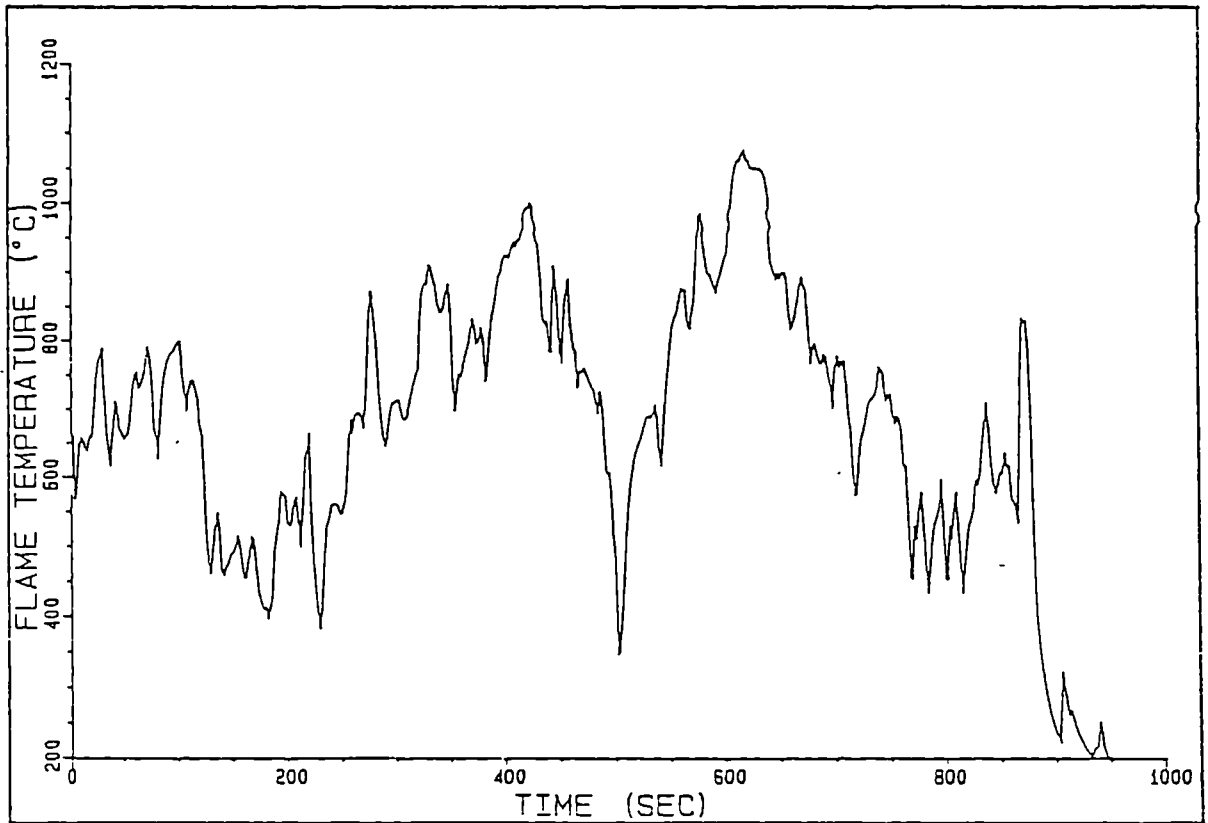


FIGURE 2.12 - TYPICAL TEMPERATURE VARIATION VS TIME AT POSITION 3 ABOVE ROLLER No. 3 , (SEE FIG. 2.6)

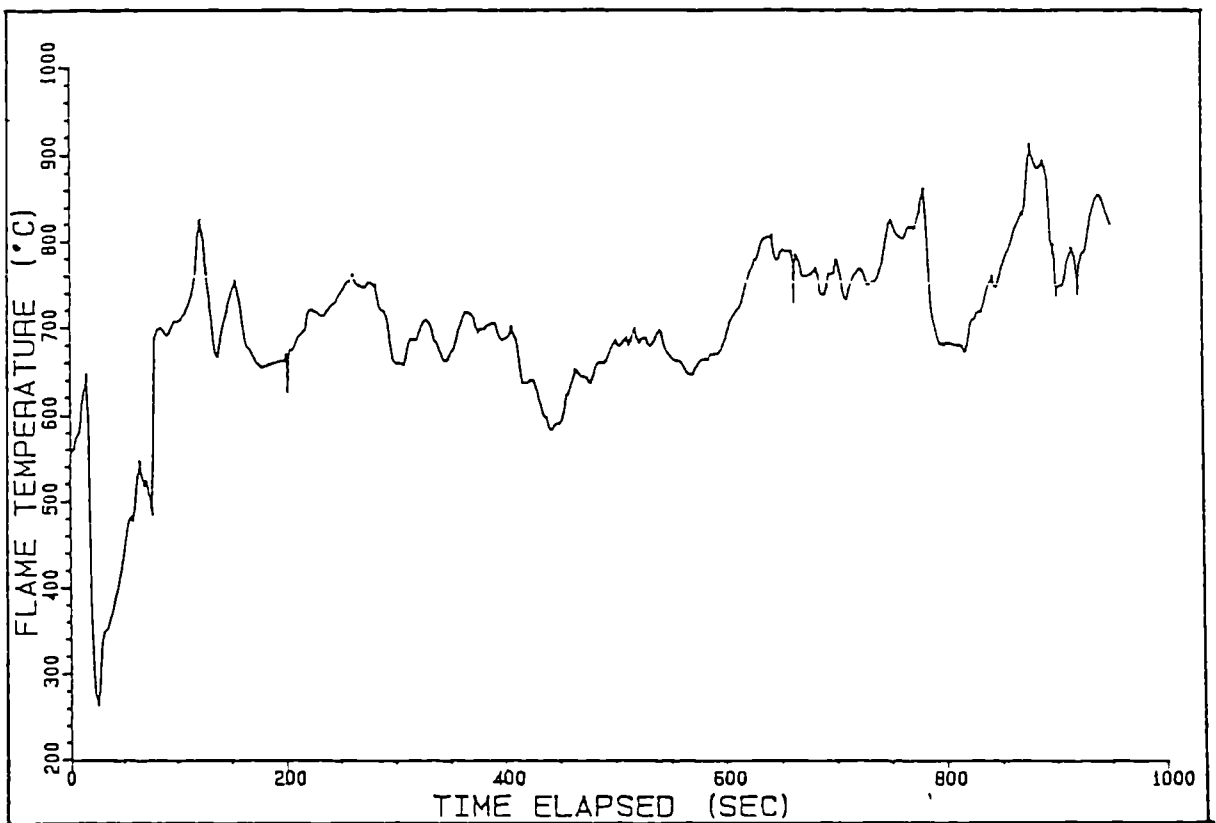


FIGURE 2.13 - TYPICAL TEMPERATURE VARIATION VS TIME AT POSITION 3 ABOVE ROLLER No. 4, (SEE FIG. 2.6)

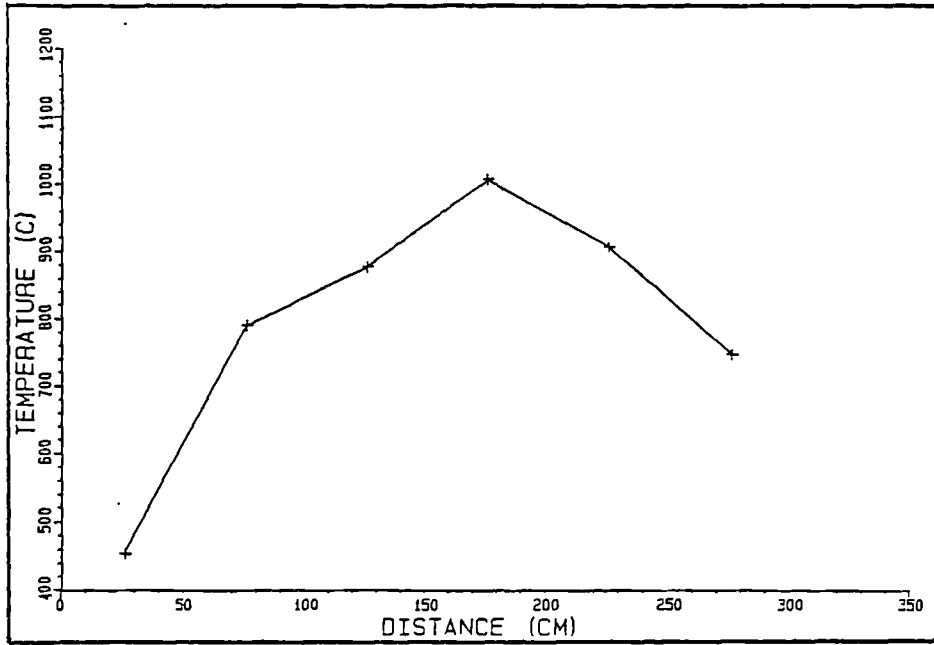


FIGURE 2.14 - TYPICAL TEMPERATURE VARIATION ACROSS THE REFUSE BED ON TOP OF ROLLER 1

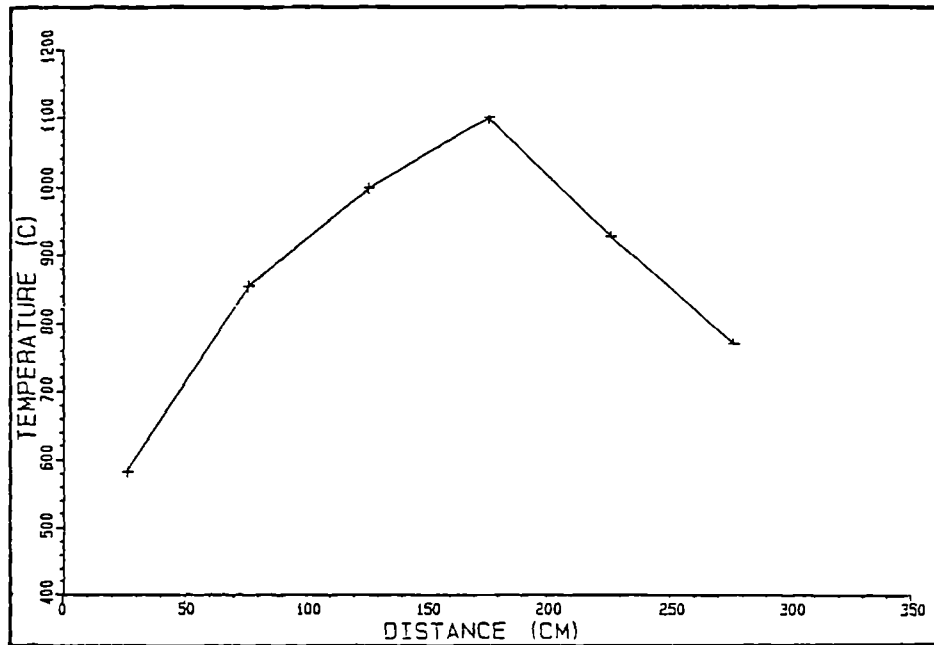


FIGURE 2.15 - TYPICAL TEMPERATURE VARIATION ACROSS THE REFUSE BED ON TOP OF ROLLER 2

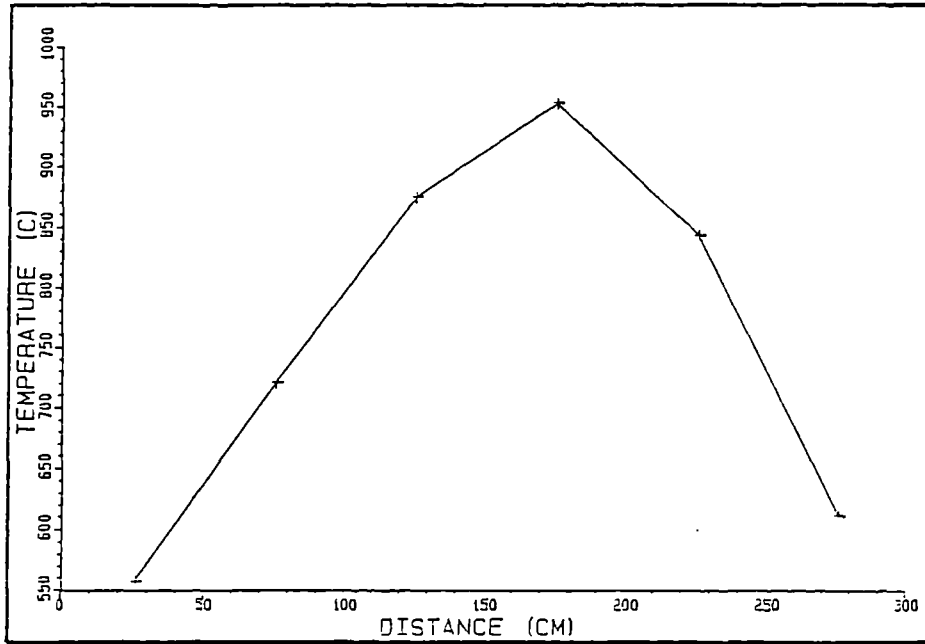


FIGURE 2.16 - TYPICAL TEMPERATURE VARIATION ACROSS THE REFUSE BED ON TOP OF ROLLER 3

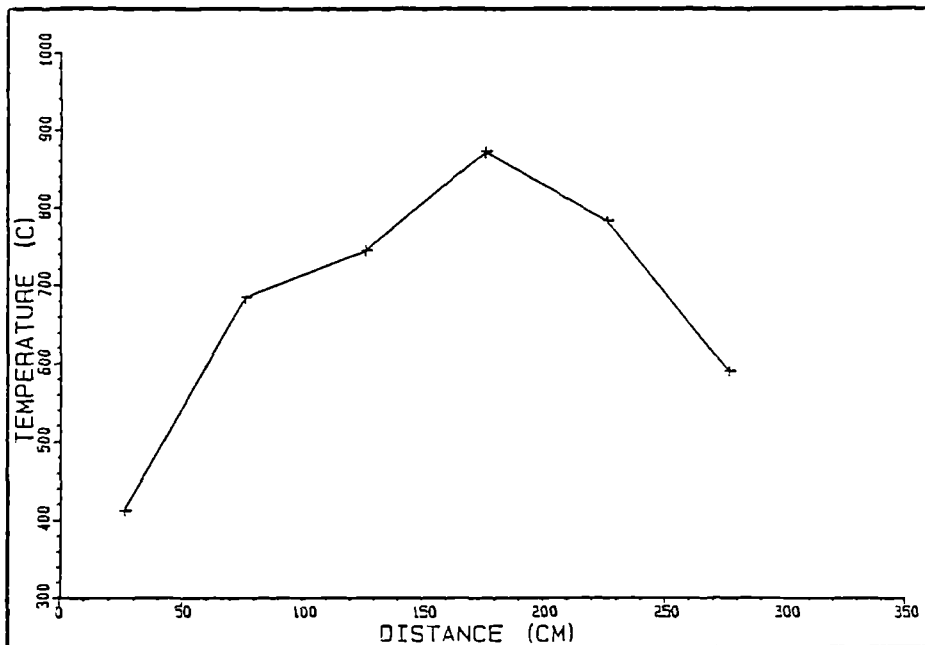


FIGURE 2.17 - TYPICAL TEMPERATURE VARIATION ACROSS THE REFUSE BED ON TOP OF ROLLER 4

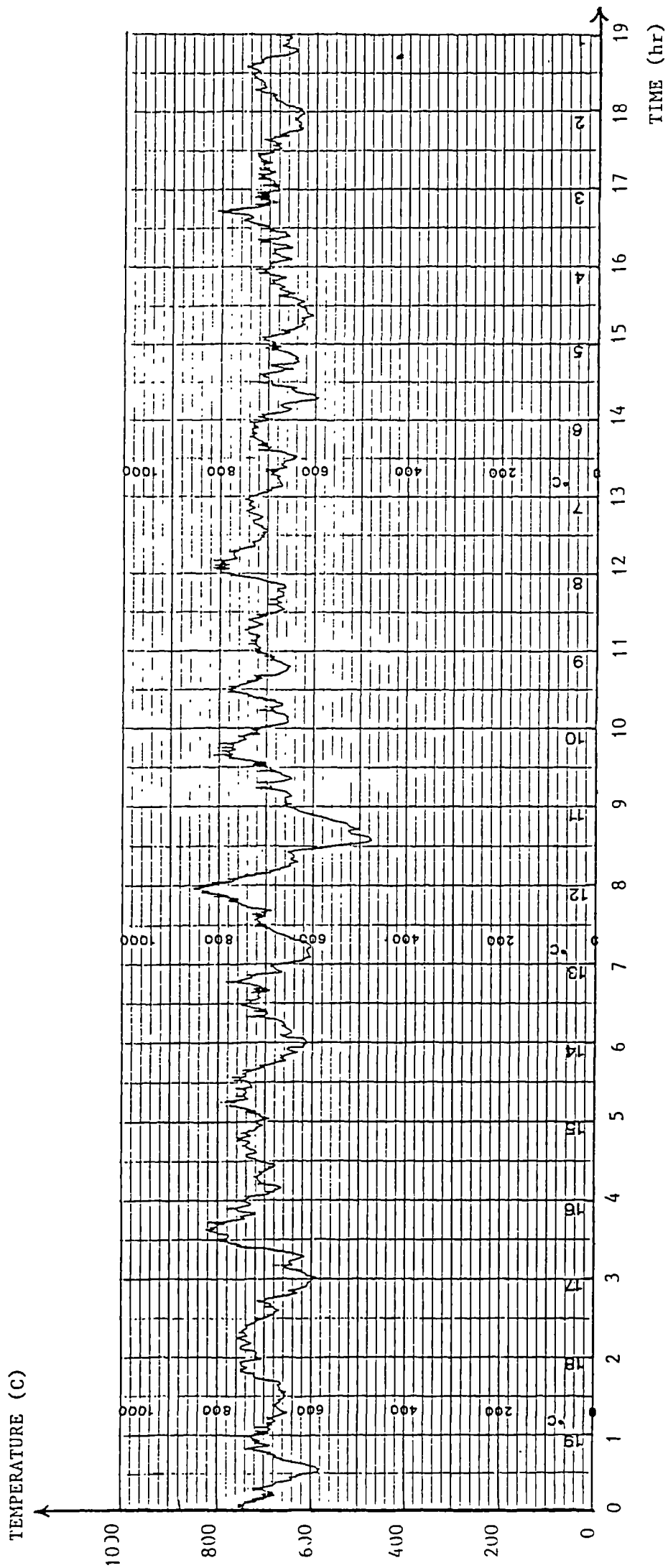


FIGURE 218 - TEMPERATURE - TIME HISTORY AT COMBUSTOR CHAMBER EXIT (POSITION TC1, SEE FIG.2.6)

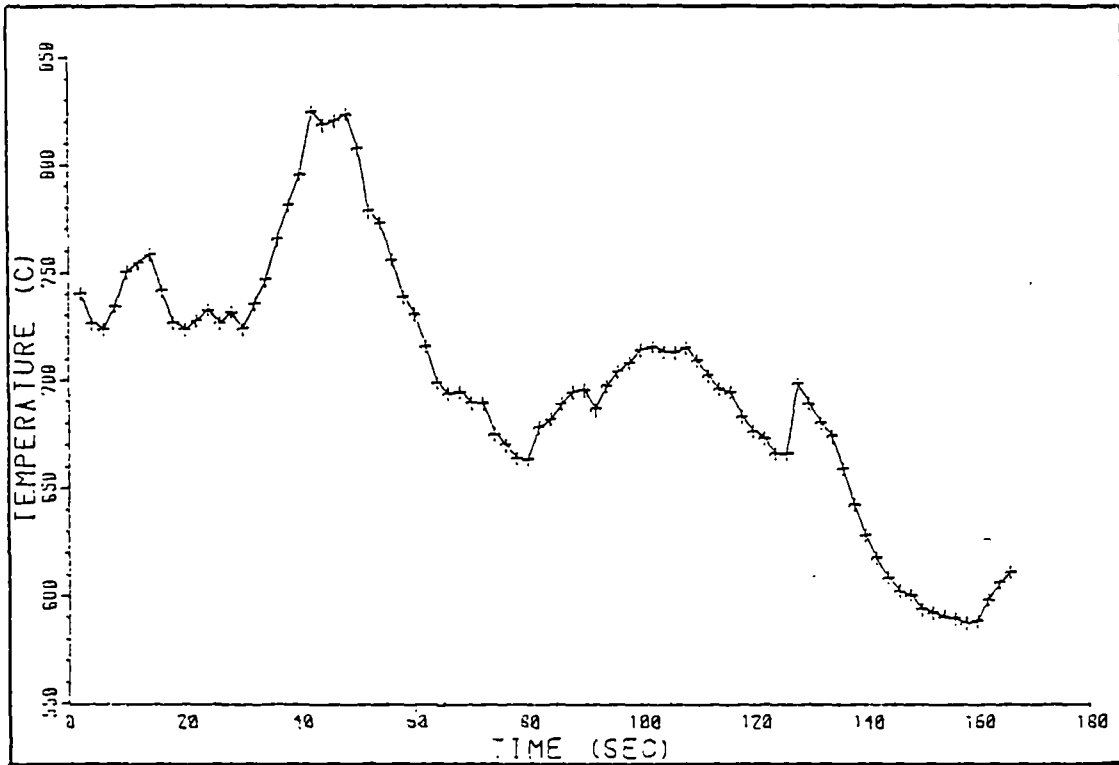


FIGURE 2.19 - TYPICAL TEMPERATURE VARIATION VS TIME AT POSITION TC2 INSIDE THE SHAFT (see fig.2.6)

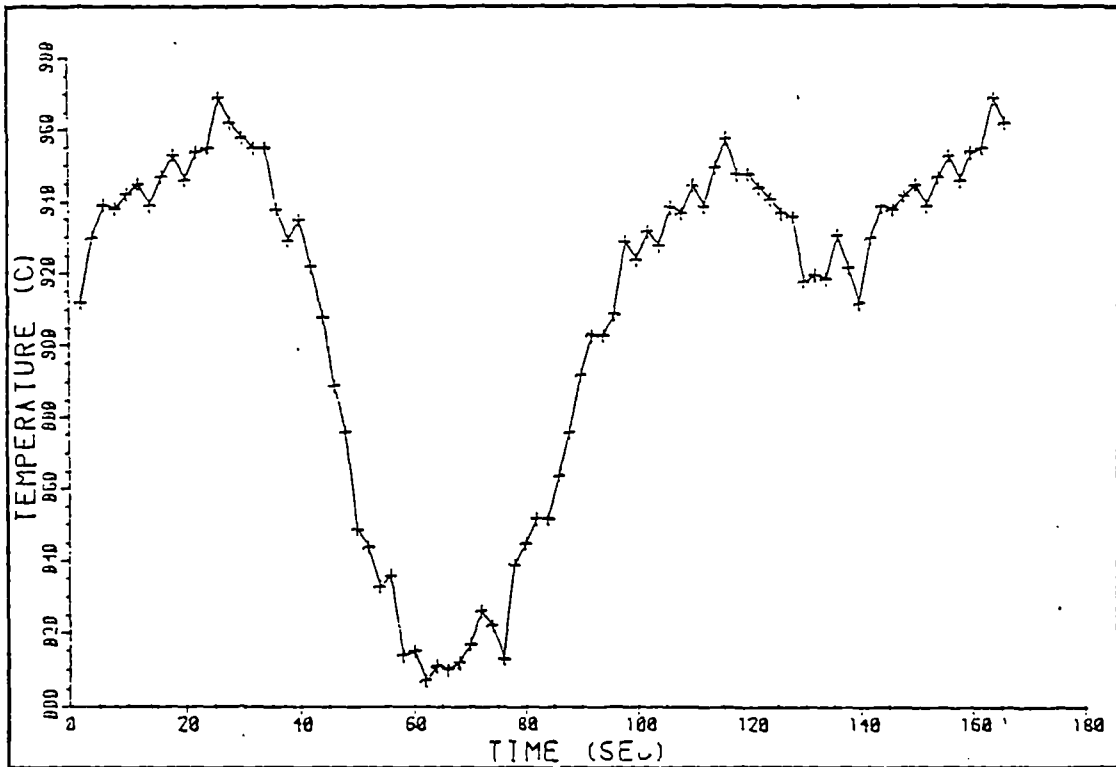


FIGURE 2.20 - TYPICAL TEMPERATURE VARIATION VS TIME AT POSITION TC3 INSIDE THE SHAFT (see fig.2.6)

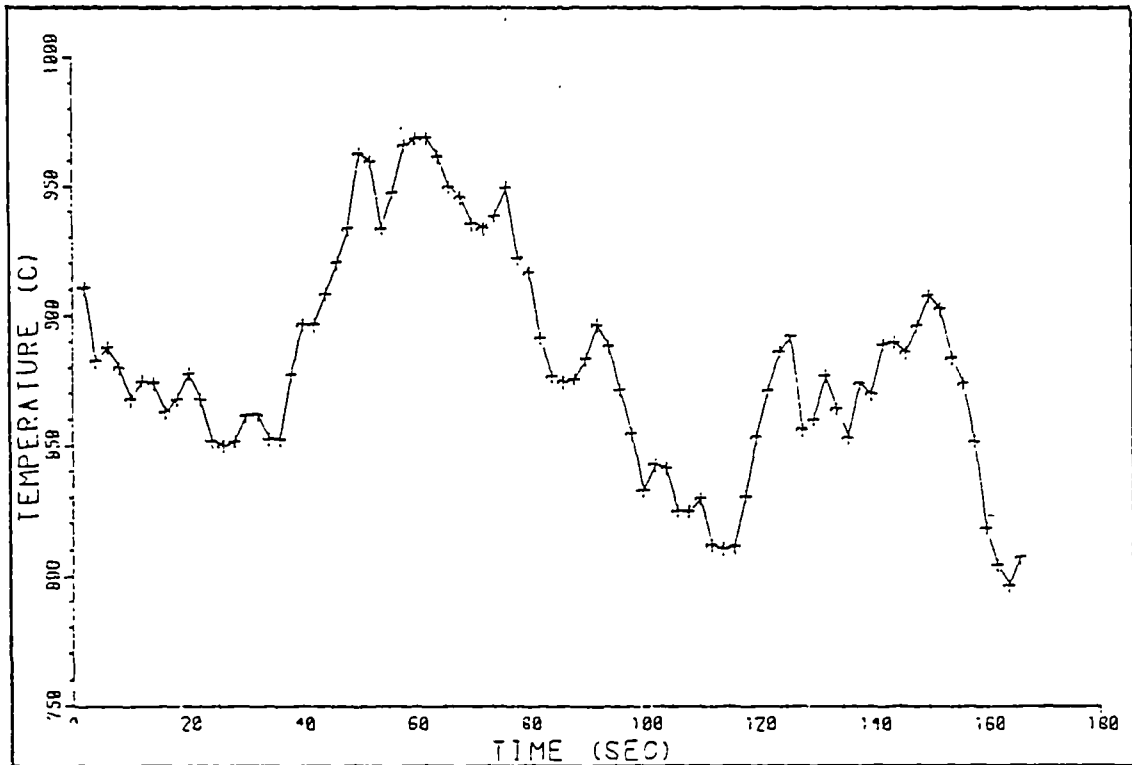


FIGURE 2.21 - TYPICAL TEMPERATURE VARIATION VS TIME AT POSITION TC4 INSIDE THE SHAFT (see fig.2.6)

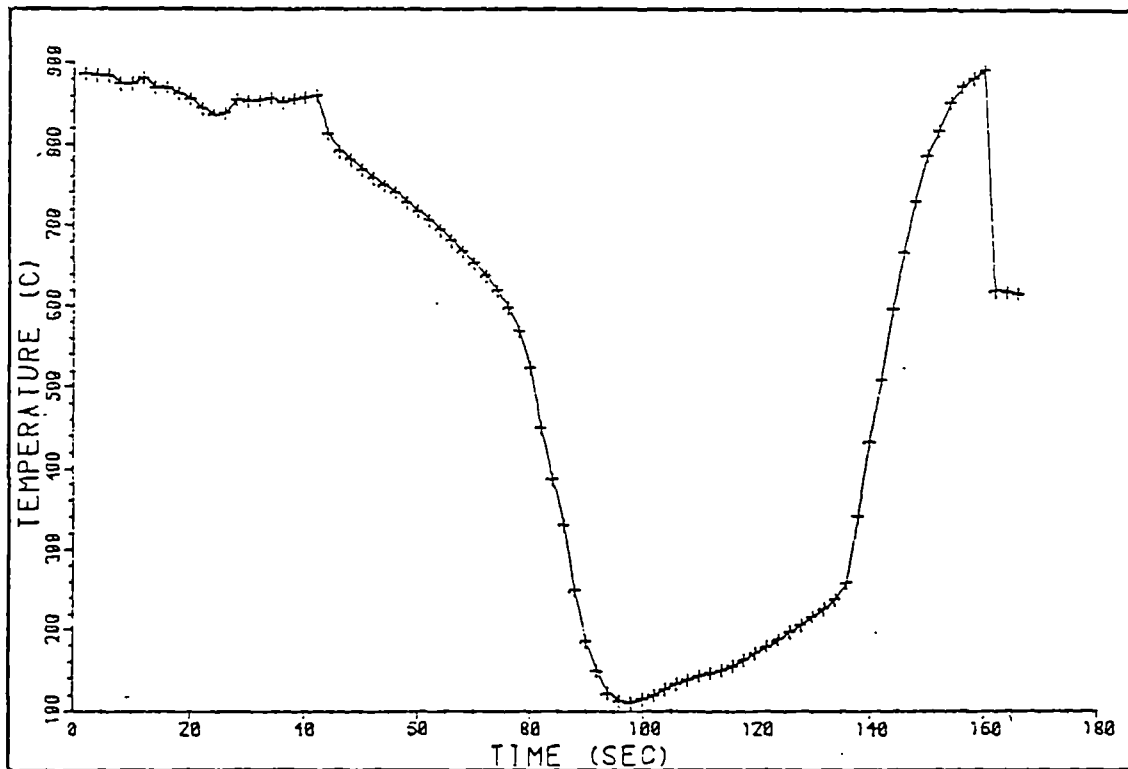


FIGURE 2.22 - TYPICAL TEMPERATURE VARIATION VS TIME AT POSITION TC5 INSIDE THE SHAFT (see fig.2.6)

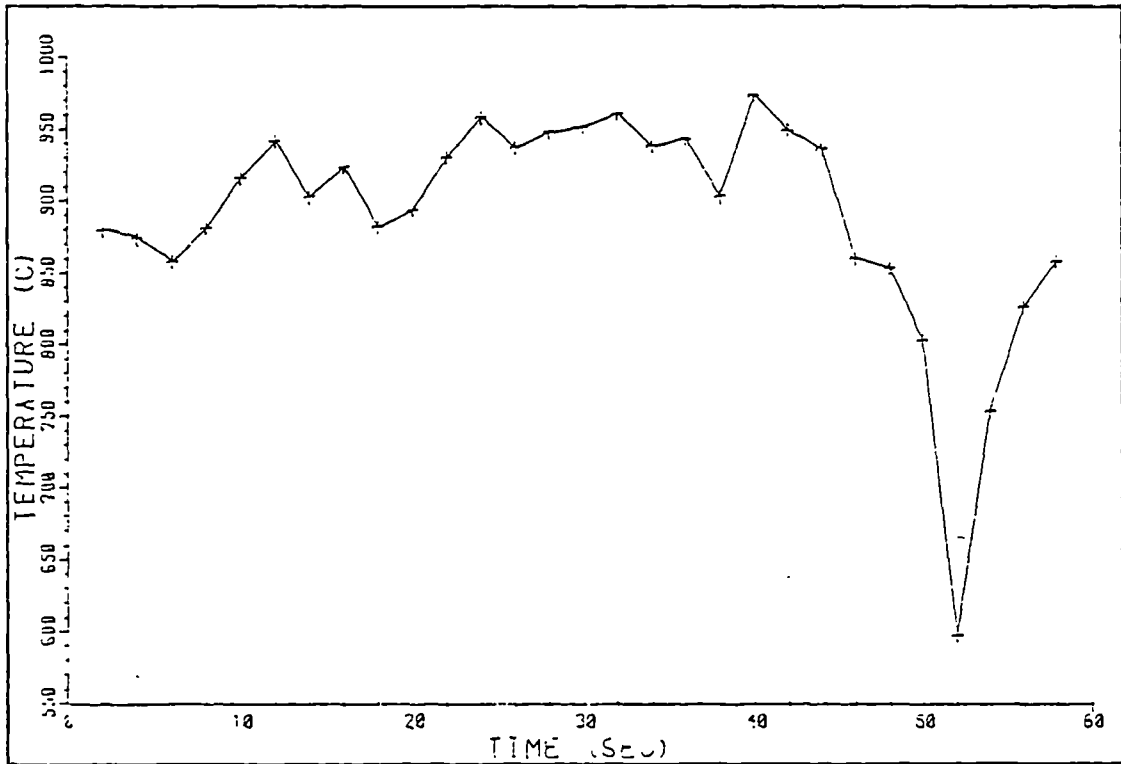


FIGURE 2.23 - TYPICAL TEMPERATURE VARIATION VS TIME AT POSITION TC6 INSIDE THE SHAFT (see fig.2.6)

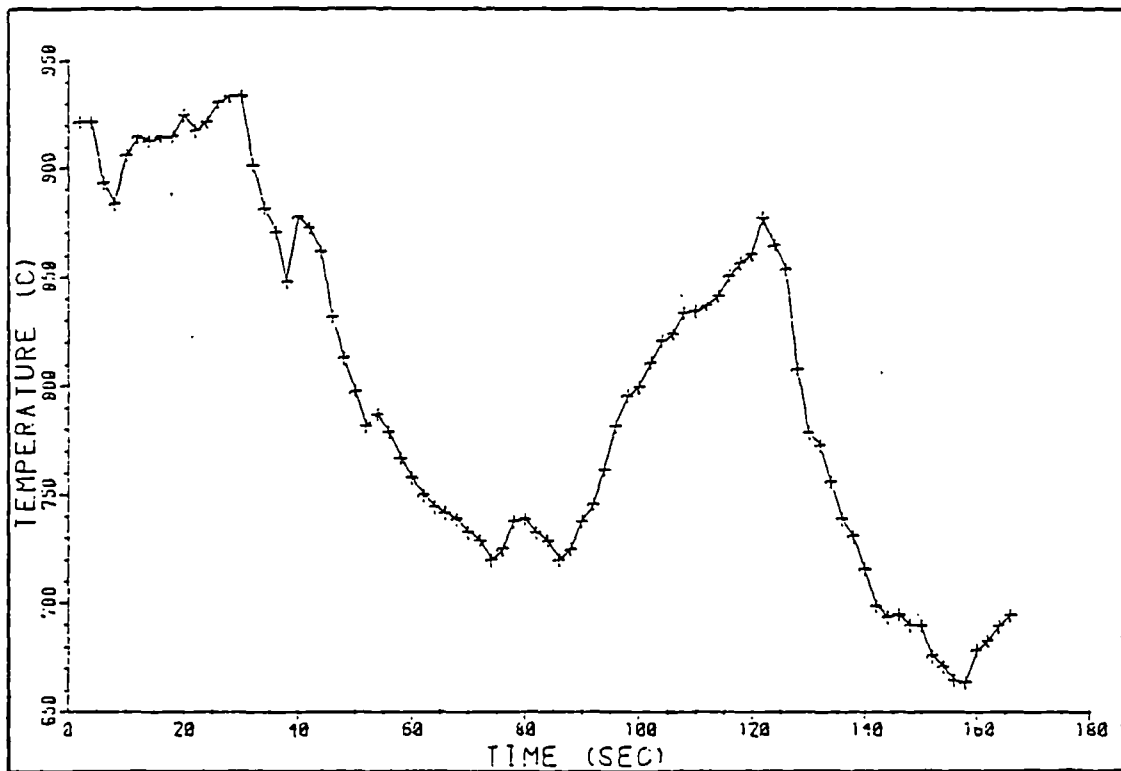


FIGURE 2.24 - TYPICAL TEMPERATURE VARIATION VS TIME AT POSITION TC7 INSIDE THE SHAFT (see fig.2.6)

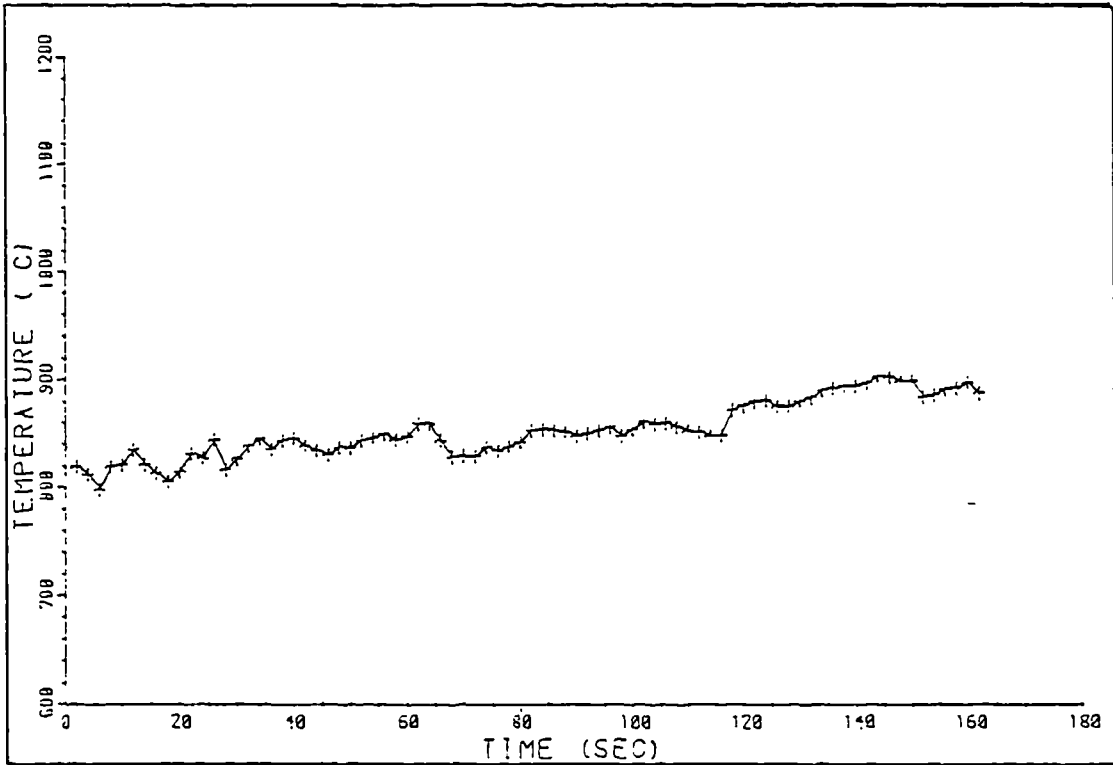


FIGURE 2.25 - TYPICAL TEMPERATURE VARIATION VS TIME AT POSITION TC8 INSIDE THE SHAFT (see fig.2.6)

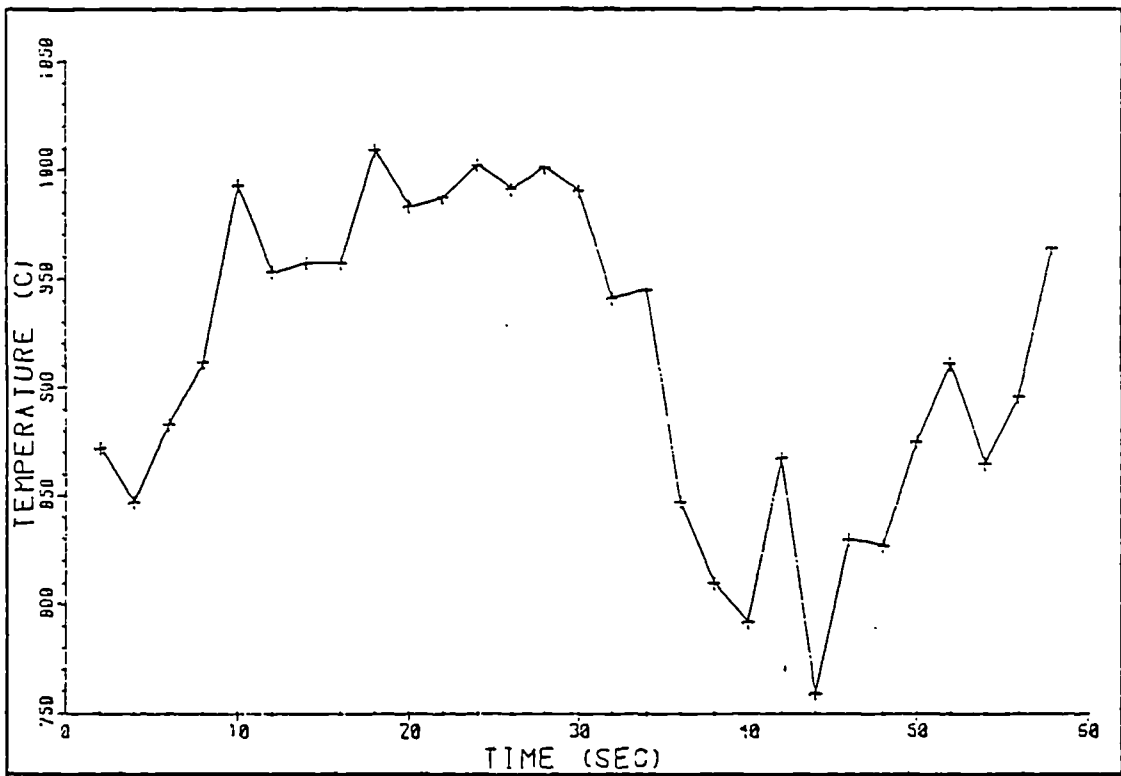


FIGURE 2.26 - TYPICAL TEMPERATURE VARIATION VS TIME AT POSITION TC9 INSIDE THE SHAFT (see fig.2.6)

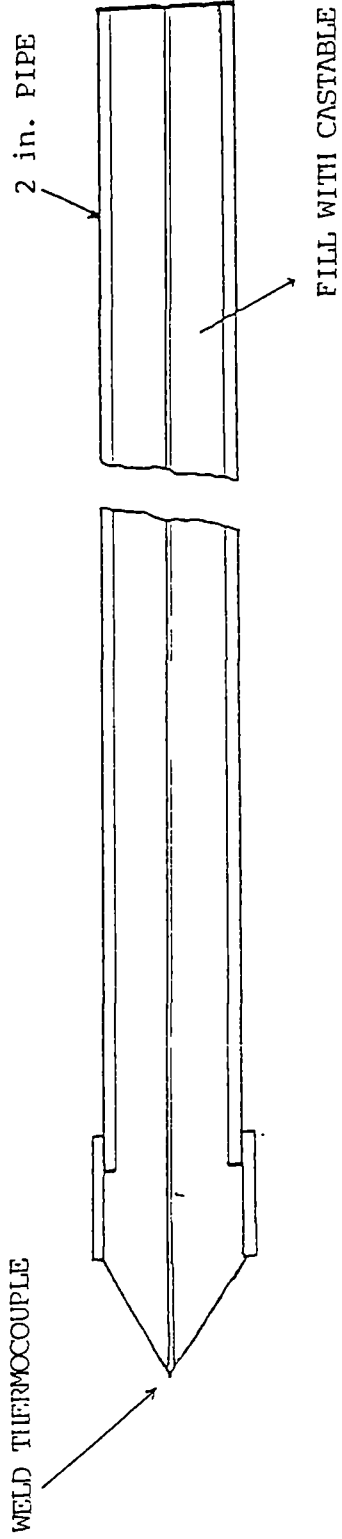
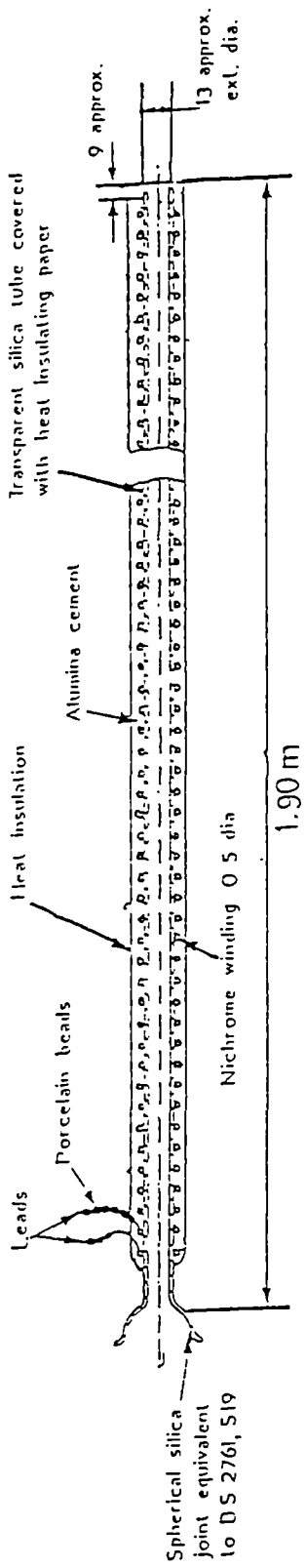


FIGURE 2-27 - SPECIAL PROBES USED FOR BED TEMPERATURE AND SO₂ (FLUE GAS ANALYSIS) DETERMINATIONS.

TEMPERATURE (°C)

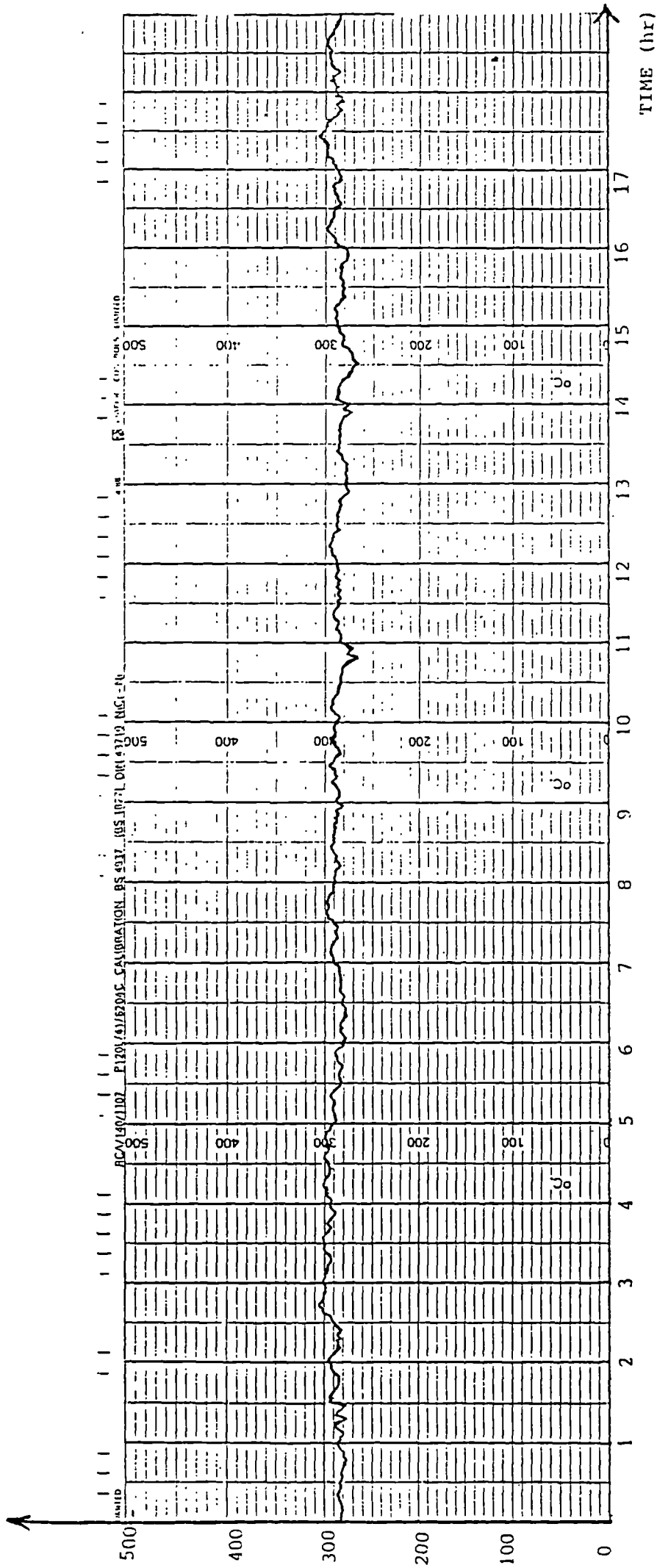


FIGURE 2-28 - TYPICAL TEMPERATURE VARIATION VS TIME AT PRECIPITATOR INLET.

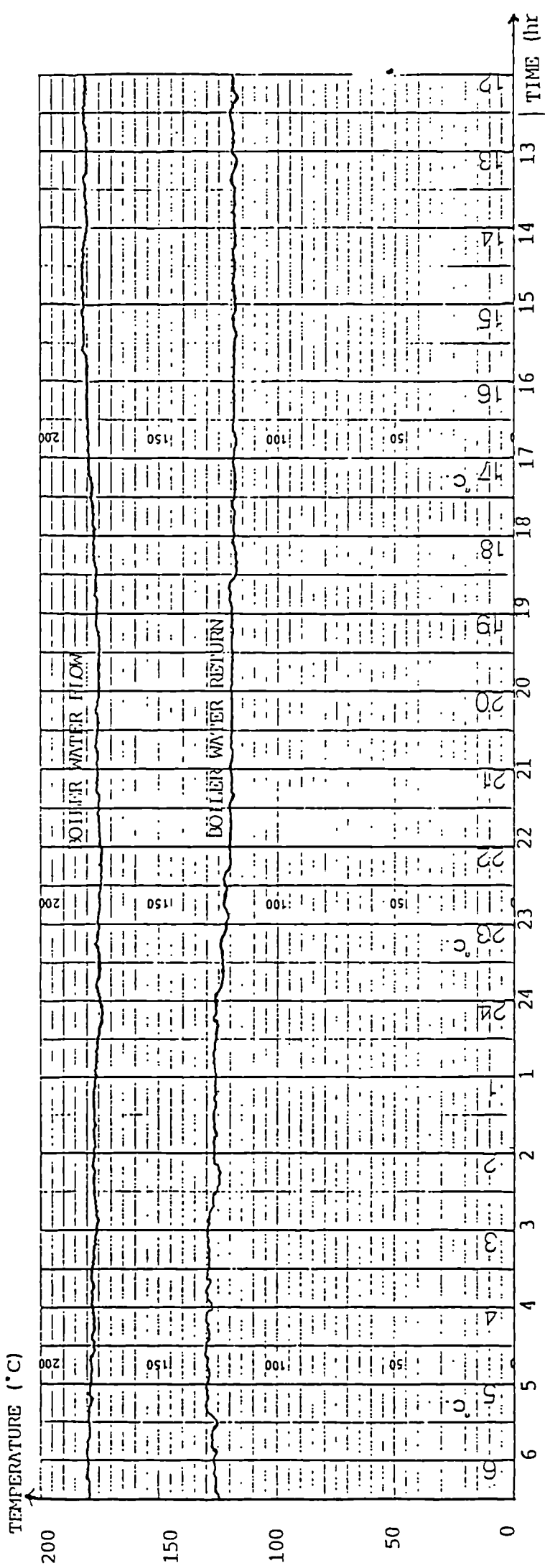


FIGURE 2-30 - TYPICAL BOILER WATER FLOW AND RETURN TEMPERATURE VARIATIONS VS TIME.

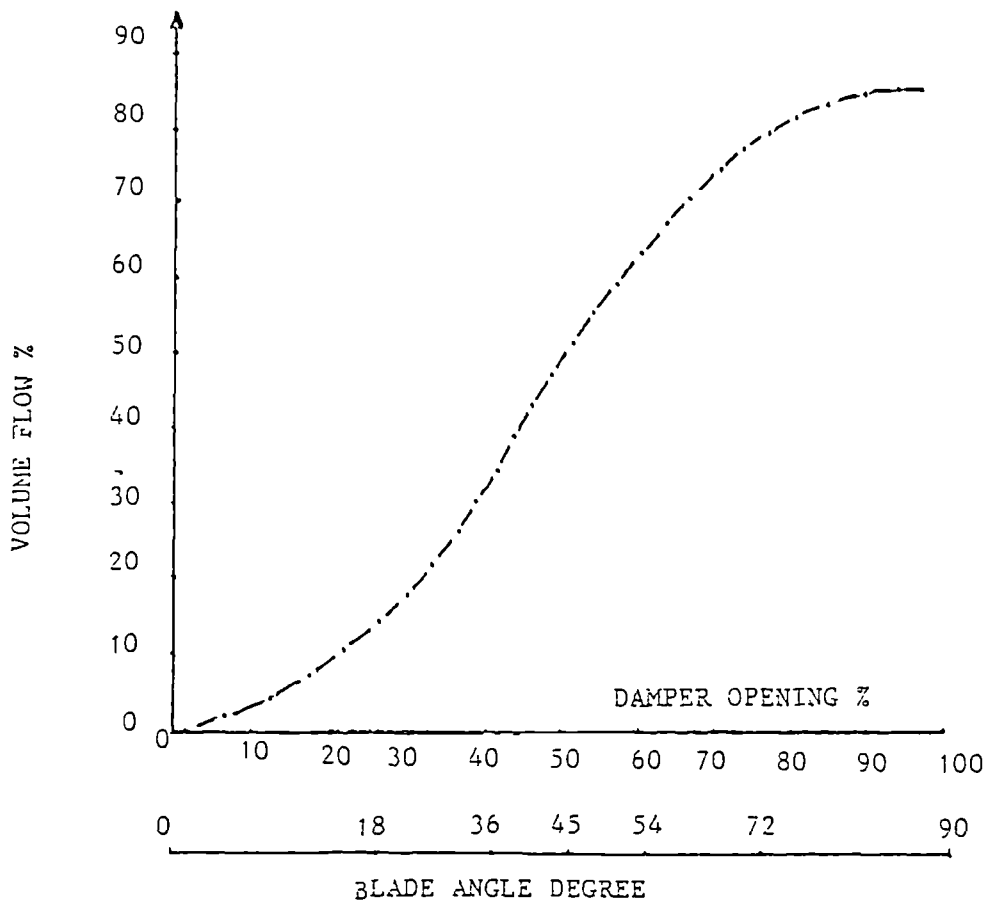


FIGURE 2.32 - APPROXIMATE EFFECT OF DAMPER BLADE (SINGLE BLADE) OPENING ON FLOWRATE (PROVIDED BY BABCOCK & WILCOX Ltd)

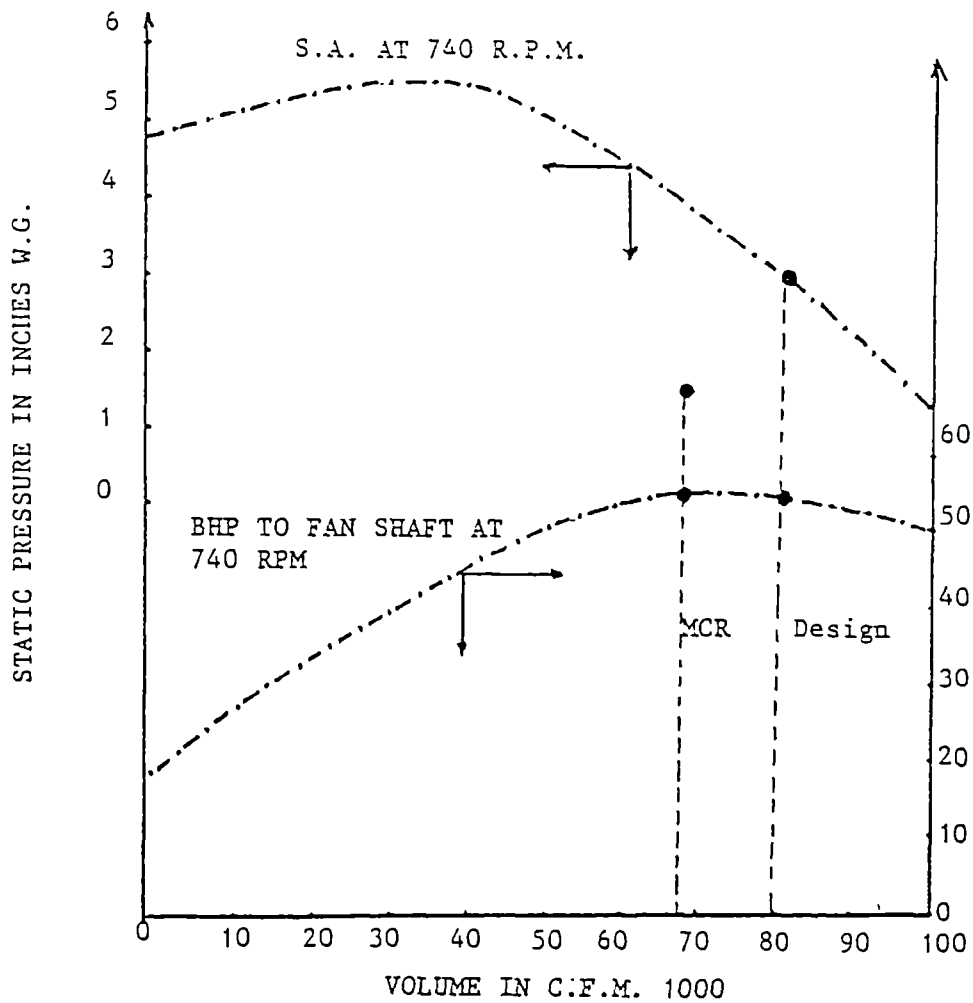


FIGURE 2.33 - ESTIMATED PERFORMANCE CURVES FOR FORCED DRAFT FAN (PROVIDED BY BABCOCK & WILCOX Ltd)

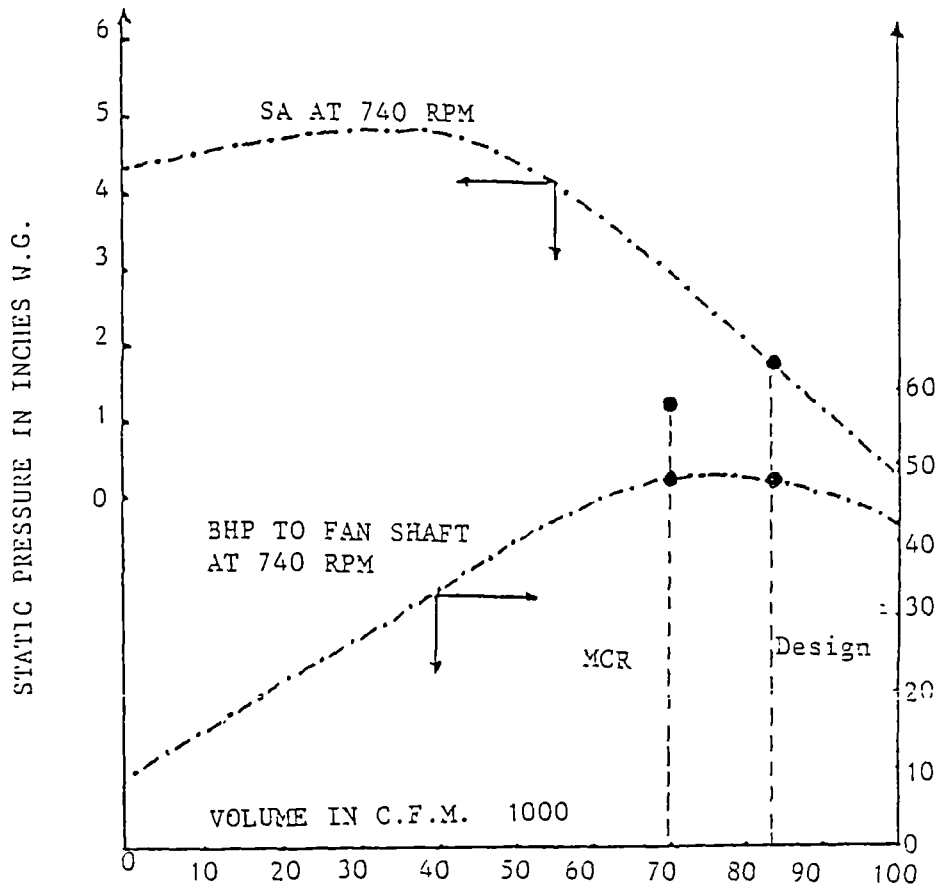


FIGURE 2.34 - ESTIMATED PERFORMANCE CURVES FOR INDUCED DRAFT FAN (PROVIDED BY BABCOCK & WILCOX Ltd.)

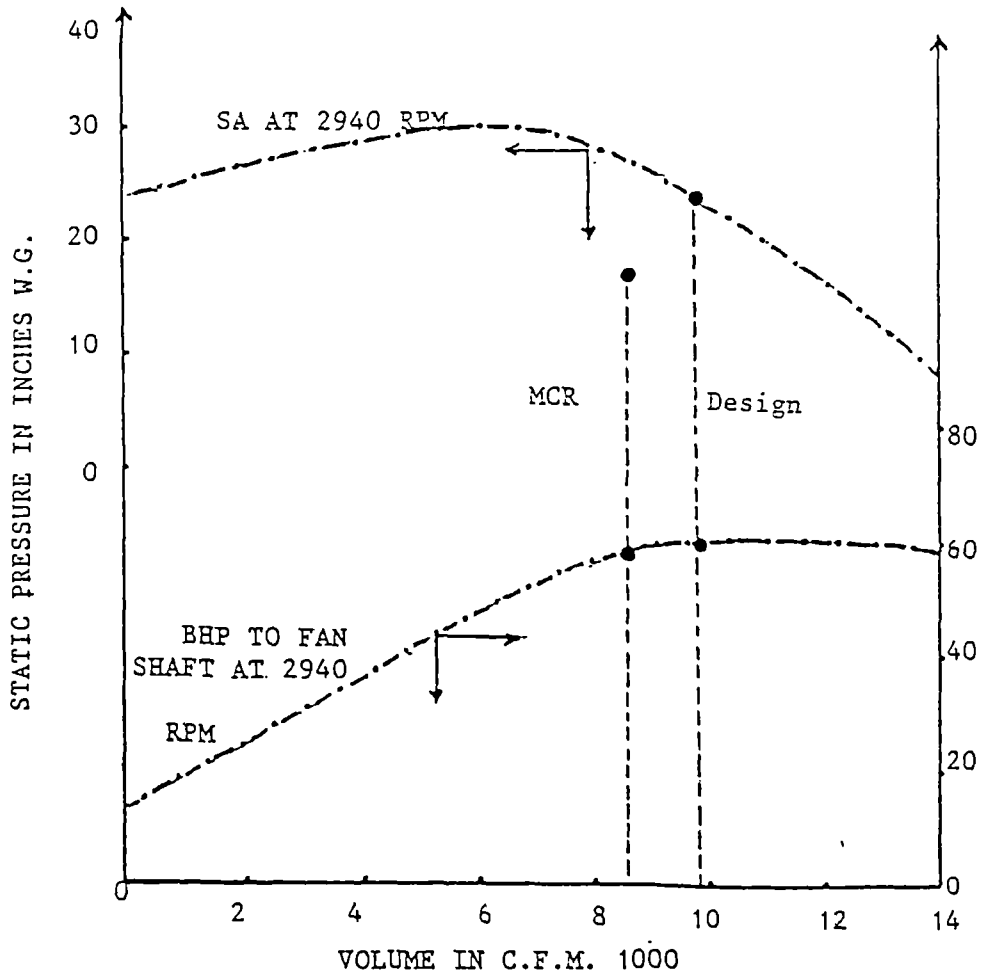


FIGURE 2.35 - ESTIMATED PERFORMANCE CURVES FOR SECONDARY AIR FAN, (PROVIDED BY BABCOCK & WILCOX)

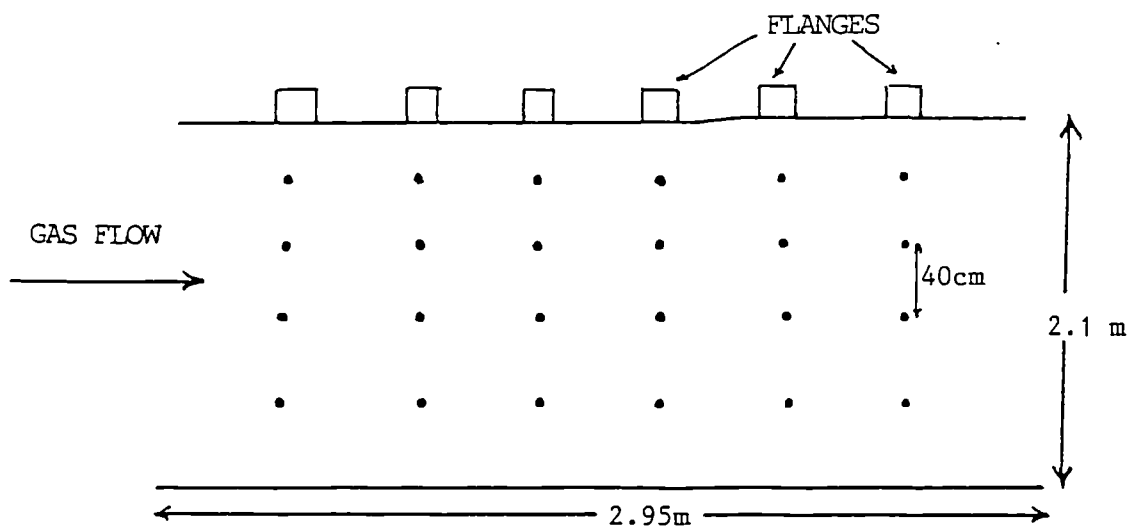
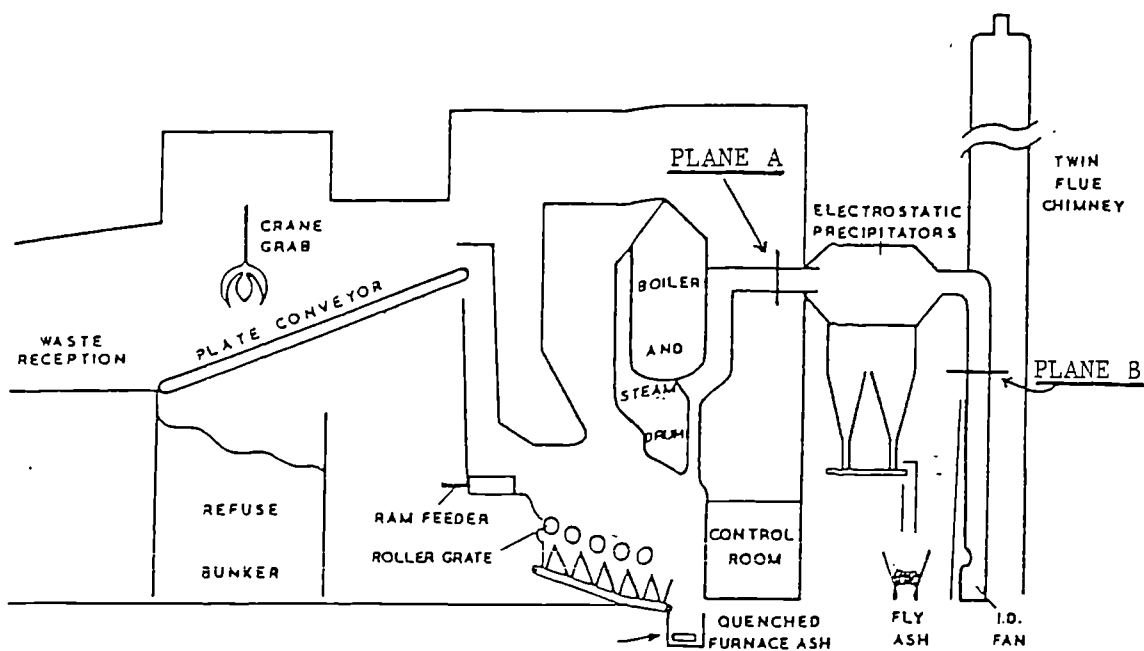
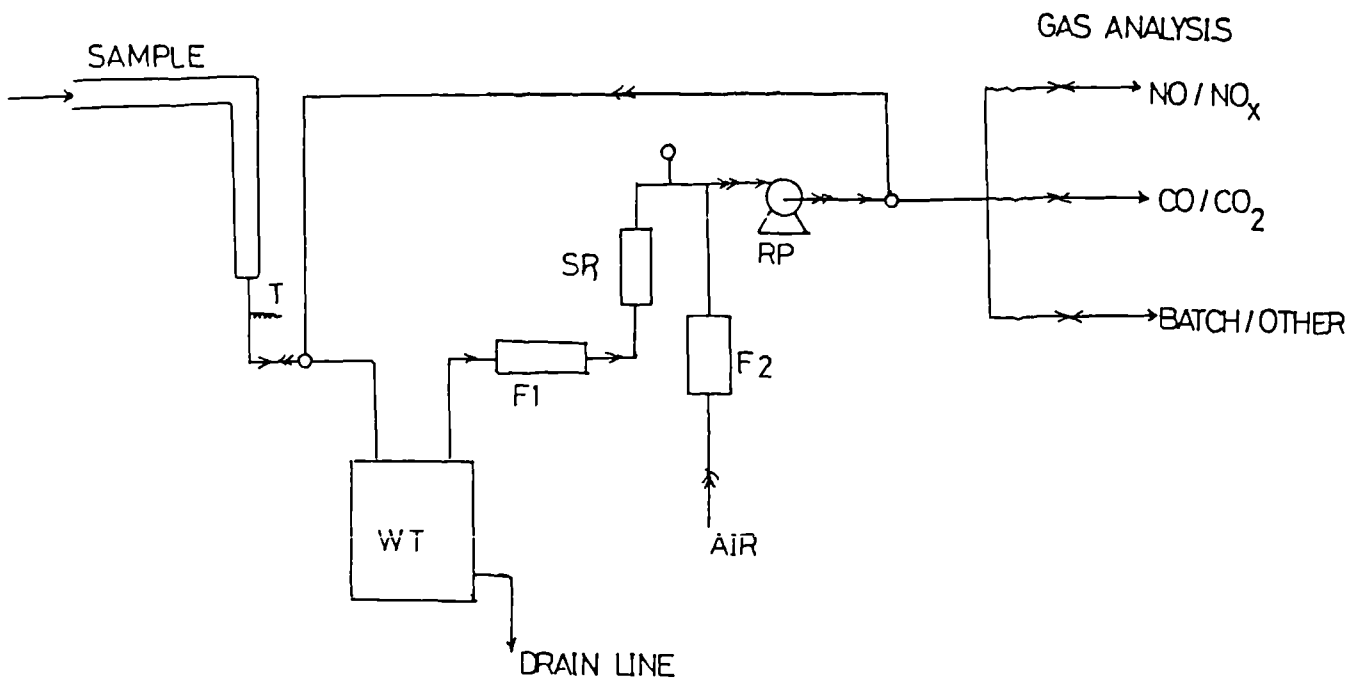
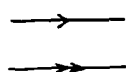


FIGURE 2.36 - SCHEMATIC OF SHEFFIELD INCINERATOR SHOWING LOCATION OF GAS SAMPLING (PLANES A & B), AT THE PRECIPITATOR INLET AND OUTLET.



KEY :



SP

T

WT

F1

F2

SR

RP

SAMPLING MODE GASEOUS FLOW

PURGING MODE AIR FLOW

SAMPLING PROBE

SAMPLING FLOW TEMPERATURE MEASURING THERMOCOUPLE

WATER TRAP

SAMPLE FILTER

PURGE AIR FILTER

SAMPLE FLOW ROTAMETER & INTEGRAL REGULATOR

SAMPLE PUMP 3 PHASE, RECIPROCATING DIAPHRAGM TYPE

FIGURE 2.37 - GAS SAMPLING LINE

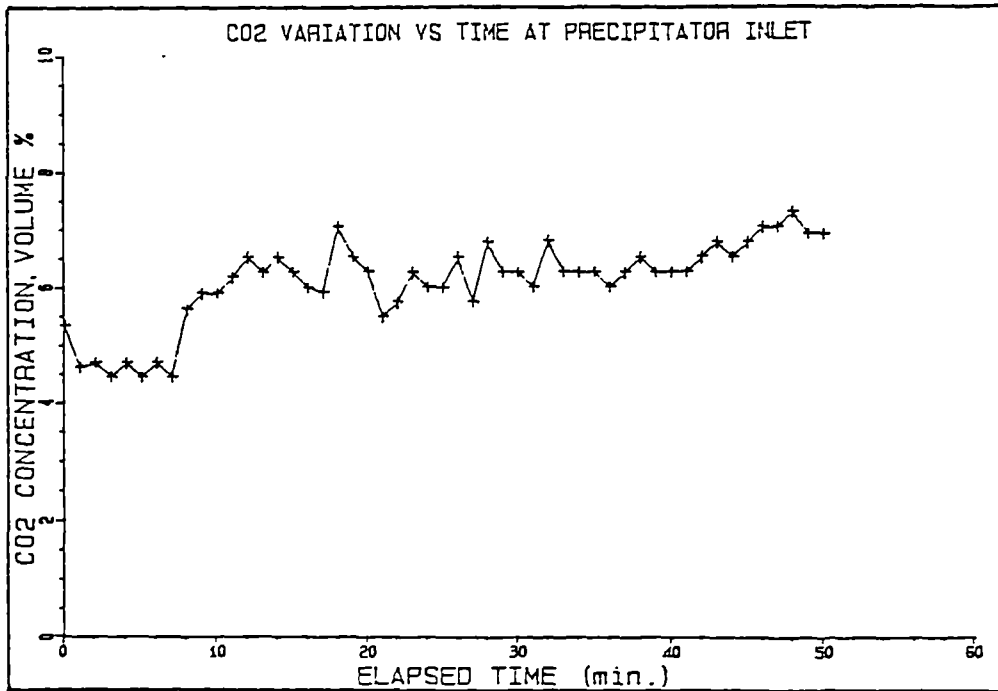


FIGURE 2.38 - TYPICAL CO2 CONCENTRATION VARIATION VS TIME AT PRECIPITATOR INLET.

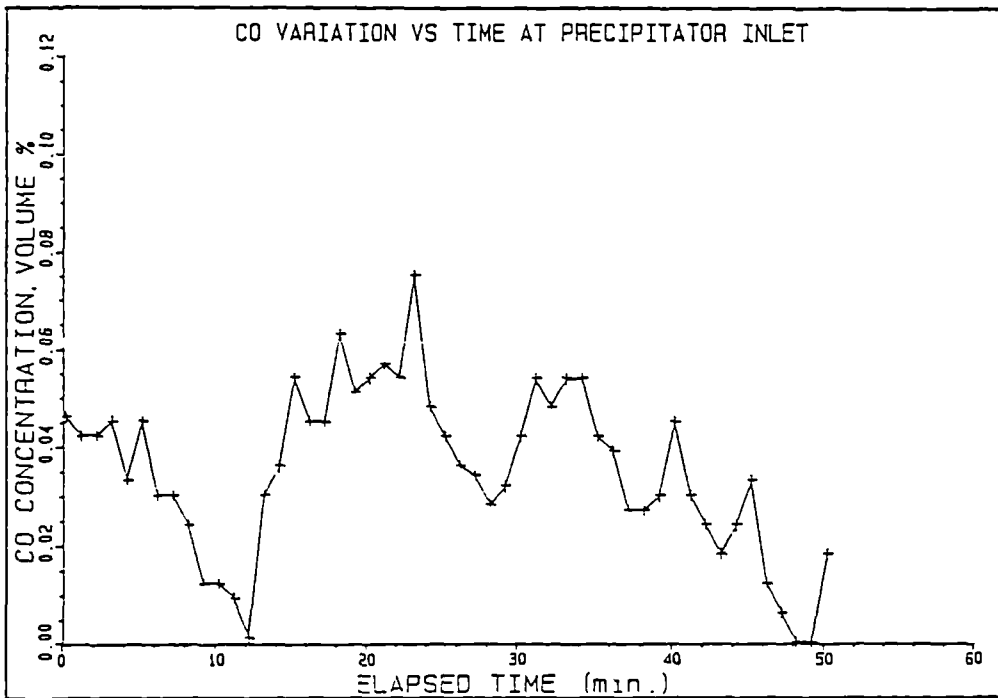


FIGURE 2.39 - TYPICAL CO CONCENTRATION VARIATION VS TIME AT PRECIPITATOR INLET.

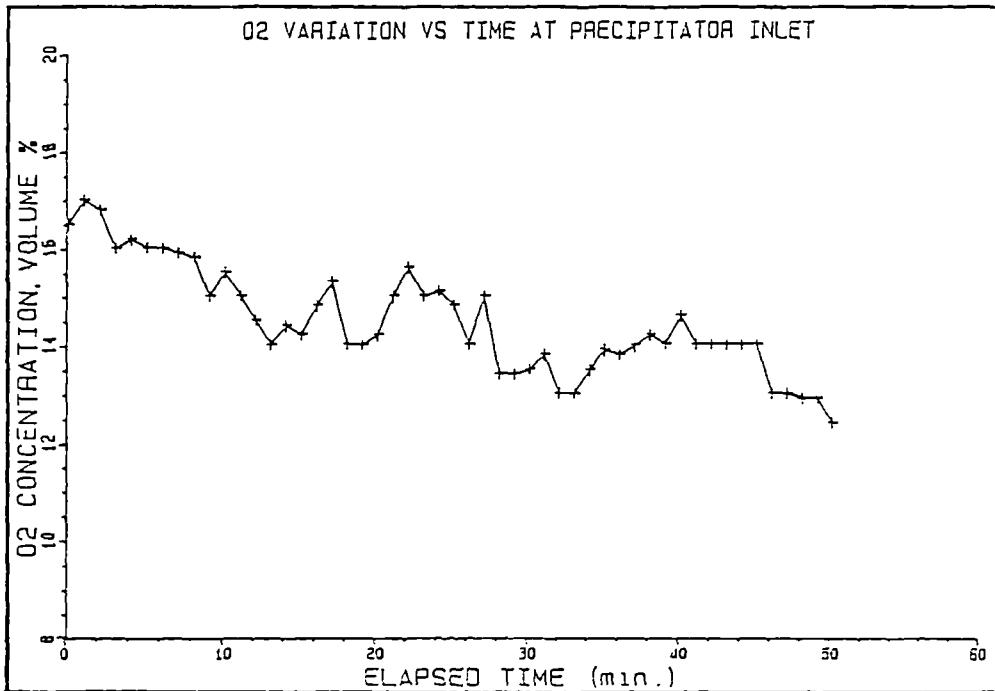


FIGURE 2.40 - TYPICAL O₂ CONCENTRATION VARIATION VS TIME AT PRECIPITATOR INLET.

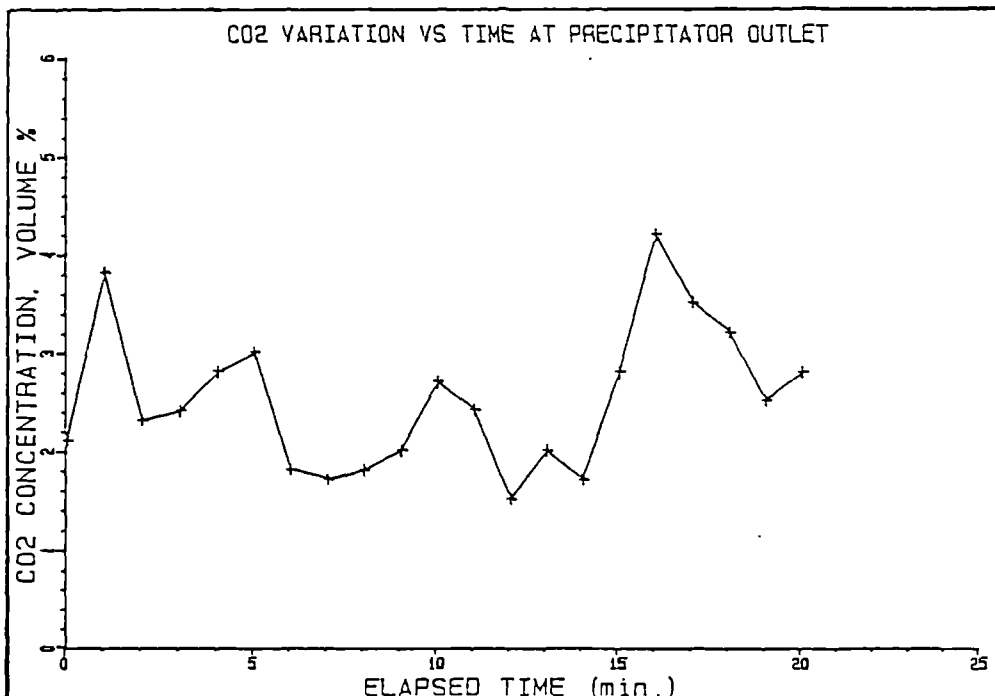


FIGURE 2.41 - TYPICAL CO₂ CONCENTRATION VARIATION VS TIME AT PRECIPITATOR OUTLET.

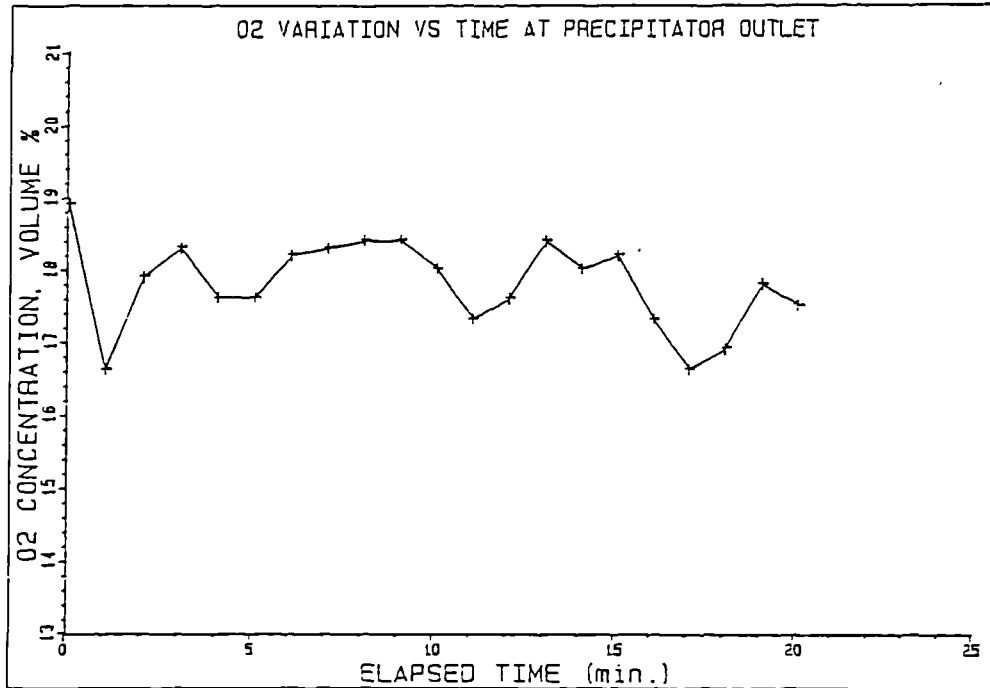


FIGURE 2.42 - TYPICAL O2 CONCENTRATION VARIATION VS TIME AT PRECIPITATOR OUTLET.

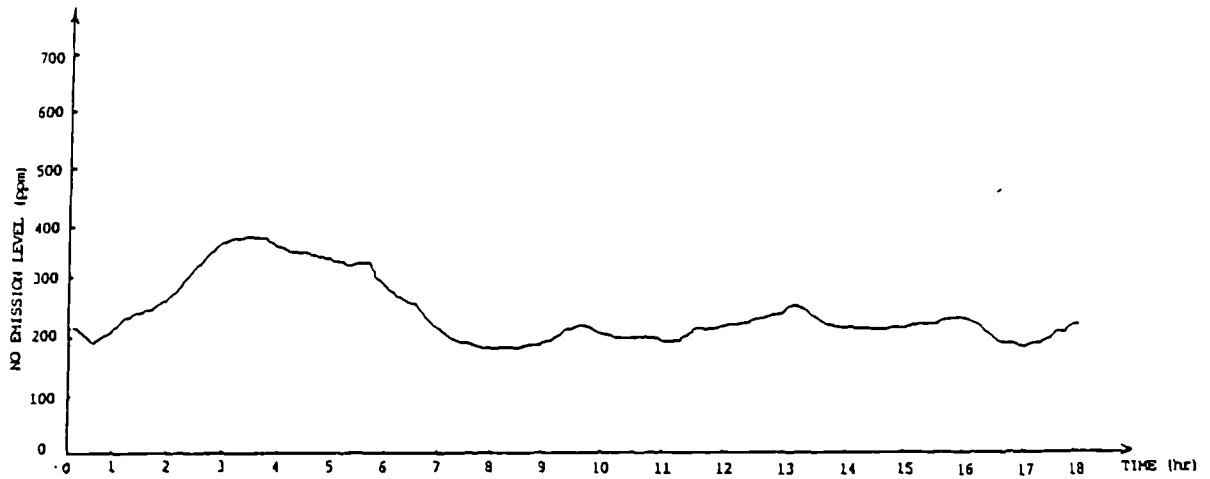
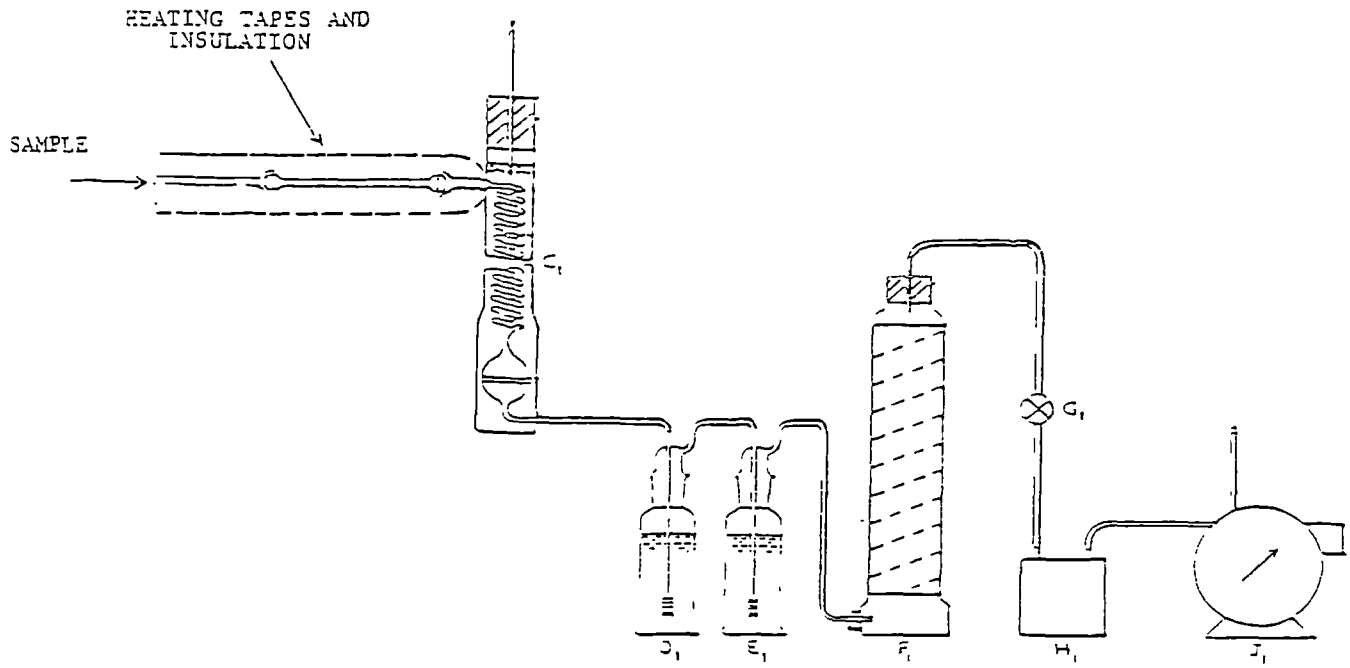


FIGURE 2.43 - TYPICAL NO CONCENTRATION VARIATION VS TIME AT PRECIPITATOR INLET.



KEY:

| | |
|----|---|
| C1 | SULPHUR TRIOXIDE COLLECTOR |
| D1 | GAS WASHING BOTTLE OF 250 ml CAPACITY COMPLYING WITH THE REQUIREMENTS OF BS 2461 WITH A SINTERED HEAD OF POROSITY GRADE NO. 1 (BS 1752) |
| E1 | SULPHUR DIOXIDE COLLECTOR |
| F1 | DRYING BOTTLE |
| G1 | NEEDLE VALVE FOR FLOW CONTROL |
| H1 | PUMP |
| J1 | GAS METER |

FIGURE 2.44 - SCHEMATIC ARRANGEMENT OF SO₂ SAMPLING TRAIN.

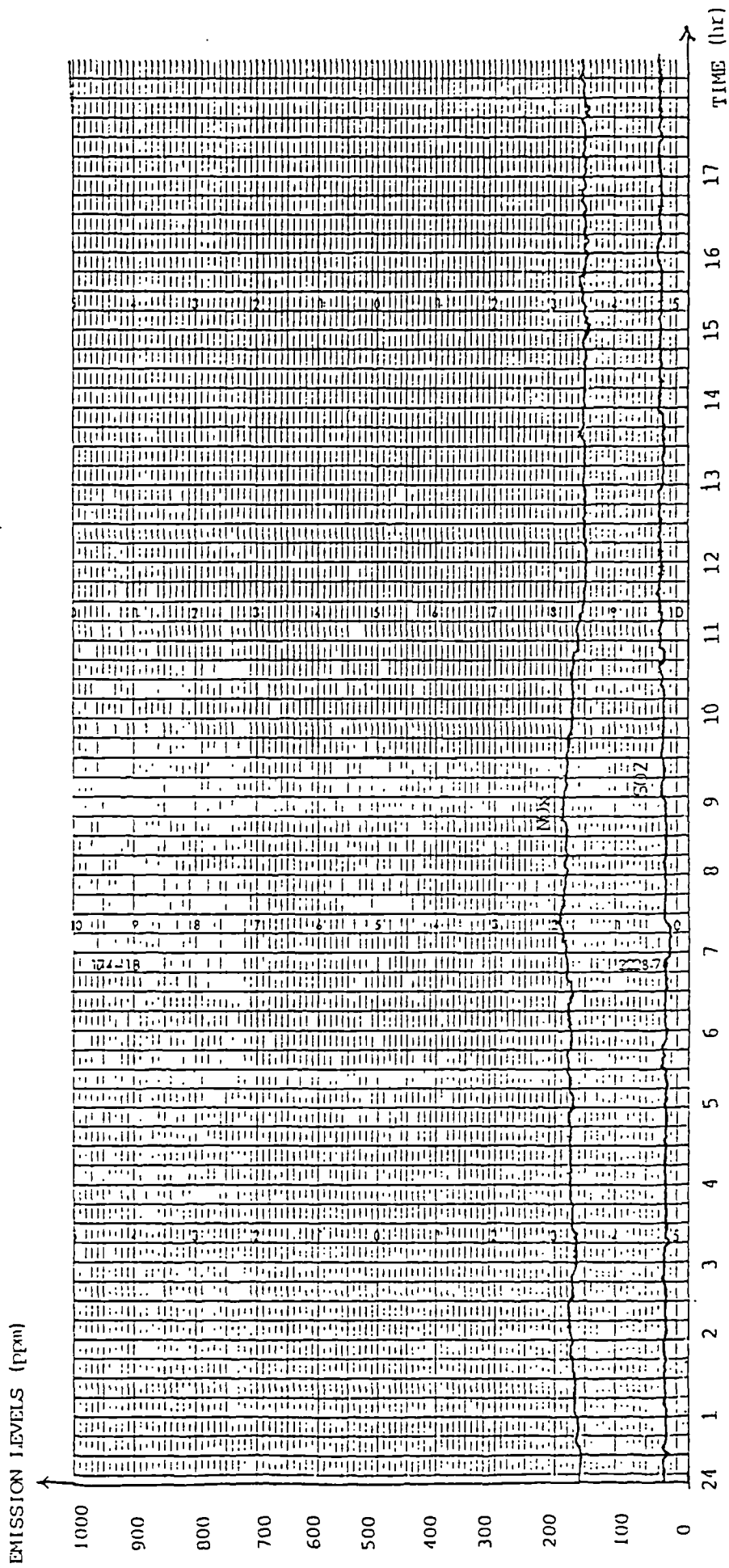


FIGURE 2.45 - TYPICAL NO AND SO₂ CONCENTRATION VARIATION VS TIME AT PRECIPITATOR OUTLET.

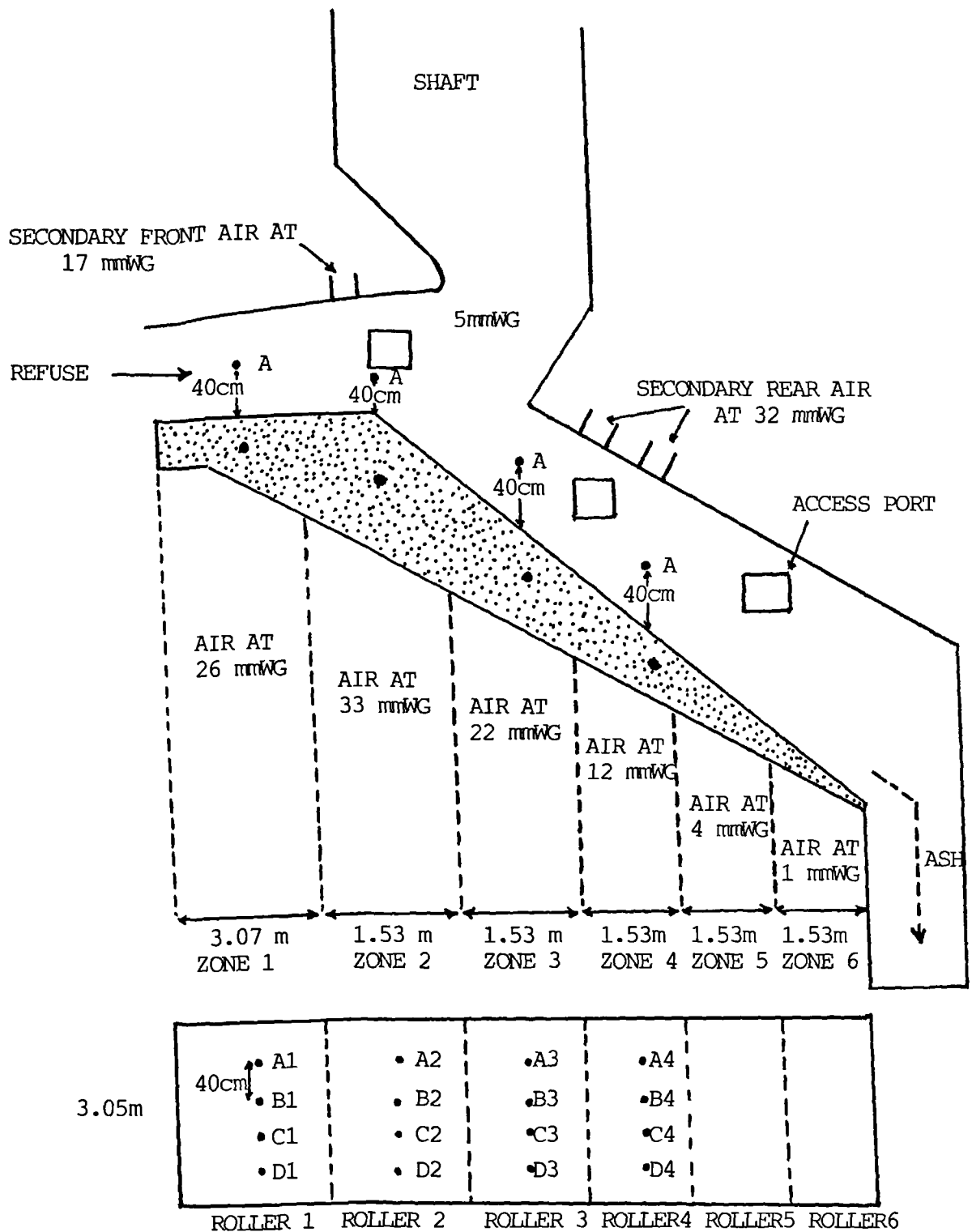


FIGURE 3.1 - SCHEMATIC OF SHEFFIELD INCINERATOR SHOWING LOCATION OF GAS SAMPLING INSIDE AND ABOVE THE REFUSE BED.

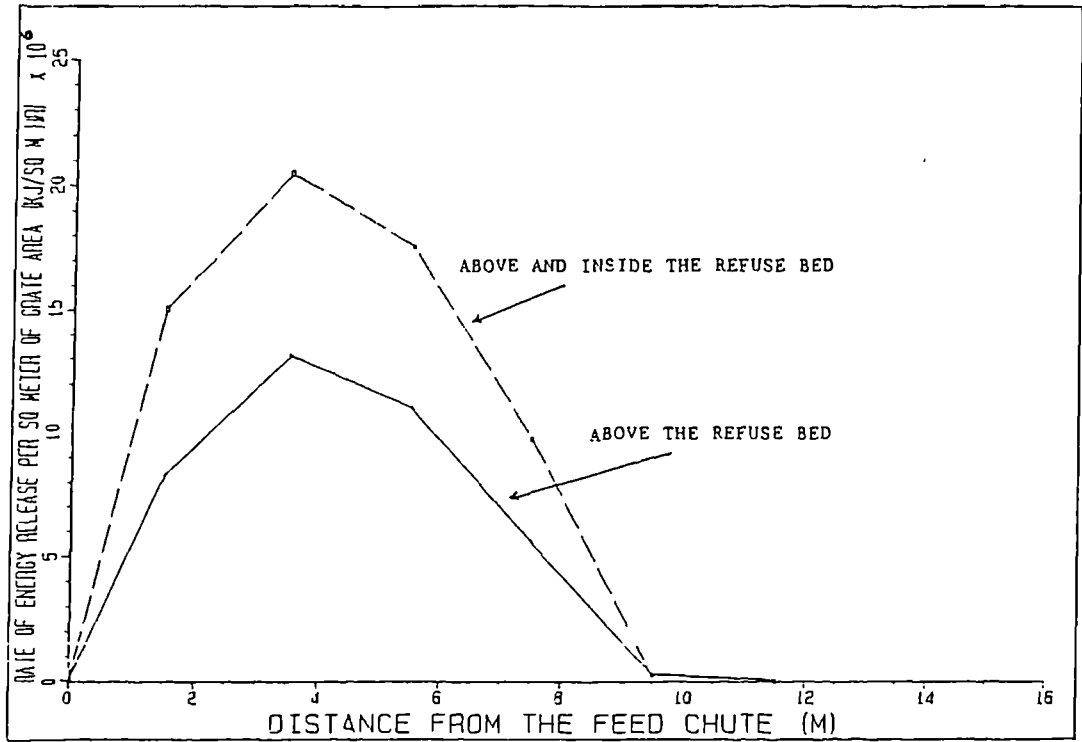


FIGURE 3.2 - ESTIMATED ENERGY RELEASE RATES FOR SHEFFIELD MUNICIPAL INCINERATOR PLANT.

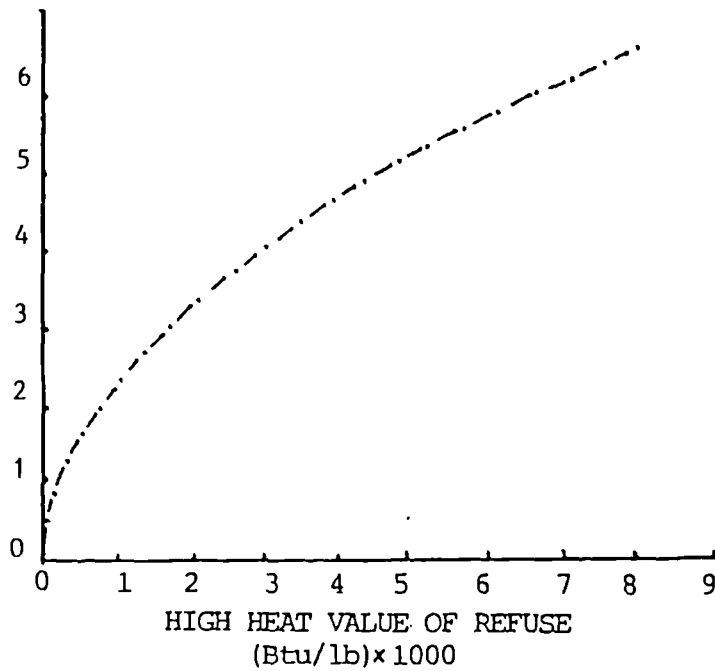


FIGURE 3.3 - VALUES OF WASTE FACTORS K (REF.44)

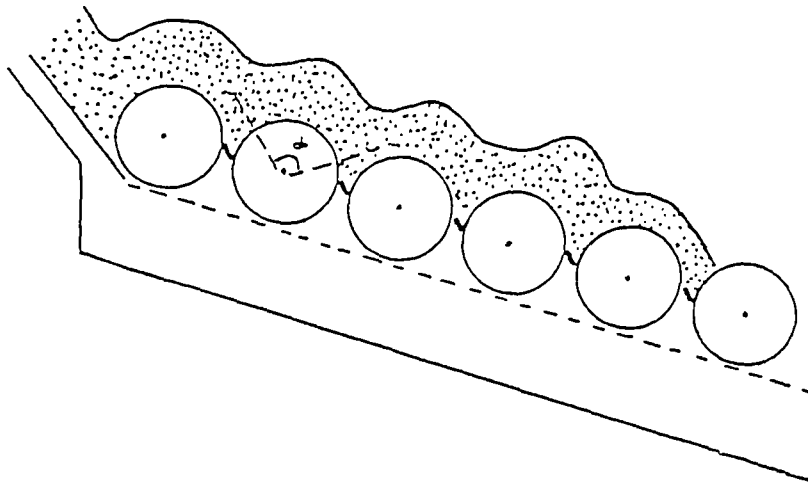


FIGURE 3.4 - SIDE VIEW OF THE ROTATING GRATE ROLLERS SHOWING THE ROTATING ANGLE (α).

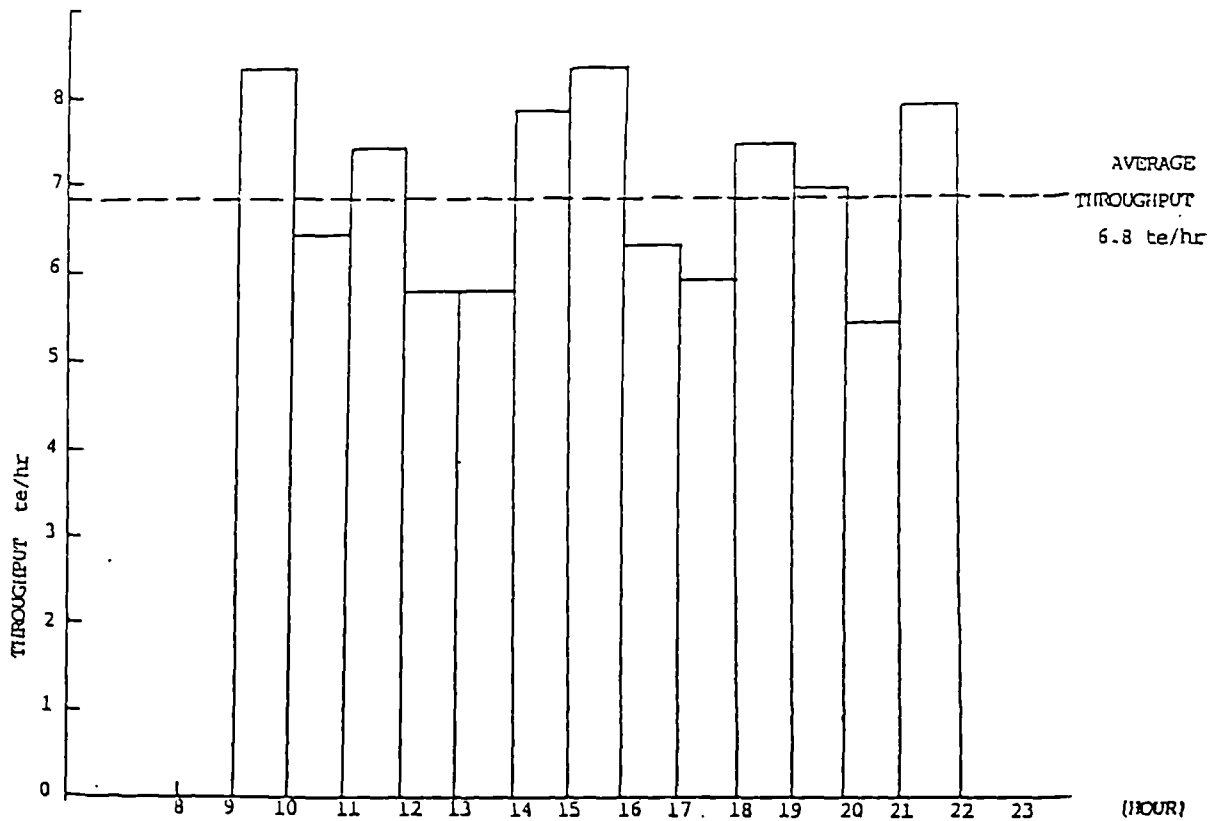


FIGURE 3.5 - HOURLY THROUGHPUT RATE OF RAW REFUSE, BOILER NO. 1 SHEFFIELD INCINERATOR.

REFUSE ARISING = 190,000 te/annum
 BULK DENSITY = 210 kg/m³
 GROSS CALORIFIC VALUE = 15000 kJ/kg
 BASIS FOR CALCULATION = 1 HOUR

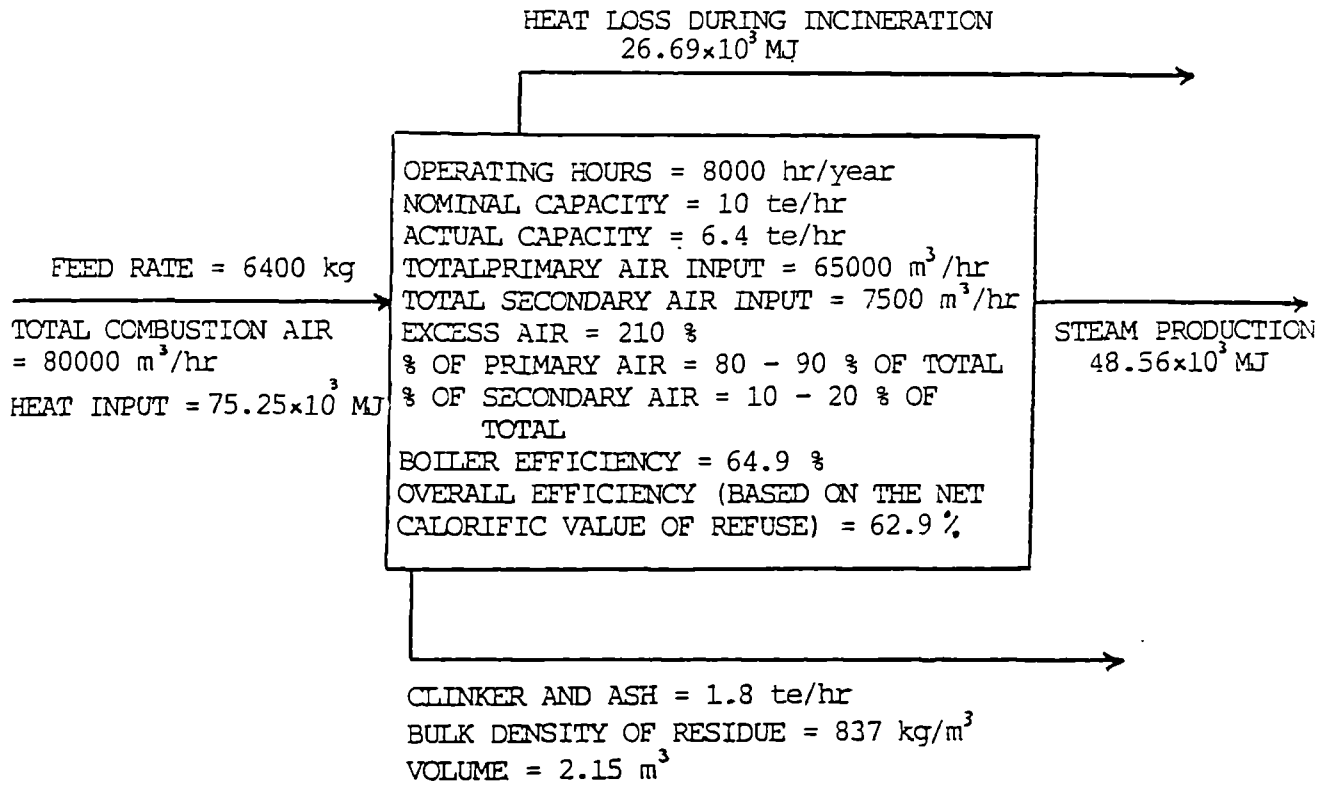


FIGURE 3.6 - SCHEMATIC MASS AND ENERGY BALANCE FOR RAW REFUSE INCINERATION IN SHEFFIELD INCINERATOR (BOILER No.1)

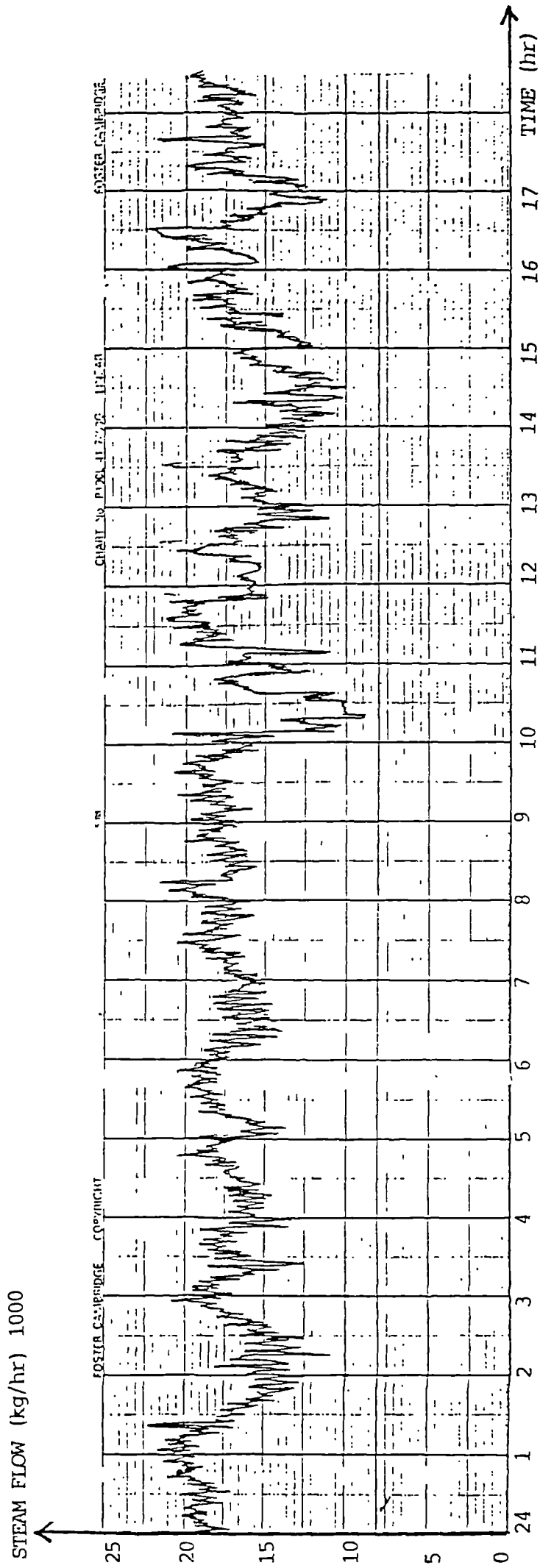


FIGURE 3.7 - TYPICAL STEAM PRODUCTION RATE VS TIME FOR BOILER NO. 1 AT SHEFFIELD INCINERATOR.

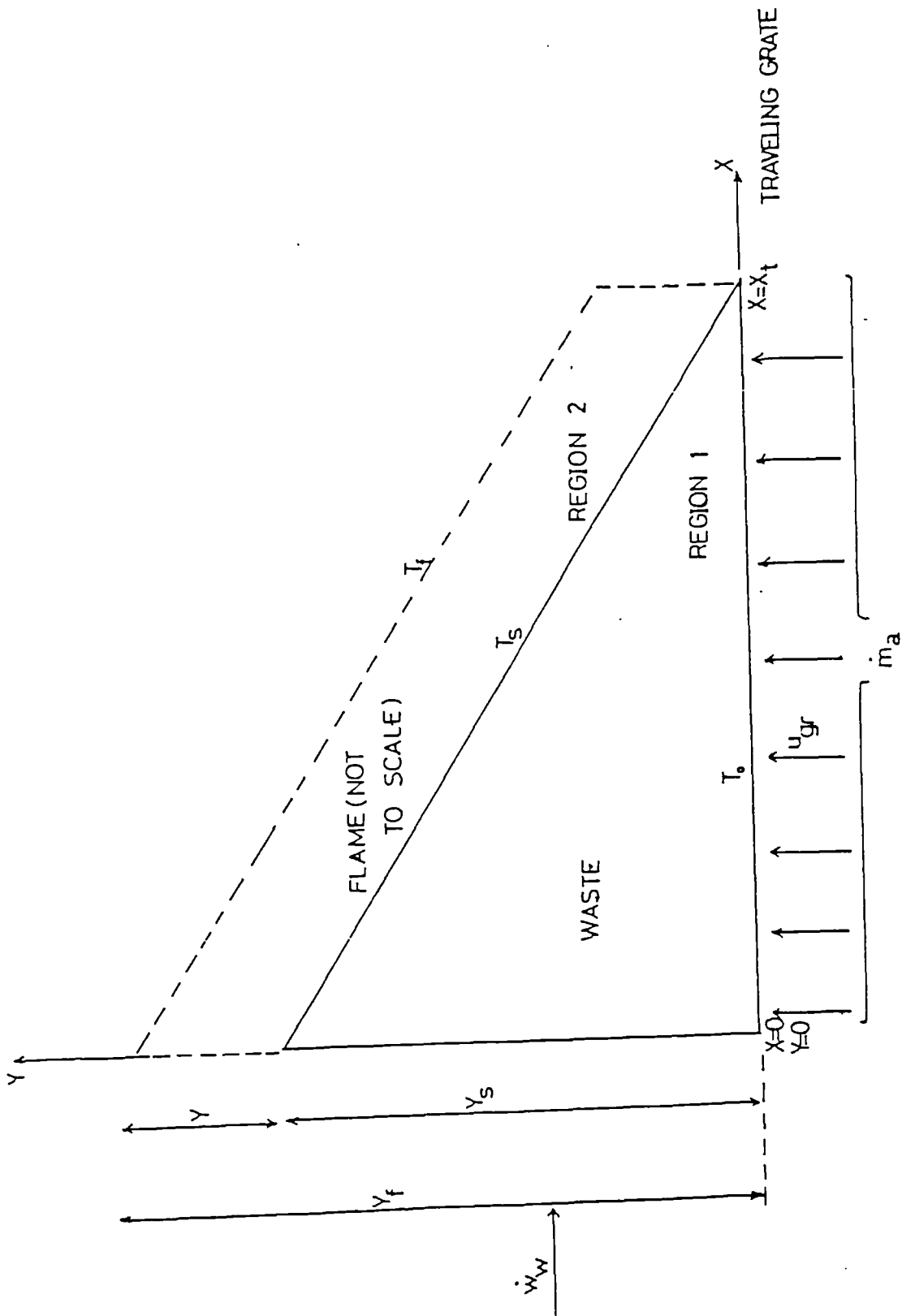
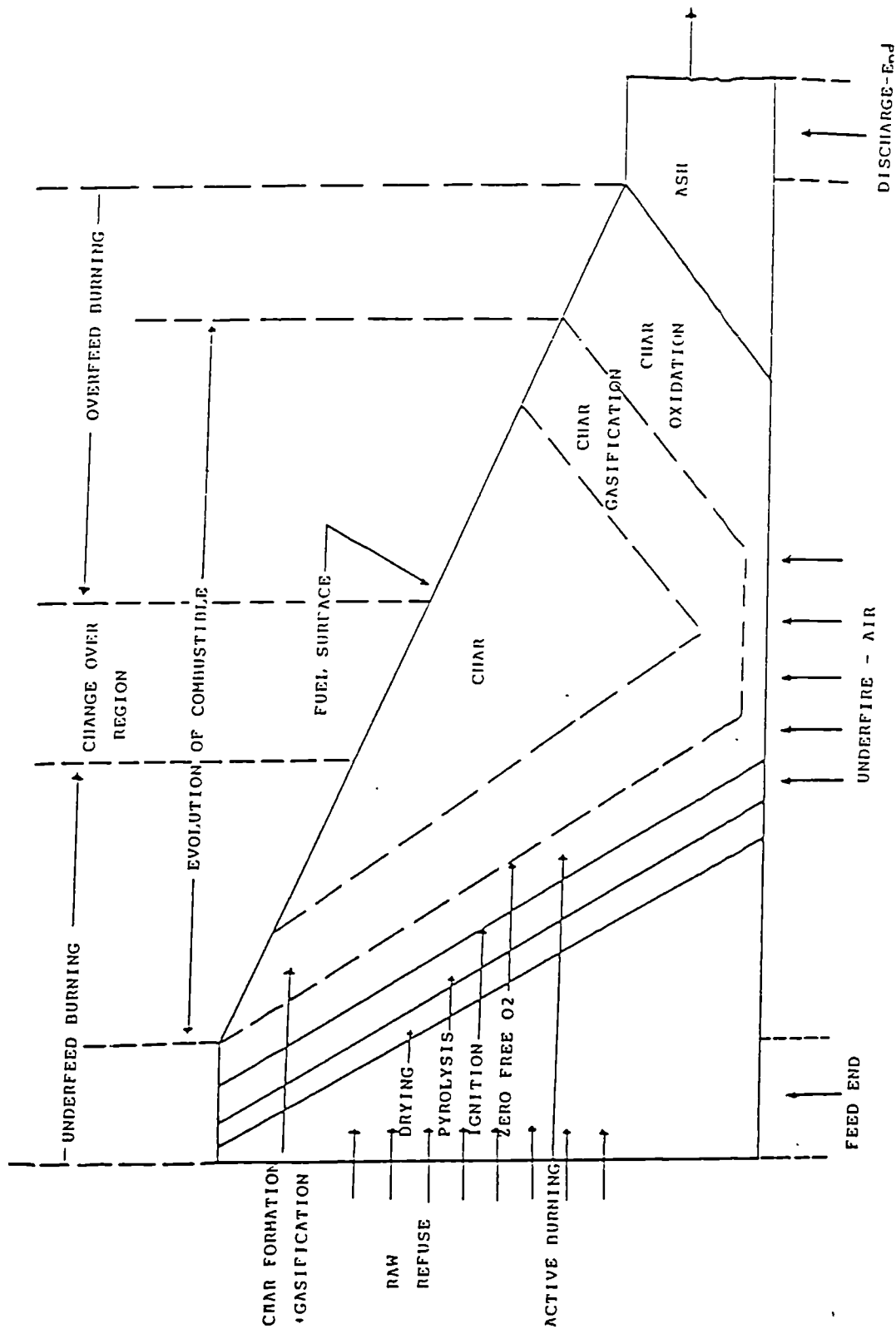


FIGURE 4.1 - Travelling grate incinerator model

FIGURE 4.2 - Simplified schematic of processes occurring in the refuse bed on a travelling grate.



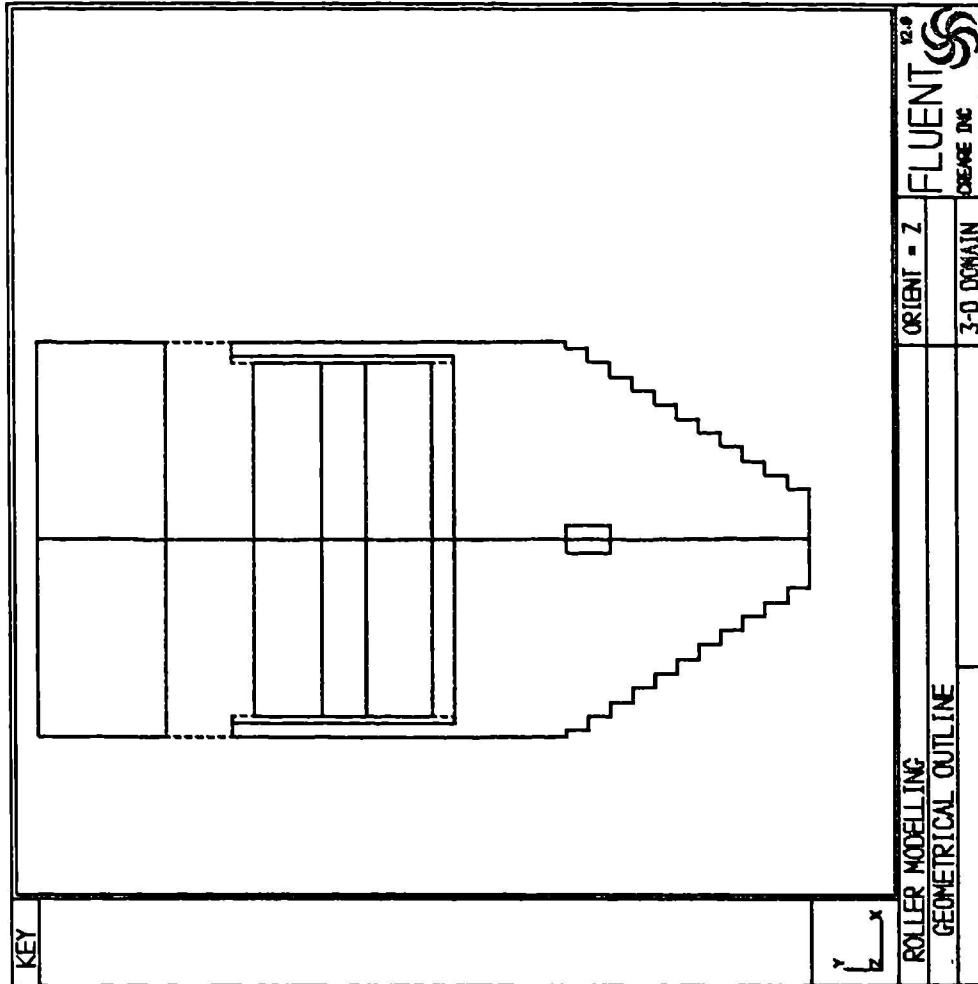


FIGURE 4.3 - The geometrical outline (2D) of the roller and the riddling hopper.

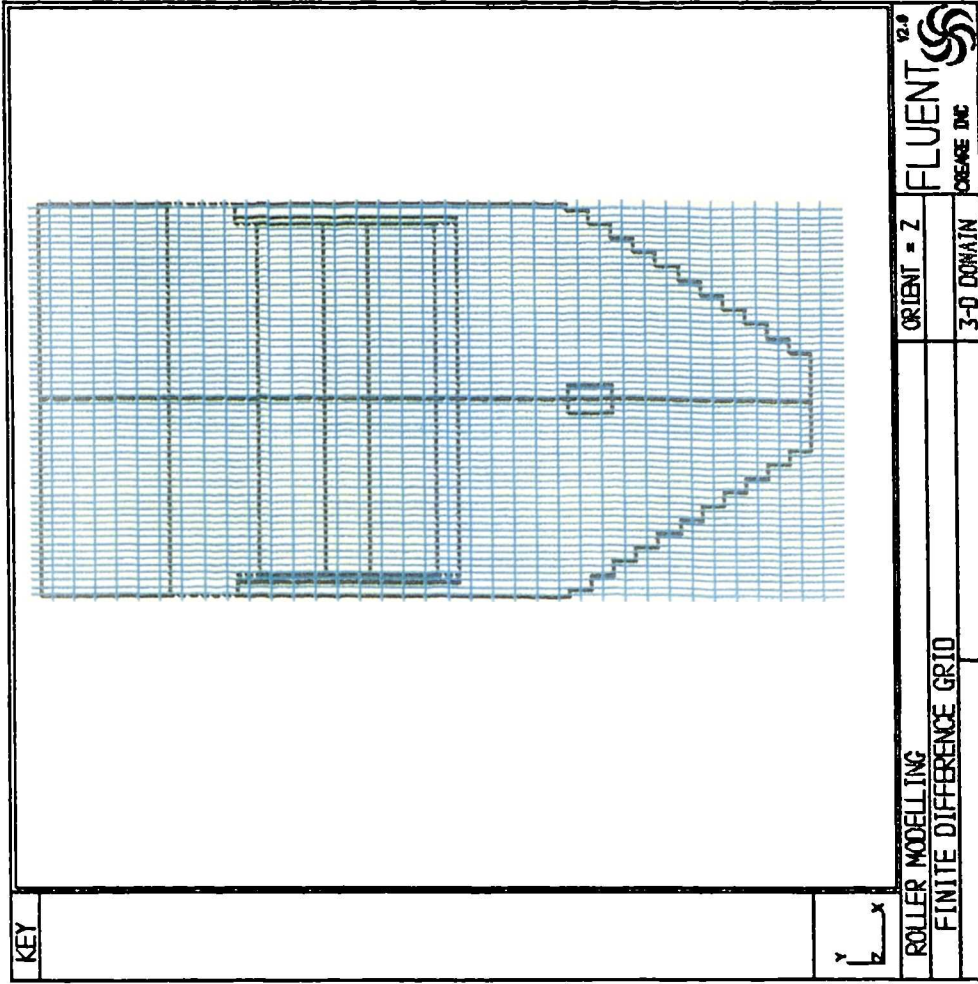


FIGURE 4.4 - The finite difference grid used for modelling of the roller and the riddling hopper.

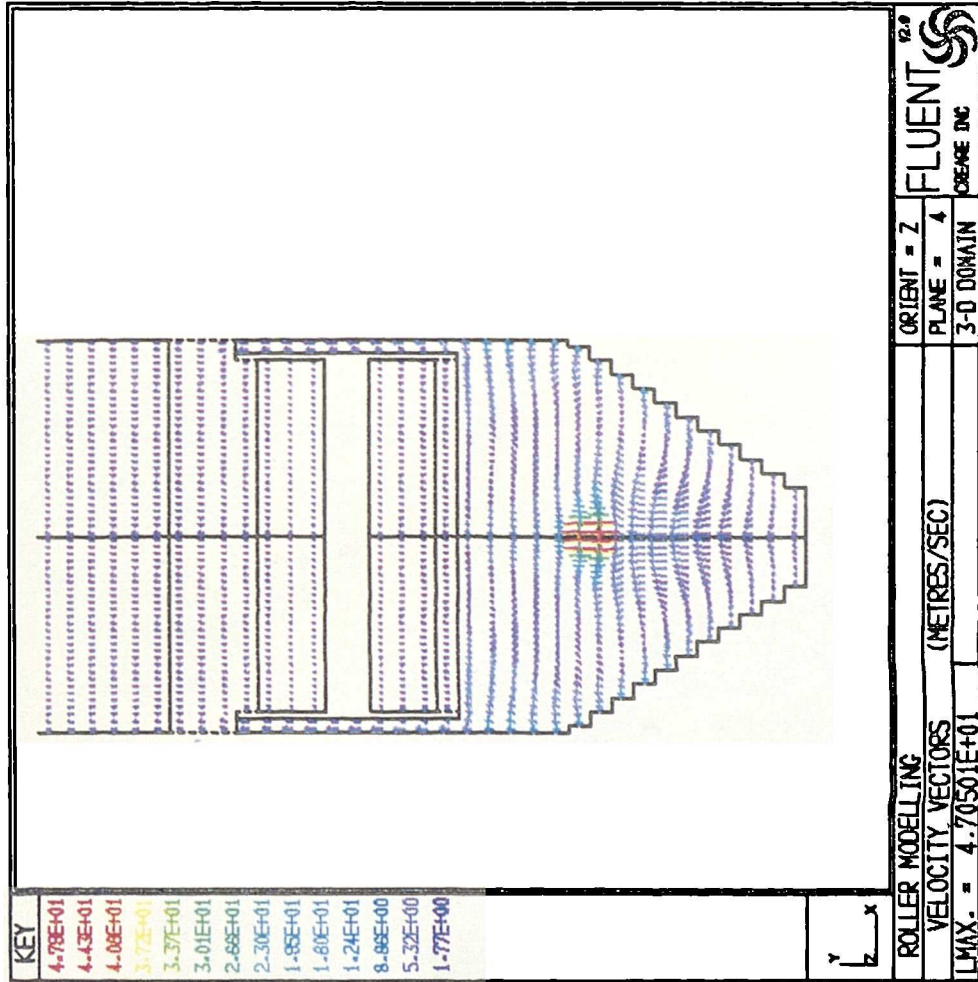


FIGURE 4.5 - Velocity vector plot (2D) for roller's isothermal flow case.

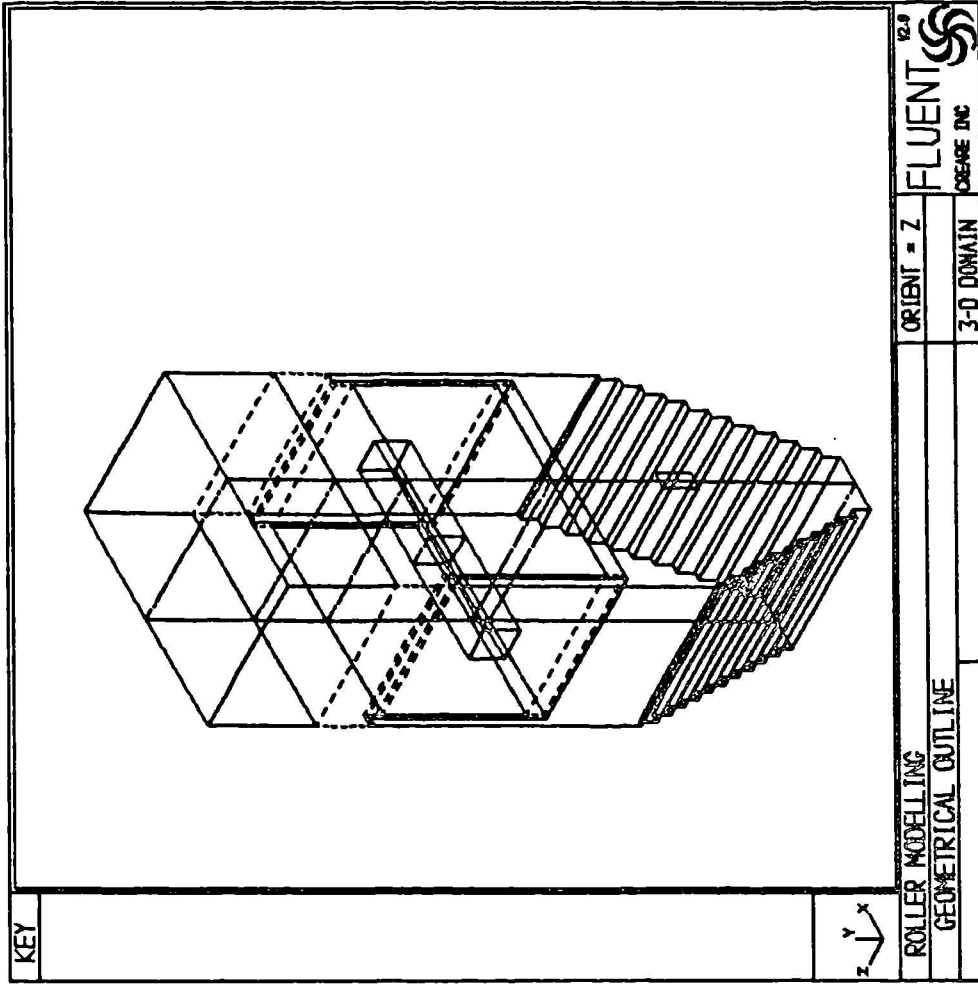


FIGURE 4.6 - Three dimensional view of the riddling hopper and the roller.

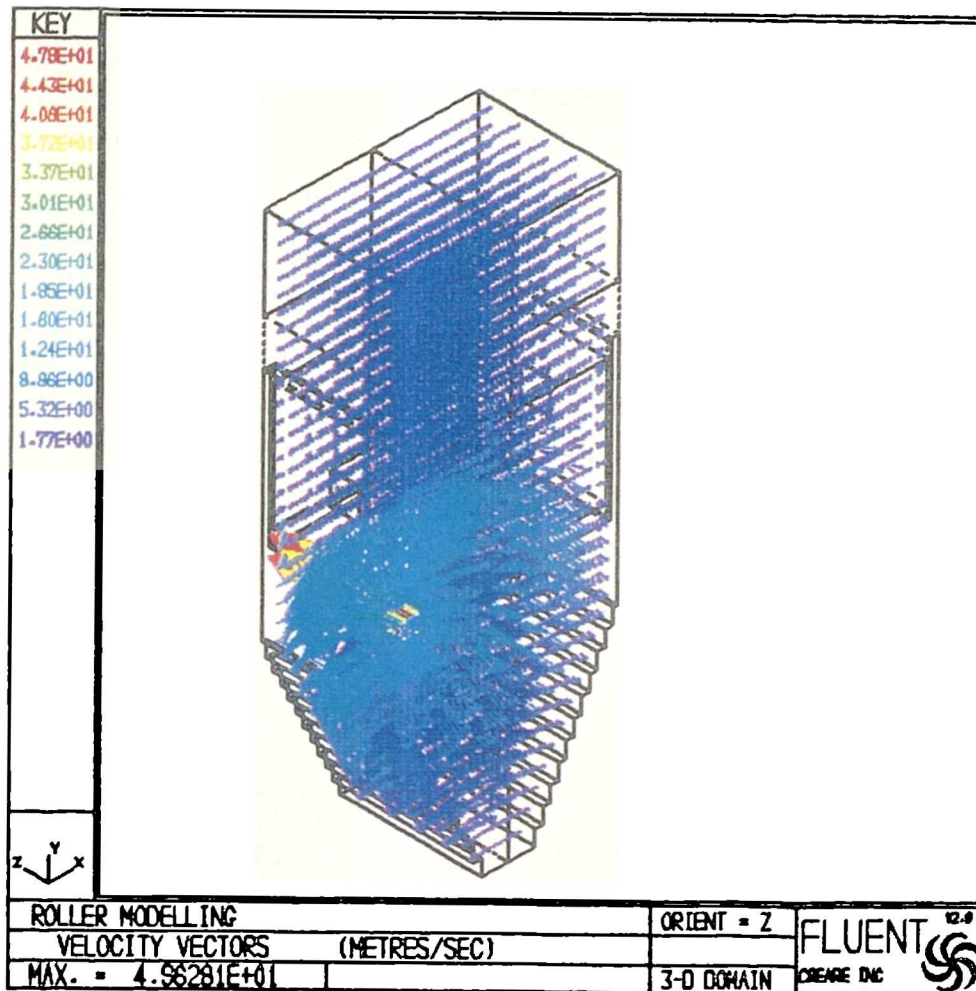


FIGURE 4.7 - Velocity vector plot (3D) for the roller's isothermal case.

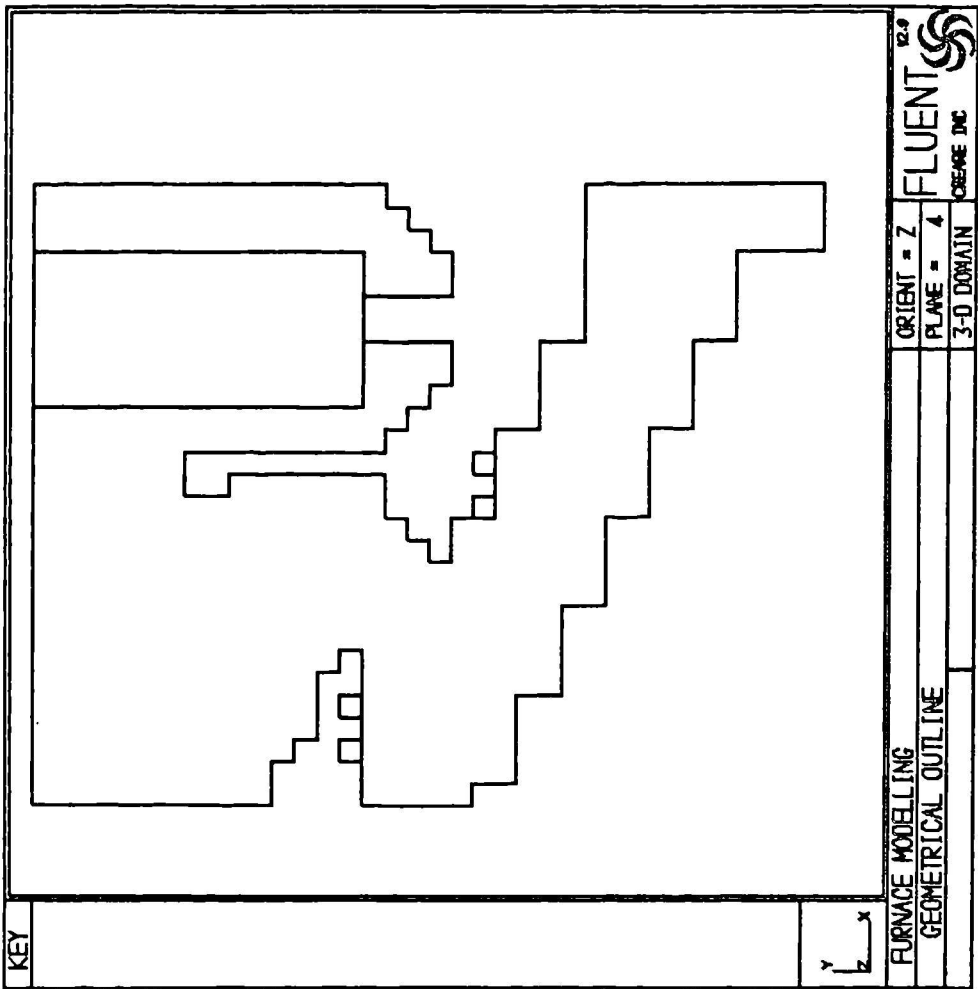


FIGURE 5.1 - The modelled Sheffield incinerator in outline (2-dimensional view).

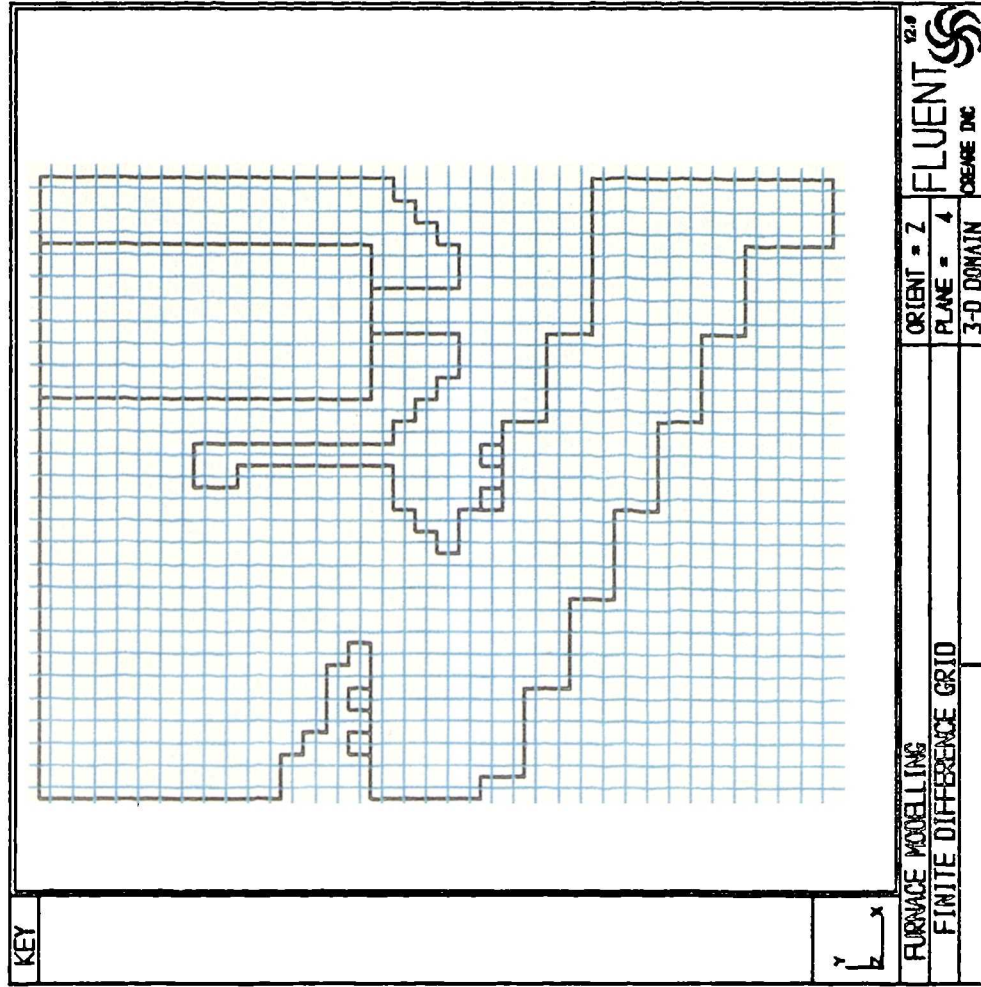


FIGURE 5.2 - The grid constructed for the Sheffield municipal incinerator.

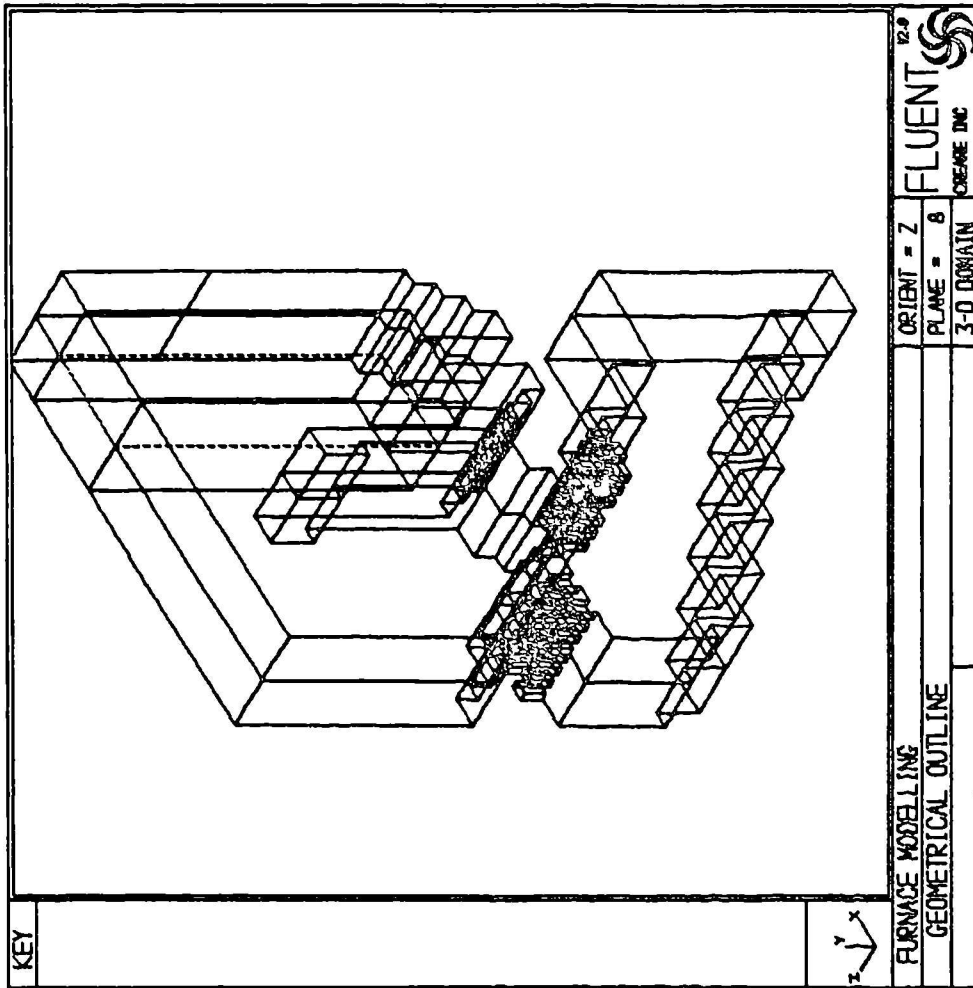


FIGURE 5.3 - Three dimensional view of the Sheffield incinerator.

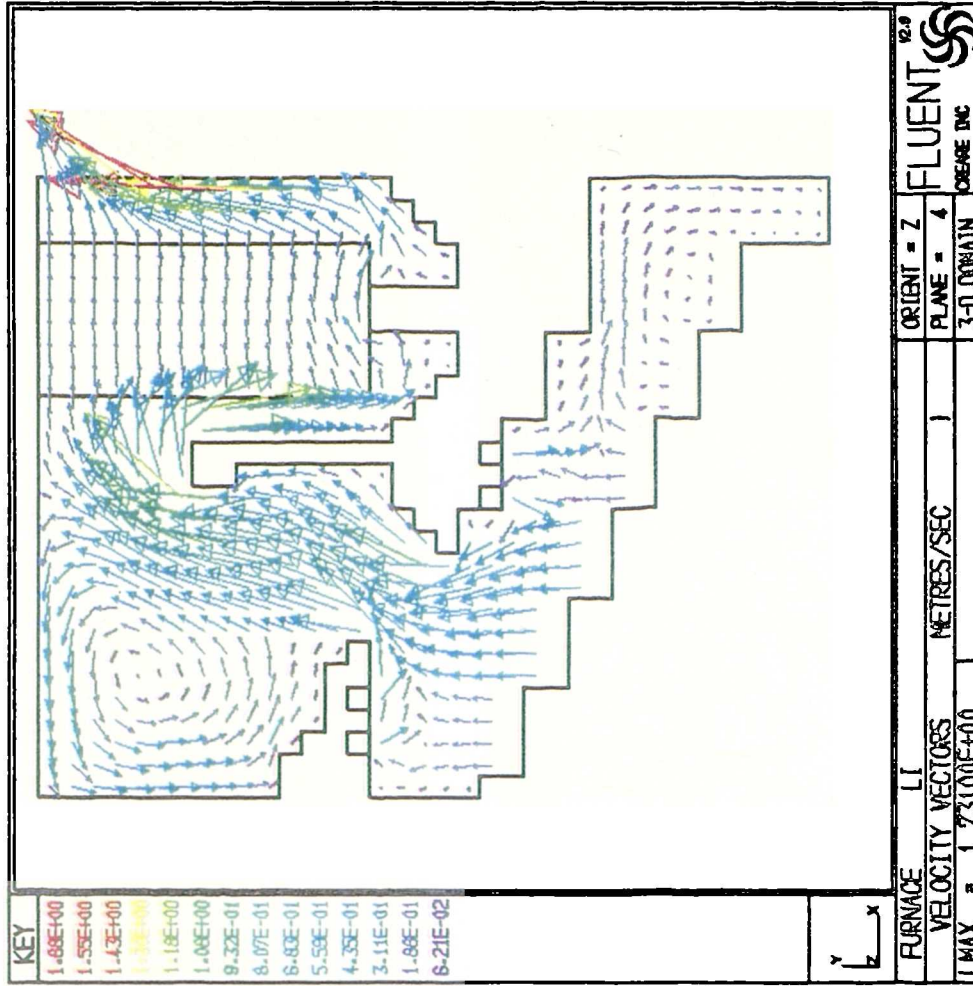


FIGURE 5.4 - Velocity vector plot in plane of secondary air slots for the isothermal flow case.

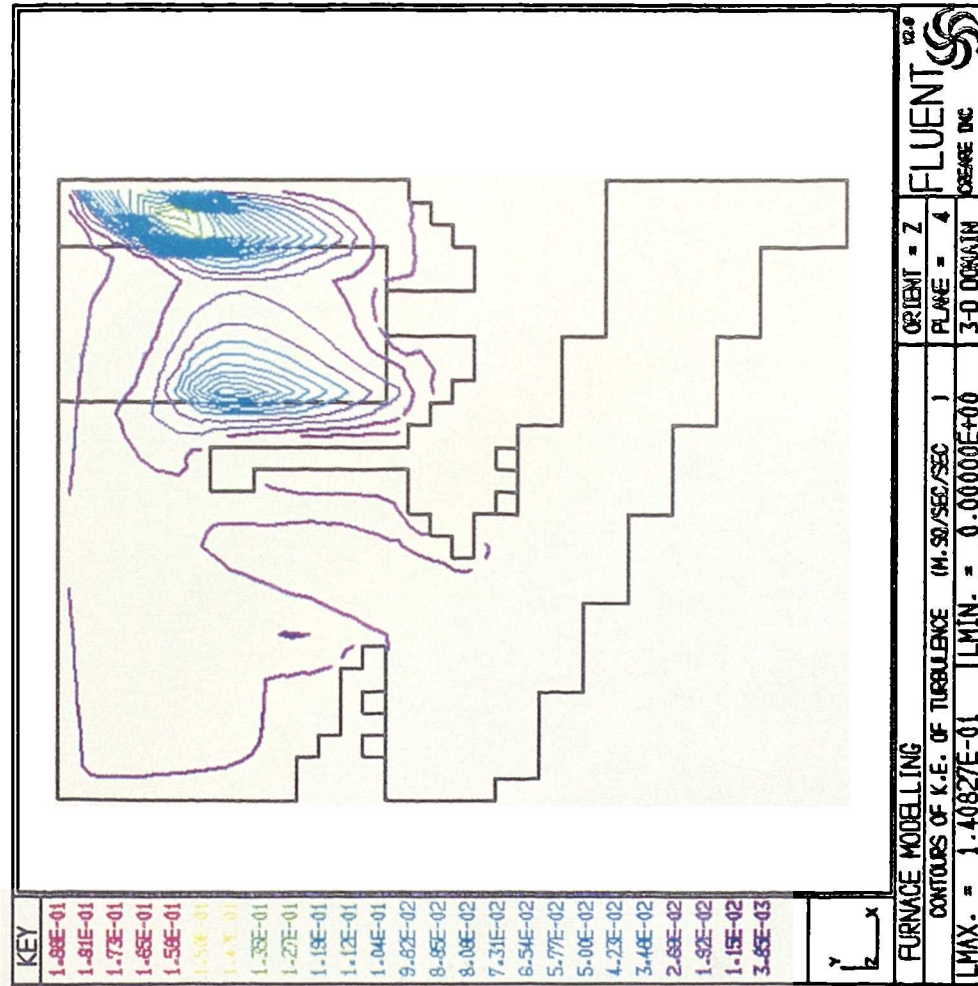


FIGURE 5.5 - Contours of K.E. of turbulence inside the incinerator (isothermal flow case).

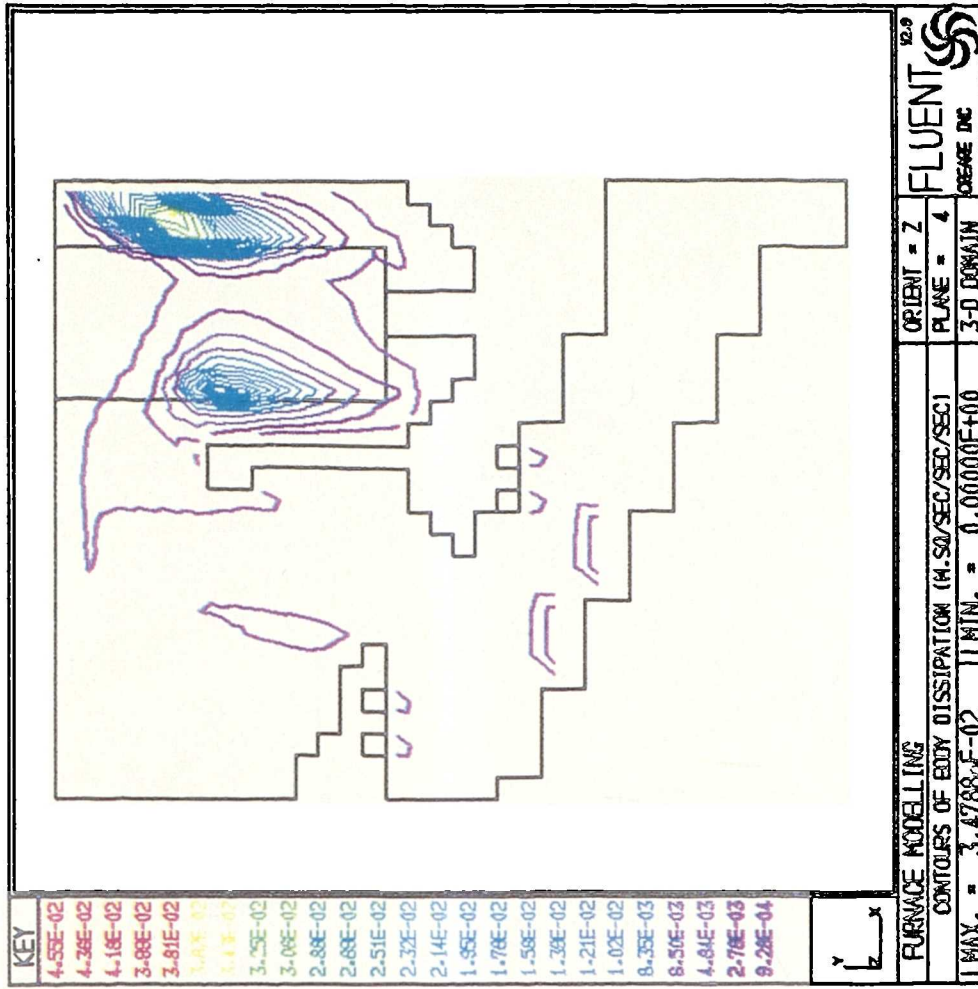


FIGURE 5.6 - Contours of eddy dissipation inside the incinerator (isothermal flow case).

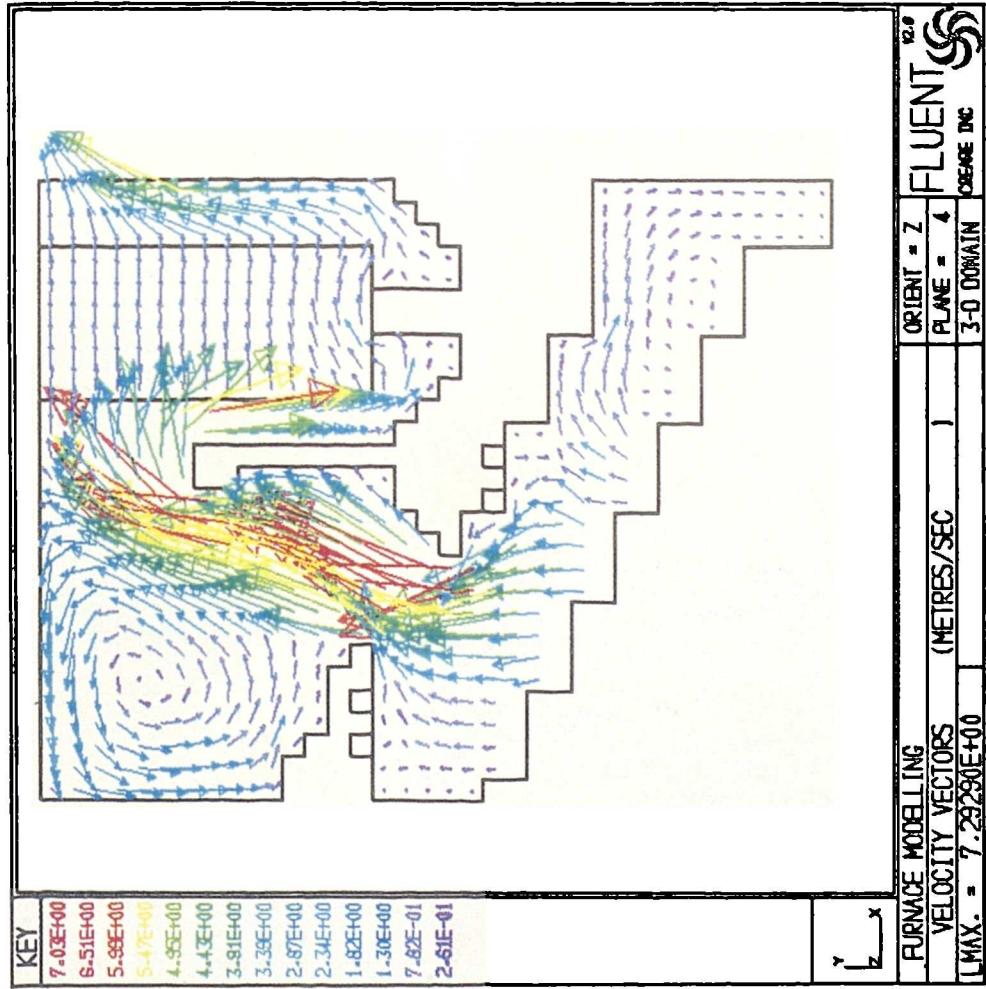


FIGURE 5.7 - Velocity vector plot in the plane of secondary air injection slots for the reacting flow case

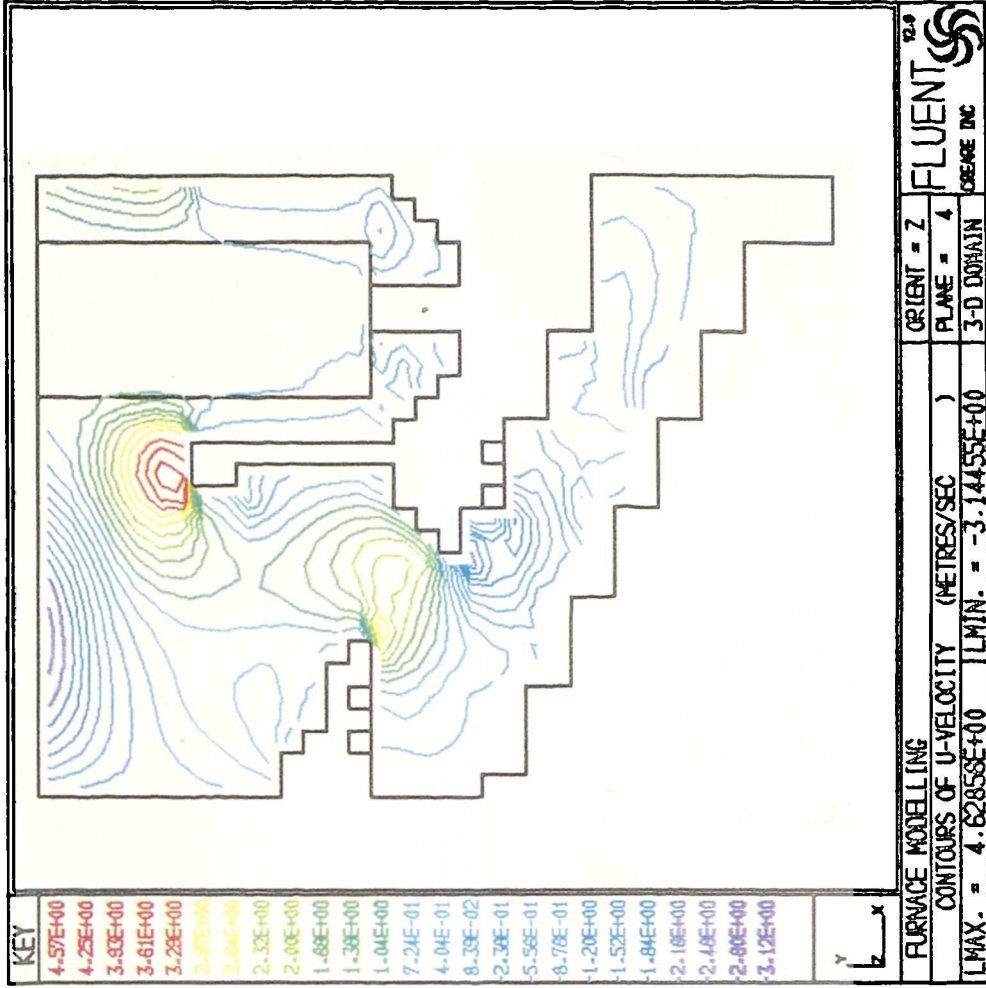


FIGURE 5.8 - Contours of u velocity in the plane of secondary air injection slots for the reacting flow case.

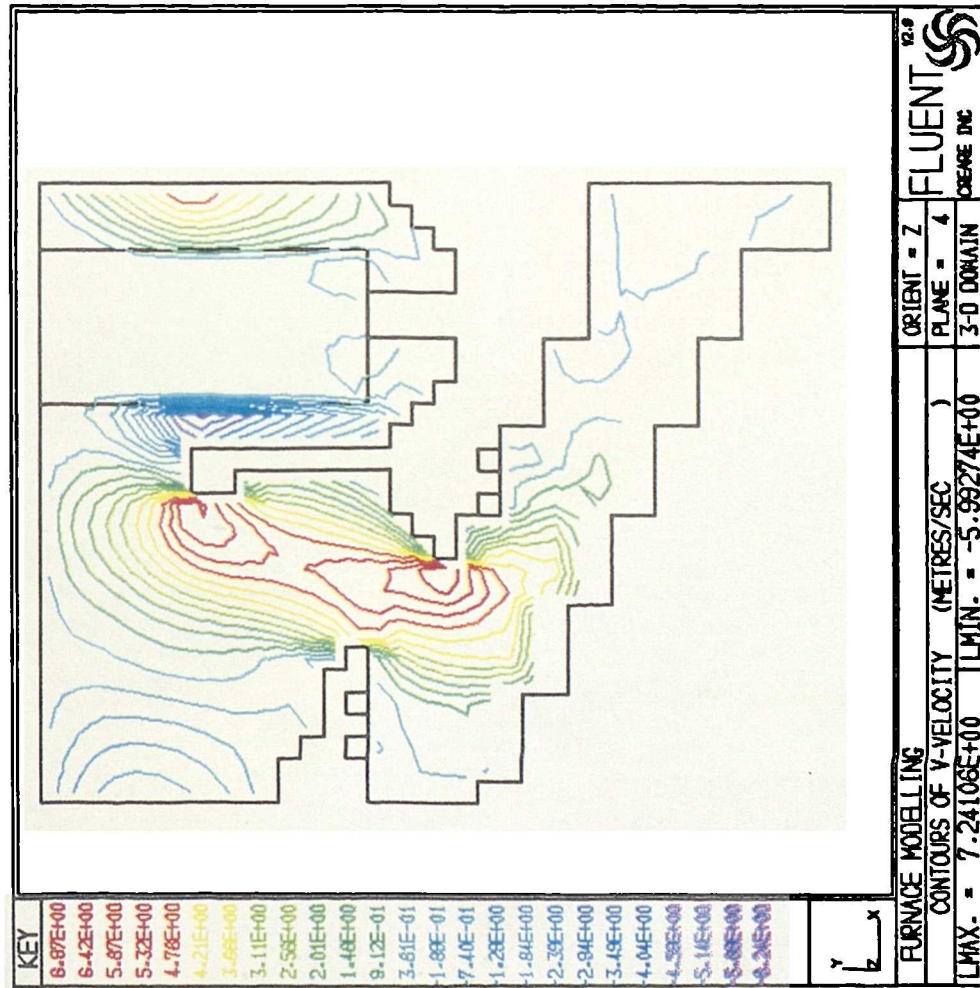


FIGURE 5.9 - Contours of v velocity in plane of secondary air slots for the reacting flow case.

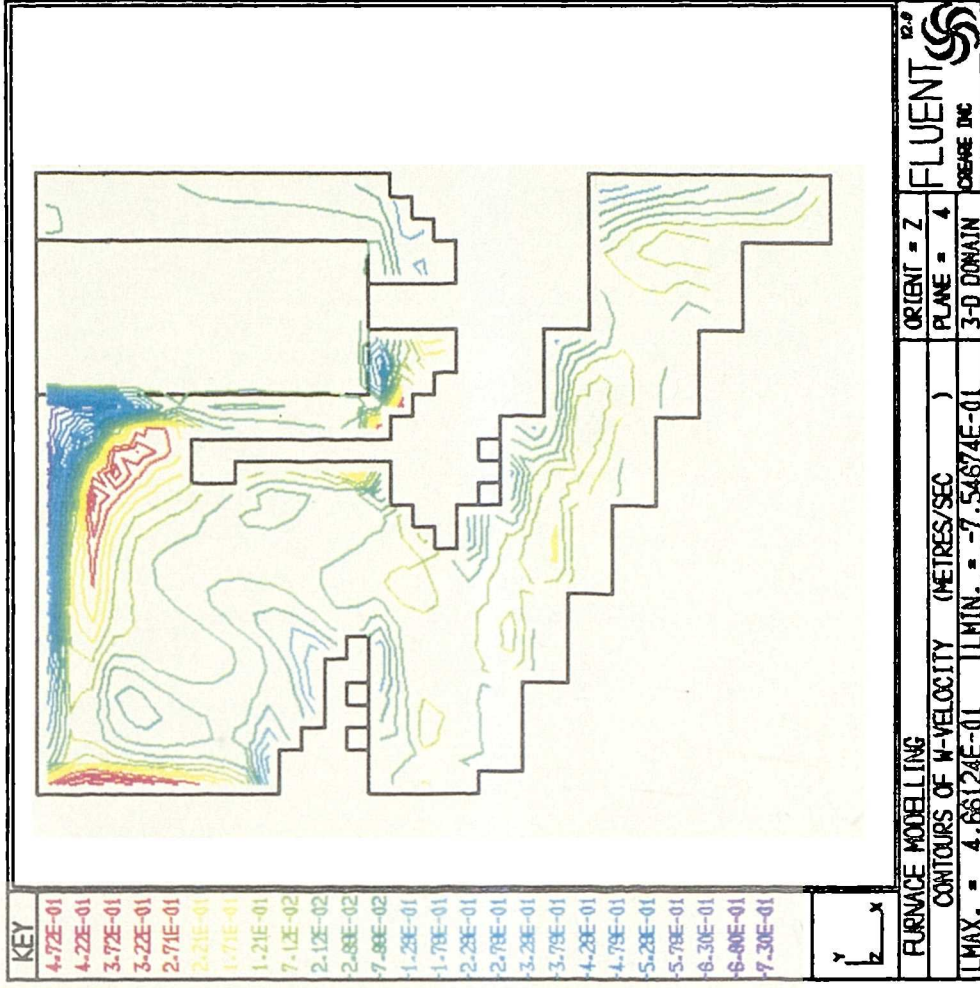


FIGURE 5.10 - Contours of w velocity in the plane of secondary air slots for the reacting case

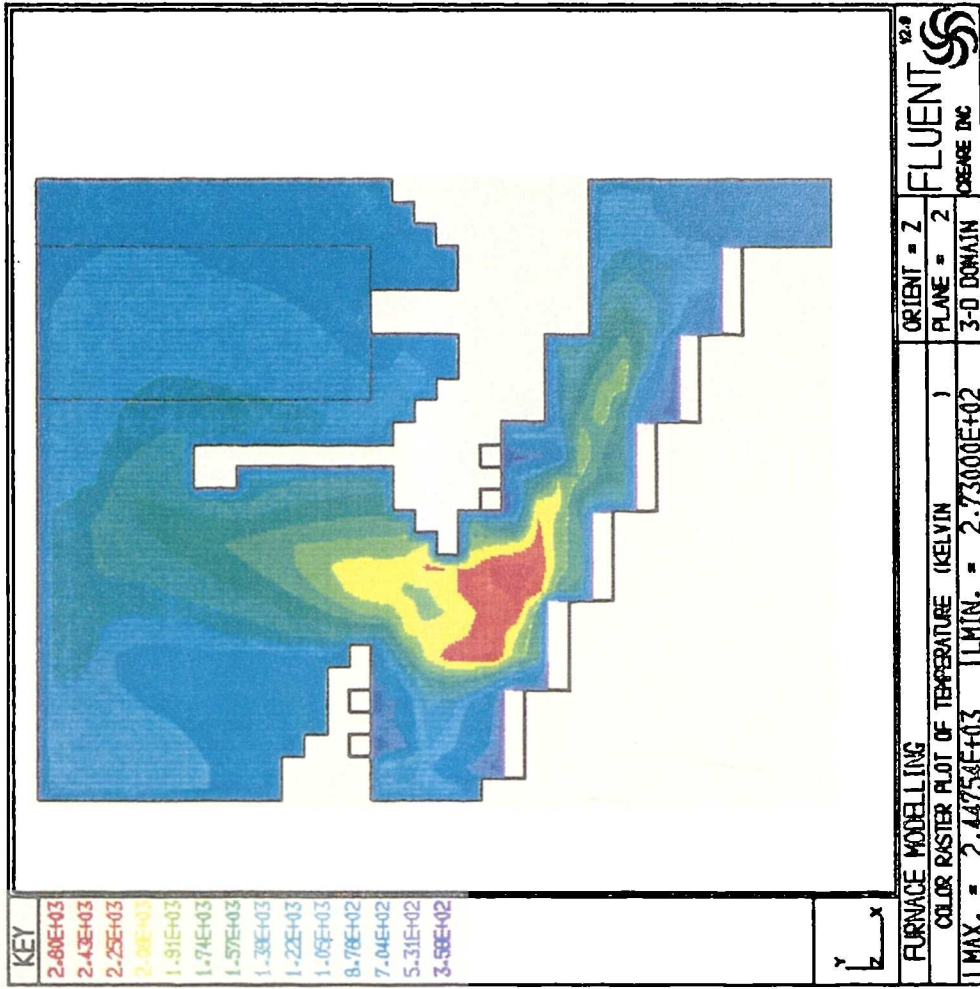


FIGURE 5.12 - Colour raster plot of temperature in plane 2 (near to the furnace side wall).

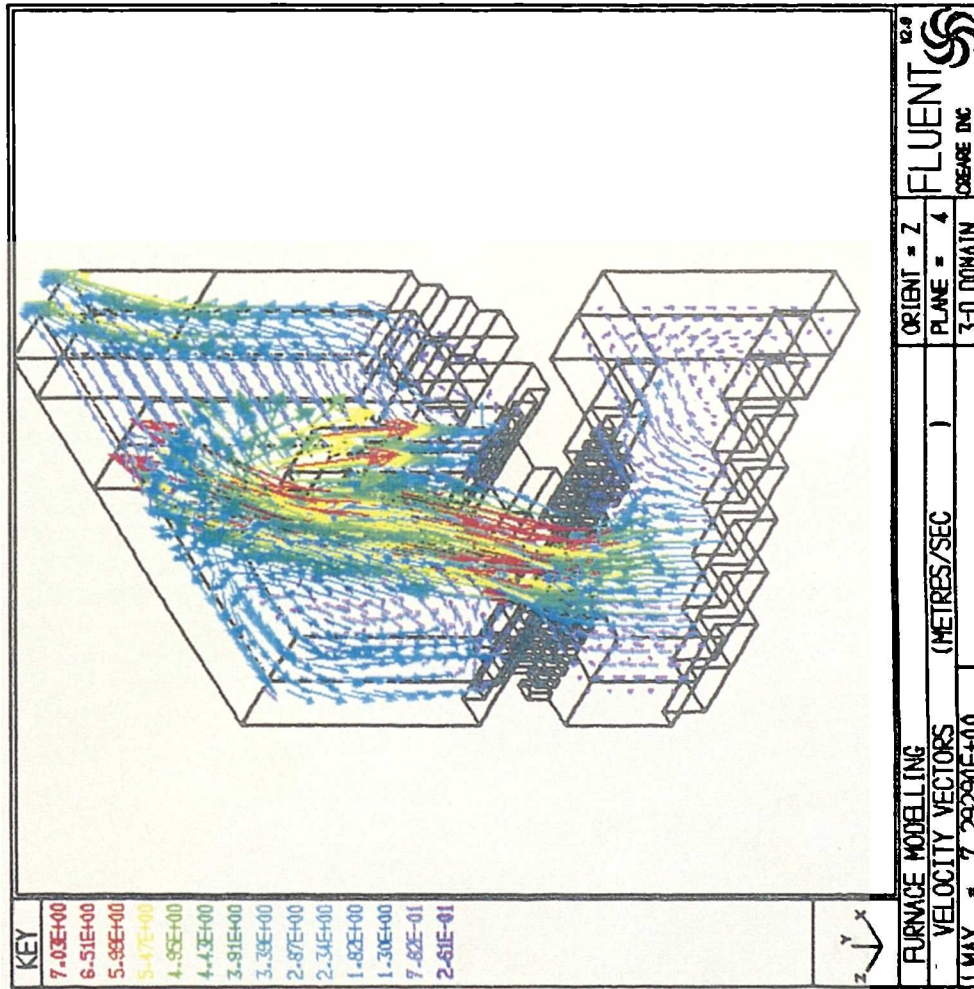


FIGURE 5.11 - Velocity vectors (3D) for the reacting flow case.

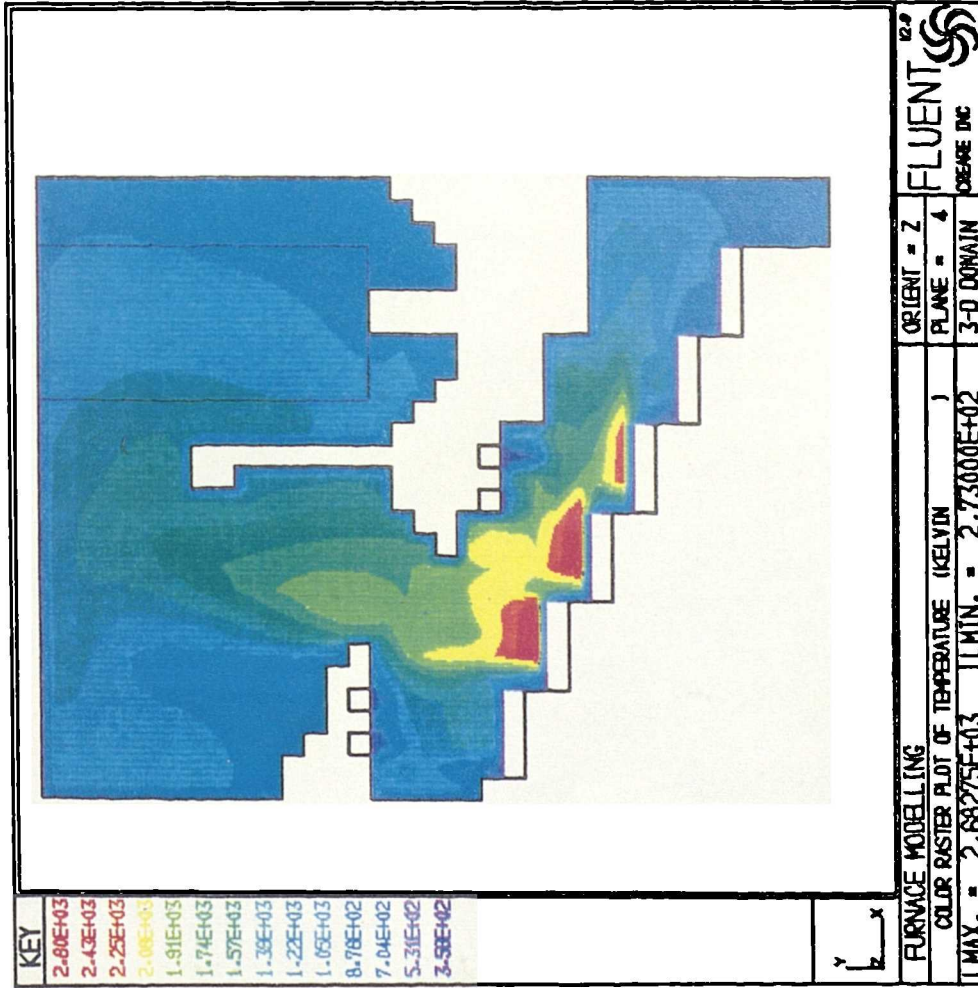


FIGURE 5.13 - Colour raster plot of temperature in plane 4 (near to the center of furnace).

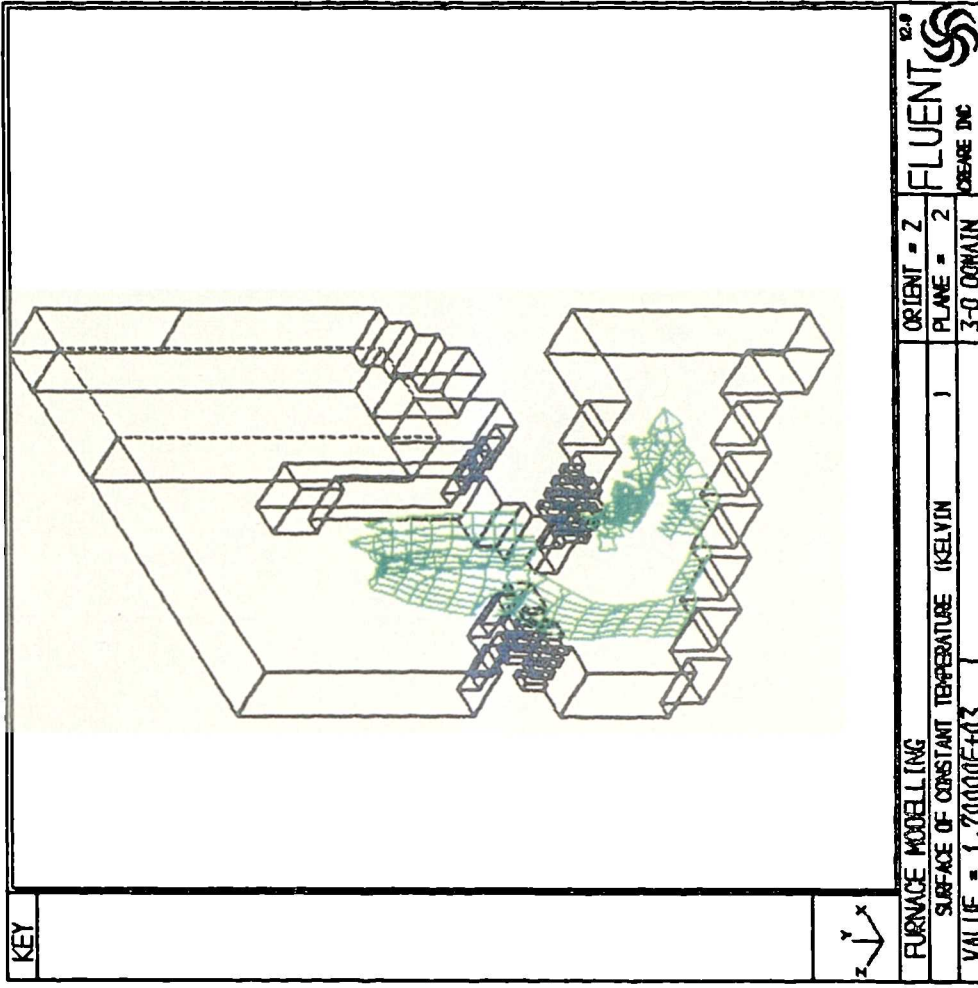


FIGURE 5.14 - Surface of constant temperature (1700 K); flame envelope.

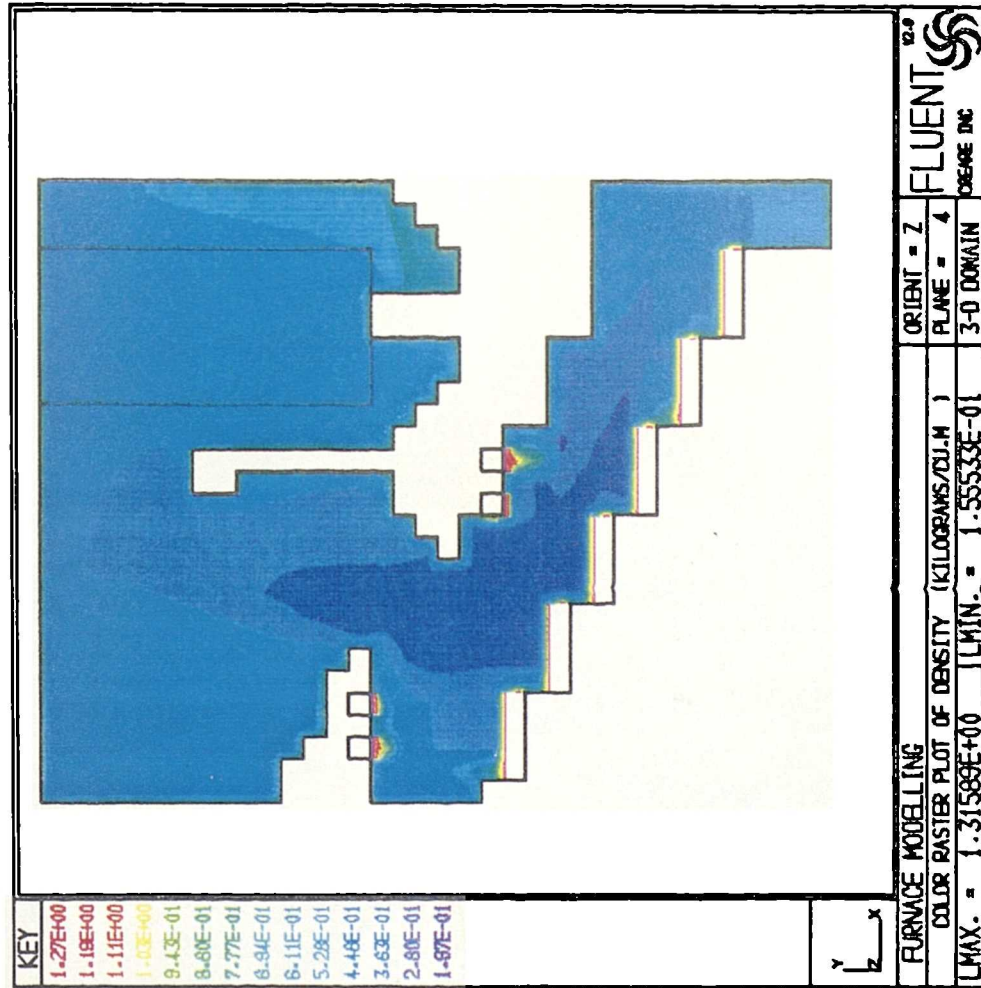


FIGURE 5.15 - Colour raster plot of density of flue gases inside the incinerator.

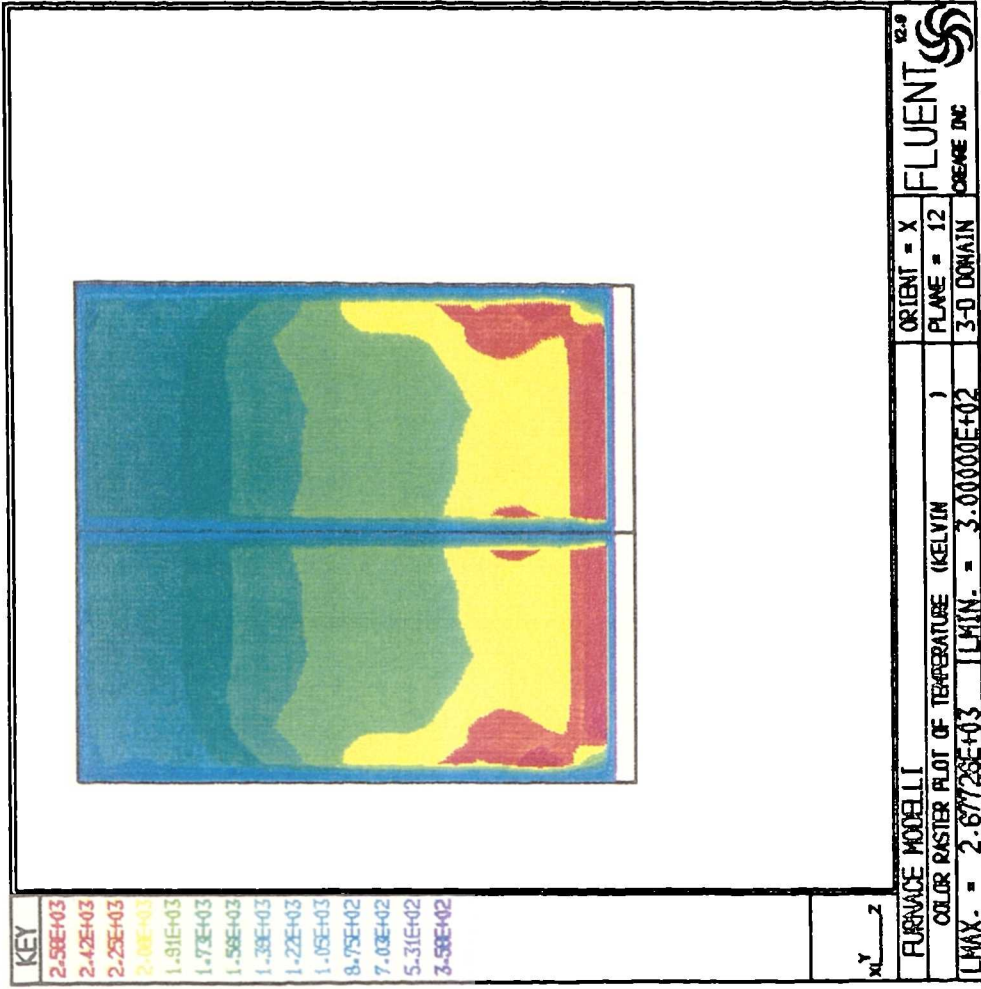


FIGURE 5.16 - Colour raster plot of temperature in the plane across the burning refuse bed on top of roller no. 2.

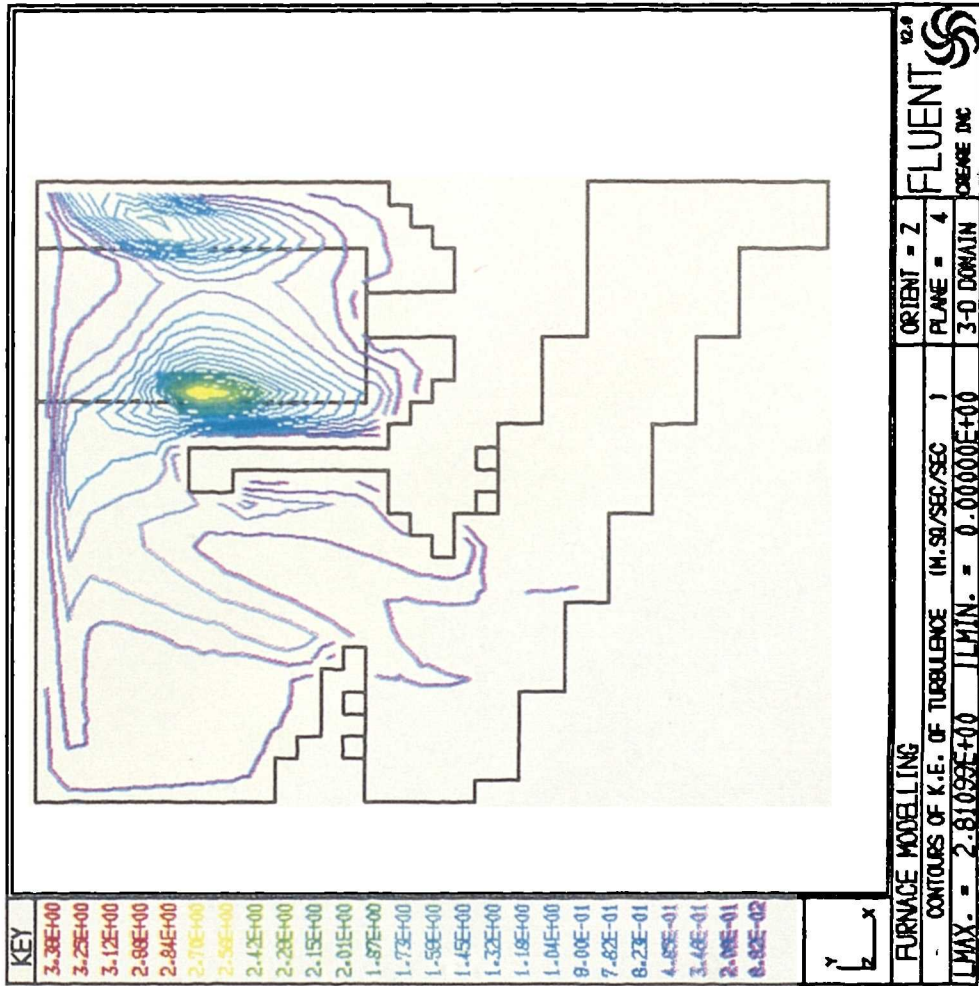


FIGURE 5.17 - Contours of K.E. of turbulence (plane 4);
 for reacting flow case.

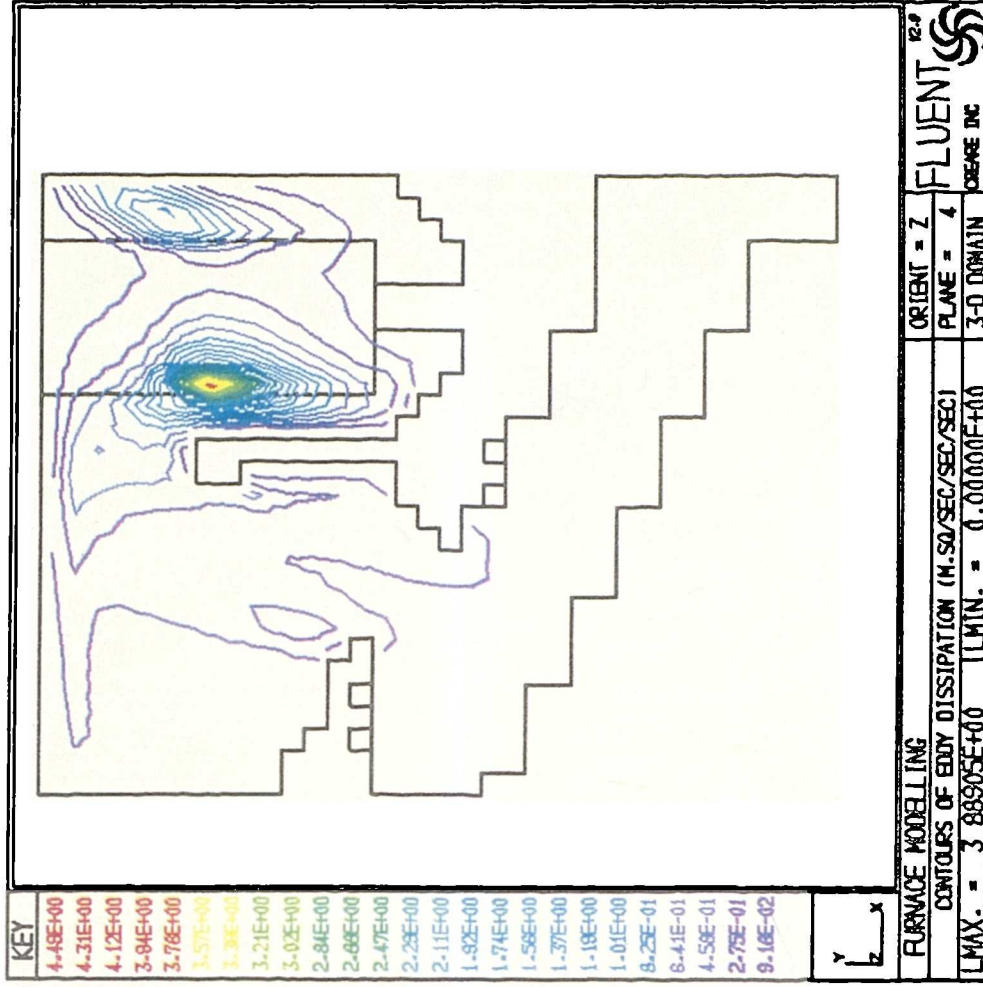


FIGURE 5.18 - Contours of eddy dissipation (plane 4);
 for reacting flow case.

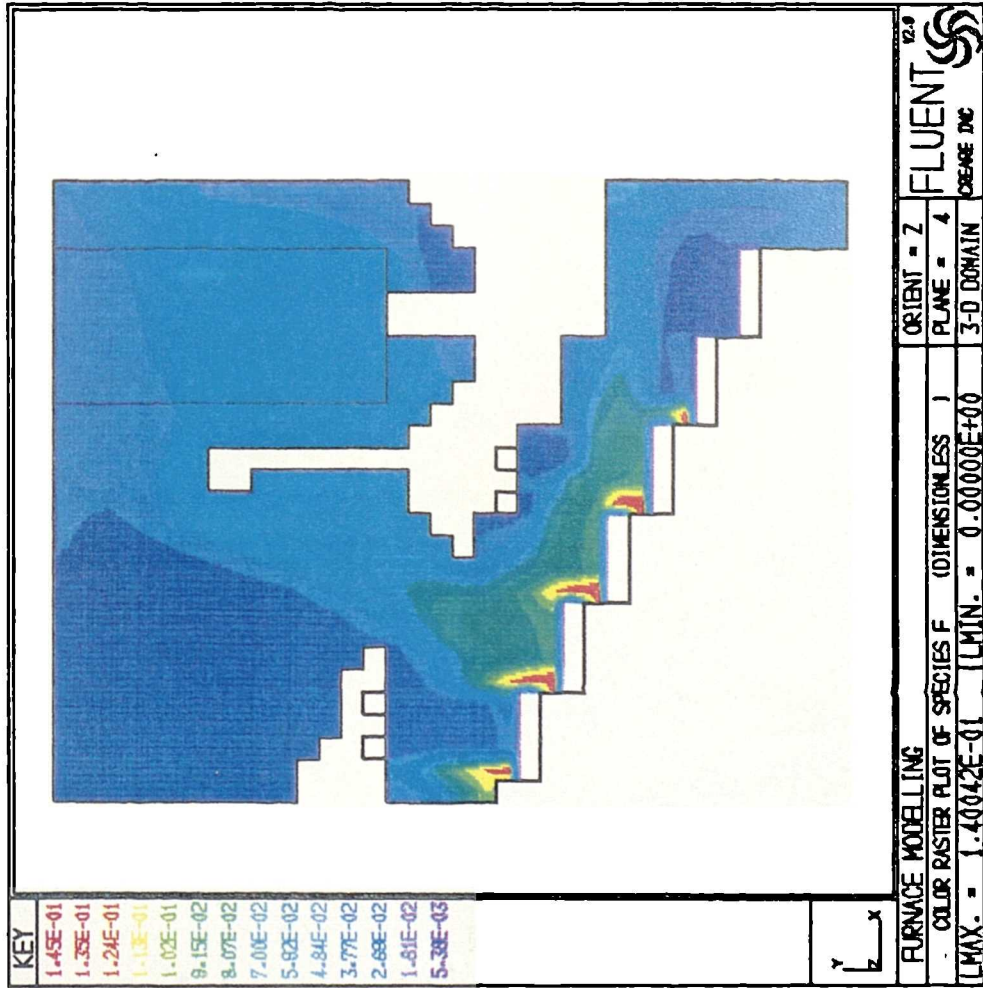


FIGURE 5.19 - Colour raster plot of unburnt fuel concentration distribution within the incinerator enclosure.

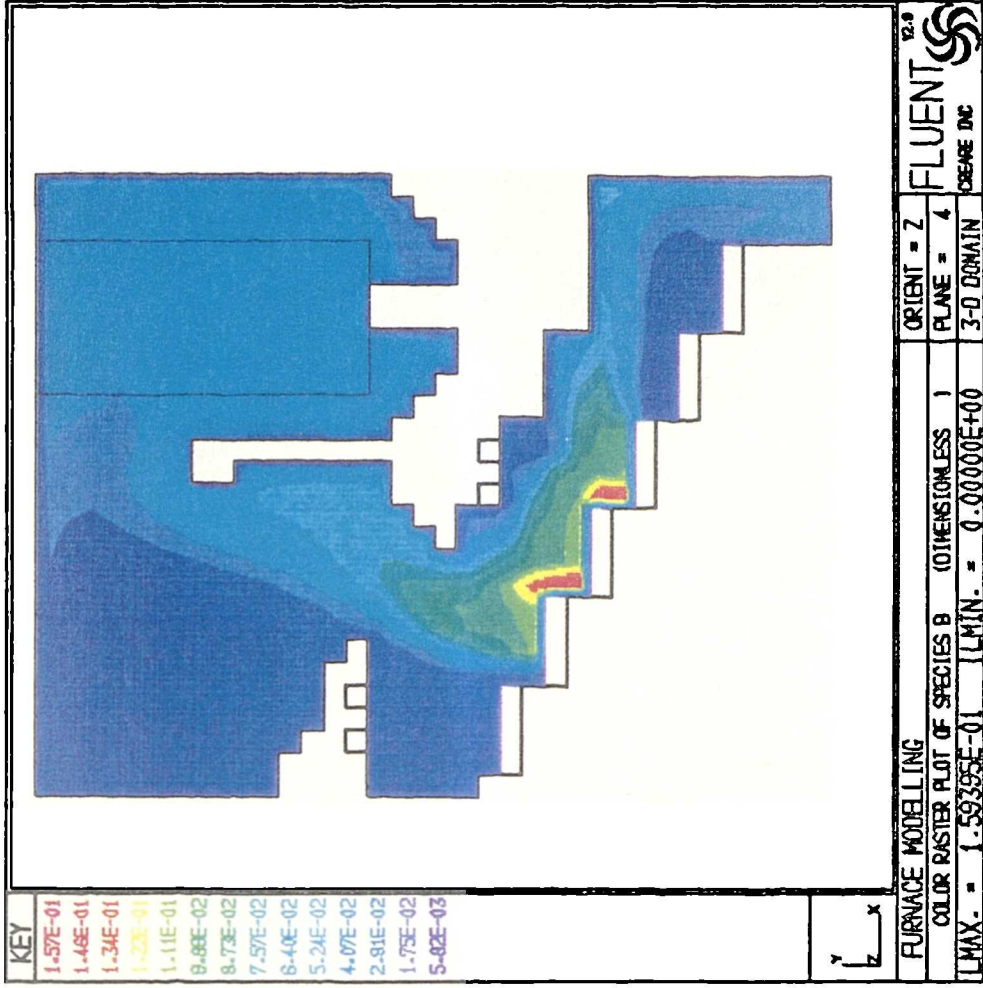


FIGURE 5.20 - Colour raster plot of CO concentration distribution within the incinerator enclosure.

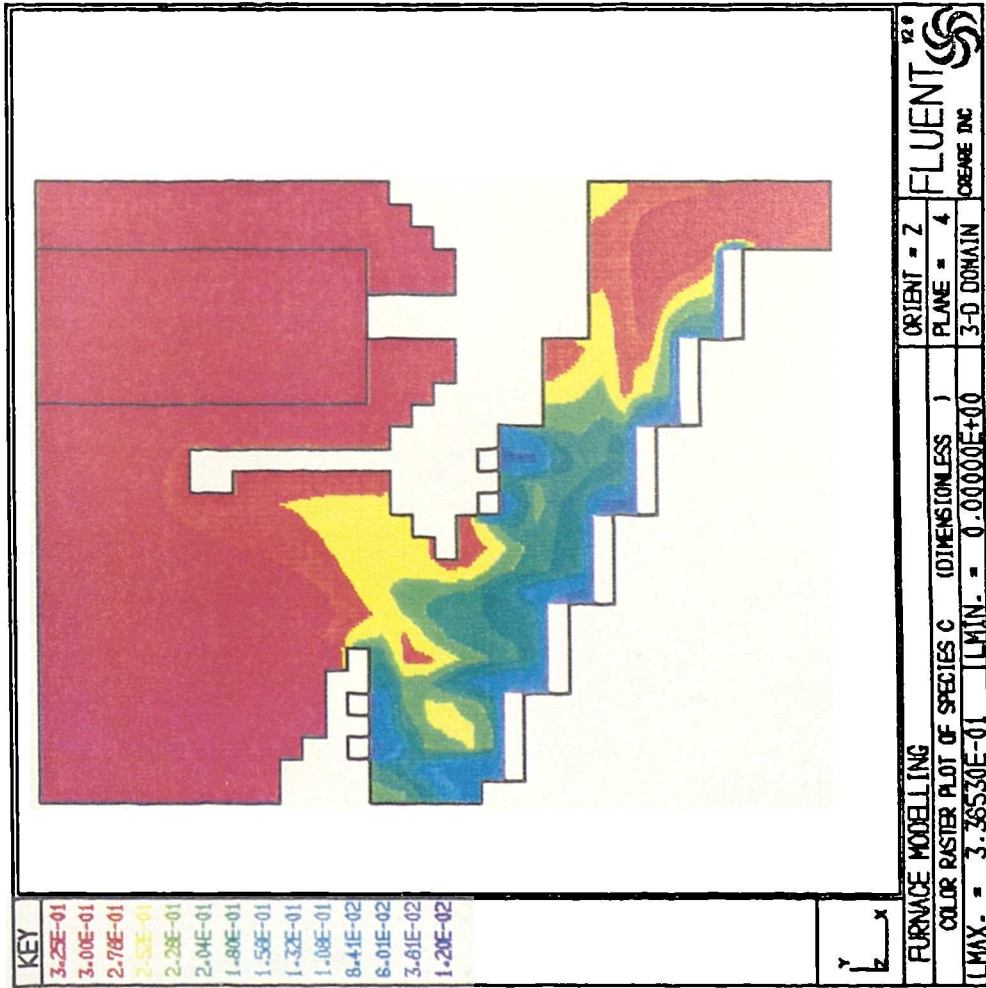


FIGURE 5.21 - Colour raster plot of CO2 concentration distribution within the incinerator enclosure.

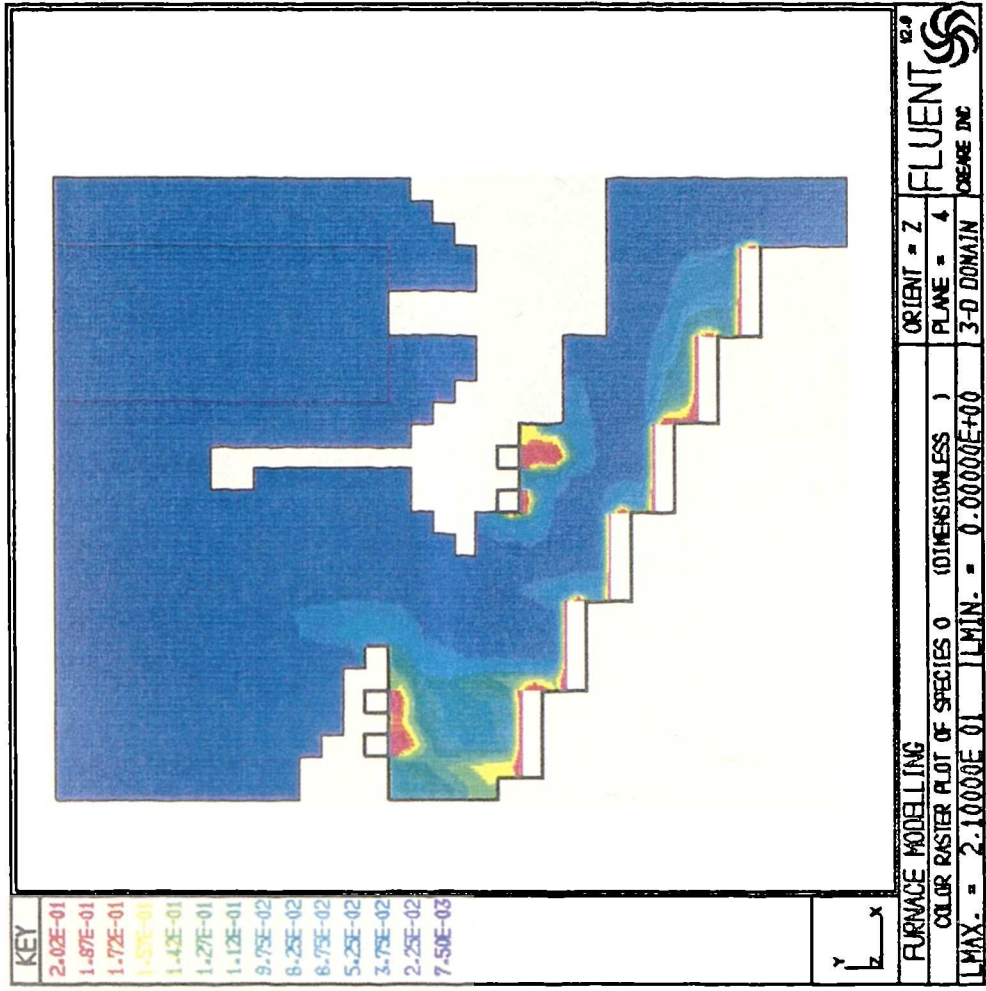


FIGURE 5.22 - Colour raster plot of O2 concentration distribution within the incinerator enclosure.

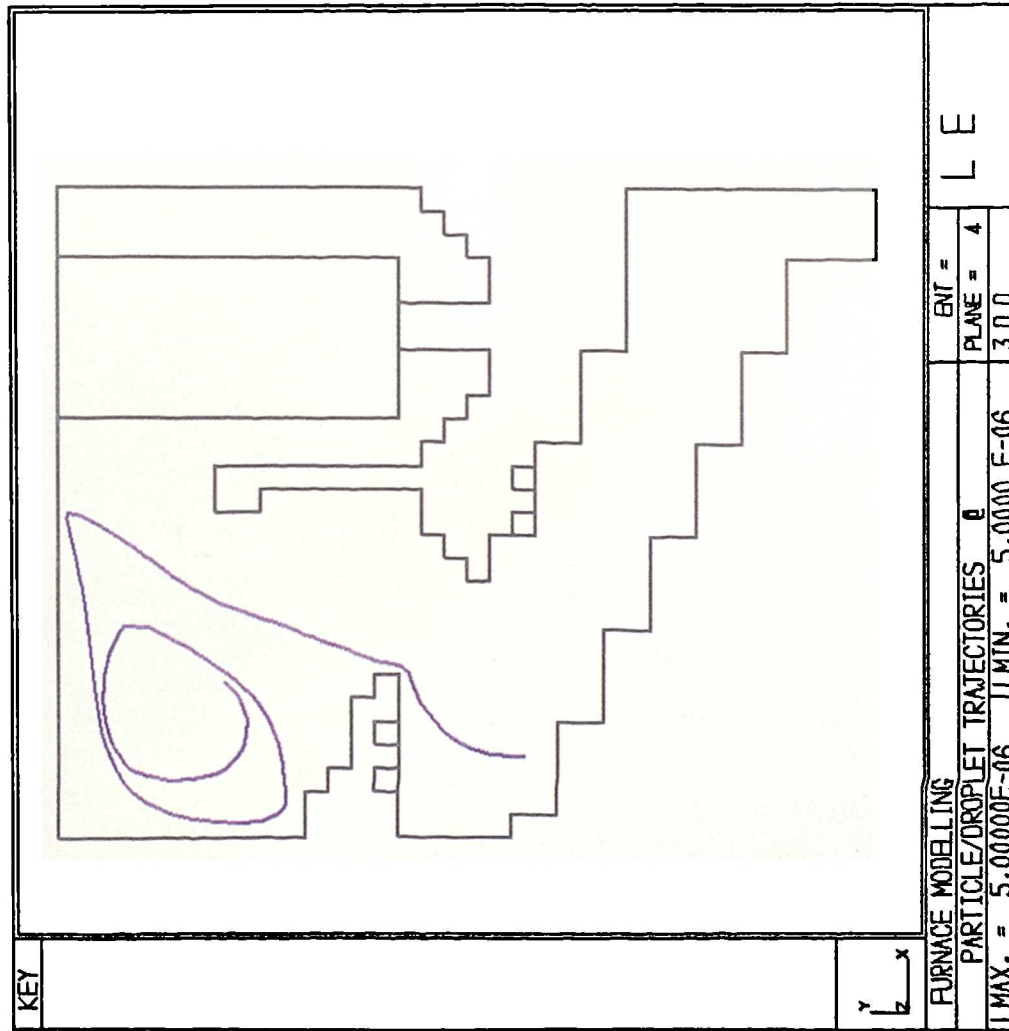


FIGURE 5.23 - Particle trajectory of injection from the top of roller no. 1

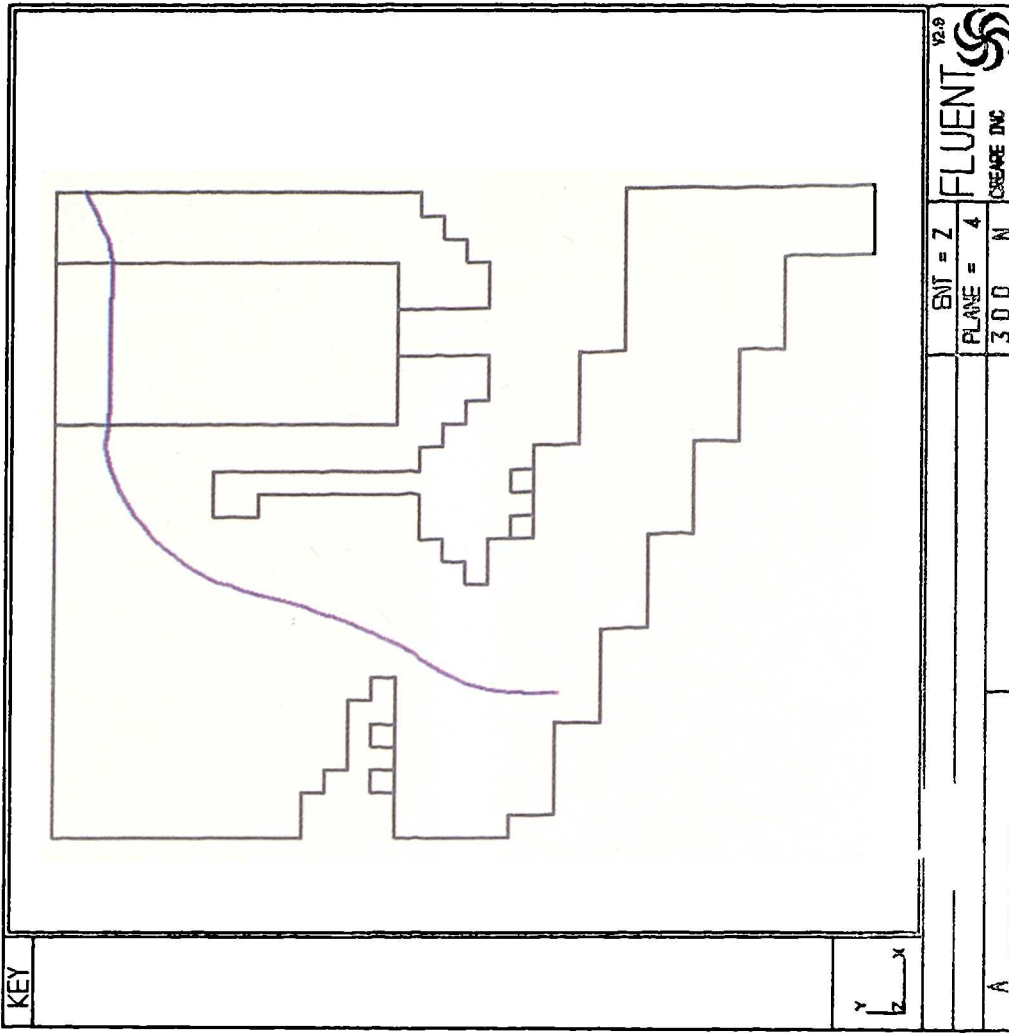


FIGURE 5.24 - Particle track of injection from the top of roller no. 2

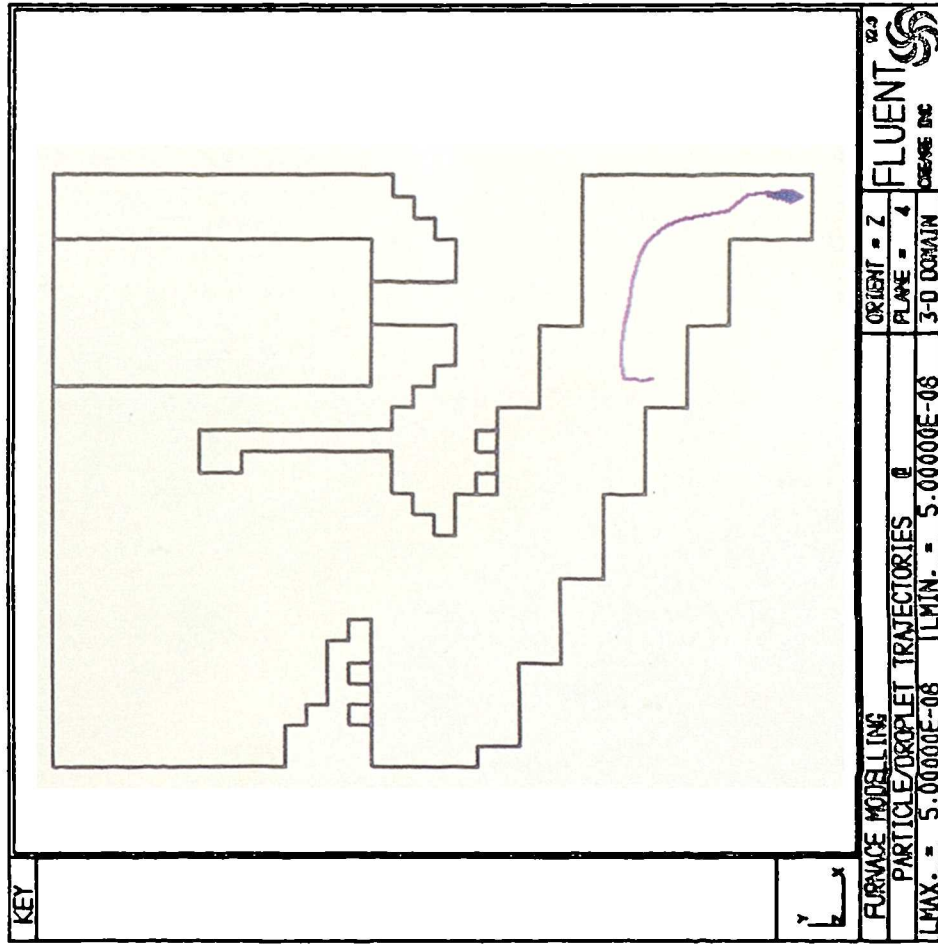


FIGURE 5.27 - Particle track of injection from the top of roller no.5

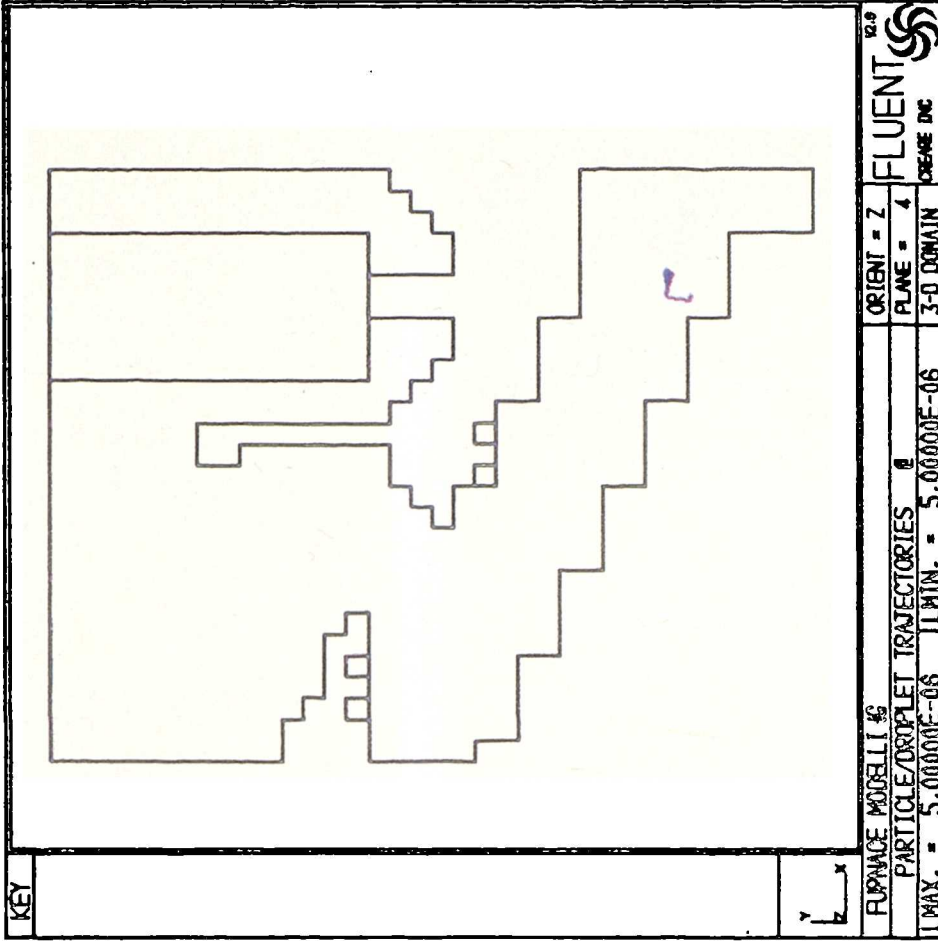


FIGURE 5.28 - Particle track of injection from the top of roller no. 6

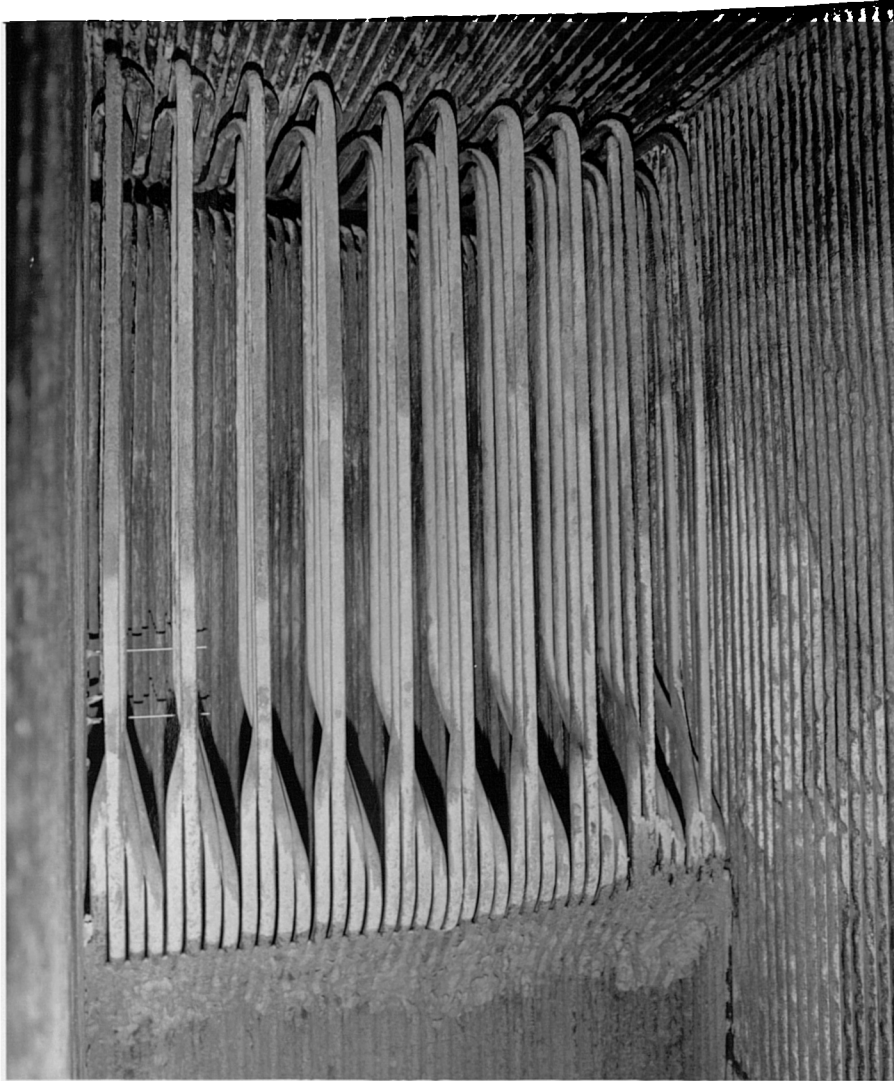
PLATE 1 - The drying oven and other equipment used for determination of density and moisture content of Sheffield refuse

PLATE 2 - The CBM computer, the analogue-digital convertor and the printer used for recording the experimental data



PLATE 3 - Plant Ni-Cr-Al thermocouples used for temperature measurement at the combustion chamber exit

PLATE 4 - Water-cooled probe and the Ni-Cr-Al thermocouple used for temperature measurement inside the radiation shaft



**PLATE 5 - End view of the water-cooled probe
used for temperature measurement inside the radia-
tion shaft**

PLATE 6 - The sampling probe cooling system

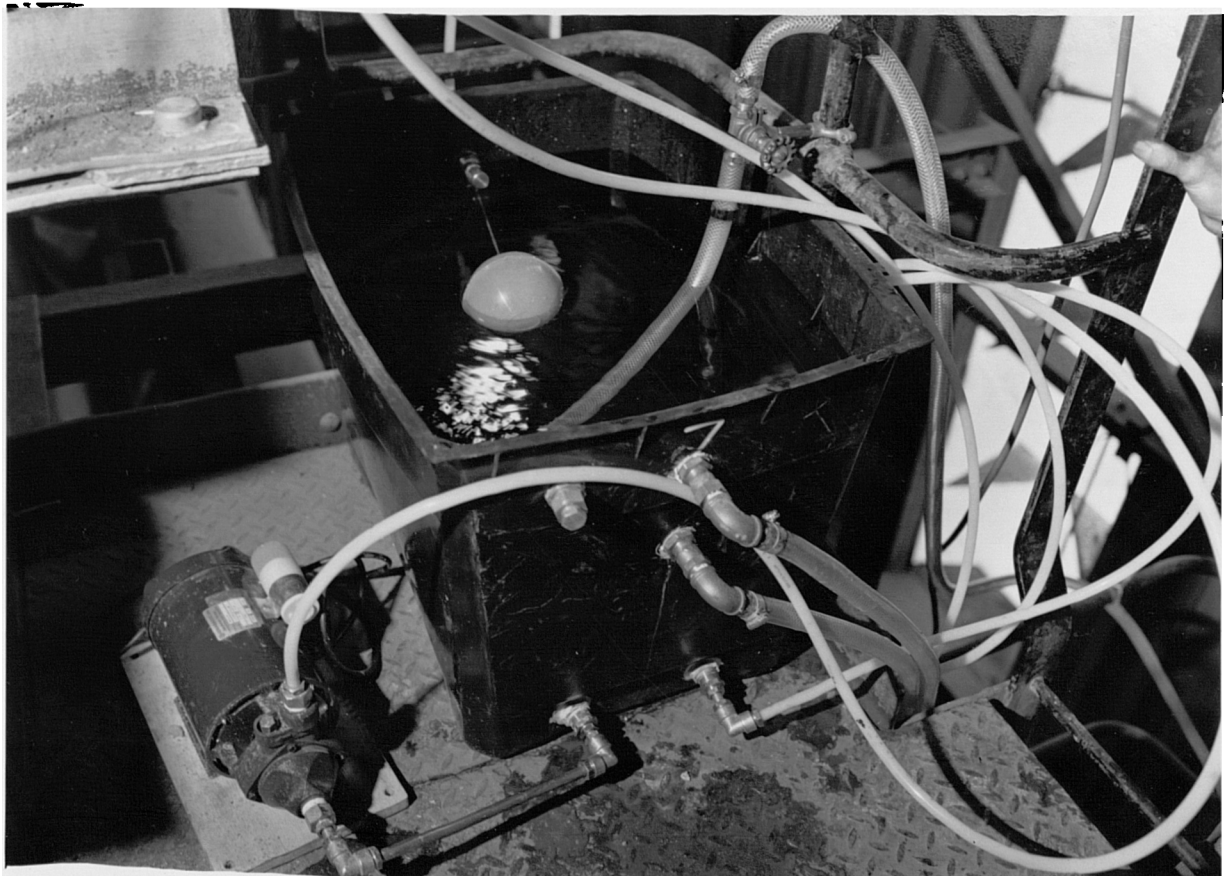
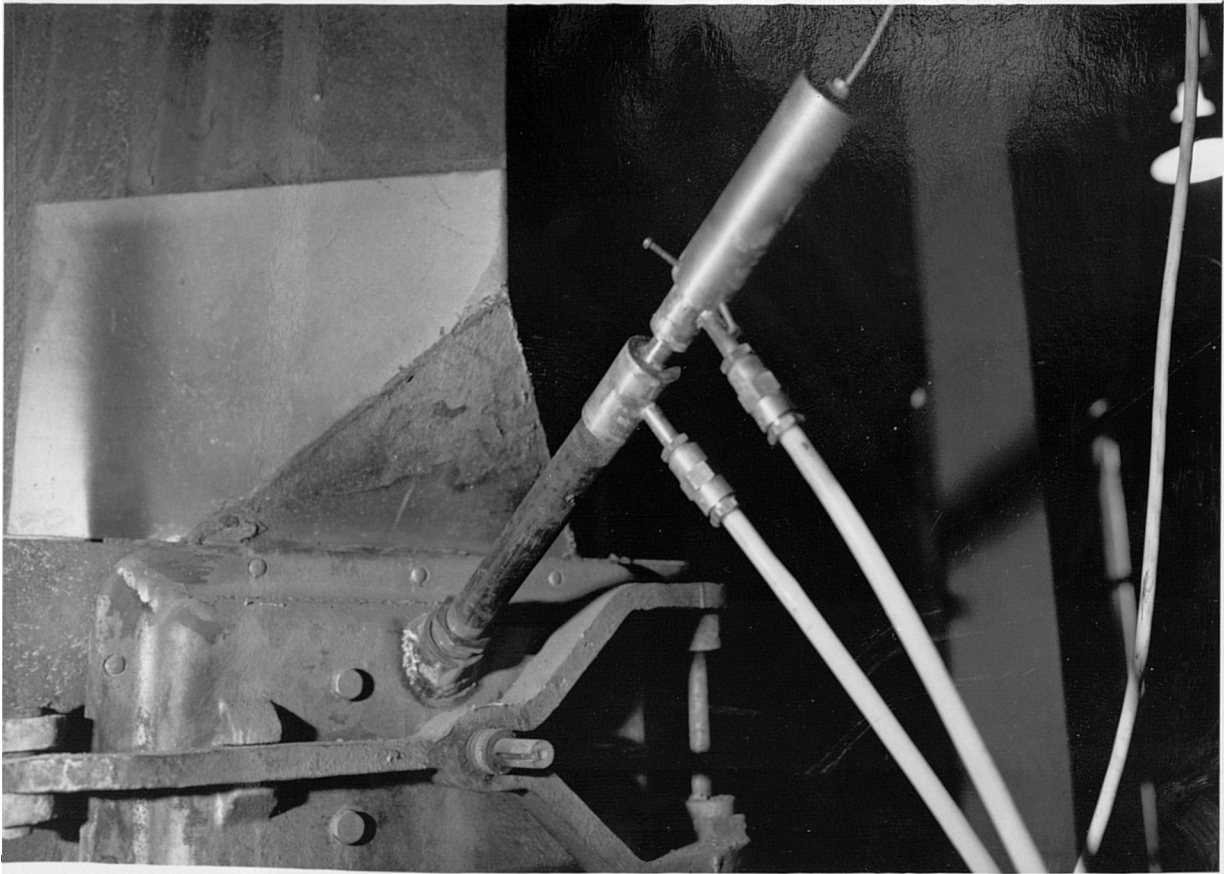


PLATE 7 - Side view of the incinerator showing location of the top access port used for gas sampling and temperature measurement inside and above the refuse bed

PLATE 8 - Side view of the incinerator showing location of middle and bottom ports used for gas sampling and temperature measurement inside and above the refuse bed

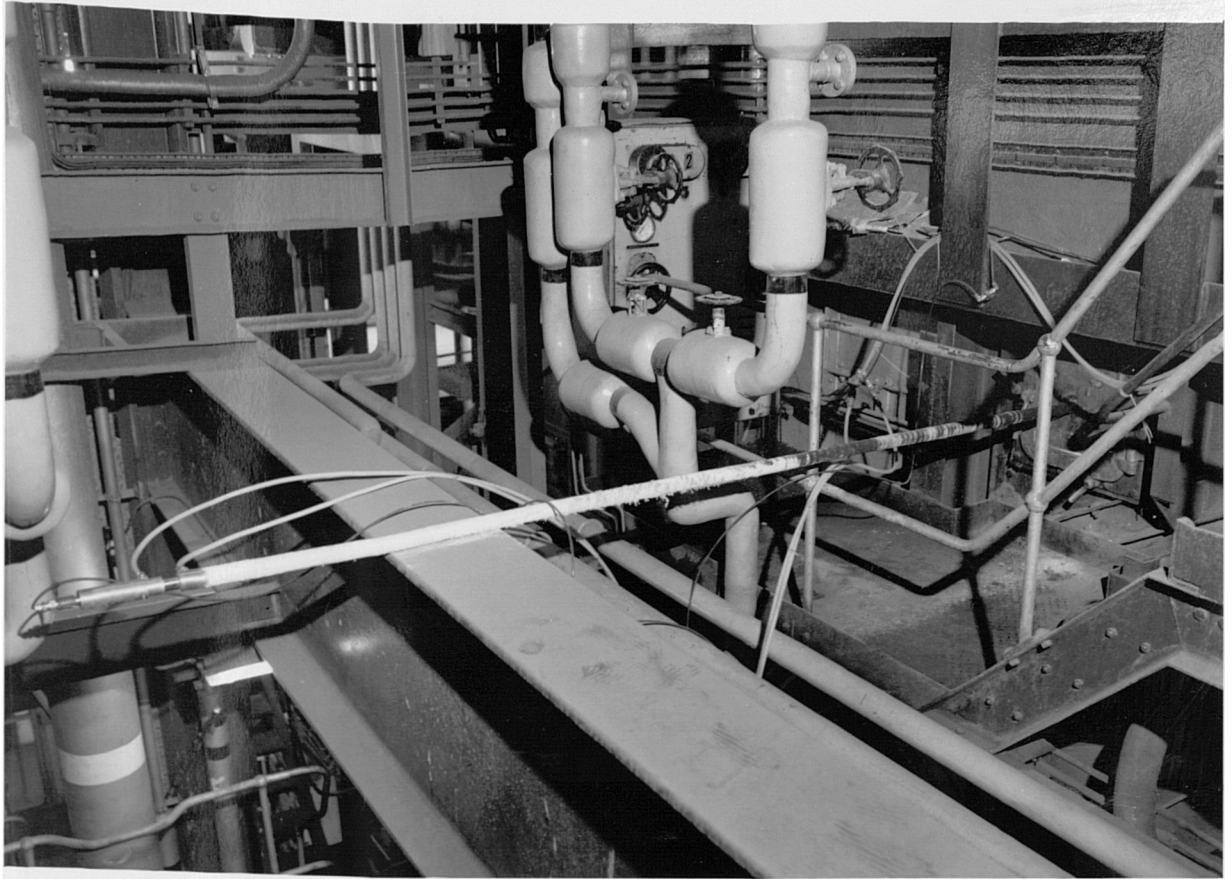


PLATE 9 - Inside view of the furnace showing location of secondary air openings on the roof arch of the furnace. As shown, most of the openings are blocked.

PLATE 10 - Inside view of the furnace showing the travelling grate. Slagging of the side walls of the furnace and the general deterioration of the refractory materials in the side areas directly above the grate can clearly be seen.

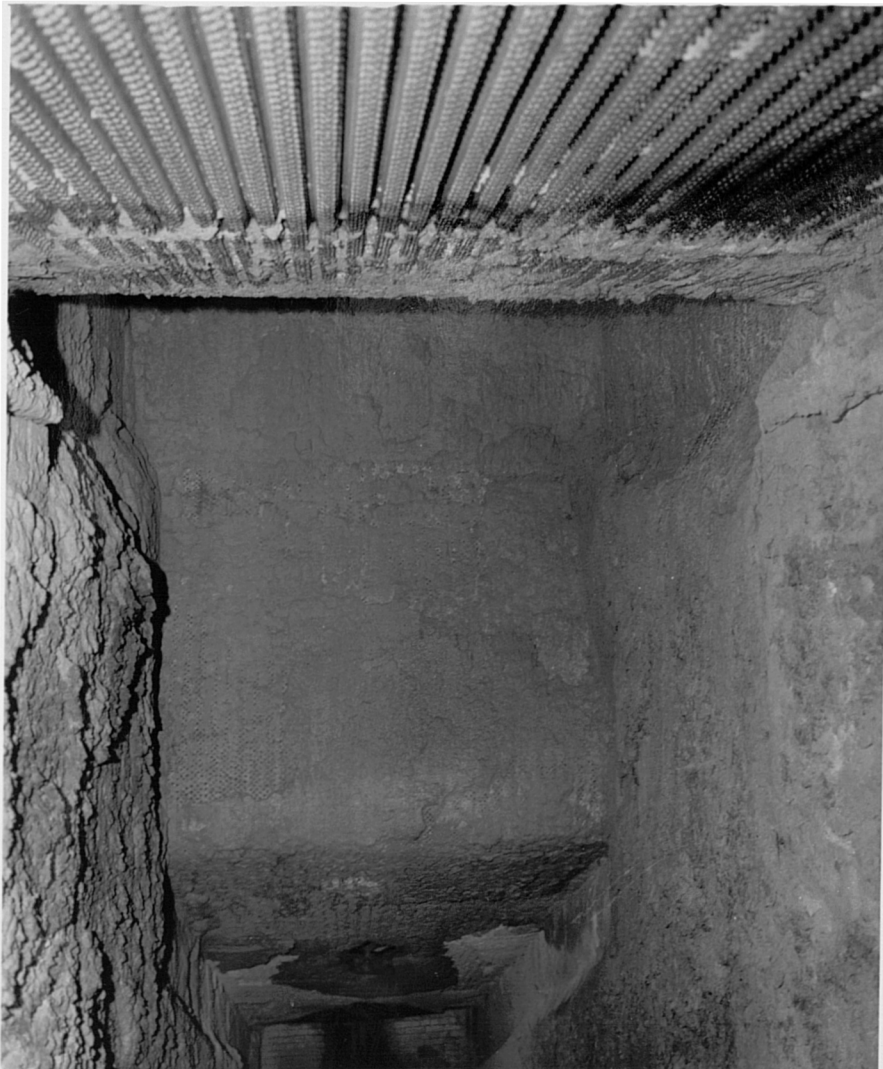
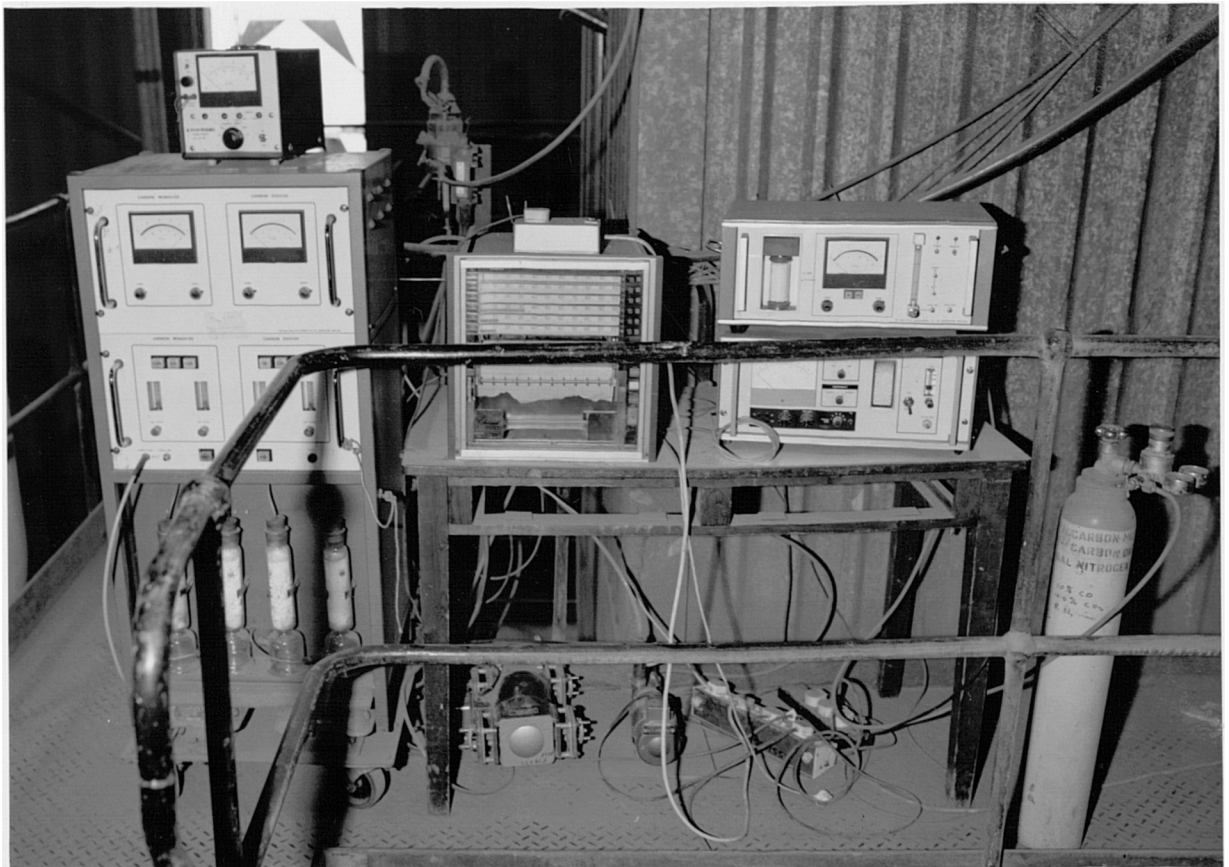
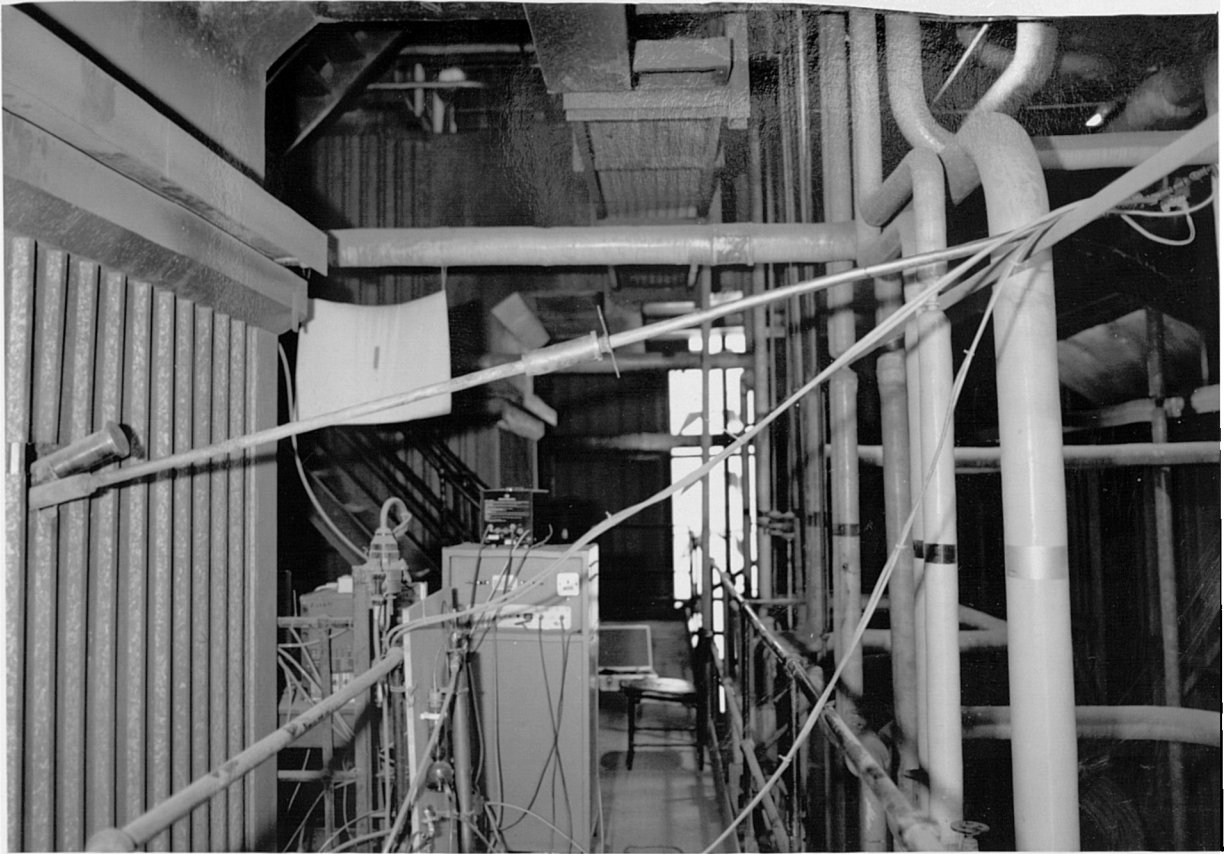


PLATE 11 - Sampling probe (water-cooled) used for determination of CO, CO₂ and O₂ concentrations at the combustion chamber exit

PLATE 12 - CO and CO₂ infra-red gas analysers , O₂ paramagnetic analyser and chart recorder used for the flue gas analysis



**PLATE 13 - Sampling train used for determination of
CO, CO₂ and O₂ concentrations in the flue gases**

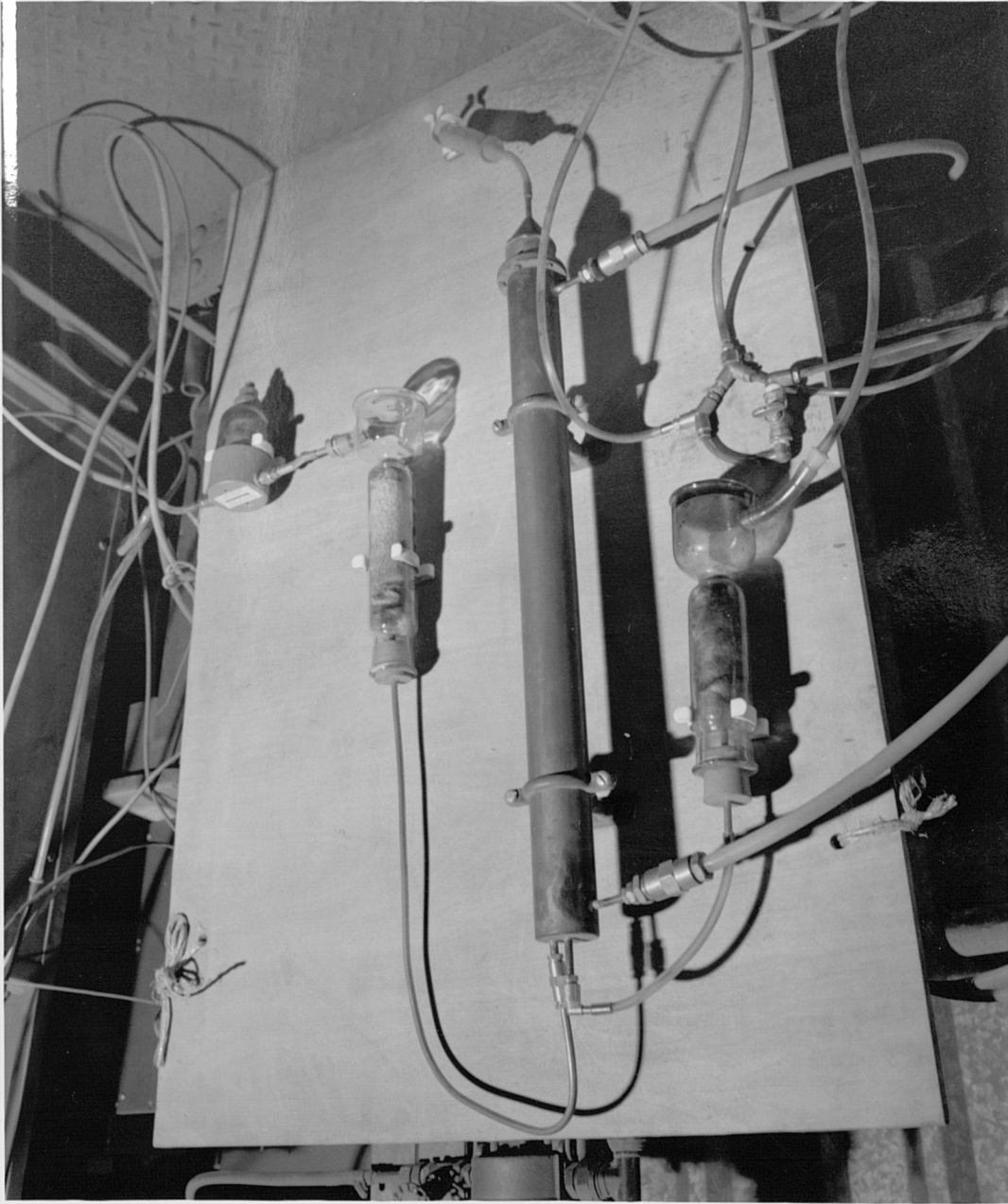


PLATE 14 - Sampling train used for determination of SO₂ and NO concentrations at the precipitator inlet

PLATE 15 - Sampling equipment (pump, gas meter, transformer, condenser, etc) used for flue gas analysis at the precipitator inlet

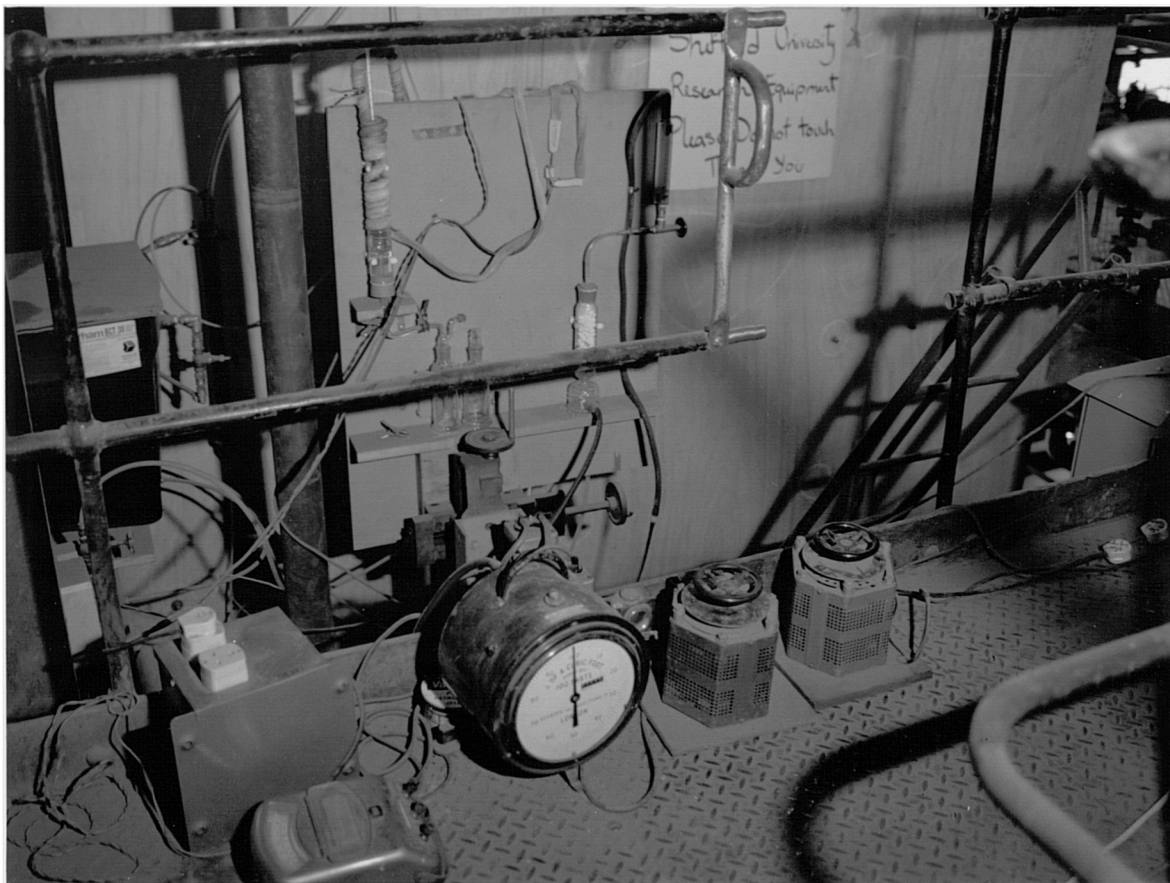
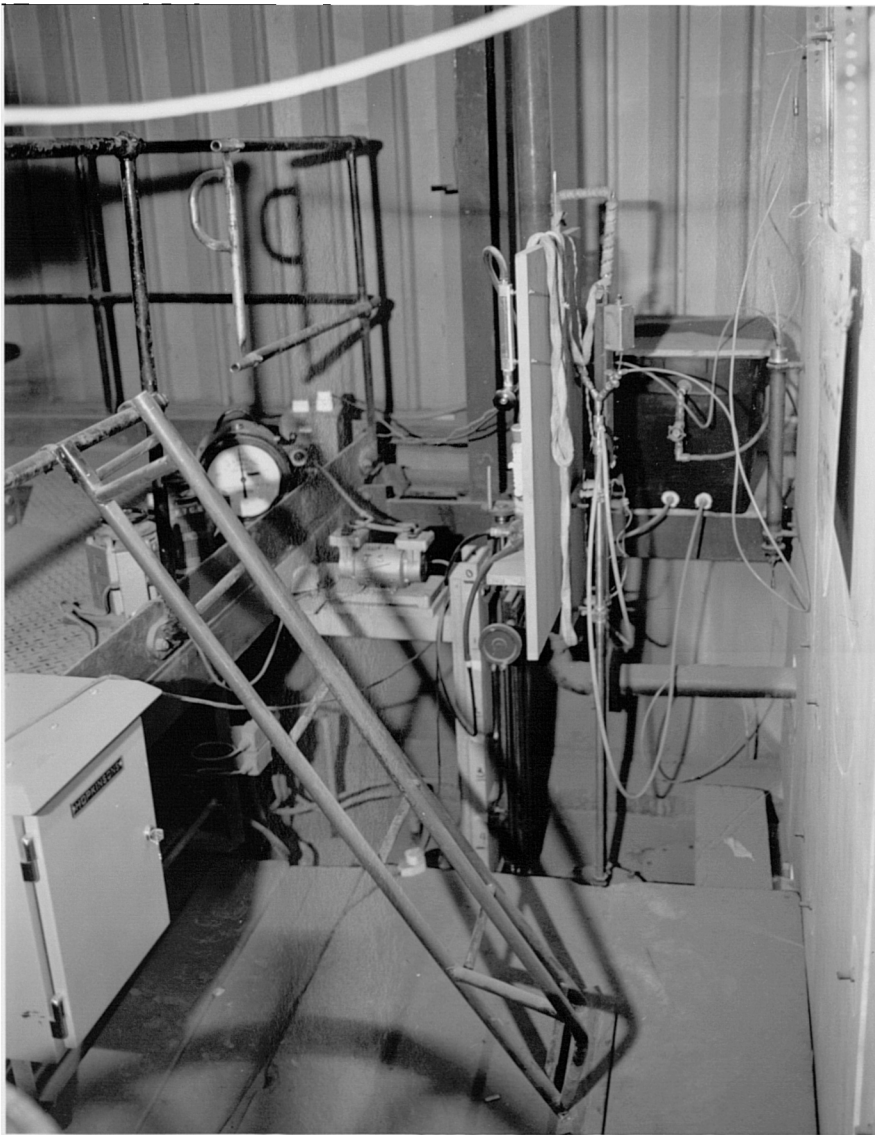
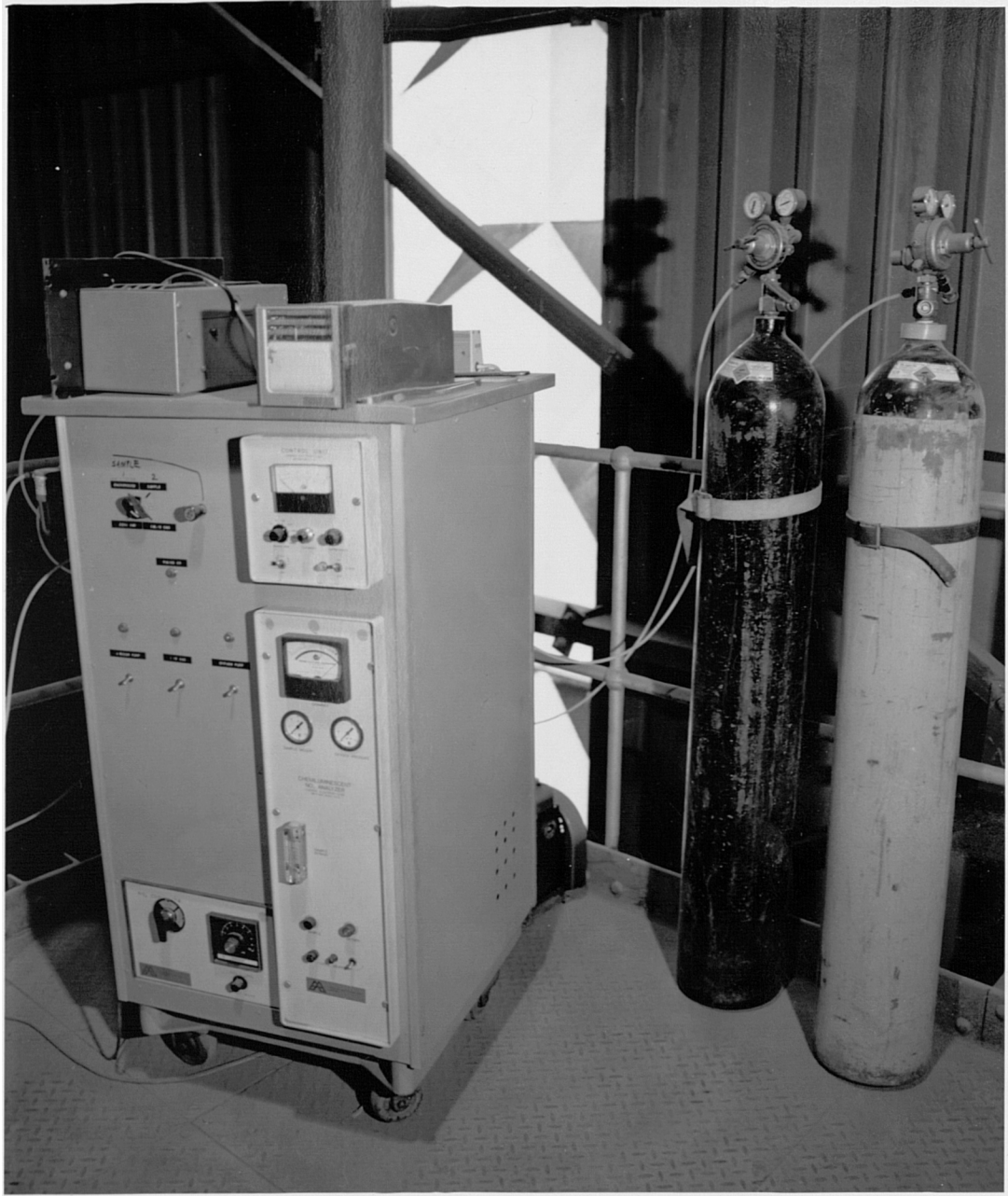


PLATE 16 - NO_x analyser (Thermal Electron Model 10A modular type) used for NO measurement at the precipitator inlet



**PLATE 17 - LAND electrochemical probe-analyser
used for determination of NO and SO₂ concentrations
at the base of chimney**

**PLATE 18 - Compressor, chart recorder and LAND
computer system used to record NO and SO₂ emission
levels**

